Phenotypic, genetic, and transcriptomic decoupling of thermal hardiness across metamorphosis in *Drosophila melanogaster*

by

Philip John Freda

B.S., Pennsylvania State University, 2005
M.S., Saint Joseph's University, 2014

AN ABSTRACT OF A DISSERTATION

submitted in partial fulfillment of the requirements for the degree

DOCTOR OF PHILOSOPHY

Department of Entomology
College of Agriculture

KANSAS STATE UNIVERSITY

Manhattan, Kansas

2018

Abstract

Complex life cycles (CLCs), developmental programs in which life-history stages are distinct in morphology, behavior, and physiology, are common throughout the biosphere. However, it is still unclear why and how CLCs evolve. The adaptive decoupling hypothesis (ADH) postulates that CLCs evolve to decouple the developmental processes that underlie traits across ontogeny to allow for independent, stage-specific responses to selection. This ultimately could lead to alternate life-history stages adapting to unique environments, thus optimizing fitness across development. However, few empirical tests of the ADH are available. Detecting genetic and transcriptomic decoupling of thermal hardiness using robust techniques in a model system, *D. melanogaster*, was the goal of this dissertation. Furthermore, this work illustrates that different life-history stages have the potential to become adapted to unique ecological niches. I performed three primary studies to test the ADH: 1.) estimation of the genetic correlation for cold hardiness between larvae and adults using isogenic lines of *D. melanogaster* to determine if unique genetic architectures underlie variation in cold stress response using standard quantitative genetic and Genome-Wide Association (GWA) methods, 2.) testing whether developmental acclimation is genetically correlated across stages, and whether acclimation alters cross-stage correlations in cold hardiness, and 3.) analysis of the transcriptional responses of both larvae and adults to extreme cold to determine if stage-specific stress response mechanisms exist across development.

Phenotypic, genetic, and transcriptomic decoupling of thermal hardiness across metamorphosis in *Drosophila melanogaster*

by

Philip John Freda

B.S., Pennsylvania State University, 2005
M.S., Saint Joseph's University, 2014

A DISSERTATION

submitted in partial fulfillment of the requirements for the degree

DOCTOR OF PHILOSOPHY

Department of Entomology
College of Agriculture

KANSAS STATE UNIVERSITY

Manhattan, Kansas

2018

Approved by:

Major Professor
Yoonseong Park

Copyright

Abstract

Complex life cycles (CLCs), developmental programs in which life-history stages are distinct in morphology, behavior, and physiology, are common throughout the biosphere. However, it is still unclear why and how CLCs evolve. The adaptive decoupling hypothesis (ADH) postulates that CLCs evolve to decouple the developmental processes that underlie traits across ontogeny to allow for independent, stage-specific responses to selection. This ultimately could lead to alternate life-history stages adapting to unique environments, thus optimizing fitness across development. However, few empirical tests of the ADH are available. Detecting genetic and transcriptomic decoupling of thermal hardiness using robust techniques in a model system, *D. melanogaster*, was the goal of this dissertation. Furthermore, this work illustrates that different life-history stages have the potential to become adapted to unique ecological niches. I performed three primary studies to test the ADH: 1.) estimation of the genetic correlation for cold hardiness between larvae and adults using isogenic lines of *D. melanogaster* to determine if unique genetic architectures underlie variation in cold stress response using standard quantitative genetic and Genome-Wide Association (GWA) methods, 2.) testing whether developmental acclimation is genetically correlated across stages, and whether acclimation alters cross-stage correlations in cold hardiness, and 3.) analysis of the transcriptional responses of both larvae and adults to extreme cold to determine if stage-specific stress response mechanisms exist across development.

Table of Contents

List of Figures

List of Tables

List of Scripts

Acknowledgements

This research was made possible via funding from the National Science Foundation's Division of Integrative Organismal Systems (NSF IOS Grant # 1256930), Division of Environmental Biology (NSF DEB Grant # 1638951), and Division of Biological Infrastructure (NSF DBI Grant # 1460802) as well as Kansas State Agricultural Research and Extension.

First and foremost, I would like to acknowledge the undergraduate and volunteer researchers who made significant portions of this dissertation possible: Jackson Alex, Nicholas Heter, Zainab Ali, Mariah Brown, Adam Schieferecke, Mary Post, Oshadhi Athukorala Arachchige, Saadia Ixchel Cleve, Ashley Wedin, and Colin Bailey. I would also like to acknowledge both Eddie Dowle and Rebekah Lambert Collier for their significant contributions on the RNAseq portion of this dissertation. I would like to thank my friends that I have made along this journey, especially my closest friends, Leonie Dohmen, Vlad Petrovan, Renan Donadelli, Jacob Alsdurf, Matt Galliart, John Coffin, Em Collin, and Deborah Stone, for keeping me grounded through, what was partially, trying times. I would also like to thank my family, Lisa Dalantinow, Matthew Freda, Buddha Dalantinow, Philip Freda, Sr., Deborah Lehman, and Enzo Dalantinow, for their ever-lasting love and support. Finally, last but definitely not least, I would like to thank my committee, Yoonseong Park, Jeremy Marshall, and Michi Tobler, and my advisors, Theodore Morgan and Gregory Ragland, for keeping me on my toes and teaching me how to learn and be a better scientist, even from afar. Thank you all very much.

The work in this dissertation is published or *submitted for publication* as follows:

Chapter 2:

Freda, P.J., Alex, J.T., Morgan, T.J., and Ragland, G.J. (2017). Genetic decoupling of thermal hardiness across metamorphosis in *Drosophila melanogaster*. Integr. Comp. Biol *57*, 999–1009.

Chapter 3:

Freda, P.J., Ali, Z.M., Heter, N., Ragland, G.J., and Morgan, T.J. (2018). *Stage-specific genotype-by-environment interactions for cold and heat hardiness in Drosophila melanogaster*. Heredity.

Dedication

This work is dedicated to my mother, Lisa, my father, Philip, my brother, Matthew, my partner, Leonie, and to those who have passed on before me for inspiring me throughout my life. For this, I thank you! Marie, John, Marie, and Frank - you are my muses.

Chapter 1 - Evolutionary Impacts of Developmental Variation

I. Developmental Variation and the Evolution of Complex Life Cycles

A required prerequisite for biological evolution is that genetic variation must exist between biological entities (Berg *et al.* 2002). Indeed, great diversity in morphology, behavior, and trophism exists, and has existed, within the biosphere due to evolutionary forces acting upon genetic variation in populations that arises from the mutability of the genetic code (Futuyma and Kirkpatrick 2017). Over time, as bouts of selection act upon variation within populations, new species adapted to distinct environmental habitats and ecological niches arise (Futuyma and Kirkpatrick 2017). However, selection can also act on genetic variation underlying the developmental regimes of individuals within a population or species, producing developmental variation strong enough that life-history phases become adapted to specific ecological niches (Moran 1994). In this way, evolutionary forces further produce diversity within the biosphere by producing intrinsic biological variation, or variation within the development regime of an organism (Bowler and Terblanche 2008).

A continuum exists for developmental variation in the natural world. Some organisms occupy the same or very similar ecological niches over development (i.e. many mammalian species and birds) while, in contrast, the vast majority exhibit life cycles in which life-history phases occupy distinct habitats and have unique fitness roles (Wald 1981; Werner 1988; Moran 1994). Systems such as these often exhibit complex life cycles (CLCs) where each life-history phase, or stage of development, differs morphologically, behaviorally, and physiologically (Moran 1994).

There are two hypothesized mechanisms for the evolution of CLCs. The first posits that alternate life stages evolve to exploit different resources during development. If each life stage

inhabits a distinct ecological niche, competition between life stages existing within the same geographic area will be limited, increasing the overall survivorship of each phase (Slade and Wassersug 1975; Heafner and Edson 1984; Moran 1994). An example of this would be lepidopteran larvae that feed on green plant matter of their host plants while adults feed primarily on nectar (Boggs 1987). The second hypothesized mechanism supposes that CLCs evolve to partition overall fitness across ontogeny. In other words, each life stage is "tasked" with a specific fitness "role(s)" across development (Bryant 1969; Moran 1994). For example, the larval stages of many terrestrial organisms are adapted primarily for feeding and growth while adult stages are associated with dispersal and/or mating. Together, these factors allow for the evolution of trait optima within certain developmental windows, deconstructing fitness into many different components across ontogeny, and enabling independent evolutionary trajectories for each life stage (Moran 1994; an extension of Lande and Arnold 1983; Slatkin 1987).

In summary, complex life cycles represent extreme but common examples of the developmental variation observed in the natural world in which development is separated into distinct life stages that are adapted to specific ecological niches and responsible for parts of overall organismal fitness. The adaptive decoupling hypothesis (Moran 1994) suggests that CLCs evolve so that each stage can respond independently to evolutionary forces while limiting effects on alternate life stages.

II. The Role of Genetic Constraint in the Evolution of Complex Life Cycles

A second postulate of the adaptive decoupling hypothesis is that the genetic correlations between traits of different life stages should be less than genetic correlations between traits of the same phase (Moran 1994). In other words, constraint, the resistance to evolutionary change (Schwenk 1995), should be weakened between stages of CLCs. According to this, the efficacy of

evolutionary forces to produce complex life cycles is therefore a function of the genetic correlation between traits across stages. Figure 1.1A conceptually illustrates the case of perfect genetic correlation ($r_g = 1$) across stages; individuals with a given phenotypic value in one stage also have the same phenotypic value in the other stage. However, Figure 1.1B illustrates the case where the genetic correlation (r_g) is 0 as there is no discernable phenotypic relationship between stage 1 and stage 2. In the second scenario, an accurate prediction of the phenotypic value in one stage cannot be made from the information available in the other. In scenario 1, a so called 'absolute' constraint exists for the trait between stages; selection on the trait in one life stage will change the phenotypic value of the trait in the other stage by the same amount (Lande and Arnold 1983). In this scenario, the same set of genetic loci (or linked loci in perfect linkage disequilibrium) control the phenotype in both stages, i.e., the genetic architecture is the same. On the other hand, in scenario 2, there is no genetic correlation, and therefore no constraint. In this scenario the genetic architecture of the phenotype is different across stages, and the potential exists for evolutionary forces to act independently on genetic variants underlying the trait in each life stage, selecting for stage-specific fitness optima (Lande and Arnold 1983; Slatkin 1987).

It is the goal of this work to determine if there is substantial support for stage-specific, independent evolutionary trajectories in a natural system using a variety of approaches including estimating the genetic correlation, and therefore, the level of constraint, for traits between distinct life stages of a complex life cycle. In other words, the overall aim of this work is to test the validity of the adaptive decoupling hypothesis.

III. Challenging Assumptions of Trait Association

In the literature, there are clear assumptions for the association of life-history traits over the course of ontogeny (Stearns 1992). Many of these associations occur classically between

growth rates and age in livestock (Hazel *et al.* 1943; Knapp and Clark 1947) but have also been observed in between other life-history traits in natural systems with complex life cycles including larval growth rate and adult body size in insects (reviewed in Chown and Gaston 2010), developmental time and body size in amphibians (Bruce 1990; Camp and Marshall 2000), juvenile body size and adult body size in amphibians (Camp *et al.* 2000), and larval host and adult body size in butterflies (Rodrigues and Moreira 2002). Ontogenetic correlation in other life-history traits, such as growth trajectories, have also been identified (Kirkpatrick *et al.* 1990; Kingsolver *et al.* 2001). Ample examples of traits that are highly genetically constrained across development exist in the literature. However, do these general patterns of life-history correlation apply to all traits and all systems?

Organisms that undergo complex life cycle transitions are subject to sometimes drastic changes in environmental pressures coupled with large-scale alterations to their body plan and morphology (Krebs and Loeschcke 1995; Ragland and Kingsolver 2008; Woods 2013). Due to these stark shifts in environment, the potential exists for trait decoupling across ontogeny. Of course, it is apparent that developmental stages separated by extreme life-history transitions, like metamorphosis, have sometimes extreme difference in function and morphology (i.e. feeding and locomotion). However, there is indeed evidence for comparative trait decoupling across the life-history transitions with shell length of a mollusk (*Mercenaria mercenaria*) (Rawson and Hilbish 1991), locomotor performance in amphibians (Shaffer *et al.* 1991; Johansson *et al.* 2010), and in social behaviors in *Drosophila melanogaster* (Anderson *et al.* 2016) as examples. There is also a body of evidence for the decoupling of various thermal phenotypes in insects which will be explored in a later section. These traits all represent various components of overall fitness, thereby directly affecting evolutionary trajectories of the species. It is, therefore, important to

challenge any established associations of life-history trait correlation as analyzing a trait of interest at only one time point during the life cycle only provides a limited view of that trait over the entirety of an organism's lifetime. In other words, phenotypic data from one age may be a poor indicator of that trait in other stages of ontogeny. Instead of controlling both the age and ontogenetic stage of the study organism, comparative studies that measure a trait of interest across the life cycle will provide a broader insight into the evolutionary history and trajectory of that trait (Bowler and Terblanche 2008).

IV. Thermal Hardiness as a Metric for Detecting Genetic Decoupling

In addition to the organism, the environment itself is not static. For organisms that have complex life cycles, the environments in which each life stage resides in can be drastically different on several ecological scales with thermal habitat being one of them. As days, weeks, and months progress, so does seasonality and climate. Organisms that start their life history in one season but finish development in another may be subject to distinct thermal extremes (Kingsolver *et al.* 2011). For example, the woolly bear caterpillar's (*Pyrrharctia Isabella*) final larval instar is subject to extreme sub-freezing conditions as it overwinters in the U.S. and southern Canada (Goettel and Philogene 1978; Layne *et al.* 1999) while the adult experiences much milder temperatures in the spring and summer. As a mechanism to combat the extreme cold, the freeze-tolerant larvae of *P. Isabella* accumulate glycerol as a cryoprotectant to inhibit freezing (Layne *et al.* 1999). In addition to seasonal changes, the microhabitats that one or more stages may reside in over development may be thermally unique. An example of this are members of the insect order Odonata, comprised of the dragonflies and damselflies, whose nymph stages are aquatic while adult stages are terrestrial and aerial (McCafferty and Provonsha 1983). In species like Odonates, in which part of their life cycles are completed in aquatic

environments, juvenile stages are likely to experience much cooler temperatures compared to the adult stage as the heat capacity of water is much higher than that of air. (Vannote and Sweeney 1980; Kingsolver *et al.* 2011). Using *Manduca* moths as a terrestrial example, larvae are more likely to experience both extremely higher temperatures and low humidity when compared to both eggs and pupae because of the larvae's larger size and the habitat in which they reside (Woods and Bonnecaze 2006; Kingsolver and Nagle 2007; Kingsolver *et al.* 2011). In addition, the development rate of *Manduca* larvae responds uniquely to changes in temperature when compared to eggs and larvae, whose developmental rate changes are similar to one another (Woods and Bonnecaze 2006; Kingsolver and Nagle 2007; Kingsolver *et al.* 2011). These examples illustrate that the thermal environments that different life stages experience may be drastically different in species with complex life cycles. Therefore, insect systems can be used to test for stage-specific thermal hardiness mechanisms.

Thermal hardiness is the ability for an organism to maintain fitness during acute exposure to thermal extremes, or in other words, the combined attributes that are employed by an organism to overcome the deleterious effects of extreme temperatures (Bale 1987). Therefore, the potential for an individual to grow, survive, and reproduce in a dynamic environment, is significantly linked to its ability to successfully mitigate damage caused by extreme temperatures. Because of this close association with overall fitness, and the potential for drastic changes between the thermal environments of different life stages, thermal hardiness is an excellent trait for investigating the potential for genetic decoupling between stages of a complex life cycle. However, experiments attempting to determine thermal hardiness correlations, or correlations in any fitness-related trait, across ontogeny are limited (except notable examples: Tucić 1979; Loeschcke and Krebs 1996; Gilchrist et al. 1997; Dierks et al. 2012). These pieces

of research, foundational as they are, measure correlated responses to selection and thus provide indirect estimates of genetic correlations. Moreover, they do not employ robust genetic approaches like Genome-Wide Association and do not utilize next generation sequencing platforms to explore the difference in gene expression on a genomic scale between stages. It is the goal of this body of work to determine if thermal hardiness phenotypes provide a means to detect trait decoupling in a natural system using robust, contemporary experimental approaches.

V. The System: *Drosophila melanogaster*

VA. Justification

There are three broad factors that make *Drosophila melanogaster* an excellent system for this body of work. The first factor is the basic biology and life cycle of the system. *D. melanogaster* is a holometabolous insect of the insect order, Diptera that has an almost worldwide distribution in temperate and tropical zones (Markow 2015). *D. melanogaster* has a complex life cycle with egg, larval, pupal, and adult stages (Ashburner *et al.* 2011). Adult females lay eggs in rotting fruits, vegetables, or other decaying materials. After hatching, larvae feed on the rotting fruit and microorganisms that inhabit it and develop through three larvae instars. After attaining proper mass, third instar wandering larvae cease feeding and move away from food to form a puparium (Ashburner *et al.* 2011). After a 4-5 day pupation, adult flies emerge with functional wings and become reproductively active within 8-12 hours (Pitnick 1996). Unlike larvae, adults primarily feed on microorganisms growing on rotting materials. The lifecycle of *D. melanogaster* is achieved in 8-10 days at 25°C (Ashburner *et al.* 2011). The habitats of *D. melanogaster* larvae and adults are distinct. In temperate regions, the fruit or other decaying matter that larvae are laid in are exposed to often extreme heat in the summer and early fall while adults are free to mitigate extreme high temperatures via flight and other behavior

mechanisms (Ashburner 1981; Dillon *et al.* 2009). On the other hand, adults overwinter in various forms of leaf litter and debris and are subject to more extreme cold (Saunders *et al.* 1989; Schmidt *et al.* 2005). This short, complex, yet predicable life cycle, coupled with the unique thermal environments each stage experiences, make *D. melanogaster* an excellent system for this study.

The rapid yet complex life cycle of *D. melanogaster* is not the only factor which makes the system well-suited for this type of study. There is a wealth of genetic tools and knowledge available for the system, including a recently sequenced and fully-annotated genome and trancriptome available on a stable, well-maintained online genetic database known as FlyBase (Gramates *et al.* 2017). The genome serves as a reference for any next generation sequenced approaches while FlyBase can be used to identify candidate loci and genetic pathways that may be associated with stage specific stress responses.

Finally, the work of previous researchers provides substantial insight into the possibility of unique genetic regions underlying thermal stress responses in *D. melanogaster* and the potential for life stage decoupling of thermal stress responses. In same way the adaptive decoupling hypothesis provides a testable hypothesis for this work, the research of Tucić (1979) provides the motivational groundwork to use *Drosophila melanogaster* as the system to detect decoupling of thermal traits in a complex life cycle. Tucić, using a complex design of classical chromosomal manipulations, was able to associate different chromosomal regions to cold hardiness in different *D. melanogaster* life stages. He found that for eggs and pupae, markers on chromosome 2 provided the highest contribution to cold hardiness while in larvae and adults, resistance to cold stress came primary from chromosome 3. Moreover, a broader result was that stages that are developmentally adjacent are more likely to share genetic regions associated with

cold hardiness. Of course, there are other notable studies including Jefferson *et al.* (1974), who discovered that different life stages of *D. pseudoobsura* exhibited distinct levels of cold tolerance, and more recently, Jensen *et al.* (2007) discovered that different developmental stages have distinct levels of both cold stress resistance and rapid-cold hardening (RCH) in *D. melanogaster*. Additionally, Bing *et al.* (2012) discovered stage-specific expression of the gene *Frost* in response to cold stress also in *D. melanogaster*. Taken together, works such as these provide significant levels of motivation for this study. It is a goal of this body of research to compliment the research of previous investigators by providing a large-scale, robust approach to detect de-coupling of thermal stress responses, including heat stress, using several contemporary tools including GWAS, and RNAseq utilizing a large isogenic population of *D. melanogaster* with full genome re-sequencing.

VB. The Drosophila Genetic Reference Panel (DGRP)

The Drosophila Genetic Reference Panel (Mackay *et al.* 2012; Huang *et al.* 2014), or the DGRP, is a collection of 205 isogenic lines of *Drosophila melanogaster*. Each of the lines' genomes have been re-sequenced and uploaded to an online database so comparisons can be made between lines and, in the case of this work, between life stages and lines. The DGRP was initiated from a natural population in Raleigh, North Carolina (dgrp2.gnets.ncsu.edu). The inbreeding design from multiple iso-female lines maintains naturally segregating variation as genetic variance among lines (genotypes). Subsets of the DGRP will be used for each of the three chapters of this dissertation.

VI. Dissertation Objectives and Outline

VIA. Tests for Genetic Decoupling of Cold Hardiness across Metamorphosis in the DGRP

Using 139 lines of the DGRP, this chapter's objective is to determine if significant genetic and phenotypic correlations exists between larval and adult cold hardiness. Both third instar larvae and 5-7 day post-eclosion adults from each line will be exposed to an acute 1 hour exposure at a lethal cold temperature. Survival will be determined for replicates of each life stage for each line. A lack of a statistical phenotypic and genetic correlation between life stages will provide evidence that cold hardiness is decoupled across life stages and that variation in cold hardiness response across ontogeny exists in natural populations. Furthermore, because of the re-sequenced genomes of the DGRP, it can be determined what SNPs are statistically associated with either larval or adult cold hardiness using a Genome-Wide Association (GWA) approach. If the majority of associated SNPs are stage-specific, this will provide further evidence that thermal hardiness maybe adaptively decoupled in this system. Furthermore, genes in which these SNPs reside can be considered as stage-specific candidates for further study. Furthermore, it will be possible to quantify the number of SNPs that are commonly statistically associated in both life stages. These loci may be under constraint by natural selection.

VIB. Tests for Decoupling of Acclimation Responses (GxE) to Cold Stress and Heat Stress across Metamorphosis in the DGRP

This chapter will attempt to extend the findings of the previous chapter by including heat stress as well as developmental acclimation to different rearing environments. Because natural systems are dynamic and seasonal, it is important to determine if decoupling exists under different thermal extremes (i.e. heat and cold) and to also determine if genotype x environment

interactions, in the form of developmental acclimation responses, can also be decoupled across the metamorphic boundary. In other words, does a three-way interaction exists between line (genotype), developmental temperature (environment), and developmental stage? Using a similar experimental protocol as chapter 1, replicates of larvae and adults, reared in two possible rearing conditions (cool and warm) will be exposed to a 1-hour acute cold stress and heat stress and the proportion of larvae and adults surviving each stress under each developmental condition will be scored. Phenotypic and genetic correlations will be estimated for each condition and stress type. Additionally, phenotypic plasticity for cold hardiness and heat hardiness will be calculated to determine if plasticity itself is also decoupled across metamorphosis.

Additionally, it is an objective of this chapter to determine if there is evidence for phenotypic and genetic correlations between cold hardiness and heat hardiness. Motivation for this question comes from the literature as it has been previously shown that the majority of loci significantly associated with survival after exposure to extreme heat or extreme cold are unique in *D. melanogaster* (Morgan and Mackay 2006; Norry *et al*. 2008). A similar result has also been illustrated in the ladybird beetle, *Cryptolaemus montrouzieri*, where the vast majority of genes significantly differentially expressed under cold or heat stress are distinct (Zhang *et al.* 2015). There is evidence for some common pathways and mechanisms underlying hardiness at both extremes, including inducible expression of heat shock proteins and other molecular chaperones (Burton *et al.* 1988) as extreme temperatures can lead to protein misfolding (Verghese *et al.* 2012). However, extreme heat and extreme cold affect cells and organisms in very different ways. For example, in chill-susceptible insects like *D. melanogaster*, cold stress causes a loss of ion and water homeostasis in the gut (Teets and Denlinger 2013; MacMillan *et al.* 2015a,b), leading to cell membrane depolarization and finally, cell death. In addition, ice formation in the

hemolymph and/or within the cytoplasm will cause mechanical damage to both intracellular structures and cell membranes (Teets and Denlinger 2013). On the other hand, heat stress has severe effects on pH with increases in temperature causing pH to drop (Denlinger and Yocum 1998; Neven 2000). This drop in pH alters the function of proteins, nucleic acids and membranes (Hochachka and Somero 1984). In addition, extreme high temperatures can disrupt many types of weak interactions including hydrogen bonds, van der Waals interactions, and even ionic bonds, severely incapacitating many biomolecules, especially proteins (Neven 2000). These factors provide a conceptual framework for how different mechanisms could be employed by *D. melanogaster* for each type of thermal stress. The distinct physiological consequences that are a result of either extreme heat or extreme cold are likely the cause of the lack of phenotypic and genetic correlation between stress types as different response mechanisms are likely at work.

VIC. Tests for Decoupling of Cold Stress Induced Gene Expression across Metamorphosis in the DGRP

RNA from a subset of genotypes from previous chapters that display the largest difference in cold hardiness across development from both extremes (i.e. high larval tolerance but low adult tolerance and low adult tolerance but high larval tolerance) were extracted from larvae and adults at four time points associated with cold stress: before exposure, half-way through exposure, at the end of exposure, and after exposure. There are two main questions this chapter will attempt to answer. The first is, do larvae and adults use distinct gene expression modules, and therefore; unique pathways and mechanisms, to combat cold stress? There may of course be common gene expression profiles between stages during and after stress, but the objective here is to determine what genes or gene pathways have a stage-specific response to cold stress. The second question is, do larval or adult genotypes with high cold hardiness have

unique, universal gene expression profiles that differ from larvae or adult genotypes that have low cold hardiness? In other words, what genetic mechanisms separate “good” and “bad” genotypes and are these mechanisms universally employed by genotypes of similar phenotypic response level?

References

Anderson BB, Scott A, Dukas R (2016). Social behavior and activity are decoupled in larval and adult fruit flies. *Behav Ecol* **27**: 820–828.

Ashburner M (1981). *The genetics and biology of* Drosophila. Academic Press: New York.

Ashburner M, Golic K, Hawley RS (2011). *Drosophila: A Laboratory Handbook*, 2nd edition. Cold Spring Harbor Laboratory Press: Cold Spring Harbor, NY.

Bale JS (1987). Insect cold hardiness: Freezing and supercooling - an ecophysiological perspective. *J Insect Physiol* **33**: 899–908.

Berg JM, Tymoczko JL, Stryer L, Berg JM, Tymoczko JL, Stryer L (2002). *Biochemistry*, 5th edn. W H Freeman: New York.

Bing X, Zhang J, Sinclair BJ (2012). A comparison of *Frost* expression among species and life stages of *Drosophila*. *Insect Mol Biol* **21**: 31–39.

Boggs CL (1987). Ecology of nectar and pollen feeding in Lepidoptera. In: Slansky FJ, Rodriguez JG (eds) *Nutritional ecology of insects, mites, spiders and related invertebrates*, Wiley: New York, pp 369–391.

Bowler K, Terblanche JS (2008). Insect thermal tolerance: what is the role of ontogeny, ageing and senescence? *Biol Rev Camb Philos Soc* **83**: 339–355.

Bruce RC, Hairston NG (1990). Life-history correlates of body-size differences between two populations of the salamander, *Desmognathus monticola*. *J Herpetol* **24**: 126.

Bryant EH (1969). A system favoring the evolution of holometabolous development. *Ann Entomol Soc Am* **62**: 1087–1091.

Burton V, Mitchell HK, Young P, Petersen NS (1988). Heat shock protection against cold stress of *Drosophila melanogaster*. *Mol Cell Biol* **8**: 3550–3552.

Camp CD, Austin RM, Marshall JL A model for the evolution of adult body size in black-bellied salamanders (*Desmognathus quadramaculatus* complex). *Can J Zool* **78**: 1712–1722.

Camp CD, Marshall JL (2000). The role of thermal environment in determining the life history of a terrestrial salamander. *Can J Zool* **79**: 1702–1711.

Chown SL, Gaston KJ (2010). Body size variation in insects: a macroecological perspective. *Biol Rev Camb Philos Soc* **85**: 139–169.

Denlinger DL, Yocum GD (1998). Physiology of heat sensitivity. In: Hallman G, Denlinger DL (eds) *Temperature sensitivity in insects and application in integrated pest management*, Westview Press: Boulder, CO, pp 7–53.

Dierks A, Kölzow N, Franke K, Fischer K (2012). Does selection on increased cold tolerance in the adult stage confer resistance throughout development? *J Evol Biol* **25**: 1650–1657.

Dillon ME, Wang G, Garrity PA, Huey RB (2009). Thermal preference in *Drosophila*. *J Therm Biol* **34**: 109–119.

Futuyma DJ, Kirkpatrick M (2017). *Evolution*, 4 edition. Sinauer Associates is an imprint of Oxford University Press: Sunderland, Massachusetts.

Gilchrist GW, Huey RB, Partridge L (1997). Thermal sensitivity of *Drosophila melanogaster*: evolutionary responses of adults and eggs to laboratory natural selection at different temperatures. *Physiol Zool* **70**: 403–414.

Goettel MS, Philogène BJR (1978). Laboratory rearing of the banded woollybear *Pyrrharctia (Isia) isabella* (Lepidoptera: Arctiidae), on different diets with notes on the biology of the species. *Can Entomol* **110**: 1077–1086.

Gramates LS, Marygold SJ, Santos G dos, Urbano J-M, Antonazzo G, Matthews BB, *et al.* (2017). FlyBase at 25: looking to the future. *Nucleic Acids Res* **45**: D663–D671.

Haefner JW, Edson JL (1984). Community invasion by complex life cycles. *J Theor Biol* **108**: 377–404.

Hazel LN, Baker ML, Reinmiller CF (1943). Genetic and environmental correlations between the growth rates of pigs at different ages. *J Anim Sci* **2**: 118–128.

Hochachka PW, Somero GN (1984). *Biochemical Adaptation*. Oxford University Press: New York.

Huang W, Massouras A, Inoue Y, Peiffer J, Ramia M, Tarone AM, *et al.* (2014). Natural variation in genome architecture among 205 *Drosophila melanogaster* Genetic Reference Panel lines. *Genome Res* **24**: 1193–1208.

Jefferson MC, Crumpacker DW, Williams JS (1974). Cold temperature resistance, chromosomal polymorphism and interpopulation heterosis in *Drosophila melanogaster*. *Genetics* **76**: 807–822.

Jensen D, Overgaard J, Sørensen JG (2007). The influence of developmental stage on cold shock resistance and ability to cold-harden in *Drosophila melanogaster*. *J Insect Physiol* **53**: 179–186.

Johansson F, Lederer B, Lind MI (2010). Trait performance correlations across life stages under environmental stress conditions in the common frog, *Rana temporaria* (S Helle, Ed.). *PLoS ONE* **5**: e11680.

Kingsolver JG, Arthur Woods H, Buckley LB, Potter KA, MacLean HJ, Higgins JK (2011). Complex life cycles and the responses of insects to climate change. *Integr Comp Biol* **51**: 719–732.

Kingsolver JG, Gomulkiewicz R, Carter PA (2001). Variation, selection and evolution of function-valued traits. In: Hendry AP, Kinnison MT (eds) *Microevolution Rate, Pattern, Process*, Springer Netherlands: Dordrecht Vol 8, pp 87–104.

Kingsolver JG, Nagle A (2007). Evolutionary Divergence in Thermal Sensitivity and Diapause of Field and Laboratory Populations of *Manduca sexta*. *Physiol Biochem Zool* **80**: 473–479.

Kirkpatrick M, Lofsvold D, Bulmer M (1990). Analysis of the Inheritance, Selection and Evolution of Growth Trajectories. *Genetics* **124**: 979–993.

Knapp B, Clark RT (1947). Genetic and environmental correlations between growth rates of beef cattle at different ages. *J Animal Sci* **6**: 174–81.

Krebs RA, Loeschcke V (1995). Resistance to thermal stress in preadult *Drosophila buzzatii*: variation among populations and changes in relative resistance across life stages. *Biol J Linn Soc* **56**: 517–531.

Lande R, Arnold SJ (1983). The measurement of selection on correlated characters. *Evolution* **37**: 1210–1226.

Layne JR, Edgar CL, Medwith RE (1999). Cold hardiness of the woolly bear caterpillar (*Pyrrharctia isabella* Lepidoptera: Arctiidae). *Am midl nat* **141**: 293–304.

Loeschcke V, Krebs RA (1996). Selection for heat-shock resistance in larval and in adult *Drosophila buzzatii*: comparing direct and indirect responses. *Evolution* **50**: 2354–2359.

Mackay TFC, Richards S, Stone EA, Barbadilla A, Ayroles JF, Zhu D, *et al.* (2012). The *Drosophila melanogaster* Genetic Reference Panel. *Nature* **482**: 173–178.

MacMillan HA, Andersen JL, Davies SA, Overgaard J (2015). The capacity to maintain ion and water homeostasis underlies interspecific variation in *Drosophila* cold tolerance. *Scientific Reports* **5**: 18607.

MacMillan HA, Andersen JL, Loeschcke V, Overgaard J (2015). Sodium distribution predicts the chill tolerance of *Drosophila melanogaster* raised in different thermal conditions. *Am J Physiol Regul Integr Comp Physiol* **308**: R823–R831.

Markow TA (2015). The secret lives of *Drosophila* flies. *eLife* **4**.

McCafferty WP, Provonsha A (1983). *Aquatic entomology: The fisherman's and ecologist's illustrated guide to Insects and their relatives*, 1st edition. Jones & Bartlett Learning: Boston.

Moran N (1994). Adaptation and constraint in the complex life cycles of animals. *Annu Rev Ecol Evol Syst* **2**: 573–600.

Morgan TJ, Mackay TFC (2006). Quantitative trait loci for thermotolerance phenotypes in *Drosophila melanogaster*. *Heredity* **96**: 232.

Neven LG (2000). Physiological responses of insects to heat. *Postharvest Biol Technol* **21**: 103–111.

Norry FM, Scannapieco AC, Sambucetti P, Bertoli CI, Loeschcke V (2008). QTL for the thermotolerance effect of heat hardening, knockdown resistance to heat and chill-coma recovery in an intercontinental set of recombinant inbred lines of *Drosophila melanogaster*. *Mol Ecol* **17**: 4570–4581.

Nylin S, Gotthard K (1998). Plasticity in Life-History Traits. *Annual Review of Entomology* **43**: 63–83.

Pitnick S (1996). Investment in testes and the cost of making long sperm in *Drosophila*. *Am Nat* **148**: 57–80.

Ragland GJ, Kingsolver JG (2008). Evolution of thermotolerance in seasonal environments: the effects of annual temperature variation and life-history timing in *Wyeomyia smithii*. *Evolution* **62**: 1345–1357.

Rawson PD, Hilbish TJ (1991). Genotype-environment interaction for juvenile growth in the hard clam *Mercenaria mercenaria* (L.). *Evolution* **45**: 1924–1935.

Rodrigues D, Moreira GRP (2002). Geographical variation in larval host-plant use by *Heliconius erato* (Lepidoptera: Nymphalidae) and consequences for adult life history. *Braz J Biol* **62**: 321–332.

Saunders DS, Henrich VC, Gilbert LI (1989). Induction of diapause in *Drosophila melanogaster*: photoperiodic regulation and the impact of arrhythmic clock mutations on time measurement. *Proc Natl Acad Sci USA* **86**: 3748–3752.

Schmidt PS, Matzkin L, Ippolito M, Eanes WF (2005). Geographic variation in diapause incidence, life-history traits, and climatic adaptation in *Drosophila melanogaster*. *Evolution* **59**: 1721–1732.

Schwenk K (1995). A utilitarian approach to evolutionary constraint. *Zoology* **98**: 251–262.

Shaffer HB, Austin CC, Huey RB (1991). The consequences of metamorphosis on salamander (Ambystoma) locomotor performance. *Physiol Zool* **64**: 212–231.

Slade NA, Wassersug RJ (1975). On the evolution of complex life cycles. *Evolution* **29**: 568–571.

Slatkin M (1987). Quantitative Genetics of Heterochrony. *Evolution* **41**: 799–811.

Stearns SC (1992). *The Evolution of Life Histories*. Oxford University Press: New York.

Strathmann RR (1993). Hypotheses on the origins of marine larvae. *Annu Rev Ecol Evol Syst* **24**: 89–117.

Teets NM, Denlinger DL (2013). Physiological mechanisms of seasonal and rapid cold-hardening in insects: Seasonal and rapid cold-hardening in insects. *Physiol Entomol* **38**: 105–116.

Tucić N (1979). Genetic capaticy for adaptation to cold resistance at different developmental stages of *Drosophila melanogaster*. *Evolution* **33**: 350–358.

Vannote RL, Sweeney BW (1980). Geographic Analysis of Thermal Equilibria: A Conceptual Model for Evaluating the Effect of Natural and Modified Thermal Regimes on Aquatic Insect Communities. *Am Nat* **115**: 667–695.

Verghese J, Abrams J, Wang Y, Morano KA (2012). Biology of the heat shock response and protein chaperones: Budding Yeast (*Saccharomyces cerevisiae*) as a model system. *Microbiol Mol Biol Rev* **76**: 115–158.

Wald G (1981). Metamorphosis: An Overview. In: Gilbert LI, Frieden E (eds) *Metamorphosis*, Springer: Boston, MA, p .

Werner EE (1988). Size, scaling, and the evolution of complex life cycles. In: Ebenman B, Persson L (eds) *Structured Populations*, Springer: Berlin, Heidelberg, p .

Woods HA (2013). Ontogenetic changes in the body temperature of an insect herbivore. *Funct Ecol* **27**: 1322–1331.

Woods HA, Bonnecaze RT (2006). Insect eggs at a transition between diffusion and reaction limitation: Temperature, oxygen, and water. *J Theor Biol* **243**: 483–492.

Zhang Y, Wu H, Xie J, Jiang R, Deng C, Pang H (2015). Transcriptome responses to heat- and cold-stress in ladybirds (*Cryptolaemus montrouzieri* Mulasnt) analyzed by deep-sequencing. *Biol Res* **48**.

Chapter 1 Figures

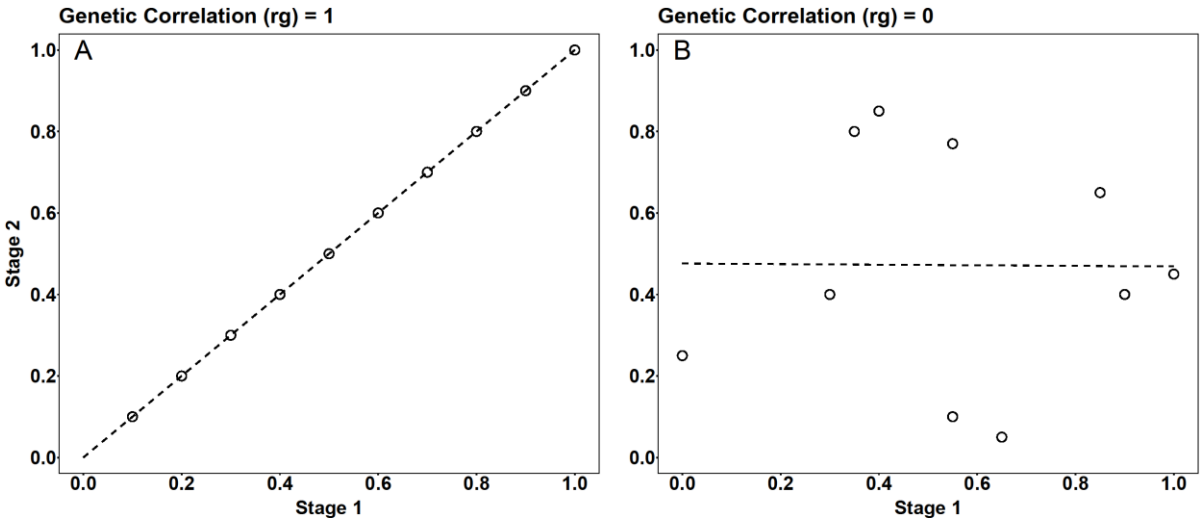

Figure 1.1 Genetic Correlations between Stages

Conceptual representation of complete coupling of a trait between stages (A) where the genetic correlation equals 1 and complete de-coupling of a trait between stages (B), where the genetic correlation is equal to 0. Axes units are hypothetical phenotypic scores with 0 being low and 1 being high.

Chapter 2 - Genetic Decoupling of Thermal Hardiness across Metamorphosis in *Drosophila melanogaster*

Abstract

As organisms age the environment fluctuates, exerting differential selection across ontogeny. In particular, highly seasonal environments expose life stages to often drastically different thermal environments. This developmental variation is particularly striking in organisms with complex life cycles, wherein life history stages also exhibit distinct morphologies, physiologies, and behaviors. Genes acting pleiotropically on thermal responses across development might constrain independent evolution within each life stage through genetic correlations. To investigate whether developmental genetic correlations constrain the evolution thermal hardiness of the fly *Drosophila melanogaster*, we applied quantitative genetic analyses to cold hardiness measured in both larvae and adults from isogenic lines of the *Drosophila* Genetic Reference Panel (DGRP), using survival at stressful low temperatures as the phenotypic metric. Using full genome resequencing data for the DGRP, we also implemented genome-wide association (GWA) analysis using Bayesian Sparse Linear Mixed Models (BSLMM) to estimate associations between naturally segregating variation and cold hardiness for both larvae and adults. Quantitative genetic analyses revealed no significant genetic correlation for cold hardiness between life stages, suggesting complete genetic decoupling of thermal hardiness across the metamorphic boundary. Both quantitative genetic and GWA analyses suggested that polygenic variation underlies cold hardiness in both stages, and that associated loci largely affected one stage or the other, but not both. However, reciprocal enrichment tests and correlations between BSLMM parameters for each life stage support some shared physiological mechanisms that may reflect common cellular thermal response pathways. Overall, these results

suggest no developmental genetic constraints on cold hardiness across metamorphosis in *D. melanogaster*, an important consideration in evolutionary models of responses to changing climates. Genetic correlations for environmental sensitivity across ontogeny remains largely unexplored in other organisms, thus assessing the generality of genetic decoupling will require further quantitative or population genetic analysis in additional species.

Introduction

As organisms progress through development, life history stages experience different environmental conditions that exert differential natural selection across the life cycle (Krebs and Loeschcke 1995; Ragland and Kingsolver 2008; Woods 2013). Moreover, different life stages typically exhibit different relationships between environmental factors and performance or fitness (Coyne 1983). This is particularly important for organisms with complex life cycles, wherein different life history stages often inhabit completely different ecological niches (Kingsolver et al. 2011). Ecophysiological models for, e.g., range limits or responses to changing climates are increasingly incorporating such stage-specific performance, increasing accuracy over models assuming a single, 'one size fits all' environment vs. performance relationship (Levy et al. 2015; Sinclair et al. 2016). Thus, considering the environmental sensitivity of the entire life cycle in the appropriate seasonal context is critical for accurate models and predictions. Yet, empirical studies typically focus on the environmental sensitivity of adult, reproductive stages, whereas juvenile life history stages have received comparatively little attention (Bowler and Terblanche 2008).

In particular, we have comparatively few data on the genetic architecture of juvenile relative to adult environmental sensitivity. The genetics of thermal sensitivity and thermal 'hardiness' (ability to maintain fitness despite acute exposure to temperature extremes) has been

especially well described in insects, but studies have focused largely on the adult stage. Numerous surveys of geographically variable populations have identified loci varying among populations or species experiencing different environmental temperatures (Bettencourt et al. 2002; Dunning et al. 2014; Garbuz et al. 2003; Lancaster et al. 2016; Sgrò et al. 2008), and some of these loci have been directly linked to thermal hardiness (Rako et al. 2007). In addition, QTL and association mapping have identified candidate loci that may segregate in natural populations (Morgan and Mackay 2006; Norry et al. 2004; Rohde et al. 2016). Studies that have explored thermal hardiness in both adult and juvenile stages suggest that loci affecting adult thermal hardiness may have no effect on juvenile thermal hardiness, i.e., there is no developmental pleiotropy. For example, laboratory selection on thermal performance in one life history stage (e.g., adults) leads to no correlated response to selection in other life stages (Tucić 1979; Loeschcke and Krebs 1996; Gilchrist et al. 1997; Dierks et al. 2012) Similarly, comparisons of hardiness among populations and species do not support cross-stage genetic correlations (Hercus et al. 2000).

The above studies all suggest that thermal hardiness may evolve independently across life stages, though they do not reveal whether this lack of correlation in underlain by different mechanisms of hardiness in different stages. To bridge this knowledge gap, we applied a combined quantitative genetic and population genomic study to estimate 1) the genetic correlation between larval and adult cold hardiness in a temperate, natural population of *Drosophila melanogaster*, and 2) genome-wide associations between naturally segregating variation and thermal hardiness for both larvae and adults. This study is the first genomic analysis of juvenile insect thermal hardiness and provides a genomic and gene-specific perspective on the remarkable genetic independence of thermal traits across a complex life cycle.

We performed all analyses using the Drosophila Genetic Reference Panel (DGRP), a collection of fully re-sequenced isogenic lines of *D. melanogaster* derived from a natural population in Raleigh, North Carolina (Huang et al. 2014; Mackay et al. 2012). Substantial genetic variation exists among the DGRP lines which captures a substantial portion of naturally occurring variation. In nature, larvae and adults experience different thermal environments because of their different habitats (feeding inside rotting fruits vs. foraging and mate finding through flight). Moreover, *D. melanogaster* overwinters primarily in the adult stage (Saunders et al. 1989), so adults of the overwintering generation in temperate environments experience more chronic and acute exposure to low temperatures compared to larvae. We focused on 139 DGRP lines, measuring larval and adult cold hardiness in each line and estimating broad sense heritabilities, a genetic correlation, and genotype-to-phenotype associations for each trait. Our results suggest 1) a complete quantitative genetic decoupling of thermal hardiness across metamorphosis, 2) that as observed in adults, larval thermal hardiness is polygenic, influenced by many loci of moderate or small effect, and 3) that individual genes with clear effects on thermal hardiness in one stage may have no detectable, pleiotropic effect on another stage. Despite apparent evolutionary independence, we found evidence for shared physiological mechanisms of cold hardiness across ontogeny. We discuss these results with respect to common cellular responses to temperature, and unique aspects of cold survival in juvenile vs. adult stages.

Methods

DGRP lines

The DGRP are 205 isogenic lines derived from a natural population in Raleigh, North Carolina (dgrp2.gnets.ncsu.edu) (Huang et al. 2014; Mackay et al. 2012). This design maintains naturally segregating variation as genetic variance among isogenic lines. The among-line genetic

variance does not capture dominance variance because each line is homozygous (Falconer and Mackay 1996). Some of these lines achieve low survival and reproductive output in the lab, thus we selected 139 vigorous lines maintained under standard rearing conditions at Kansas State University for several years that exhibit no obvious fitness problems under standard rearing conditions.

Line Rearing and maintenance

All experimental animals were reared on cornmeal, molasses, and yeast media with propionic acid and benzoic acid added as anti-fungal and anti-bacterial agents. To encourage egg laying, vials were sprinkled with dry active yeast. All rearing was performed under a 12h/12h light-dark cycle at 25°C. Experimental flies from 139 isogenic DGRP lines were reared in vials started from 5 males and 5 females. The parents were sorted under light CO2 anesthesia and then placed on fresh media for oviposition. Every 24 hours, the parents were transferred to fresh media over 6 days. The first set of replicate vials (day 1) were discarded to limit the effects of anesthesia on egg-laying. Progeny (experimental individuals) were collected from the vials on days 2-6, creating replicates 1-5. Parents were discarded 24h after their final transfer on day 6. A maximum of 5 serial replicates for each line and each life stage were created using this design. Experimental individuals were collected for larval and adult assays at predetermined developmental time points (see below).

Survival Assays

Larval assays were performed at 120h (5d) post-oviposition, using third instar feeding larvae that were extracted from replicate vials using a 20% w/v sucrose solution following the protocol of Nöthiger (1970). The solution was poured into the vial and the media was disturbed to allow larvae to float to the top of the liquid. Larvae were then extracted from the solution with

a soft brush, briefly washed in ddH_2O, and then transferred to a paper towel to dry for approximately one minute. After drying, 20 larvae were transferred, using a soft brush, to a vial with fresh media. To determine if this extraction method had any effect on larval survival, we tested cold shock survival for a subset of 10 lines (minimum of four replicates per line) extracted mechanically (using just a soft brush) versus extraction using the sucrose solution (Figure A.1). We found that survival of flies extracted using the sucrose solution was slightly higher (6.7%; $p = 0.017$) than that of larvae extracted mechanically. This result may be due to mechanical injury of forcibly removing the larvae from the food. Additionally, there was no significant interaction between line and extraction method ($p = 0.10$), suggesting that the differences among lines are unlikely to be caused by different responses to the sucrose solution. After successful extraction, we poked holes into the media to facilitate larval burrowing and feeding. Experimental vials were then immersed in a recirculating bath (ECO RE 2025, Lauda Corporation) containing a 50/50 mixture of distilled water and propylene glycol held at the test temperature for a 1h exposure time. Thermocouples placed in empty food vials confirmed that the food did not freeze during any of the experimental exposures. Empty vials with adults reached the test temperature only slightly faster than vials containing food and larvae (~ 3 minutes faster averaged across temperatures) representing a difference of only five percent of the 1h exposure. After exposure, vials were removed from the bath and returned to standard rearing conditions. After 9d (216h), larval survivorship was assessed as the proportion of successfully eclosed individuals (Bing et al. 2012); proportion of successful pupation yielded qualitatively similar results.

For the adult assays, adults (12 days post-oviposition) were extracted from replicate vials under light CO2 anesthesia. A total of 10 male and 10 female adults per replicate and per line were then sorted, sexed, and transferred to fresh media. Males and females were kept in separate

vials and placed under standard rearing conditions for 5 more days to recover from any effects of anesthesia. During recovery, adults were transferred to new food after 3d to avoid mortality associated with old, rotting food. After the 5d had elapsed, 5-7 day post-eclosion (408h post-oviposition) adults were transferred to empty vials with sexes kept separate and exposed to the test temperatures as described above. After exposure, the adults were transferred to fresh media (sexes separated) and placed under standard rearing conditions for 24h to recover. The proportion that had survived was assessed by counting the number of adults capable of coordinated movement and flight (Colinet and Hoffmann 2012; Kelty and Lee 2001; Overgaard et al. 2005).

Experimental Design

Organisms generally exhibit a roughly logistic relationship between survival and temperature at extreme (stressful) temperatures (Lee, 2012). We wished to initially describe this curve over a set of temperatures for a subset of lines in order to determine whether survival at a single temperature near the LD50 (temperature producing 50% survival) could accurately predict the shape of the full curve. For larvae, a subset of 28 lines were randomly selected and for adults, a subset of 36 lines were randomly selected. Larval survival curves were generated from survival data after 1h exposures at -8° C, -7° C, -6° C, -5° C, -4° C, -3° C, and -2° C (Figure A.2a). Adult survival curves were generated after exposures at -7° C, -6° C, -5° C, -4° C, -3° C, -2° C, and -1° C. (Figure A.2b). These temperature ranges were previously determined to span the range from 0% to 100% survival in most tested lines. For each life stage, survival at each of the 7 test temperatures was regressed against cumulative survival summed across all test temperatures. Based on these results, we selected -5° C as the appropriate, single test temperature exhibiting

the strongest, highly significant correlation with cumulative survival across temperatures (Adults: R^2 = 0.91; Larvae, R^2= 0.95; Figure A.3).

Subsequently, we tested survival at -5° C for all 139 lines using the assays described above. The factorial experimental design was as follows: 139 lines X 2 life stages X 5 replicate vials per life stage. Each vial contained 20 larvae and 20 adults (10 males, 10 females), respectively.

Quantitative Genetics

Broad sense heritability (H^2) of cold hardiness in larvae and adults was estimated as the proportion of variance among lines divided by the total variance (sum of the variance among and within lines) (Lynch and Walsh 1998). Variance components were estimated using generalized linear mixed models (GLMMs) with a logit link function implemented in lme4 (glmer function; Bates et al. 2015) in R (R Core Team 2017). Line and replicate were modeled as random effects. Sex was only determined for adults. Thus, in the adult model we included a fixed effect of sex (estimates within sexes were qualitatively similar). We estimated 95% confidence intervals on the heritability estimates by implementing 500 bootstrap replicates (resampling with replacement from the 139 DGRP lines) of the GLMMs and calculating H^2 for each replicate. We estimated the genetic correlation between larval and adult hardiness as:

$$r_g = \frac{COV_{AL}}{\sqrt{\sigma_A^2 \times \sigma_L^2}}$$

where COV_{AL} is the covariance between adult and larval cold hardiness and σ_A^2 and σ_L^2 are the variance components among lines for adults and larvae, respectively. These values were estimated using generalized linear mixed models with logit link functions implemented in glmer, as above. The σ_A^2 and σ_L^2 values were estimated as the among line variance from the separate

adult and larval models used for the heritability calculations above. We estimated COV_{AL} as the among-line variance from a generalized linear mixed model of the combined larval and adult data including a fixed effect of developmental stage and random effects of line, line-by-stage interaction, and replicate nested within line (Harbison et al. 2013) . As above, we estimated confidence intervals using 500 bootstrap replicates.

GWAS

We performed a Genome-Wide Association (GWA) analysis to estimate the effects of alleles at individual loci and across the genome on both larval and adult cold hardiness. The analysis included SNP and INDEL genotypes at 6,149,882 chromosomal positions across the genome identified by Mackay et al. (2012) and Huang et al. (2014) using full genome resequencing. We applied a Bayesian Sparse Linear Mixed Model (BSLMM) separately to raw larval data (survival) and to the residuals of a generalized linear model with logit link function fitting adult survival data and including a fixed effect of sex (to remove the effects of sex prior to GWA; implemented in glmer (lme4 in R). The BSLMM model accounts for linkage among markers and relatedness among individuals (Zhou et al. 2013). We implemented the BSLMM in gemma (Zhou et al. 2013), which uses a Bayesian, Markov Chain Monte Carlo (MCMC) approach to fit the following model:

$$y = \mu + \boldsymbol{X}\beta + u + \epsilon$$

where β is a vector of genetic marker effects, $\boldsymbol{X}$ is a matrix of genotypes, u is a vector of random effects, and ϵ is a vector of errors. The parameter u can be decomposed into $\boldsymbol{X}\alpha$, where α is a vector modeling the infinitesimal genetic effects of each locus, whereas β models the additional effects of moderate or large-effect loci. The BSLMM model includes an additional hyperparameter gamma which estimates the inclusion probability of each locus, i.e. the

probability that each locus has a non-zero effect on the phenotype while accounting for all effects at all other loci. Manhattan plots of inclusion probabilities for SNPs higher than 0.00275 in adults and higher than 0.00375 in larvae (top 0.01% of SNPs) were produced in R using the package, qqman (Turner 2014). Finally, gemma also estimates the posterior distribution for the total Percent Variance Explained (PVE) by genotype (across all loci), and the number of loci with measurable effects on the genotype. For sets of loci identified as 'candidates' based on β values and inclusion probabilities, we applied enrichment analysis using DAVID (Huang et al. 2009a,b) to test for overrepresentation of functional categories among loci that mapped to gene models predicted in the *D. melanogaster* genome release version 5.36.

We also characterized the correlated effects of loci, focusing on genome-wide effects. We estimated the spearman (non-parametric) correlation between individual locus effect size estimates for larval and adult cold hardiness produced by the BSLMM above, including only loci with non-zero inclusion probabilities. We performed these correlations between the larval and adult β values (measureable effects) and α values (infinitesimal effects). We also performed this same correlation for α values of all loci regardless of inclusion probability. Inclusion probabilities modify the way that the β coefficients are modeled, but α coefficients contribute to PVE regardless of inclusion probability. Though linkage disequilibrium (LD) decays over short genomic distances in *D. melanogaster* (Long et al. 1998), LD among loci will still violate the assumption of independence for the spearman rank test. To mitigate non-independence, we estimated the 95% confidence interval of the spearman correlation from 1000 bootstrap replicates randomly resampling loci across the genome. And, we performed two-tailed permutation tests to assess statistical significance, estimating the correlation for 1000 data sets where larval values were randomly shuffled relative to adult values.

Results

Mean survival after a one-hour exposure to -5° C was significantly higher in adults compared to larvae (proportion surviving ± standard error; Adults = 0.73 ± 0.052; Larvae = 0.60 ± 0.064; $p < 0.001$, Figure A.4). Likewise, broad sense heritability was higher in adults (model including sex as a fixed effect) compared to larvae (adult H^2= 0.44, 0.38 - 0.50 95% CI; larvae H^2= 0.22, 0.16 - 0.27), though both were significantly greater than zero (1000 permutations produced no values as extreme as the point estimates). Treating sexes separately, estimates of adult broad sense H^2 for males and females were 0.48 (0.41 - 0.54 95% CI) and 0.57 (0.50 - 0.63 95% CI), respectively. There was no significant genetic correlation between survival at -5° C in larvae and adults (Figure 2.1; n = 139, r_g = 0.085, 95% CI = -0.053 - 0.18, p = 0.12).

From the posterior inclusion probabilities estimated in the BSLMM models, we inferred that 1 - 146 (95% CI, median=57) and 0 - 234 (95%CI, median=90) loci had measurable effects on larval and adult cold hardiness, respectively. However, most inclusion probabilities for individual SNPs were low (only 1 and 13 loci with gamma > 0.025 in larvae and adults, respectively), whereas point estimates of Percent Variance Explained (PVE) were relatively high (median = 41, 3 - 91, 95% CI, larvae; median = 53, 3 - 99 95% CI, adults). The top 100 loci associated with each trait are listed in Tables A.1 and A.2 along with the per-locus estimates of β (genetic effect) and γ (inclusion probability), ranked according to effect size weighted by inclusion probability ($\beta \times \gamma$). As with any statistical cutoff, the choice of 100 loci is somewhat arbitrary, but falls within the range of the number of loci with measurable effects as inferred from the BSLMM. Most loci had the highest inclusion probabilities in either larvae or adults, but not both (Figure 2.2). Only 1,803 loci had non-zero inclusion probabilities for both larval and adult models, no more than would be expected by chance alone (p = 0.38, Fisher's exact test).

However, the ‘top 100’ lists for adults and larvae shared three gene ids in common, significantly more than would be expected by chance alone (p = 0.014, Fisher’s exact test). To further explore this overlap, we tested whether gene models harboring SNPs with high inclusion probabilities in adults also tended to harbor SNPs with high inclusion probabilities in larvae. Reciprocal enrichment tests supported this hypothesis; inclusion probabilities in larvae for the top 100 gene models with the highest inclusion probabilities in adults were substantially greater than expected by chance alone (none of 10,000 random permutations generated a median inclusion probability as high as the observed value; the reciprocal test yielded the same result; Script A.1). The ‘top 100’ list for adults was enriched for several functional categories including Uniprot keyword ‘alternate splicing’ and the INTERPRO domain ‘Low-density lipoprotein (LDL) receptor’ (Table A.3), while there was no significant enrichment of any category in the ‘top 100’ list for larvae.

Correlation analysis of the estimated larval and adult BSLMM parameters revealed limited evidence for genetic correlation between larval and adult cold hardiness. In particular, there was a non-significant correlation between the β values, or large genetic effects for the larval and adult models (median r = -0.004, -0.005 - 0.002, 95% CI, p = 0.15). However, there was a slight but highly significant positive correlation between the α values, or infinitesimal effects for the larval and adult models. This was true for only the subset of loci with non-zero inclusion probabilities in either model (median r = 0.090, 0.082 -0.094 95% CI) and for all loci (median r = 0.059, 0.058 - 0.061 95%CI). In both cases no value as extreme as the point estimate (median) were produced in 1,000 permutations.

Discussion

Genetic constraint and evolution across ontogeny

Both larval and adult cold hardiness were highly heritable under laboratory conditions, suggesting that the Raleigh, NC population of origin for the DGRP harbors substantial segregating genetic variation for cold hardiness visible to natural selection. Heritability estimates in this study very likely overestimate heritability in the field because 1) they are broad-sense estimates that include non-additive effects, and 2) environmental variance is greater in the field (Fisher 1930; Merilä and Sheldon 2000; McCleery et al. 2004). However, inter-population variation in thermal hardiness has been demonstrated many times in *D. melanogaster* and is likely underlain by heritable, genetic variation within populations (Hoffman et al. 2002; Hoffman et al. 2003; Krebs and Feder 1997). The results of the BSLMM models of genetic association further suggest that both larval and adult cold hardiness behave largely as polygenic traits, with generally low inclusion probabilities and moderate effect sizes for associated genetic variants.

Despite apparently ample genetic variation for larval and adult cold hardiness, we found no evidence for a genetic correlation between the two traits. The estimate for r_g was low, and not significantly different from zero. These results align with the results of previous studies that have inferred a lack of correlation through measurements of correlated response to selection (Dierks et al. 2012; Gilchrist et al. 1997; Loeschcke and Krebs 1996; Tucić 1979), and implies that different sets of segregating variants must influence thermal hardiness at different life stages. Here we have directly tested this hypothesis, and indeed, there was little overlap between the sets of variants most strongly associated with each trait, and no correlation in effect sizes for loci with non-zero inclusion probabilities in the BSLMMs. Tucić et al. (1979) found similar results on the whole-chromosome level in the sense that chromosomal variants accounted for different

amounts of cold hardiness variation in different stages. But, the most proximal life stages (e.g., consecutive larval instars) did tend to share similar patterns of chromosome-hardiness associations, suggesting that at a small enough developmental increment, genetic correlations may exist.

The above results suggest that cold hardiness is relatively free to evolve independently across ontogeny, an important consideration for evolutionary models of seasonality and response to changing climates (Kingsolver et al. 2011). In contrast, other studies have identified ontogenetic correlations that more severely constrain the evolution of, e.g., growth trajectories (Kingsolver et al. 2001; Kirkpatrick et al. 1990) and sexual dimorphism (Badyaev 2002; Chippindale et al. 2001). Induced physiological responses or composite metrics of performance (e.g., growth rate) may generally be less developmentally constrained compared to traits related to morphology and body size or condition (Kingsolver et al. 2015). Different life stages often occur in distinct seasons, and without genetic constraint natural selection should simultaneously optimize (i.e., select for highest fitness) thermal performance/fitness in each life stage (Ragland and Kingsolver 2008). There are no studies that clearly illustrate differential selection and evolutionary responses of different life stages in nature. But, there is at least one appropriate data set that measures evolutionary differences in both larval and adult fly cold hardiness across 16 Drosophilid species spanning millions of years of evolution and a variety of temperate-and tropical-origin species (Mitchell et al. 2013). Mitchell et al. (2013) focused on the effect of acclimation, which appears to be phylogenetically unconstrained. We applied an additional phylogenetically independent contrast to their published cold hardiness values (see Script A.2) and found a relatively high correlation between larval and adult cold hardiness after correcting for phylogeny ($r = 0.70$, $p = 0.004$). Given the evidence for lack of correlation within populations

of *D. melanogaster*, this result is consistent with two hypotheses: 1) evolved differences among species do not reflect standing genetic variation segregating in natural populations, and 2) correlational natural selection favors either increased or decreased hardiness across ontogeny (i.e., in all life stages). The first would be difficult to test, though there is evidence that standing variation contributes to physiological differences among species (Barrett and Schluter 2008). The second hypothesis is plausible because most, if not all of the species included in Mitchell et al. (2013) are likely multivoltine with overlapping generations, which will tend to decrease heterogeneity of the thermal environment across life history stages. Further phylogenetic analysis and comparisons of closely related sister species may further elucidate the relative roles of correlational selection and standing genetic variation in shaping thermal hardiness across ontogeny.

Stage-specificity and common genetic effects

Although estimates of genetic correlations and the bulk of genetic variants with measurable effects identified via GWA support the capacity for independent evolution in larvae and adults, there was also a background signal of shared causal genetic variants. In particular, there was a small but significant correlation between the α values, or infinitesimal effects of the BSLMM in larvae and adults. In addition, there was small, but statistically significant overlap between sets of genes harboring the top 100 SNP variants most strongly associated with larval and adult cold hardiness. Finally, gene models harboring SNPs with the highest inclusion probabilities (higher values represent greater statistical confidence in a SNP effect) in adults also exhibited significantly higher inclusion probabilities in larvae than would be expected by chance alone (and vice versa). We performed an additional enrichment test to identify functional

categories (GO and KEGG) that might be associated with cold hardiness across stages, but no individual categories were notably enriched or statistically significant (Script A.3).

Evidence for common allelic effects across development is not unexpected, given that cold injury is often mediated at the cellular level (Teets and Denlinger 2013), which should have some common effects in larvae and adults. For example, modifications to cell membrane ratios of fatty acid types (Bennett and Lee 1997; Michaud and Denlinger 2007; Tomcala et al. 2006) and phospholipids (Koštál, 2010; Overgaard et al., 2005) are associated with maintenance of membrane fluidity in cold tolerant insects. Increased expression of heat shock proteins, aquaporins, and antioxidant enzymes also associate with various metrics of cold hardiness in insects (Colinet et al. 2010; Philip and Lee, 2010; Yocum, 2001). And recently, the maintenance of ion homeostasis during cold exposure has been linked to cold hardiness (MacMillan et al., 2015a,b).

The observation that most genetic variants had measureable effects on only one life stage may be largely because of the very different tissue composition and developmental status of adults versus larvae, a hypothesis suggested by (Bowler and Terblanche 2008). The ability of adults to survive cold shocks in our assays should be mainly due to resistance to cold injury, whereas larval survival to pupation is influenced by resistance to cold injury and subsequent, successful development to pupation. Indeed, many of the genes harboring variants most strongly associated with larval cold hardiness have known functions in developmental processes (functional annotations for the top 100 list in Table A.1). Yet, variants affecting cellular cold injury resistance through the mechanisms described above ought to affect both larval and adult cold hardiness. So, why are so few of these variants present in the DGRP, which captures segregating variation from the source population in Raleigh, NC?

Our observations of mainly stage-specific genetic effects are consistent with an alternative hypothesis explaining the lack of genetic correlation between larval and adult thermal hardiness; natural selection against variants with stage-specific effects may be weaker than natural selection against variants that affect hardiness across the life cycle. All else being equal, a variant exposed to more bouts of selection (e.g., a variant that affects cold hardiness across ontogeny) will have greater effects on fitness than a variant exposed to fewer bouts of selection (e.g., a stage-specific variant). Thus, selection should more efficiently cull 'cross-ontogeny' causal variants compared to stage-specific variants. This hypothesis assumes that the average strength of selection is relatively homogenous across ontogeny, which would be more likely to apply to multivoltine species with overlapping generations such as *D. melanogaster*. In principal, laboratory selection on DGRP-derived base populations coupled with pooled resequencing of populations pre- and post-selection could be applied to test this hypothesis.

Genetics of cold hardiness

Both the quantitative genetic and GWA analyses suggest that cold hardiness as measured in this study is a complex, polygenic trait in both adults and larvae. Several studies have identified QTL with moderate to major effect on thermal hardiness phenotypes in *D. melanogaster* (Morgan and Mackay 2006; Norry et al. 2004; Norry et al. 2007; Rako et al. 2007; Rand et al. 2010). However, most of these studies relied to some extent on comparisons of laboratory selected lines or a small set of inbred lines. In contrast, variants in the DGRP reflect genetic variation segregating in natural populations, (Mackay et al. 2012) and variation maintained in the relatively large number of lines is less influenced by chance sampling and fixation compared to studies that compare many fewer selected or laboratory lines. Moreover, previous studies compare lines or populations likely to have fixed alternate QTL alleles in

different thermal environments, whereas large effect QTL are probably transient in a panmictic population with large effective population size such as would be expected for *D. melanogaster* (Agrawal et al. 2001). Thus, the polygenic nature of cold hardiness in this study is probably a reasonable representation of variation available to respond to selection in a given geographic population.

No variants exceeded a 3% inclusion probability for association with larval cold hardiness, but there was a single apparent outlier SNP with a 28% inclusion probability for adult cold hardiness (Figure. 2.2a). This SNP occurs in the gene *shawl*, a voltage-gated potassium channel. The *shawl* gene also harbored a different SNP variant whose non-zero inclusion probability, while lower (4%), fell within the upper 90th percentile of inclusion probabilities for all variants in the larval analysis. Ion balance is increasingly recognized as an important determinant of thermal hardiness and performance in insects. (Macmillan et al. 2015a,b). However, most previous work has focused on ion balance in the gut and Malpighian tubules, whereas *shawl* appears to be expressed primarily in anatomical regions associated with the central nervous system (see modEncode anatomy expression data in Flybase) and like other voltage-gated potassium channels, may function primarily in action potential propagation. In relation to other genetic studies of cold hardiness we also note a SNP with a moderate inclusion probability (3.4%, but in the top ten for weighted effect size; Table A.2) for adult cold hardiness within the gene *shaggy*, a likely ortholog of human Glycogen Synthase 3 Kinase (GSK3) that has previously been associated with an adult cold hardiness QTL in *D. melanogaster* (Rand et al. 2010).

Whether the variants identified in this study contribute to cold adaptations in nature depends on either the ecological relevance of the test conditions, or the genetic correlation

between the measured phenotype and a field-relevant phenotype such as survival of a transient cold snap. We did not apply thermal ramping, which tends to better represent ecologically relevant conditions, and ramping rates in nature may vary substantially among life history stages that exploit different microclimates (Sinclair 2001; Terblanche et al. 2011). The slightly slower ramping rate for larvae compared to adults (see methods) in this study was relatively minor, but likely does reflect real difference in nature, e.g., the internal temperature of a partially liquefied, rotting apple vs. ambient air temperatures.

Beyond better characterization of the phenotypic targets of natural selection, identification of associations between variants and environmental conditions among populations could also strengthen the case for the adaptive value of a given variant. Of two pooled sequencing studies examining genetic variation among high and low latitude populations of *D. melanogaster* in North America (Fabian et al. 2012) and Australia (Kolaczkowski et al. 2011), the North American study identified both *shawl* and *shaggy* as highly differentiated among populations from Florida and Pennsylvania (as quantified using outlier analysis of Fst values; see table S5 in (Fabian et al. 2012).

Summary

Our results suggest that there is no detectable genetic correlation for thermal hardiness between larvae and adults. Furthermore, allelic variants associated with cold hardiness mostly affected the phenotype in only one of the two life stages. However, there was a weak signal of common allelic effects across both life stages that may be consistent with cellular mechanisms universally effected by cold exposure across development. Overall, the results suggest that a single genome can provide independent evolutionary solutions to selection pressures that may vary across development, allowing for thermal strategies to evolve freely in distinct life stages.

This is an important consideration as the world's climate, and particularly seasonality, rapidly changes. Evolutionary responses in thermal hardiness may be relatively unconstrained by cross-stage, or developmental pleiotropy in species with similar life histories to *D. melanogaster*, though further empirical work will be necessary to evaluate the generality of this genetic architecture.

Acknowledgements

Stocks obtained from the Bloomington Drosophila Stock Center (NIH P40OD018537) were used in this study. I would like to thank Mary Post, Colin Bailey, Adam Schieferecke, Saadia Cleve, Oshadhi Athukorala Arachchige, Ashley Wedin, Nicholas Heter, Mariah Brown, and Jackson Alex for their help with this project. This chapter was published in 2017 by Oxford Academic in the journal *Integrative and Comparative Biology*, volume 57, issue 5, from pages 999-1009, and titled "Genetic Decoupling of Thermal Hardiness across Metamorphosis in *Drosophila melanogaster*" (DOI: 10.1093/icb/icx102).

References

Agrawal AF, Brodie Iii ED, Rieseberg LH. 2001. Possible consequences of genes of major effect: transient changes in the G-matrix. Microevolution Rate, Pattern, Process. Springer. p. 33-43.

Barrett RDH and Schluter D (2008) Adaptation from standing genetic variation. *Trends in Ecology & Evolution* 23(1): 38–44.

Bates D, Mächler M, Bolker B and Walker S (2015) Fitting Linear Mixed-Effects Models Using **lme4**. *Journal of Statistical Software* 67(1). Available at: http://www.jstatsoft.org/v67/i01/ (accessed 17/09/16).

Bennett V and Lee R (1997) Modeling seasonal changes in intracellular freeze-tolerance of fat body cells of the gall fly *Eurosta solidaginis* (Diptera, Tephritidae). *Journal of Experimental Biology* 200(1): 185–192.

Bettencourt BR, Kim I, Hoffmann AA and Feder ME (2002) Response to natural and laboratory selection at the *Drosophila* hsp70 genes. *Evolution; International Journal of Organic Evolution* 56(9): 1796–1801.

Bing X, Zhang J and Sinclair BJ (2012) A comparison of Frost expression among species and life stages of *Drosophila*: Frost expression in *Drosophila*. *Insect Molecular Biology* 21(1): 31–39.

Bowler K and Terblanche JS (2008) Insect thermal tolerance: what is the role of ontogeny, ageing and senescence? *Biological Reviews of the Cambridge Philosophical Society* 83(3): 339–355.

Colinet H and Hoffmann AA (2012) Comparing phenotypic effects and molecular correlates of developmental, gradual and rapid cold acclimation responses in *Drosophila melanogaster*:Cold acclimation and stress response. *Functional Ecology* 26(1): 84–93.

Colinet H, Lee SF and Hoffmann A (2010) Knocking down expression of Hsp22 and Hsp23 by RNA interference affects recovery from chill coma in *Drosophila melanogaster*. *Journal of Experimental Biology* 213(24): 4146–4150.

Coyne JA, Bundgaard J and Prout T (1983) Geographic Variation of Tolerance to Environmental Stress in *Drosophila pseudoobscura*. *The American Naturalist* 122(4): 474–488.

Dierks A, Kölzow N, Franke K and Fischer K (2012) Does selection on increased cold tolerance in the adult stage confer resistance throughout development? *Journal of Evolutionary Biology* 25(8): 1650–1657.

Dunning LT, Dennis AB, Sinclair BJ, Newcomb RD and Buckley TR (2014) Divergent transcriptional responses to low temperature among populations of alpine and lowland species of New Zealand stick insects (*Micrarchus*). *Molecular Ecology* 23(11): 2712–2726.

Duun Rohde P, Krag K, Loeschcke V, Overgaard J, S&#xf8, Rensen P and Nygaard Kristensen T (2016) A quantitative genomic approach for analysis of fitness and stress related traits in a *Drosophila melanogaster* model population. *International Journal of Genomics* 2016: e2157494.

Falconer DS and Mackay TFC (1996) *Introduction to Quantitative Genetics* (4 edition.). Harlow u.a.: Pearson.

Fisher RA (2000) *The Genetical Theory of Natural Selection* (1 edition.). Oxford: Oxford University Press.

Garbuz D, Evgenev MB, Feder ME and Zatsepina OG (2003) Evolution of thermotolerance and the heat-shock response: evidence from inter/intraspecific comparison and interspecific hybridization in the *virilis* species group of *Drosophila*. I. Thermal phenotype. *Journal of Experimental Biology* 206(14): 2399–2408.

Gilchrist GW, Huey RB and Partridge L (1997) Thermal sensitivity of *Drosophila melanogaster*: evolutionary responses of adults and eggs to laboratory natural selection at different temperatures. *Physiological Zoology* 70(4): 403–414.

Harbison ST, McCoy LJ and Mackay TF (2013) Genome-wide association study of sleep in *Drosophila melanogaster*. *BMC Genomics* 14: 281.

Hercus MJ, Berrigan D, Blows MW, Magiafoglou A and Hoffmann AA (2000) Resistance to temperature extremes between and within life cycle stages in *Drosophila serrata*, *D. birchii* and their hybrids: intraspecific and interspecific comparisons. *Biological Journal of the Linnean Society* 71(3): 403–416.

Hoffmann AA, Anderson A and Hallas R (2002) Opposing clines for high and low temperature resistance in *Drosophila melanogaster*. *Ecology Letters* 5(5): 614–618.

Hoffmann AA, Scott M, Partridge L and Hallas R (2003) Overwintering in *Drosophila melanogaster*: outdoor field cage experiments on clinal and laboratory selected populations help to elucidate traits under selection. *Journal of evolutionary biology* 16(4): 614–623.

Huang DW, Sherman BT and Lempicki RA (2009a) Systematic and integrative analysis of large gene lists using DAVID bioinformatics resources. *Nature Protocols* 4(1): 44–57.

Huang DW, Sherman BT and Lempicki RA (2009b) Bioinformatics enrichment tools: paths toward the comprehensive functional analysis of large gene lists. *Nucleic Acids Research* 37(1): 1–13.

Huang W, Massouras A, Inoue Y, Peiffer J, Ràmia M, Tarone AM, Turlapati L, Zichner T, Zhu D, Lyman RF, Magwire MM, Blankenburg K, Carbone MA, Chang K, Ellis LL, Fernandez S, Han Y, Highnam G, Hjelmen CE, Jack JR, Javaid M, Jayaseelan J, Kalra D, Lee S, Lewis L, Munidasa M, Ongeri F, Patel S, Perales L, Perez A, Pu L, Rollmann SM, Ruth R, Saada N, Warner C, Williams A, Wu Y-Q, Yamamoto A, Zhang Y, Zhu Y, Anholt RRH, Korbel JO, Mittelman D, Muzny DM, Gibbs RA, Barbadilla A, Johnston JS, Stone EA, Richards S, Deplancke B and Mackay TFC (2014) Natural variation in genome architecture among 205 *Drosophila melanogaster* Genetic Reference Panel lines. *Genome Research* 24(7): 1193–1208.

Kelty JD and Lee RE (2001) Rapid cold-hardening of *Drosophila melanogaster* (Diptera: Drosophiladae) during ecologically based thermoperiodic cycles. *Journal of Experimental Biology* 204(9): 1659–1666.

Kingsolver JG, Woods HA, Buckley LB, Potter KA, MacLean HJ and Higgins JK (2011) Complex life cycles and the responses of insects to climate change. *Integrative and Comparative Biology* 51(5): 719–732.

Koštál V (2010) Cell structural modifications in insects at low temperatures. *low temperature biology of insects. Cambridge University Press, Cambridge* 116–140.

Krebs RA and Feder ME (1997) Natural variation in the expression of the heat-shock protein HSP70 in a population of *Drosophila melanogaster* and its correlation with tolerance of ecologically relevant thermal stress. *Evolution* 51(1): 173.

Krebs RA and Loeschcke V (1995) Resistance to thermal stress in preadult *Drosophila buzzatii*: variation among populations and changes in relative resistance across life stages. *Biological Journal of the Linnean Society* 56: 517–531.

Lancaster LT, Dudaniec RY, Chauhan P, Wellenreuther M, Svensson EI and Hansson B (2016) Gene expression under thermal stress varies across a geographical range expansion front. *Molecular Ecology* 25(5): 1141–1156.

Levy O, Buckley LB, Keitt TH, Smith CD, Boateng KO, Kumar DS and Angilletta MJ (2015) Resolving the life cycle alters expected impacts of climate change. *Proc. R. Soc. B* 282(1813): 20150837.

Loeschcke V and Krebs RA (1996) Selection for heat-shock resistance in larval and in adult *Drosophila buzzatii*: comparing direct and indirect responses. *Evolution* 50(6): 2354–2359.

Long AD, Lyman RF, Langley CH and Mackay TFC (1998) Two sites in the *Delta* gene region contribute to naturally occurring variation in bristle number in *Drosophila melanogaster*. *Genetics* 149(2): 999–1017.

Lynch M and Walsh B (1998) *Genetics and Analysis of Quantitative Traits* (1 edition.). Sunderland, Mass: Sinauer Associates.

Mackay TFC, Richards S, Stone EA, Barbadilla A, Ayroles JF, Zhu D, Casillas S, Han Y, Magwire MM, Cridland JM, Richardson MF, Anholt RRH, Barrón M, Bess C, Blankenburg KP, Carbone MA, Castellano D, Chaboub L, Duncan L, Harris Z, Javaid M, Jayaseelan JC, Jhangiani SN, Jordan KW, Lara F, Lawrence F, Lee SL, Librado P, Linheiro RS, Lyman RF, Mackey AJ, Munidasa M, Muzny DM, Nazareth L, Newsham I, Perales L, Pu L-L, Qu C, Ràmia M, Reid JG, Rollmann SM, Rozas J, Saada N, Turlapati

L, Worley KC, Wu Y-Q, Yamamoto A, Zhu Y, Bergman CM, Thornton KR, Mittelman D and Gibbs RA (2012) The *Drosophila melanogaster* Genetic Reference Panel. *Nature* 482(7384): 173–178.

MacMillan HA, Andersen JL, Davies SA and Overgaard J (2015) The capacity to maintain ion and water homeostasis underlies interspecific variation in *Drosophila* cold tolerance. *Scientific Reports* 5: 18607.

MacMillan HA, Ferguson LV, Nicolai A, Donini A, Staples JF and Sinclair BJ (2015) Parallel ionoregulatory adjustments underlie phenotypic plasticity and evolution of *Drosophila* cold tolerance. *Journal of Experimental Biology* 218(3): 423–432.

McCleery RH, Pettifor RA, Armbruster P, Meyer K, Sheldon BC and Perrins CM (2004) Components of variance underlying fitness in a natural population of the great tit *Parus major*. *The American Naturalist* 164(3): E62–E72.

Merilä J and Sheldon BC (2000) Lifetime reproductive success and heritability in nature. *The American Naturalist* 155(3): 301–310.

Michaud MR and Denlinger DL (2007) Shifts in the carbohydrate, polyol, and amino acid pools during rapid cold-hardening and diapause-associated cold-hardening in flesh flies (*Sarcophaga crassipalpis*): a metabolomic comparison. *Journal of Comparative Physiology B* 177(7): 753–763.

Mitchell KA, Sinclair BJ and Terblanche JS (2013) Ontogenetic variation in cold tolerance plasticity in *Drosophila*: is the Bogert effect bogus? *Die Naturwissenschaften* 100(3): 281–284.

Morgan TJ and Mackay TFC (2006) Quantitative trait loci for thermotolerance phenotypes in *Drosophila melanogaster*. *Heredity* 96(3): 232–242.

Norry FM, Dahlgaard J and Loeschcke V (2004) Quantitative trait loci affecting knockdown resistance to high temperature in *Drosophila melanogaster*. *Molecular Ecology* 13(11): 3585–3594.

Norry FM, Sambucetti P, Scannapieco AC, Gomez FH, Loeschcke V. 2007. X-linked QTL for knockdown resistance to high temperature in Drosophila melanogaster. Insect Molecular Biology 16(4):509-513.

Nöthiger R (1970) Sucrose density separation: A method for collecting large numbers of *Drosophila* larvae. *Dros. Inf. Serv* 45: 177.

Overgaard J, Sørensen JG, Petersen SO, Loeschcke V and Holmstrup M (2005) Changes in membrane lipid composition following rapid cold hardening in *Drosophila melanogaster*. *Journal of Insect Physiology* 51(11): 1173–1182.

Philip BN and Lee RE (2010) Changes in abundance of aquaporin-like proteins occurs concomitantly with seasonal acquisition of freeze tolerance in the goldenrod gall fly, *Eurosta solidaginis*. *Journal of Insect Physiology* 56(7): 679–685.

R Core Team (2017) *R: A language and environment for statistical computing.* R Foundation for Statistical Computing, Vienna, Austria. URL: http://www.R-project.org/.

Ragland GJ and Kingsolver JG (2008) Evolution of thermotolerance in seasonal environments: the effects of annual temperature variation and life-history timing in *Wyeomyia smithii*. *Evolution; International Journal of Organic Evolution* 62(6): 1345–1357.

Rako L, Blacket MJ, McKechnie SW and Hoffmann AA (2007) Candidate genes and thermal phenotypes: identifying ecologically important genetic variation for thermotolerance in the Australian *Drosophila melanogaster* cline. *Molecular Ecology* 16(14): 2948–2957.

Rand DM, Weinreich DM, Lerman D, Folk D, Gilchrist GW. 2010. Three selections are better than one: clinal variation of thermal QTL from independent selection experiments in Drosophila. Evolution 64(10):2921-2934.

Saunders DS, Henrich VC and Gilbert LI (1989) Induction of diapause in *Drosophila melanogaster*: photoperiodic regulation and the impact of arrhythmic clock mutations on time measurement. *Proceedings of the National Academy of Sciences of the United States of America* 86(10): 3748–3752.

Sgrò CM, Milton CC, Jensen LT, Frydenberg J, Loeschcke V, Batterham P and Hoffmann AA (2008) Nucleotide diversity in the Hsp90 gene in natural populations of *Drosophila melanogaster* from Australia. *Insect Molecular Biology* 17(6): 685–697.

Sinclair BJ, Marshall KE, Sewell MA, Levesque DL, Willett CS, Slotsbo S, Dong Y, Harley CDG, Marshall DJ, Helmuth BS and Huey RB (2016) Can we predict ectotherm responses to climate change using thermal performance curves and body temperatures? *Ecology Letters* 19(11): 1372–1385.

Teets NM and Denlinger DL (2013) Physiological mechanisms of seasonal and rapid cold-hardening in insects: Seasonal and rapid cold-hardening in insects. *Physiological Entomology* 38(2): 105–116.

Tomcala A, Tollarova M, Overgaard J, Simek P and Kostal V (2006) Seasonal acquisition of chill tolerance and restructuring of membrane glycerophospholipids in an overwintering insect: triggering by low temperature, desiccation and diapause progression. *Journal of Experimental Biology* 209(20): 4102–4114.

Tucić N (1979) Genetic capacity for adaptation to cold resistance at different developmental stages of *Drosophila melanogaster*. *Evolution* 33(1): 350–358.

Turner SD (2014) qqman: an R package for visualizing GWAS results using Q-Q and manhattan plots. *biorXiv* DOI: 10.1101/005165.

Woods HA (2013) Ontogenetic changes in the body temperature of an insect herbivore. *Functional Ecology* 27(6): 1322–1331.

Yocum GD (2001) Differential expression of two HSP70 transcripts in response to cold shock, thermoperiod, and adult diapause in the Colorado potato beetle. *Journal of Insect Physiology* 47(10): 1139–1145.

Zhou X, Carbonetto P and Stephens M (2013) Polygenic modeling with bayesian sparse linear mixed models. *PLOS Genetics* 9(2): e1003264.

Chapter 2 Figures

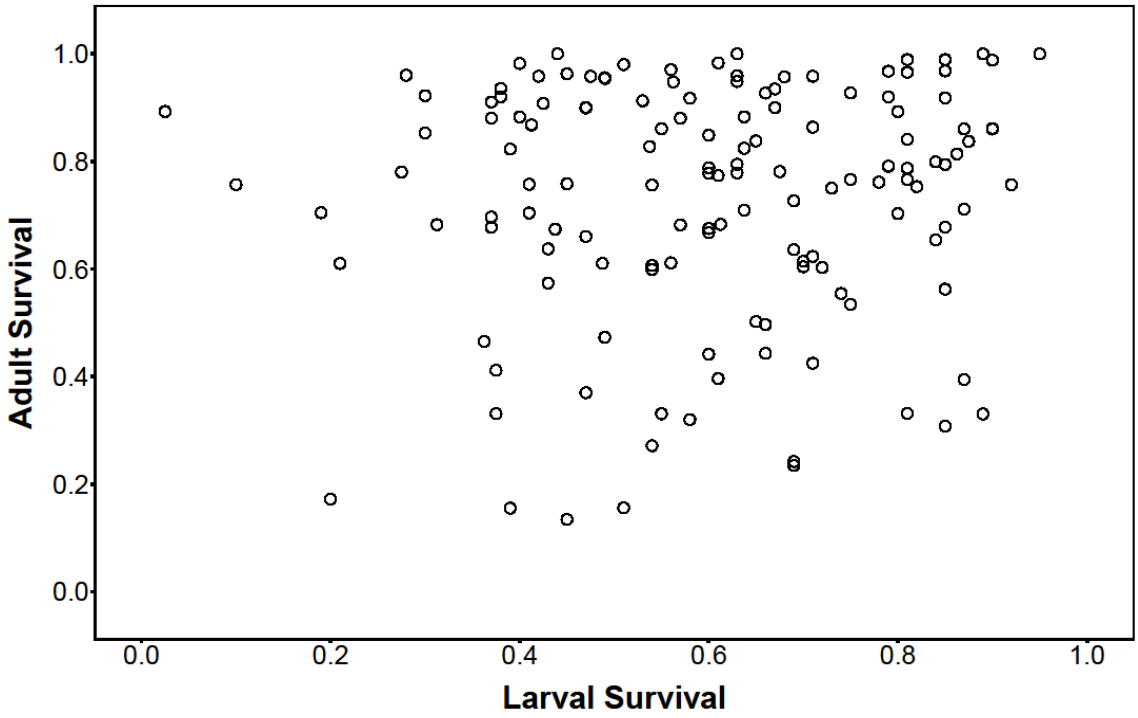

Figure 2.1 Larval vs. Adult Cold Hardiness

Scatterplot of average larval survival (proportion surviving) vs. average adult survival after a 1h exposure to -5 °C. Each circle represents one of the 139 DGRP lines. Both the phenotypic (r^2 = 0.00525, *p*-value = 0.3966) and genetic correlation (r_g = 0.085, p = 0.12) are not significantly different from zero.

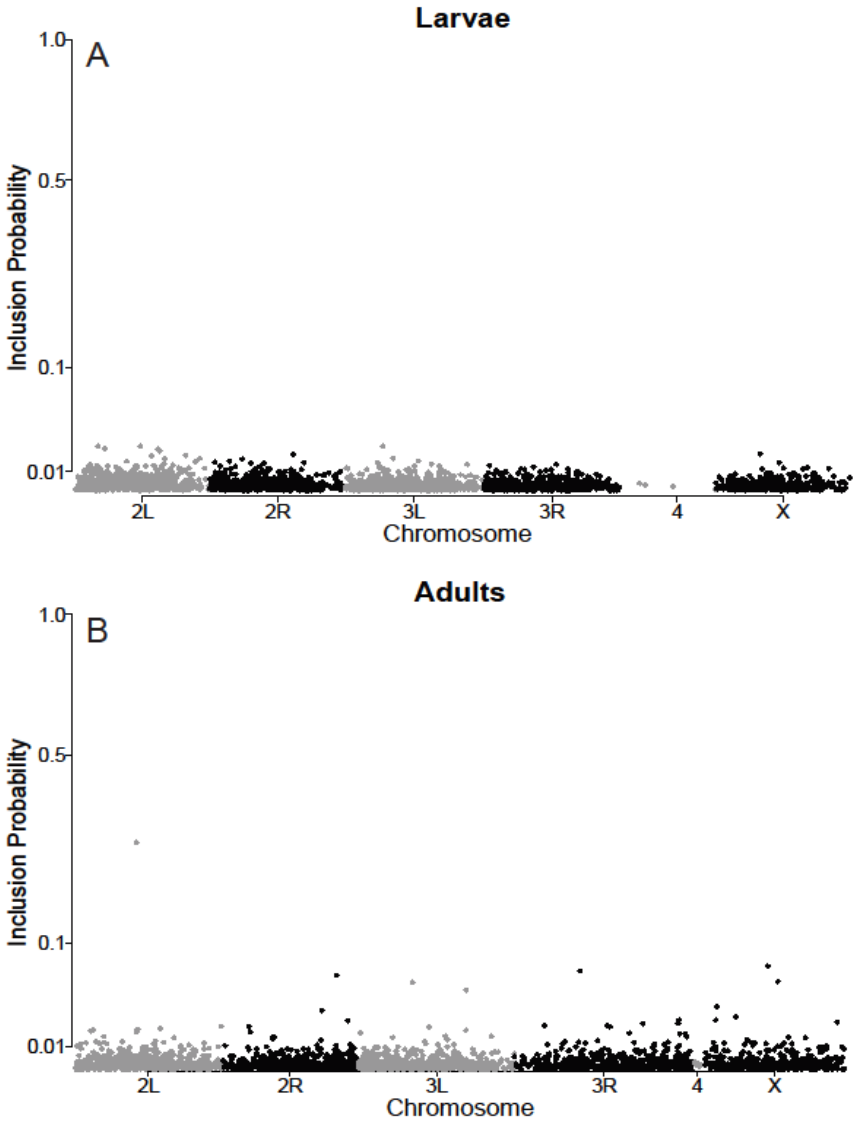

Figure 2.2 Manhattan Plots

Manhattan plots of inclusion probabilities for the top 0.01% of SNPs (highest inclusion probabilities) in larvae (A) and adults (B). Inclusion probabilities (the probability that each locus has a non-zero effect on the phenotype while accounting for all effects at all other loci) for SNPs are plotted against genomic position. The y-axis (inclusion probability) is square-root scaled to compress the range.

Chapter 3 - Stage-Specific Genotype-by-Environment Interactions for Cold and Heat Hardiness in *Drosophila melanogaster*

Abstract

Environments often vary across a life cycle, imposing fluctuating natural selection across development. Such fluctuating selection can drive evolutionary responses specific to distinct life-history stages. However, selection and genetic variation, phenotypic plasticity, and their interaction (GxE), as well as genetic correlation across development dictate stage-specific evolution. Thus, quantifying genetic covariance of fitness-related traits and plasticity across development is vital to determine whether stage-specific adaptation occurs in nature. Additionally, the interaction of genetic variation and environmental plasticity (GxE) may be stage-specific, leading to a 3-way interaction between genotype, environment, and development or GxDxE. To test for these patterns in a natural system, we exposed larvae and adults of *Drosophila melanogaster* isogenic lines derived from a natural population to extreme heat and cold after developmental acclimation to cool (18°C) and warm (25°C) conditions and measured genetic variance for thermal hardiness. We detected significant GxE that was specific to larvae and adults for cold and heat hardiness (GxDxE), but no significant genetic correlation across development for either trait at either acclimation temperature. However, cross-development phenotypic correlations for acclimation responses suggest that plasticity itself may be developmentally constrained, though rigorously testing this hypothesis requires more experimentation. In general, we find evidence for thermal niche adaptation across development as larvae are more heat-hardy while adults are more cold-hardy. These results illustrate the potential for stage-specific adaptation within a complex life cycle and highlight the importance

of measuring traits at appropriate developmental stages and environmental conditions when predicting evolutionary responses to changing climates.

Introduction

As organisms proceed through development, they typically experience predictable changes in their environment driven by, for example, shifts in resource use or transitions from feeding to reproductive behaviors (Krebs and Loeschcke 1995; Ragland and Kingsolver 2008; Woods 2013). These developmentally variable environments may result in life stage-specific evolutionary responses. For example, complex life cycles often include developmental stages with distinct morphology, physiology, and behavior linked to developmentally shifting ecological niches (Moran 1994; Kingsolver 2011), (McGraw and Antonovics 1983; Schluter et al. 1991).

As with any environmentally sensitive trait, stage-specific evolutionary responses are modulated by genetic variation, plastic responses, and their interaction, typically termed 'gene by environment interactions', or GxE (West-Eberhard 1989; Pigliucci 2005). The evolutionary response is proportional to the strength of selection and the amount of heritable genetic variance. Expanding this to a multivariate perspective, genetic correlations among traits or among the expression of the same trait across developmental stages may limit evolutionary responses. These limits represent lack of genetic variation for particular trait combinations; in other words, tightly correlated traits respond to selection as a unit, in combinations that may or may not convey the highest fitness (Lande and Arnold 1983; Via and Lande 1985). Thus, negative genetic correlation among fitness-related traits across development may constrain stage-specific responses (Price and Langen 1992; Roff 1996). Whereas, the absence of genetic correlation

facilitates the independent response of traits in each developmental stage (Tucić 1979; Loeschcke and Krebs 1996; Gilchrist et al. 1997; Dierks et al. 2012).

Determining the level of genetic constraint between fitness-related traits across development is thus critical to understanding the mechanisms by which environmental adaptations evolve in organisms with complex life cycles (Levy et al. 2015; Sinclair et al. 2016). Thermal hardiness, the ability to maintain performance despite stressful environmental conditions, is one of the best-studied traits with respect to environmental adaptation (Hoffmann and Watson 1993; Bale and Hayward 2010). However, most empirical studies focus on only a single developmental stage, typically reproductive adults (Bowler and Terblanche 2008). However, Freda et al. (2017) recently showed that genetic variation for cold hardiness in *Drosophila melanogaster* is not genetically constrained across different developmental stages. Quantitative genetic analyses revealed ample, heritable genetic variation for thermal hardiness in adult flies and in earlier (larval) developmental stages, with no evidence for genetic correlations across stages. This lack of genetic correlation suggests that thermal hardiness can evolve to independently maximize fitness in juvenile and adult stages that experience different thermal habitats (Kelty and Lee 1999; Gibert and Huey 2001; Overgaard et al. 2008; Andersen et al. 2016).

Although the results of Freda et al. (2017) suggest a lack of developmental genetic constraint, this study was conducted in a single, homogenous developmental environment (25°C constant), which does not account for plasticity in response to variable thermal conditions encountered in nature. A comprehensive understanding of the genotypic response to variable environments is critical because genotype-by-environment interactions (GxE), specifically the relationship between genotypes associated with thermal hardiness and developmental

temperature, can change genetic variances and covariances (De Jong 1990). In particular, developmental acclimation, physiological changes that occur as a result of different environments experienced during development, can have lasting effects on thermal hardiness across the life cycle (Colinet and Hoffmann 2012; Fallis et al. 2014; Gerken et al. 2015). For example, exposing developing larval stages to relatively cold environments typically improves cold hardiness in adult flies (Overgaard et al. 2008; Koštál et al. 2011; Fallis et al. 2014; Gerken et al. 2015; Everman et al. 2017). However, the effects of developmental temperature on larval thermal hardiness are unknown, but a three-way interaction between Genotype, Developmental Stage, and Environment (GxDxE) could affect the expression of genetic (co)variances among developmental stages and ultimately evolutionary responses.

Figure 1 conceptually illustrates hypothetical relationships among trait values (here, a metric of cold hardiness) measured across developmental stages, developmental acclimation temperatures, and genotypes. Within an acclimation temperature, significant genetic correlations occur when there is variance among genotypes (genetic variance), but each genotype performs similarly in the larval and adult stage. This is not the case for DGRP isofemale lines acclimated at 25°C (Freda et al. 2017), illustrated in Figure 1 by the crossing orange lines, each representing the performance of a single genotype in the larval and adult stages. Acclimating at a lower developmental temperature is well known to increase cold hardiness in adult *Drosophila melanogaster* (Overgaard et al. 2008; Koštál et al. 2011; Fallis et al. 2014; Gerken et al. 2015; Everman et al. 2017), illustrated in all panels in Figure 3.1 by higher average hardiness values for the blue (acclimated at 18°C) lines vs. the orange (acclimated at 25°C) lines. Acclimation may have no effect on (Fig. 3.1A), increase (Fig. 3.1B), or decrease (Fig. 3.1C) genetic variance. However, in order to cause cross-stage genetic correlations, developmental acclimation must

maintain some variance among genotypes, and those genotypes must perform similarly at that acclimation temperature in both life stages (Fig. 3.1D). In other words, the blue lines representing genotypes in Figure 3.1 must be roughly parallel, preserving the rank order of genotypes across stages. In Figure 3.1D, a GxDxE produces a genetic correlation between stages acclimated at 18°C, driven mainly by a genetically variable acclimation response that universally increases hardiness of both stages relative to acclimation at 25°C. These scenarios are specific to our example of developmental acclimation in *D. melanogaster* and are not exhaustive. However, they illustrate how environmental temperature might fundamentally change genetic correlation structure, and thus genetic constraint (Steppan et al. 2002).

To examine the evolutionary potential of developmental acclimation, and its effects on GxDxE, we measured genetic (co)variance of thermal hardiness in *D. melanogaster* across larval and adult stages and across developmental acclimation temperatures in a factorial design (Figure B.1). In nature, developmental acclimation represents an important short-term response to temporal and spatial environmental variability, though different developmental stages may experience a different range of environments. In temperate regions, *D. melanogaster* larvae experience extreme high temperatures during spring and summer within their oviposition site. (Ashburner 1981; Dillon et al. 2009). However, *D melanogaster* adults overwinter in leaf litter and orchard debris (Saunders et al. 1989; Schmidt et al. 2005) and thus are more likely to experience extreme cold temperatures. This difference in the thermal stressors between adult and larval stages may result in developmental stage specific adaptation or maladaptation, depending on the genetic covariance across stages and environments. Whether adaptive or maladaptive, the results could drastically affect long-term evolutionary trajectories of the species.

In this study, we explore genetic variability in cold hardiness, heat hardiness, and developmental acclimation by exposing both larvae and adults from 39 genotypes (isofemale lines) from the Drosophila Genetic Reference Panel (DGRP) (Mackay et al. 2012; Huang et al. 2014). The 39 genotypes were developmentally acclimated by rearing at warm and cool temperatures followed by acute heat and cold stress exposures. We used this factorial design (illustrated in Figure B.1) to test the effect of developmental acclimation on genetic variances, across stage covariances, and the occurrence of GxDxE. In addition, we also tested whether plasticity itself (i.e., change in thermal hardiness across developmental acclimation treatments) is genetically correlated across developmental stages, and if there is a genetic correlation between plasticity in cold and heat hardiness.

Methods

Drosophila Genetic Reference Panel (DGRP) lines

The DGRP is comprised of 205 isogenic lines of *Drosophila melanogaster* that were initiated from a single natural population in Raleigh, North Carolina (dgrp2.gnets.ncsu.edu) (Mackay et al. 2012; Huang et al. 2014). This design maintains naturally segregating variation as genetic variance among isogenic lines. A total of 39 genotypes were used in this study, which represent a subset of the 139 used previously to test for genetic correlation across developmental stages in cold hardiness (Freda et al. 2017). All genotypes were obtained from the Bloomington Drosophila Stock Center (Indiana University).

Line Rearing and Maintenance

All flies were reared on media containing cornmeal, molasses, and yeast. Propionic acid and benzoic acid were also added as anti-fungal and anti-bacterial agents. To increase oviposition rates, vials were lightly sprinkled with dry active yeast. Experimental flies were

developmentally acclimated by rearing from egg-to adult at 18°C or 25°C on a 12/12 light-dark cycle. Experimental flies were collected for assays at predetermined developmental time points for larval and adult measurements (see below). All experimental flies were the progeny of adults reared at low densities (5 males and 5 females per vial). These parents were sorted under light CO_2 anesthesia and then placed on fresh media for oviposition. Oviposition occurred at 25°C for all experimental flies. These vials containing 5 males and 5 female parents were transferred every 24h to fresh media for 6 days. After each transfer, vials from the previous day, containing eggs, were then moved to the cool (18°C) or warm (25°C) developmental acclimation temperature. The first set of replicate vials (day 1) were discarded to remove any residual effect of anesthesia on oviposition rates.

Survival Assays

Larval assays were conducted at 120h (5d) post-oviposition for replicates developmentally acclimated at 25°C and 168 h (7d) post-oviposition for those developmentally acclimated at 18°C, using third instar feeding larvae that were extracted from media using a 20% w/v sucrose solution following the protocol of Nöthiger (1970) and Freda et al. (2017) In the larval vials, small holes were made in the media to facilitate larval burrowing and feeding. During the heat and cold hardiness measurements, larval vials were immersed in a recirculating bath (ECO RE 2025, Lauda Corporation) containing a 50/50 mixture of distilled water and propylene glycol held at the test temperature (see below) for a total of 1h. To confirm that the food did not freeze during the cold stress assays, thermocouples were inserted into vials with food. No evidence of freezing was observed. After exposure, vials were removed from the recirculating bath and placed in a 25°C for recovery, regardless of developmental acclimation

condition of the larvae. After 9d (216h), the proportion of successfully eclosed adults was used to score larval survivorship (Bing et al. 2012).

Adult assays were performed on 5-7d post-eclosion flies. For flies developmental acclimated at 25°C, adults emerged and were collected 10-12d post-oviposition. In flies developmentally acclimated at 18°C, emergence and collection occurred 19-21d post-oviposition. Experimental flies were sorted and separated into groups of 10 by sex under light CO2 anesthesia upon eclosion. Separate, same sex vials were returned to their respective developmental acclimation conditions (12/12 light-dark at either 18°C or 25°) for 5 days to recover before cold or heat hardiness was measured. Adults were transferred to new food after 3d during this 5d period to ensure that the food was fresh. After 5d of recovery, adult flies 5-7d old (5-7 d post-eclosion; 408h post-oviposition) were placed in empty vials and exposed to either cold (-6.5°C) or heat (38°C) stress for 1 hour. After this exposure, flies were transferred to vials containing fresh media and placed at 25°C, 12/12 light-dark environment for recovery. After 24h, the proportion of adults (males and females) per line capable of coordinated movement and flight was used to score adult survival (Colinet and Hoffmann 2012; Gerken et al 2015; Kelty and Lee 2001; Overgaard et al. 2005).

To test if vials with food and empty vials reached test temperatures at significantly different times, iButtons® (Part Number: DS1925L; Maxim Integrated™) were placed at the bottom of empty vials (adults) and buried within the food in food (larval) vials. For cold stress, empty vials, which are used in adult assays, reached the test temperature (-6.5°C) only slightly faster (~3 minutes faster on average) than vials containing food, representing a difference of only five percent of the 1h exposure. For heat stress, there was only a 1-minute average difference

between food vials and empty vials with food vials reaching 38°C 1 minute faster (a difference of 1.7% of the 1h exposure).

Experimental Design

At extreme, stressful temperatures, organisms generally display a roughly logistic relationship between survival and temperature (Lee and Denlinger 1991). To simplify measurements, we wished to capture as much of the variation in survival as possible using a single temperature. Freda et al. 2017 applied -5°C as the stressful cold temperature because survival after exposure to -5°C was most highly correlated with cumulative survival across a range of stressful temperature exposures in both larvae and adults compared to other tested, single temperature exposures. However, a lower stress temperature (-6.5°C) was used in this study because adults had relatively high survival following cold stress at -5°C compared to larvae when reared at 25°C in the previous study. Developmental acclimation at 18°C increases cold hardiness (Ayrinhac et al. 2004; Fallis et al. 2014; Gerken et al. 2015), and a lower test temperature avoids overdispersed data (many vials with a survival proportion of 1). For heat stress, we generated survival curves of both larvae and adults from four DGRP lines (data not show) using survival data after a 1h exposures to 36°C, 37°C, 37.5°C, 38°C, and 39°C. For both larvae and adults, 38°C was selected as the test temperature because the average survival in both larvae and adults was closest to 50% at this temperature (LD50). This temperature is also in agreement with the LD50 of similar heat stress experiments on other *D. melanogaster* genotypes (Fallis et al. 2012; Morgan and Mackay 2006).

Cold stress survival was tested at -6.5° C, while heat stress survival was tested at 38°C for all 39 genotypes in a full factorial design. The full factorial experimental design was as follows for both cold and heat stress experiments and is visualized in Figure B.1: 39 genotypes X

2 developmental stages X 2 developmental acclimation temperatures X 5 replicate vials for each genotype, developmental stage, sex (adults only), and developmental acclimation temperature. Each replicate consisted of a total of 20 individuals (20 larvae or a total of 20 adults with 10 males and 10 females assayed in separate vials to not allow mating to occur). Although vials were separated by sex we did not separate sexes in the analyses as sex was not determined for larvae.

Thermal Hardiness, Plasticity, and GxDxE

We modeled the effects of temperature, stage, genotype (line), and their interactions on thermal hardiness using a generalized linear model with a logit link function and binomial distribution implemented in the *glmer* function in R (R Core Team 2018). Terms retained in the best fit model were interpreted as significantly affecting thermal hardiness. The full model was specified as:

$$logit(y) = stage + temp + stage * temp + line + rep(line) + line \times stage + line \times temp + line \times stage \times temp$$

where *stage, temp, and line* model the effects of developmental stage, developmental acclimation temperature, and genotype. All factors including genotype (line) were modeled as random effects, and all factors excluding line were modeled as fixed effects (rep(line) indicates replicate nested within line). Here, GxE is modeled by the *line x temp* term, while *line x stage x temp* models GxDxE. We excluded sex from the models because sex could not be determined for larvae that did not successfully eclose. We used backward model selection to identify the best fit model, first dropping fixed terms, then random terms, and comparing model Akaike Information

Criterion (AIC) among models. The model yielding the lowest AIC score was selected as the best fit model for cold and heat hardiness (Table B.1). Finally, we estimated thermal plasticity (β) as the difference between survival when developmentally acclimated at 18°C compared to survival when developmentally acclimated at 25°C for both cold hardiness and heat hardiness assays.

Heritability and genetic correlation

The broad sense heritabilities (H^2) of cold hardiness and heat hardiness within developmental stages and developmental acclimation temperatures were estimated as the proportion of the variance among lines divided by the total variance (among and within lines). The heritability is broad sense because the among-line variance does not separate the dominance in this isogenic line design (Falconer and Mackay 1996; Lynch and Walsh 1998). Variance components for cold/heat hardiness within each stage x developmental temperature combination were estimated using generalized linear mixed models similar to the one described above. The adult model for each metric (cold or heat hardiness) at each developmental acclimation temperature was:

$$logit(y) = sex + line + rep(line)$$

The larval model was the same, except that it excluded the effect of sex. We also estimated the broad-sense heritability of plasticity for each stage and each trait (cold or heat hardiness) as the proportion of variance associated with GxE divided by the total variance in the following model:

$$logit(y) = sex + temp + line + line * temp + rep(line)$$

Where *line x temp* models GxE, and the fixed effect of sex was only included for adults. We estimated 95% confidence intervals (CIs) for each estimate by repeating the variance component calculation 500 times on data sets where genetic line was randomly sampled with replacement.

We also tested the hypothesis that the heritability estimates were significantly different from random expectations by estimating a null distribution, randomly permuting the association between replicates and lines (within stages and temperatures) 1,000 times and comparing the observed H^2 estimate to the null distribution using a two-tailed test.

The genetic correlations between larval and adult thermal hardiness under each developmental acclimation treatment were estimated as:

$$r_g = \frac{COV_{AL}}{\sqrt{\sigma_A^2 \times \sigma_L^2}}$$

where COV_{AL} represents the covariance between adult and larval thermal hardiness and σ_A^2 and σ_L^2 are the variance among lines for adults and larvae, respectively. Variances and covariances were estimated using generalized linear mixed models as above. The values for σ_A^2 and σ_L^2 were estimated as the among line variance from the separate adult and larval models that were used to estimate broad-sense heritabilities. We estimated COV_{AL} as the among-line variance from a generalized linear mixed model of the combined larval and adult data including a fixed effect of developmental stage (Harbison et al. 2013) and random effects of line, line-by-stage interaction, line-by-developmental acclimation temperature and replicate nested within line. Confidence intervals were estimated, and permutation tests performed as above. Genetic correlations were also calculated across developmental acclimation temperatures and across trait type (heat hardiness and cold hardiness) within developmental stages using equation one, substituting developmental acclimation temperature or stress type for stage. Phenotypic correlations were estimated for all the above comparisons using the Pearson correlation of line means. Though our experimental design did not allow us to estimate the genetic correlation for plasticity across stages and traits, we did estimate the phenotypic correlations as above, where

plasticity (β) was estimated as the difference in mean survival at 18°C vs. 25°C developmental acclimation temperatures.

Results

Plasticity and Stage-Specific Thermal Hardiness

Developmental acclimation increased cold hardiness at 18°C (Fig. 3.2A). However, the effect differed between larvae and adults (best model included a stage-by-temperature interaction; Table B.1A) with a 22.36% increase in survival in larvae, and 32.23% increase in adults between flies reared at 18°C vs 25°C. There was also an effect of developmental acclimation temperature on heat hardiness, with survival in larvae increasing by 16.05% and survival in adults increasing by 12.44% between flies reared at 25°C vs. 18°C. however there was no significant stage-by-temperature interaction (Table B.1B; Fig. 3.2B).

Adults were significantly more cold hardy, on average, than larvae under both developmental acclimation conditions (Fig. 3.2A; 43.06% and 33.19% increased survival in adults relative to larvae at 18°C and 25°C, respectively). Conversely, larvae were more heat-hardy on average compared to adults under both developmental acclimation conditions (Fig. 3.2B; 5.68% and 9.30% increased survival for larvae relative to adults at 18°C and 25°C, respectively), though the stage difference was not as dramatic as for cold hardiness.

On average, cold stress survival was more plastic than heat stress survival in both larvae and adults, with non-overlapping 95% CIs (Adults: mean β cold stress: 32.23%, 95% CI 25.64 — 38.81; mean β heat stress: -12.44%, 95% CI -19.36 — -5.51; Larvae: mean β cold stress: 22.36%, 95% CI 17.24 — 27.47; mean β heat stress: -16.05%, 95% CI -23.28 — -8.82). These data also illustrate that adults exhibited greater plasticity for cold hardiness, on average, than

larvae, though 95% CIs overlap. In contrast, larvae were more plastic for heat hardiness on average, but 95% CIs overlap for this comparison as well.

Genotype-by-Development-by-Environment (GxDxE) Interactions

The best model of cold hardiness, including data from all stages, developmental acclimation temperatures, and lines, included a line-by-stage-by-temperature interaction, suggesting a GxDxE interaction for cold hardiness (Table B.1A). In particular, among-genotype variance for cold hardiness decreased markedly at 18°C relative to 25°C for adults, as variable genotypes at 25°C collapsed to similar cold hardiness at 18°C (Fig. 3.3A). Likewise, there was significant GxDxE for heat hardiness (best model included a line-by-stage-by-temperature interaction; Table B.1B), though in this case variances among lines remained roughly comparable across developmental acclimation temperatures in both stages (Fig. 3.3B). Note that Figure 3.3 illustrates norms of reaction, or the relationships between hardiness and acclimation temperature for each genotype. Average thermal hardiness for genotypes across stages relative to predictions in Figure 1 appear in the discussion.

Heritability

Broad-sense heritability (H^2) for cold-stress survival and heat stress survival for each developmental stage under both developmental acclimation conditions were all significantly different from zero based on permutation tests (Table 3.1A,B), suggesting that the population in Raleigh, NC, from which the DGRP was founded, has substantial segregating genetic variance for thermal hardiness that is visible to natural selection. Adults exhibited slightly higher H^2 for cold-hardiness under both developmental acclimation conditions when compared to larvae. The H^2 estimates for heat hardiness were greater in magnitude than the H^2 for cold hardiness in both larvae and adults. As is observed in H^2 for cold-stress survival, adults have higher H^2 for heat-

stress survival compared to larvae. Finally, plasticity itself was also heritable for both cold hardiness and heat hardiness in both adults and larvae, though estimates were generally lower than those for cold and heat hardiness (Table 3.1C).

Cross-Stage, Cross-Temperature, and Cross-Trait Correlations

Cross-stage genetic (r_g) and phenotypic (r_P) correlations between cold-stress survival in larvae and adults under both developmental acclimation conditions were not significantly different from zero, with comparable results for heat stress survival (Table 3.2A; Figure B.2A,B). Plasticity of larval cold hardiness and plasticity of adult cold hardiness were positively phenotypically correlated (Table 3.2A; Figure B.3A; $r_P = 0.34$, $p = 0.034$). Plasticity of heat hardiness was also positively correlated between larvae and adults, though not significantly (Table 3.2A Figure B.3A; $r_P = 0.24$, $p = 0.14$).

In contrast, the genetic and phenotypic correlations between developmental acclimation-temperature *within* developmental stages (18°C vs. 25°C) were all significant for both cold and heat hardiness (Table 3.2B). Thus, genotypes that tended to be more hardy at one developmental acclimation temperature were also more hardy at the other developmental acclimation temperature. Genetic and phenotypic correlations between cold hardiness and heat hardiness within stages and developmental acclimation temperatures were all non-significant (Table 3.2C; Figure B.4) except for larvae developmentally acclimated at 18°C (Figure B.4A). In addition, estimates of correlations between plasticity of cold hardiness and plasticity of heat hardiness within developmental stages were not significantly different from zero (Table 3.2C; Figure B.3B).

Discussion

Plasticity and GxDxE

Plastic responses of thermal hardiness to developmental acclimation temperature have been well documented in adult *D. melanogaster* (Overgaard et al. 2008; Colinet and Hoffmann 2012; Gerken et al. 2015) and other organisms (Cuculescu 1998; Chatterjee et al. 2004; Das et al. 2004; Terblance et al. 2005). Our data support these previous observations, and provide evidence that acclimation also affects larval thermal hardiness. In both larvae and adults, acclimation at a temperature close to the stress temperatures resulted in a significant increased cold hardiness when reared at 18°C and heat hardiness when reared 25°C (Fig. 3.2A,B; Fig. 3.3). The current and previous studies suggest that natural selection likely favors plastic responses to temperature across the life cycle in multivoltine species that experience often extreme seasonal variation, like *D. melanogaster* (Lynch and Gabriel 1987; Jentsch et al. 2007; Lande 2009; Kodra et al. 2011; Noh et al. 2017), though most data sets including our own do not provide an explicit test for adaptive plasticity.

Though the average trend was towards greater hardiness at the acclimation temperature closest to the stressful temperature, there was substantial genetic variance in reaction norms in both developmental stages (GxE, though this is subsumed by GxDxE, see below). This variance includes genotypes with reaction norms that are negative acclimators, e.g., with greater cold hardiness when acclimated at 25°C vs. 18°C or greater heat hardiness when reared at 18°C vs. 25°C (Fig. 3.3). To our knowledge, this is the first record of negative acclimators occurring in *D. melanogaster* larvae but negative acclimators have also been recorded in *D. melanogaster* adults in previous studies investigating thermal hardiness (Fallis et al. 2014; Gerken et al. 2015). Overall, there are less negative acclimators in both stages under cold stress and the variance

associated with the *line x temp* term is larger for heat stress vs. cold stress (cold stress *line x temp* $\sigma^2 = 0.041$; heat stress *line x temp* $\sigma^2 = 0.11$). This could suggest that cold hardiness plasticity is constrained among genotypes more than heat hardiness.

Though both life stages harbored genetic variance for reaction norms, the variability was stage-specific, supported by a significant Genotype-by-Development-by-Environment interactions (GxDxE) for cold and heat hardiness. In particular, developmental acclimation at the temperature closest to the stressful temperature increased thermal hardiness on average (Fig. 3.2A,B; Fig. 3.3), but this developmental acclimation effect does not produce similar phenotypes for each genotype between larvae and adults, which would otherwise result in a significant cross developmental stage genetic correlation (Fig. 3.4; Table 3.2A). Note that at both 18 and 25°C, genotypes exhibit a crossing pattern in Figure 3.4, whereas roughly parallel lines would suggest similar trait values in both stages for a given genotype (Fig. 1D). Our discovery of GxDxE interactions for both cold and heat hardiness suggest a complex mechanism underlying the expression of genetic variation across ontogeny and thermal environment. Thus, there is ample genetic variance in cold and heat hardiness within environments and plasticity for thermal hardiness that may respond to stage-specific natural selection.

Thermal Hardiness is Genetically Decoupled across Development

As suggested by the patterns underlying the observed GxDxE, we found no detectable genetic correlations across life stages for either cold or heat hardiness at either acclimation temperature (Table 3.2A, FigureB.2A,B). Thus, the previous observation that thermal hardiness is not genetically correlated across development (Freda et al. 2017) is robust to different developmental acclimation temperatures (18°C and 25°C) and to the performance metric, despite significant broad-sense heritability for both cold hardiness and heat hardiness (Table 3.1A,B).

These results provide additional evidence that distinct genetic architectures underlie variation in cold stress hardiness in larvae and adults of *D. melanogaster* (Freda et al. 2017) and provide initial evidence of developmental stage independence for heat stress hardiness and acclimation responses as well. Our results are comparable to those found in previous studies that also illustrate lack of correlations between thermal hardiness phenotypes in alternate developmental stages in holometabolous insects (Tucić 1979; Loeschcke and Krebs 1996; Gilchrist et al. 1997; Dierks et al. 2012). We refer to this lack of genetic correlation as 'genetic decoupling', a pattern that has been observed for other traits in other organisms such as shell length of the hard clam, *Mercenaria mercanaria* (Rawson and Hilbish 1993), locomotor performance in the salamander *Ambystoma californiense* (Shaffer et al. 1991) and in the Common Frog, *Rana temporaria* (Johansson et al. 2010), and social behaviors in *D. melanogaster* (Anderson et al. 2016). Recently, genetic decoupling of cold hardiness was discovered across ages within the adult developmental stage in *D. melanogaster*, indicating that this phenomenon is not limited to drastic life history transitions like metamorphosis (Everman and Morgan 2018). These findings illustrate the potential for many traits to be genetically decoupled across development in a host of systems and over a variety of developmental windows. Furthermore, this body of evidence points to the importance of measuring quantitative genetic parameters at the appropriate developmental stage (and perhaps even age within stage), as selection typically fluctuates across development (Kingsolver et al. 2011).

Though thermal hardiness *per se* appears to be genetically decoupled across stages, evidence for decoupling of plasticity (the acclimation response) is equivocal. Our experimental design did not allow us to directly estimate genetic correlations of plasticity (β) across life stages, but estimated phenotypic correlations were positive for both cold and heat hardiness, though only

statistically significant for cold hardiness (Figure B.4A). This raises the possibility that similar sets of genetic variants may affect the acclimation response in both larvae and adults, a somewhat surprising result given the lack of cross-stage genetic correlations for thermal hardiness at either acclimation temperature. However, a more complex quantitative genetic experimental design (e.g., split brood) and/or mutant genetic screens will be necessary to directly test this hypothesis. Nevertheless, this result provides evidence that selection may constrain the acclimation response of a stress-related trait across development but not the stress response mechanism(s), allowing each developmental stage to adapt to their unique environmental stressors while maintaining a general plastic response common across development.

In addition to the evidence suggesting genetic decoupling of thermal hardiness, our results show that larvae were more heat-hardy while adults were more cold-hardy (Fig. 3.2A,B). Higher cold hardiness in adult vs larval *Drosophila* has been widely observed (Czajka and Lee 1990; Jensen et al. 2007; Bing et al. 2012). However, to our knowledge, there are no other reports of higher heat tolerance in larvae compared to adults. This trend persisted at both developmental acclimation temperatures, but was more pronounced when flies were developmentally acclimated at the temperature closer to the test temperature (Fig. 3.2A,B). Stage-specific thermal phenotypes are a common observation across insects (Neargarder et al. 2003; Marias et al. 2009; Kingsolver et al. 2011; Radchuk et al. 2013) and other taxa (Diederich and Pechenik 2013; Turschwell et al. 2017). Our findings and these others are consistent with the adaptive decoupling hypothesis, which postulates that different developmental stages are relatively free to evolve in response to unique niches that vary across the life cycle, allowing for stage-specific niche adaptation (Moran 19994).

Different morphologies, behaviors, and physiologies allow each stage in a complex life cycle to be specialized for different environments. Extreme differences in appendages, mouthparts, digestive systems, etc. between larval and adult stages of holometabolous insects clearly illustrate decoupling at the morphological level. Our results support decoupling of physiology as well, in this case, thermal stress responses that often include highly conserved cellular responses such as inducible heat shock protein production. The observed differences in thermal hardiness are consistent with differences in larval and adult thermal niches. Larvae are generally unable to move from the area in which they are oviposited, often a rotting piece of fruit that may contain high levels of ethanol through fermentation of organic matter and is exposed relatively extreme high temperatures (David and Van Herrewege 1983; Lachaise et al. 1988; Feder et al. 1997). Because larvae have limited movement relative to adults, they likely require mechanisms to tolerate sustained high temperatures (Dillon et al. 2009). Conversely, adults can mitigate high temperatures by either moving via flight or behaviorally dispersing heat via other mechanisms (reviewed in Dillon et al. 2009). However, adults of *D. melanogaster* experience more extreme cold temperatures compared to larvae because adults are the primary overwintering stage (Saunders et al. 1989; Schmidt et al. 2005). In addition to diapause-related responses such as ovarian developmental arrest (Saunders et al. 1989), overwintering adults also tend to be more resistant to other environmental stressors which may include cold hardiness (Schmidt et al. 2005; Czajka and Lee 1990). Both the higher basal cold tolerance of adults compared to larvae and the marked effect of developmental acclimation at a lower rearing temperatures in adults (Fig. 3.2A) support the idea that the adult stage is more well suited for colder environments. Conversely, larvae exhibit a more pronounced developmental acclimation to heat stress from warmer rearing conditions (Fig. 3.2B), providing evidence that larvae are

more well suited for extreme heat. Given the observed lack of cross-stage genetic correlation in this and previous studies, we contend that genetic decoupling of thermal physiology facilitates the independent evolution of larval and adult thermal physiology that maximize fitness in relatively warmer and cooler environments, respectively.

Cross-Environment and Cross-Trait Correlations

Although a lack of genetic correlation was observed between developmental stages, we estimated strong genetic and phenotypic correlation for thermal hardiness across developmental acclimation conditions within developmental stages for both cold hardiness and heat hardiness (Table 3.2B). These results indicate that, within a developmental stage, many segregating genetic variants influencing thermal hardiness under one developmental acclimation condition are likely to also influence thermal hardiness in the other developmental acclimation condition. In other words, acclimation responses, however strong (e.g., cold acclimation in adults; Fig. 3.3A), do not completely change the underlying physiological responses to temperature stress. Thus, plastic responses activated by changes in developmental acclimation condition can affect overall survival by either enhancing or inhibiting the efficacy of established mechanisms used to combat thermal stress while the genetic architectures underlying these mechanisms remain largely unchanged (Schlichting and Smith 2002).

In contrast, heat hardiness and cold hardiness were not genetically correlated in both larvae developmentally acclimated at 25°C and adults under both developmental acclimation conditions (Table 3.2C; Figure B.4). We also investigated the relationship between cold stress plasticity (β_C) and heat stress plasticity (β_H) within developmental stages and found no correlation between the two in both larvae and adults (Figure B.3B). This result indicates that some mechanisms underlying cold hardiness and heat hardiness (and acclimation responses

affecting each trait) are distinct and that *D. melanogaster* larvae and adults probably employ unique mechanisms to deal with each stress type. Indeed, it has been shown that the majority of loci significantly associated with or significantly differentially expressed during heat hardiness and cold hardiness are unique in *D. melanogaster* (Morgan and Mackay 2006; Norry et al. 2008) and other insects (Zhang et al. 2015). At the sub-cellular level there is evidence for some common pathways and mechanisms underlying hardiness at both extremes (inducible expression of heat shock proteins; Burton et al. 1988) However, extreme heat and extreme cold affect cells (Hochachka and Somero 1984; Denlinger and Yocum 1998; Neven 2000) and tissues (Teets and Denlinger 2013; MacMillan et al. 2015a,b) in very different ways. The distinct physiological consequences of extreme heat or extreme cold are likely the cause of the lack of phenotypic and genetic correlation between stress types as different response mechanisms are likely at work.

Surprisingly, cold hardiness and heat hardiness were moderately genetically correlated in larvae developmentally acclimated at 18°C (Table 3.2C; Figure B.4A). Though we did not observe any significant cross-stage genetic correlations at any developmental acclimation temperature, this result does illustrate how the environment can influence genetic covariance among traits. Given that larvae appear to be less cold stress adapted, developmental acclimation at 18°C may be chronically stressful, upregulating a general stress response that protects against multiple stressors. There is evidence for a general stress response in yeasts and *Drosophila* (Gasch et al. 2000; Sørensen et al. 2017), and other studies have documented that acclimation in one environment enhances resistance to multiple stressors (Hoffmann 1990; Krebs and Loeschcke 1994; Aggarwal et al. 2013). If such general, protective responses often produce genetic correlations among stress responses, the correlated evolution of multi-stress resistance in response to natural selection imposed by one particular stressor may be a general phenomenon.

Indeed, artificial selection on one stressor often results in the correlated evolution of other stress responses (Hoffmann and Parsons 1989: Bubliy and Loeschcke 2005). However, our results suggest that these multi-trait correlations, and thus correlated evolution may depend on both developmental stage and on the developmental environment.

Summary

Overall, our results provide substantial evidence that different sets of segregating genetic variants influence thermal hardiness and developmental acclimation in larval and adult *D. melanogaster*. We do provide evidence that environmental variation can substantially alter genetic correlations among traits (heat hardiness and cold hardiness), but not genetic correlations across development. Our results are consistent with the apparent, independent, stage-specific adaptation to distinct thermal niches by different developmental stages in insects. However, the specific physiological responses to thermal stress that are unique to juvenile and adult stages remain undescribed and require further study. Furthermore, it is important to determine if species with similar life histories also exhibit unconstrained thermal hardiness responses across ontogeny. This knowledge is an important consideration to make when attempting to model the evolutionary trajectories of species in a world where the climate and seasonality may rapidly change.

Acknowledgements

This work was supported by National Science Foundation awards NSF DEB 1638951 and NSF IOS 1256930 to G.J.R. and NSF DBI 1460802 to T.J.M. This work was also supported by the Kansas State Agricultural Research and Extension. At the time of this dissertation's submission, this chapter was submitted in 2018 to the journal *Heredity*.

References

Aggarwal, D.D., Ranga, P., Kalra, B., Parkash, R., Rashkovetsky, E., and Bantis, L.E. (2013). Rapid effects of humidity acclimation on stress resistance in *Drosophila melanogaster*. Comp Biochem Physiol C Toxicol Pharmacol *166*, 81–90.

Anderson, B.B., Scott, A., and Dukas, R. (2016). Social behavior and activity are decoupled in larval and adult fruit flies. Behav. Ecol *27*, 820–828.

Ashburner, M. (1981). The genetics and biology of *Drosophila* (New York: Academic Press).

Ayrinhac, A., Debat, V., Gibert, P., Kister, A.-G., Legout, H., Moreteau, B., Vergilino, R., and David, J.R. (2004). Cold adaptation in geographical populations of *Drosophila melanogaster*: phenotypic plasticity is more important than genetic variability. Funct. Ecol *18*, 700–706.

Bale, J.S., and Hayward, S.A.L. (2010). Insect overwintering in a changing climate. J. Exp. Biol *213*, 980–994.

Bing, X., Zhang, J., and Sinclair, B.J. (2012). A comparison of *Frost* expression among species and life stages of *Drosophila*. Insect Mol. Biol. *21*, 31–39.

Bowler, K., and Terblanche, J.S. (2008). Insect thermal tolerance: what is the role of ontogeny, ageing and senescence? Biol Rev Camb Philos Soc. *83*, 339–355.

Bubliy, O.A., and Loeschcke, V. (2005). Correlated responses to selection for stress resistance and longevity in a laboratory population of *Drosophila melanogaster*. J. Evol. Biol *18*, 789–803.

Burton, V., Mitchell, H.K., Young, P., and Petersen, N.S. (1988). Heat shock protection against cold stress of *Drosophila melanogaster*. Mol. Cell. Biol *8*, 3550–3552.

Chatterjee, N., Pal, A.K., Manush, S.M., Das, T., and Mukherjee, S.C. (2004). Thermal tolerance and oxygen consumption of *Labeo rohita* and *Cyprinus carpio* early fingerlings acclimated to three different temperatures. J Therm Biol. *29*, 265–270.

Colinet, H., and Hoffmann, A.A. (2012). Comparing phenotypic effects and molecular correlates of developmental, gradual and rapid cold acclimation responses in *Drosophila melanogaster*: *Cold acclimation and stress response*. Funct. Ecol *26*, 84–93.

Cuculescu, M., Hyde, D., and Bowler, K. (1998). Thermal tolerance of two species of marine crab, *Cancer pagurus* and *Carcinus maenas*. J Therm Biol. *23*, 107–110.

Czajka, M.C., and Lee, R.E. (1990). A rapid cold-hardening response protecting against cold shock injury in *Drosophila melanogaster*. J. Exp. Biol *148*, 245–254.

Das, T., Pal, A.K., Chakraborty, S.K., Manush, S.M., Chatterjee, N., and Mukherjee, S.C. (2004). Thermal tolerance and oxygen consumption of Indian Major Carps acclimated to four temperatures. J Therm Biol. *29*, 157–163.

David, J.R., and Van Herrewege, J. (1983). Adaptation to alcoholic fermentation in Drosophila species: relationship between alcohol tolerance and larval habitat. Comp Biochem Physiol A Mol Integr Physiol *74*, 283–288.

De Jong, G. (1990). Genotype-by-environment interaction and the genetic covariance between environments: multilocus genetics. Genetica *81*, 171–177.

Denlinger, D.L., and Yocum, G.D. (1998). Physiology of heat sensitivity. In Hallman, G.J., Denlinger D.L. (Eds). Temperature Sensitivity in Insects and Application in Intergrated Pest Management, (Boulder, CO: Westview Press), pp. 7–54.

Diederich, C., and Pechenik, J. (2013). Thermal tolerance of *Crepidula fornicata* (Gastropoda) life history stages from intertidal and subtidal subpopulations. Mar Ecol Prog Ser. *486*, 173–187.

Dierks, A., Kölzow, N., Franke, K., and Fischer, K. (2012). Does selection on increased cold tolerance in the adult stage confer resistance throughout development? J. Evol. Biol. *25*, 1650–1657.

Dillon, M.E., Wang, G., Garrity, P.A., and Huey, R.B. (2009). Thermal preference in *Drosophila*. J Therm Biol. *34*, 109–119.

Everman, E.R., and Morgan, T.J. (2018). Antagonistic pleiotropy and mutation accumulation contribute to age-related decline in stress response. Evolution *72*, 303–317.

Everman, E.R., Freda, P.J., Brown, M., Schieferecke, A.J., Ragland, G.J., and Morgan, T.J. (2018). Ovary development and cold tolerance of the invasive pest *Drosophila suzukii* (Matsumura) in the central plains of Kansas, United States. Environ. Entomol. *47*, 1013–1023.

Falconer, D.S., and Mackay, T.F.C. (1996). Introduction to Quantitative Genetics (Essex: Longman Group Limited).

Fallis, L.C., Fanara, J.J., and Morgan, T.J. (2012). Genetic variation in heat-stress tolerance among South American *Drosophila* populations. Genetica *139*, 1331–1337.

Fallis, L.C., Fanara, J.J., and Morgan, T.J. (2014). Developmental thermal plasticity among *Drosophila melanogaster* populations. J Evol Biol. *27*, 557–564.

Feder, M.E., Blair, N., and Figueras, H. (1997). Natural thermal stress and heat-shock protein expression in Drosophila larvae and pupae. Funct. Ecol *11*, 90–100.

Freda, P.J., Alex, J.T., Morgan, T.J., and Ragland, G.J. (2017). Genetic decoupling of thermal hardiness across metamorphosis in *Drosophila melanogaster*. Integr. Comp. Biol *57*, 999–1009.

Gasch, A.P., Spellman, P.T., Kao, C.M., Carmel-Harel, O., Eisen, M.B., Storz, G., Botstein, D., and Brown, P.O. (2000). Genomic expression programs in the response of yeast cells to environmental changes. Mol. Biol. Cell *11*, 4241–4257.

Gerken, A.R., Eller, O.C., Hahn, D.A., and Morgan, T.J. (2015). Constraints, independence, and evolution of thermal plasticity: Probing genetic architecture of long- and short-term thermal acclimation. Proc. Natl. Acad. Sci. U.S.A. *112*, 4399–4404.

Gibert, P., and Huey, R.B. Chill-coma temperature in *Drosophila*: effects of developmental temperature, latitude, and phylogeny. Physiol Biochem Zool. *74*, 429–434.

Gilchrist, G.W., Huey, R.B., and Partridge, L. (1997). Thermal sensitivity of *Drosophila melanogaster*: evolutionary responses of adults and eggs to laboratory natural selection at different temperatures. Physiol Zool. *70*, 403–414.

Harbison, S.T., McCoy, L.J., and Mackay, T.F. (2013). Genome-wide association study of sleep in *Drosophila melanogaster*. BMC Genom. *14*, 281.

Hochachka, P.W., and Somero, G.N. (1984). Biochemical Adaptation (New York: Oxford University Press).

Hoffmann, A.A. (1990). Acclimation for desiccation resistance in *Drosophila melanogaster* and the association between acclimation responses and genetic variation. J Insect Physiol. *36*, 885–891.

Hoffmann, A.A., and Parsons, P.A. (1989). Selection for increased desiccation resistance in *Drosophila melanogaster*: Additive genetic control and correlated responses for other stresses. Genetics *122*, 837–845.

Hoffmann, A.A., and Watson, M. Geographical variation in the acclimation responses of *Drosophila* to temperature extremes. Am. Nat. *142*, 93–113.

Huang, W., Massouras, A., Inoue, Y., Peiffer, J., Ramia, M., Tarone, A.M., Turlapati, L., Zichner, T., Zhu, D., Lyman, R.F., et al. (2014). Natural variation in genome architecture among 205 *Drosophila melanogaster* Genetic Reference Panel lines. Genome Res. *24*, 1193–1208.

Jensen, D., Overgaard, J., and Sørensen, J.G. (2007). The influence of developmental stage on cold shock resistance and ability to cold-harden in *Drosophila melanogaster*. J Insect Physiol. *53*, 179–186.

Jentsch, A., Kreyling, J., and Beierkuhnlein, C. (2007). A new generation of climate-change experiments: events, not trends. Front. Ecol. Environ. *5*, 365–374.

Johansson, F., Lederer, B., and Lind, M.I. (2010). Trait performance correlations across life stages under environmental stress conditions in the common frog, *Rana temporaria*. PLoS ONE *5*, e11680.

Kelty, J.D., and Lee, Jr, R.E. (1999). Induction of rapid cold hardening by cooling at ecologically relevant rates in *Drosophila melanogaster*. J Insect Physiol. *45*, 719–726.

Kelty, J.D., and Lee, Jr, R.E. (2001). Cold-hardening of *Drosophila melanogaster*. J. Exp. Biol *204*, 1659–1666.

Kingsolver, J.G., Arthur Woods, H., Buckley, L.B., Potter, K.A., MacLean, H.J., and Higgins, J.K. (2011). Complex life cycles and the responses of insects to climate change. Integr. Comp. Biol *51*, 719–732.

Kodra, E., Steinhaeuser, K., and Ganguly, A.R. (2011). Persisting cold extremes under 21st-century warming scenarios. Geophys. Res. Lett. *38*, 1–5.

Krebs, R.A., and Loeschcke, V. (1994). Effects of exposure to short-term hear stress on fitness components in *Drosophila melanogaster*. J. Evol. Biol. *7*, 39–49.

Krebs, R.A., and Loeschcke, V. (1995). Resistance to thermal stress in preadult *Drosophila buzzatii*: variation among populations and changes in relative resistance across life stages. Biol. J. Linn. Soc *56*, 517–531.

Lachaise, D., Cariou, M.-L., David, J.R., Lemeunier, F., Tsacas, L., and Ashburner, M. (1988). Historical Biogeography of the *Drosophila melanogsater* species subgroup. In Hecht, M.K, Wallace, B., Prance, G.T. (Eds) Evoltionary Biology, Evolutionary Biology, (Boston, MA: Springer), p.

Lande, R. (2009). Adaptation to an extraordinary environment by evolution of phenotypic plasticity and genetic assimilation. J. Evol. Biol. *22*, 1435–1446.

Lande, R., and Arnold, S.J. (1983). The measurement of selection on correlated characters. Evolution *37*, 1210–1226.

Lee, R. (1991). Insects at Low Temperature (Springer US).

Levy, O., Buckley, L.B., Keitt, T.H., Smith, C.D., Boateng, K.O., Kumar, D.S., and Angilletta, M.J. (2015). Resolving the life cycle alters expected impacts of climate change. Proc. R. Soc. B *282*, 20150837.

Loeschcke, V., and Krebs, R.A. (1996). Selection for heat-shock resistance in larval and in adult *Drosophila buzzatii*: comparing direct and indirect responses. Evolution *50*, 2354–2359.

Lynch, M., and Gabriel, W. (1987). Environmental tolerance. Am. Nat. *129*, 283–303.

Lynch, M., and Walsh, B. (1998). Genetics and Analysis of Quantitative Traits (Sunderland, Mass: Sinauer Associates is an imprint of Oxford University Press).

Mackay, T.F.C., Richards, S., Stone, E.A., Barbadilla, A., Ayroles, J.F., Zhu, D., Casillas, S., Han, Y., Magwire, M.M., Cridland, J.M., et al. (2012). The *Drosophila melanogaster* Genetic Reference Panel. Nature *482*, 173–178.

MacMillan, H.A., Andersen, J.L., Davies, S.A., and Overgaard, J. (2015a). The capacity to maintain ion and water homeostasis underlies interspecific variation in *Drosophila* cold tolerance. Scientific Reports *5*, 18607.

MacMillan, H.A., Andersen, J.L., Loeschcke, V., and Overgaard, J. (2015b). Sodium distribution predicts the chill tolerance of *Drosophila melanogaster* raised in different thermal conditions. Am. J. Physiol. Regul. Integr. Comp. Physiol. *308*, R823–R831.

McGraw, J.B., and Antonovics, J. (1983). Experimental ecology of *Dryas octopetala* ecotypes: I. Ecotypic differentiation and life-cycle stages of selection. J. Ecol. *71*, 879.

Moran, N. (1994). Adaptation and constraint in the complex life cycles of animals. Annu. Rev. Ecol. Evol. Syst. *2*, 573–600.

Morgan, T.J., and Mackay, T.F.C. (2006). Quantitative trait loci for thermotolerance phenotypes in *Drosophila melanogaster*. Heredity *96*, 232.

Neargarder, G., Dahlhoff, E.P., and Rank, N.E. (2003). Variation in thermal tolerance is linked to phosphoglucose isomerase genotype in a montane leaf beetle. Funct. Ecol. *17*, 213–221.

Neven, L.G. (2000). Physiological responses of insects to heat. Postharvest Biol Technol. *21*, 103–111.

Noh, S., Everman, E.R., Berger, C.M., and Morgan, T.J. (2017). Seasonal variation in basal and plastic cold tolerance: Adaptation is influenced by both long- and short-term phenotypic plasticity. Ecol. Evol *7*, 5248–5257.

Norry, F.M., Scannapieco, A.C., Sambucetti, P., Bertoli, C.I., and Loeschcke, V. (2008). QTL for the thermotolerance effect of heat hardening, knockdown resistance to heat and chill-coma recovery in an intercontinental set of recombinant inbred lines of *Drosophila melanogaster*. Mol. Ecol. *17*, 4570–4581.

Nöthiger, R. (1970). Sucrose density separation: A method for collecting large numbers of *Drosophila* larvae. Dros. Inf. Serv *45*, 177.

Overgaard, J., Sørensen, J.G., Petersen, S.O., Loeschcke, V., and Holmstrup, M. (2005). Changes in membrane lipid composition following rapid cold hardening in *Drosophila melanogaster*. J Insect Physiol. *51*, 1173–1182.

Overgaard, J., Tomčala, A., Sørensen, J.G., Holmstrup, M., Krogh, P.H., Šimek, P., and Koštál, V. (2008). Effects of acclimation temperature on thermal tolerance and membrane phospholipid composition in the fruit fly *Drosophila melanogaster*. J Insect Physiol. *54*, 619–629.

Pigliucci, M. (2005). Evolution of phenotypic plasticity: where are we going now? Trends Ecol Evol. *20*, 481–486.

R Core Team (2018). R: a language and environment for statistical computing. (Vienna, Austria: R Foundation for Statistical Computing).

Radchuk, V., Turlure, C., and Schtickzelle, N. (2013). Each life stage matters: the importance of assessing the response to climate change over the complete life cycle in butterflies. J. Animal Ecol. *82*, 275–285.

Ragland, G.J., and Kingsolver, J.G. (2008). Evolution of thermotolerance in seasonal environments: the effects of annual temperature variation and life-history timing in *Wyeomyia smithii*. Evolution *62*, 1345–1357.

Rawson, P.D., and Hilbish, T.J. (1991). Genotype-environment interaction for juvenile growth in the hard clam *Mercenaria mercenaria* (L.). Evolution *45*, 1924–1935.

Roff, D.A. (1996). The evolution of genetic correlations: An analysis of patterns. Evolution *50*, 1392–1403.

Saunders, D.S., Henrich, V.C., and Gilbert, L.I. (1989). Induction of diapause in *Drosophila melanogaster*: photoperiodic regulation and the impact of arrhythmic clock mutations on time measurement. Proc. Natl. Acad. Sci. U.S.A. *86*, 3748–3752.

Schlichting, C.D., and Smith, H. (2002). Phenotypic plasticity: linking molecular mechanisms with evolutionary outcomes. Evol. Ecol. *16*, 189–211.

Schluter, D., Price, T.D., and Rowe, L. (1991). Conflicting selection pressures and life history trade-offs. Proc. Royal Soc. Lond. [Biol] *246*, 11–17.

Schmidt, P.S., Matzkin, L., Ippolito, M., and Eanes, W.F. (2005). Geographic variation in diapause incidence, life-history traits, and climatic adaptation in *Drosophila melanogaster*. Evolution *59*, 1721–1732.

Shaffer, H.B., Austin, C.C., and Huey, R.B. (1991). The consequences of metamorphosis on salamander (Ambystoma) locomotor performance. Physiol. Zool. *64*, 212–231.

Sinclair, B.J., Marshall, K.E., Sewell, M.A., Levesque, D.L., Willett, C.S., Slotsbo, S., Dong, Y., Harley, C.D.G., Marshall, D.J., Helmuth, B.S., et al. (2016). Can we predict ectotherm responses to climate change using thermal performance curves and body temperatures? Ecol. Lett. *19*, 1372–1385.

Sørensen, J.G., Schou, M.F., and Loeschcke, V. (2017). Evolutionary adaptation to environmental stressors: a common response at the proteomic level. Evolution *71*, 1627–1642.

Steppan, S.J., Phillips, P.C., and Houle, D. (2002). Comparative quantitative genetics: evolution of the G matrix. Trends Ecol. Evol. *17*, 320–327.

Teets, N.M., and Denlinger, D.L. (2013). Physiological mechanisms of seasonal and rapid cold-hardening in insects: Seasonal and rapid cold-hardening in insects. Physiol. Entomol. *38*, 105–116.

Terblanche, J.S., Sinclair, B.J., Jaco Klok, C., McFarlane, M.L., and Chown, S.L. (2005). The effects of acclimation on thermal tolerance, desiccation resistance and metabolic rate in *Chirodica chalcoptera* (Coleoptera: Chrysomelidae). J Insect Physiol. *51*, 1013–1023.

Tucić, N. (1979). Genetic capaticy for adaptation to cold resistance at different developmental dtages of *Drosophila melanogaster*. Evolution *33*, 350–358.

Turschwell, M.P., Balcombe, S.R., Steel, E.A., Sheldon, F., and Peterson, E.E. (2017). Thermal habitat restricts patterns of occurrence in multiple life-stages of a headwater fish. Freshw. Sci. *36*, 402–414.

Via, S., and Lande, R. (1985). Genotype-environment interaction and the evolution of phenotypic plasticity. Evolution *39*, 505.

West-Eberhard, M.J. (1989). Phenotypic plasticity and the origins of diversity. Annu. Rev. Ecol. Evol. Syst. *20*, 249–278.

Woods, H.A. (2013). Ontogenetic changes in the body temperature of an insect herbivore. Funct. Ecol. *27*, 1322–1331.

Zhang, Y., Wu, H., Xie, J., Jiang, R., Deng, C., and Pang, H. (2015). Transcriptome responses to heat- and cold-stress in ladybirds (*Cryptolaemus montrouzieri* Mulasnt) analyzed by deep-sequencing. Biol. Res. *48*.

Chapter 3 Figures

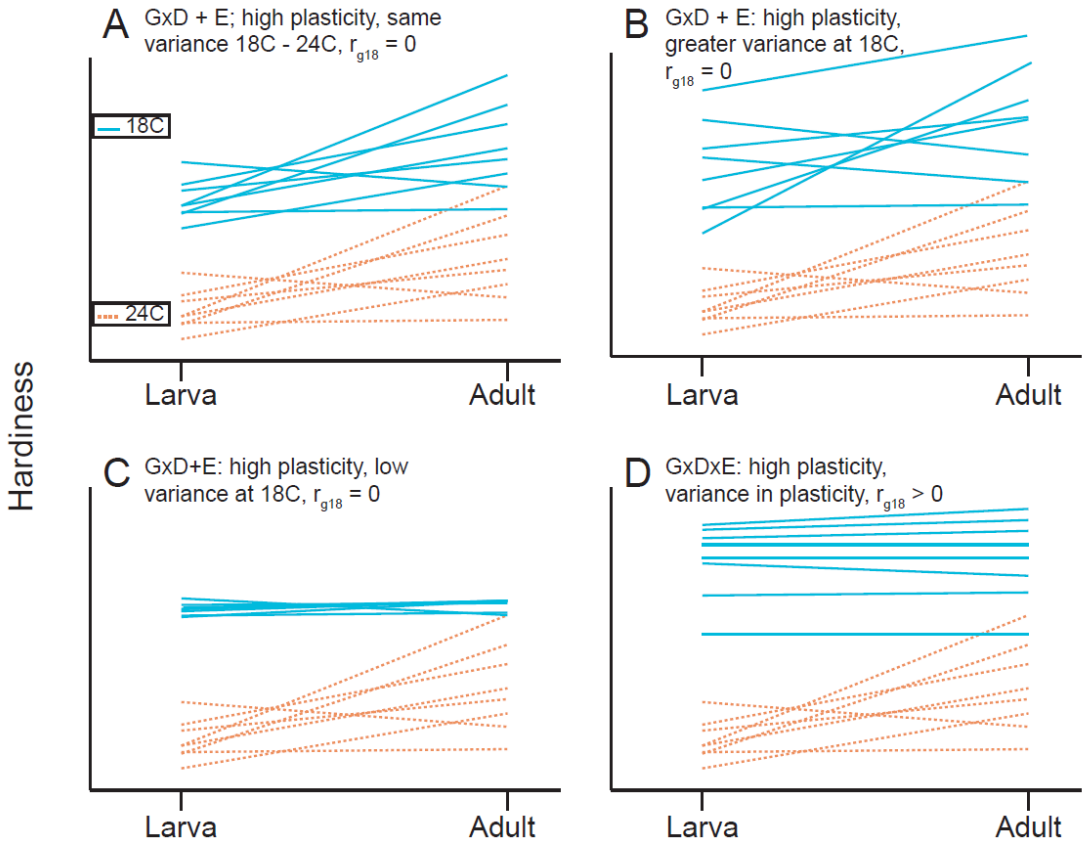

Figure 3.1 Examples of Interactions Between Genotype, Environment, and Development

Hypothetical relationship between genetic (co)variance, developmental stage, and acclimation temperature. Each colored line represents the relationship between larval and adult cold hardiness for a single genotype reared at either 18°C (blue/solid; cool) or 25°C (orange/dashed; warm). In these examples, genetic variation exists for thermal hardiness but crossing lines (genotypes) illustrates a lack of genetic correlation between stages at 25°C (r_{g25} = 0). Acclimation at 18°C compared to 25°C increases mean hardiness in all scenarios and either A) does not change genetic variance, B) increases or C) decreases variance in both stages. In scenarios, A-C, the relative rank of genotypes does not change in response to rearing temperature (lines remain crossing), resulting in a lack of genetic correlation at 18°C (i.e. r_{g18} = 0). These

scenarios illustrate an effect of acclimation environment (E) independent of Genotype by Development (GxD) interactions. In contrast, (D) illustrates a GxDxE wherein changes in genotype rank order at 18°C cause a positive genetic correlation, illustrated by roughly parallel blue lines.

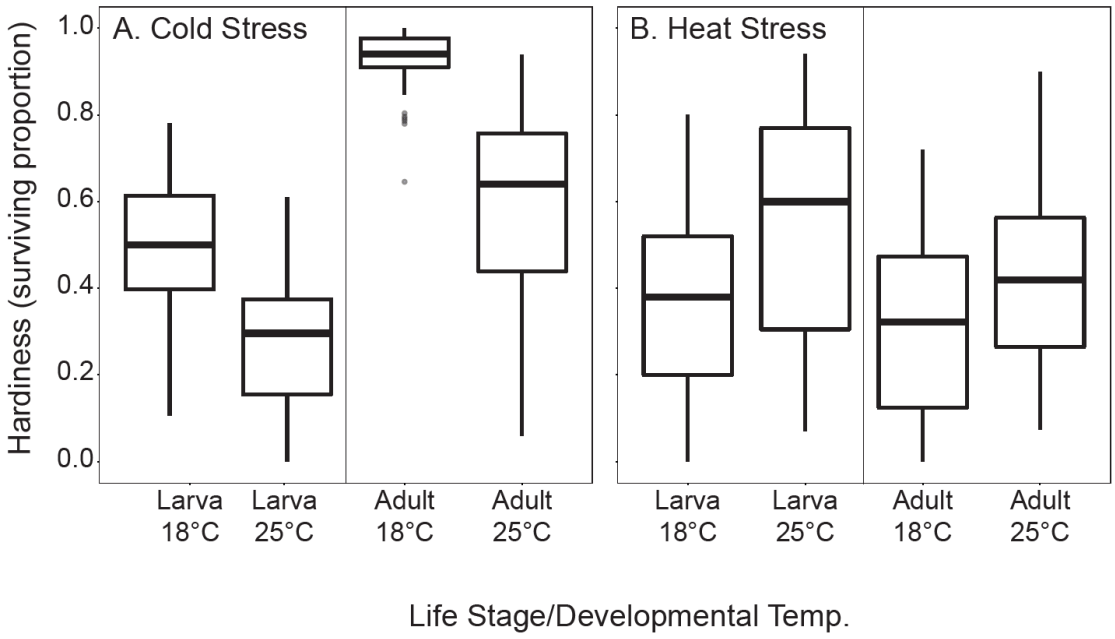

Figure 3.2 Average Adult vs. Average Larval Thermal Hardiness

Adult and larval thermal hardiness at different acclimation temperatures and life stages, and the relationship between hardiness across stages. Boxplots represent the 1st and 3rd quartiles, median, and 1.5xIQR for the distribution of cold (A) and heat (B) hardiness for all 39 DGRP lines under both acclimation conditions (18 or 25°C).

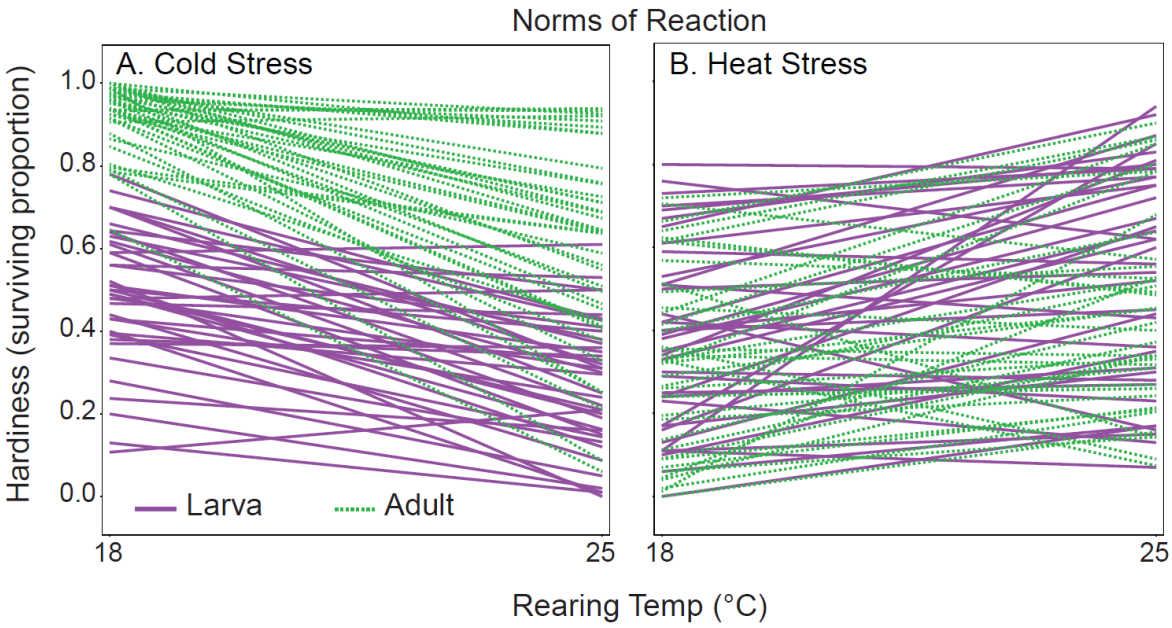

Figure 3.3 Norms of Reaction across Acclimation Temperature in Larvae and Adults

Norms of reaction relating cold stress (A) and heat stress (B) to acclimation temperature in larvae and adults. Each line represents the mean hardiness for a genotype at both rearing temperatures. Purple/solid lines represent larval data while green/dashed lines represent adult data.

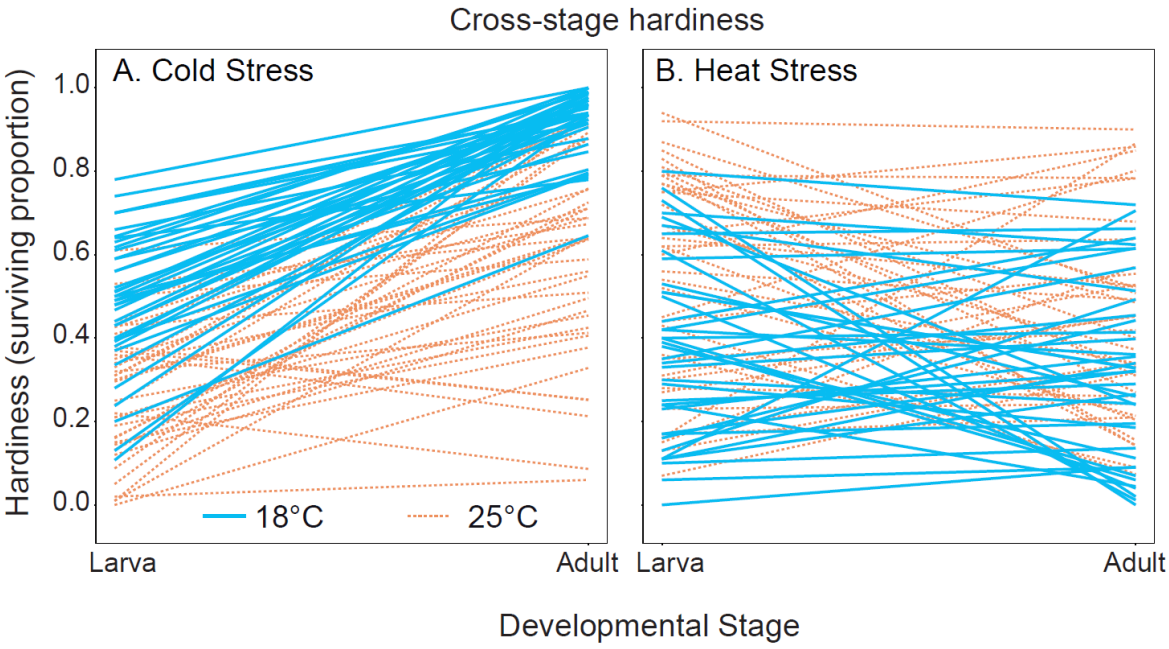

Figure 3.4 Average Thermal Hardiness across Development in each Genotype

Average cold (a) and heat (b) hardiness for each genotype measured in the larval or the adult stage. Each line represents the average values for a single genotype measured after rearing at either 18C (blue/solid) or 25C (orange/dashed). This figure re-plots the data in Figure 3.3 to illustrate how genetic variance changes across life stages; compare to Table 3.2, which provides hypothesized patterns of genetic variance vs. rearing environment vs. developmental stage.

Chapter 3 Tables

	Stage	Rearing Temp.	trait	H^2
a.				
	Adult	18	cold	0.25 (0.11 - 0.36) ***
				0.13 (0.062 - 0.19)
	Larva	18	cold	***
	Adult	25	cold	0.35 (0.20 - 0.44) ***
				0.21 (0.073 - 0.34)
	Larva	25	cold	***
b				
	Adult	18	heat	0.45 (0.29 - 0.56) ***
	Larva	18	heat	0.30 (0.17 - 0.41) ***
	Adult	25	heat	0.36 (0.24 - 0.45) ***
	Larva	25	heat	0.34 (0.25 - 0.42) ***
c				
			cold	0.13 (0.058 - 0.20)
	Adult	18 & 25	plasticity	***
			cold	0.069 (0.037 - 0.11)
	Larva	18 & 25	plasticity	***
			heat	0.17 (0.086 - 0.27)
	Adult	18 & 25	plasticity	***
			heat	0.13 (0.065 - 0.21)
	Larva	18 & 25	plasticity	***

Table 3.1 Heritability Estimates for Thermal Hardiness

Heritability estimates for cold hardiness (cold), heat hardiness (heat), and plasticity of cold and heat hardiness. The point estimate is followed by the 95% Confidence Interval, in parentheses. *** indicates $p < 0.001$ based on permutation tests.

Comparison	Stage(s)	Rearing Temp(s).	trait	r_p	r_g
a					
Cross-stage	Adult vs. Larva	18	cold	0.019	0.16 (-0.26 - 0.49)
Cross-stage	Adult vs. Larva	25	cold	0.010	0.055 (-0.51 - 0.59)
Cross-stage	Adult vs. Larva	18	heat	0.023	0.051 (-0.33 - 0.48)
Cross-stage	Adult vs. Larva	25	heat	0.020	0.14 (-0.15 - 0.40)
Cross-stage	Adult vs. Larva	18 & 25	cold plasticity	0.34 (0.091 - 0.57) *	-
Cross-stage	Adult vs. Larva	18 & 25	heat plasticity	0.24 (0.014 - 0.49)	-
b					
Cross-temp	Adult	18 vs. 25	cold	0.34*	0.73 (0.32 - 0.88)*
Cross-temp	Larva	18 vs. 25	cold	0.26*	0.68 (0.44 - 0.89)*
Cross-temp	Adult	18 vs. 25	heat	0.31*	0.45 (0.17 - 0.57)*
Cross-temp	Larva	18 vs. 25	heat	0.33*	0.64 (0.35 - 0.85)*
c					
Cross-trait	Adult	18	heat vs. cold	0.070	0.11 (0.0067 – 0.11)
Cross-trait	Adult	25	heat vs. cold	0.00021	0.10 (-0.21 – 0.26)

Cross-trait	Larva	18	heat vs. cold	0.16*	0.51 (0.20 - 0.73)*
Cross-trait	Larva	25	heat vs. cold	0.037	0.15 (-0.41 - 0.71)
Cross-trait	Adult	18 & 25	heat vs. cold plasticity	0.17 (-0.23 - 0.25)	-
Cross-trait	Larva	18 & 25	heat vs. cold plasticity	0.016 (-0.13 - 0.40)	-

Table 3.2 Genetic and Phenotypic Correlation Estimates

Genetic (r_G) and phenotypic (r_P) correlation estimates for cold hardiness (cold), heat hardiness (heat), and plasticity of cold and heat hardiness across stages (a; adult vs. larvae), temperatures (b; 18 vs. 25C), and traits (c; cold vs. heat hardiness). The point estimate is followed by the 95% Confidence Interval, in parentheses. * indicates $p < 0.05$ based on permutation tests for r_G or $p < 0.05$ for r_P based on linear regression.

Chapter 4 - Unique Cold-Induced Gene Expression across Developmental Stages but not among Different Cold Hardiness Phenotypes in *D. melanogaster*

Abstract

The environment that an organism experiences during their life cycle changes over seasons. Additionally, organisms are in a constant state of physiological and morphological change during growth and development. These changes are dramatic for organisms that undergo complex life cycles, possibly allowing each life stage to evolve unique responses to changing habitats and stress. In the holometabolous insects, including *Drosophila melanogaster*, previous research has illustrated that a lack of genetic correlation across the metamorphic boundary for thermal hardiness, with unique genomic regions associated with thermal stress in larva and adults. However, it is not currently understood if larvae and adults achieve cold hardiness via similar mechanisms. To address this question, we exposed 6 isogenic genotypes previously found to show differential phenotypic performance across metamorphosis in *D. melanogaster* to an acute exposure to extreme cold and measured whole-body RNA from 4 time points following cold-exposure to determine the expression trajectories of cold-induced genes. Furthermore, we determined the level of differential expression within phenotypic classes in each life stage to determine if the mechanisms of cold hardiness are similar among genotypes. Together, we find that the expression profiles of adults and larvae are unique and that many established mechanisms of adult cold hardiness are not activated in larvae. Additionally, we provide evidence that genotypes with different larval and adult cold hardiness achieve these phenotypes in genotypically unique ways. These results provide evidence that the mechanisms employed by

larvae and adults to respond to cold stress are unique and decoupled across the metamorphic boundary in *D. melanogaster*. Additionally, we also provide evidence that there are multiple ways to achieve cold hardiness across ontogeny in *D. melanogaster*.

Introduction

The environment an organism experiences is dynamic. As an organism develops, many biotic and abiotic factors are altered and shifted such as resource availability, predator abundance, and thermal environment. (Krebs and Loeschcke 1995; Ragland and Kingsolver 2008; Woods 2013). These changes in the environment may result in stage-specific evolutionary trajectories as selective pressures are altered in response to changes in the external environment. In organisms with complex cycles, where alternate developmental stages exhibit distinct morphologies, physiologies, and behaviors, stage specific adaptation may result in responses to distinct ecological niches (i.e. larval stages associated with feeding and growth and adult stages associated with mating and dispersal) (McGraw and Antonovics 1983; Scluter et al. 1991; Moran 1994; Kingsolver 2011).

If stage-specific adaptation occurs in natural systems, then these stage specific responses will be facilitated if little to no genetic correlations exists for traits across life stages (Moran 1994). This conclusion has been inferred or empirically observed in several studies that explore thermal hardiness in insects and are discussed below. Thermal hardiness is the ability of animals to maintain performance after experiencing extreme thermal conditions and has been used as a metric to study environmental adaptation in many insect systems (Hoffmann and Watson 1993; Bale and Hayward 2010). Several studies have documented a lack of correlation between thermal hardiness phenotypes in different life stages in holometabolous insects via direct quantitative genetic assessment (Loeschcke and Krebs 1996; Gilchrist et al. 1997; Dierks et al. 2012) or

indirect responses to selection (Tucić, 1979). We recently demonstrated a lack of both phenotypic and genetic correlations for cold hardiness between adults and larvae of *D. melanogaster* as well as unique statistical associations of genomic regions with the variation observed in thermal hardiness in each of these life stages (Freda et al. 2017). In summary, significant evidence exists for the decoupling of genetic variation for thermal hardiness across the metamorphic boundary in several holometabolous insect systems. However, substantial evidence has not been provided to determine if different developmental stages employ unique physiological responses (whether genetically variable or not) to combat thermal stress.

Mechanisms by which insects cope with the detrimental effects of extreme cold include alterations to cell membranes, cryoprotect synthesis, use of molecular chaperones, and alterations to ion transport mechanisms across cell membranes (reviewed in Teets and Denlinger 2013). Furthermore, it has been empirically illustrated that a loss of ion homeostasis between cells and the intracellular space results in cold injury in *D. melanogaster* (MacMillan et al. 2015a,b; MacMillan et al. 2016). Despite these discoveries, the majority of mechanistic explorations of insect cold hardiness occur in the adult stage only (Bowler and Terblanche 2008). Therefore, it is currently not established whether larvae employ similar mechanisms to deal with extreme cold. This may be due to greater interest in the literature focusing on overwintering strategies in adults. However, analyzing how larvae combat cold stress could determine if larvae employ fundamentally distinct physiological responses compared to adults. One way to explore this knowledge gap is to analyze gene expression in both larvae and adults in response to cold stress and look for patterns unique to either life stage. Furthermore, if genes involved in established mechanisms of cold hardiness implicated in previous studies that focused on the adult stage are

not found to be significantly expressed in larvae, a foundation would be laid to investigate stage-specific thermal hardiness in larvae.

A small number of studies have examined differential gene expression in response to thermal stress across the metamorphic boundary in insects. Bing et al. (2012) determined that, in response to cold stress exposure, *Frost* (*Fst*), a gene that has been implicated in cold shock survival in *Drosophila* (Goto 2001; Qin et al. 2005; Colinet et al. 2010), was upregulated in 3rd instar larvae and 5d post-eclosion adults but was not significantly up-regulated in any other life stage, including 20d post-eclosion adults, eggs, pupae, and other larval instars. Also, Shi et al. (2013) discovered distinct transcript abundances among multiple stages of the parasitoid wasp, *Cotesia vestalis*. They discovered that four different heat shock proteins had differential expression among several life stages under different developmental temperatures, including across the metamorphic boundary. Studies such as these highlight the possibility that different thermal hardiness mechanisms could be facilitated by distinct forms of regulation across ontogeny or that stage-specific mechanisms in response to stressful conditions may exist in species that exhibit complex life cycle transitions. It is a purpose of this work to determine if unique patterns of thermal stress-induced gene expression emerge on a transcriptomic scale in *D. melanogaster* across the metamorphic boundary.

A secondary purpose of this work is to determine if genotypes of similar phenotypic performance (i.e. low cold hardiness or high cold hardiness) elicit similar mechanisms to cope with thermal stress. From studies like Freda et al. (2017), it is apparent that there is ample phenotypic variation in response to cold stress in both larvae and adults within a sampled population. The observation of this variation in phenotypic response leads to the question, do high or low performing genotypes achieve their respective cold hardiness via universal

mechanisms or can cold hardiness be achieved in different ways? Universal patterns of gene expression within phenotypic classes could point to mechanisms that have an important role in maintaining performance in response to thermal stress. However, if these patterns do not emerge, it may be possibly that high performance may be achieved via multiple mechanisms. The latter possibility implies that cold hardiness itself is largely quantitative, with many loci, mechanisms, and pathways that could attribute to the greater stress response.

To answer these questions, we measured whole body transcriptomes of both larvae and adults from six Drosophila Genetic Reference Panel (DGRP) (dgrp2.gnets.ncsu.edu) (Mackay et al. 2012; Huang et al. 2014) genotypes exhibiting high phenotypic performance in one life stage but not the other: 3 with high adult cold hardiness and low larval cold hardiness and 3 with low adult cold hardiness and high larval cold hardiness (Freda et al. 2017). We obtained samples from 4 time points before, during, and after a 1h exposure to acute cold stress to determine the expression trajectories of genes related to cold stress in larvae and adults and to assess differences in expression profiles of these genes between phenotypic classes. Our results suggest that the cold-induced gene expression patterns of larvae and adults are distinct. Furthermore, many genes associated with established mechanisms of cold hardiness in adults are not significantly up-regulated in larvae. We also find that cold hardiness is largely uniquely achieved in both larvae and adults with only several genes significantly differentially expressed between phenotypic classes. These results provide evidence that both the response to thermal stress is unique in larvae and adults and that cold hardiness is achieved in unique ways among genotypes in *D. melanogaster*.

Methods

Drosophila Genetic Reference Panel (DGRP) Lines

The DGRP is a collection of isogenic and re-sequenced lines of *Drosophila melanogaster* originating from a single, natural population in Raleigh, North Carolina (dgrp2.gnets.ncsu.edu) (Mackay et al. 2012; Huang et al. 2014). We used 6 DGRP genotypes (lines) in this study that were selected because of their extreme difference in cold hardiness (measured as proportion surviving after a 1h acute exposure to cold stress) across metamorphosis from a previous study (Freda et al. 2017) (Figure C.1). There were 3 genotypes exhibiting high cold hardiness in the larval stage but low cold hardiness in the adult stage. These are denoted as High Larval (HL) genotypes (DGRP lines 441, 832, and 913). We refer to the remaining 3 genotypes exhibiting low cold hardiness in the larval stage but high cold hardiness in the adult stage as High Adult (HA) genotypes (DGRP lines 358, 380, and 486). These genotypes were selected to investigate differential gene expression in response to cold stress among phenotypic classes within stages while also allowing for the detection of differential gene expression in response to cold stress between developmental stages. All genotypes were obtained from the Bloomington Drosophila Stock Center at Indiana University.

DGRP Line Rearing

All experimental flies were reared on media containing cornmeal, molasses, and yeast. Both propionic acid and benzoic acid were added to reduce fungal and bacterial growth in the culture. Fly vials were sprinkled with dry, active yeast to facilitate oviposition. Experimental flies were reared from egg to adult at 25°C on a 12/12 light-dark cycle. Experimental flies were collected for the cold stress assay at distinct developmental windows as larvae and adults (see below). Experimental flies that were used in this study were the progeny of 5 male and 5 female

parents. The parents were collected from cultures and sorted for sex under light CO_2 anesthesia. The parents were then put onto fresh media to allow for mating/oviposition, which was also at 25°C, 12/12 light-dark. Every 24h, the parents were transferred to fresh media for four consecutive days to produce each replicate for the study, leaving 3 experimental replicates per life stage and per genotype. The first replicate vials from day 1 were discarded to remove any residual effect of anesthesia on oviposition.

Cold Stress Assay and Experimental Design

Larvae exposed to cold stress were third instar feeding larvae extracted from cultures 120h (5d) post-oviposition using a 20% w/v sucrose solution following the protocol of Nöthiger (1970) and Freda et al. (2017). Adults were collected, sorted, and separated by sex in groups of 5 under light CO2 anesthesia 10-12d post-oviposition. Separate vials containing only males or females were returned to 25°C/12-12 light-dark for 5 days to recover before the cold stress assay.

We wished to capture and investigate gene expression before, during, and after an acute 1h cold stress in both larvae and adults of each genotype. To do this, we extracted RNA from whole flies from a total of 4 time points: 0 mins, 30 mins, 60 mins, and 90 mins, where 0 mins represents flies sampled before stress, 30 and 60 mins represent during stress, and 90 mins represents recovery after stress. Immediately before the cold stress assay, 10 larvae and 10 adults (consisting of 5 males and 5 females) of each of the 6 DGRP genotypes were flash frozen with liquid N_2 and stored in 1.5 mL Eppendorf tubes. These individuals serve as "0 mins" controls. For the remaining three time points, 10 adult flies per time point, previously kept separated by sex, were combined and placed in empty vials. A total of 10 larvae per line and time point, extracted from media, were placed in vials containing only a vial flug (Genesee Scientific, Catalog # 49-102) moistened with ddH_2O to inhibit desiccation. Vials of larvae and adults were

then immersed in a recirculated bath containing a 50/50 aqueous mixture of propylene glycol and ddH_2O set at the test temperature of -5°C. After 30 mins had elapsed a replicate of larvae and adults of each line were removed from the bath, flash frozen, and stored at -80°C. At the end of the exposure, 60 mins, all vials were removed from the bath. Of the remaining two replicates, one was immediately flash frozen and stored at -80°C and the other was kept at 25°C for another 30 mins until they were also flash frozen and stored for later RNA extraction. This process was repeated over the next two consecutive days to produce two additional biological replicates for each genotype, stage, and time point.

RNA Extraction, Library Preparation, and Sequencing

Three pooled replicates each containing 10 whole larvae or 10 whole adults (5 males and 5 females) per genotype and time point were homogenized with a pestle in Tri-reagent (Zymo) and RNA was extracted using the Zymo direct-zol total RNA extraction kit. Extracted samples were quantified using a nanodrop before library preparation.

Pooled samples were prepared using a RNA-tag sequencing approach (for details see: Lohmen et al 2016). Briefly, RNA samples were fragmented using an Mg+ buffer before a poly-T segment is annealed to the poly-A tail of the mRNA. Reverse transcription (RT) was started from the now double stranded poly-A section using SMARTscribe reverse transcriptase (Clontech) which adds additional 'C' nucleotides to the 3' end of the cDNA (3'-RACE). RT template switching is achieved with the inclusion of a RNA oligo with a complementary stretch of 'G' bases completing extension. Following RT two rounds of PCR, Illumina adapters and barcodes were added for sequencing. Resulting libraries (final cleaning step using Ampure beads) were sequenced on 5 lanes as 100bp single end reads on an Illumina HiSeq 2500 at Kansas University's Genome Sequencing Core Laboratory. Samples had an average of 6M SE reads.

Reads were mapped to the *Drosophila melanogaster* reference genome (version 6.06) obtained from FlyBase (Gramates et al. 2017) using STAR (Dobin et al. 2013). Total mapped reads averaged >95% across all samples. Read counts per gene and per isoform were generated using RSEM (Li & Dewey 2011).

Differential Expression

The edgeR package was used in R (R Core Team 2018) to apply generalized linear models to the read count data (Robinson et al. 2010) to determine significantly differentially expressed genes both between stages and between phenotypes (HL and HA). Genes that were not represented by at least a single read were discarded from further analysis, leaving 13,457 genes. Variation in read depth was normalized using the weighted trimmed mean of M-values (TMM) method (Robinson & Oshlack 2010) and significant differential expression was determined using a Benjamini and Hochberg false discovery rate (FDR) threshold of 0.05. A Multi-Dimensional Scaling (MDS) plot was generated using the top 500 differentially expressed genes (determined by fold-change) to illustrate distances between gene expression profiles of each sample.

Cross-Stage Comparisons

A full model with all possible interactions was fitted in edgeR including 3-way interaction between line (genotype), stage, and time point:

$$y = stage + time\ point + stage\ \times\ time\ point + line + line \times\ stage + line\ \times\ time\ point + line\ \times stage \times time\ point$$

Any genes that had a significant 3-way interaction (FDR > 0.05) were excluded from the analysis to control for any significant variation in gene expression among lines or stages. A total of 124

genes had a significant 3-way interaction and were excluded from further analysis to only include genes with low levels of random noise among genotypes.

A reduced model was then fit to explore differences in gene expression between each time point (30 mins, 60 mins and 90 mins) compared to constitutive expression (0 mins) in each life stage average across genotype:

$$y = stage + time\ point + stage\ \times\ time\ point + line + line \times\ stage + line\ \times\ time\ point$$

We designed post-hoc linear contrasts to test for differences between life stages in the change from 0 mins to 30, 60, and 90 mins. For example, we tested whether the log fold change from 0 to 30 mins in larvae differed significantly from the log fold change from 0 to 30 mins in adults. This generated 3 lists of genes, one for each time point comparison, that were significantly different in their expression profiles between stages.

Finally, we performed a clustering analysis on the time series of transcript expression including each stage, and using $\log_2$ fold changes estimated between 30, 60, and 90 mins vs. the 0 min time point. The goal was to identify transcripts with similar expression trajectories across time within each life stage, but not necessarily across life stages. For example, the approach described below would cluster sets of transcripts that all increased similarly in abundance over time in larvae, but all similarly decreased in expression over time in adults. All transcripts significantly differentially expressed across time or between stages were included, resulting in a 1,561 (genes) by 6 (3 $\log_2$ fold change estimates per stage) matrix. We estimated a Euclidean distance matrix between rows, then estimated hierarchical clustering relationships using the

complete linkages method as implemented in the R function *hclust*. We used a dynamic tree-cutting algorithm to initially cluster co-expressed transcripts, then merged clusters whose first principal components were correlated at $r > 0.75$ using the *cutreeDynamic* and *mergeCloseModules* functions from the R Weighted Gene Coexpression Network Analysis (*WGCNA*) package (Langfelder and Horvath 2008). We visually represent these clusters in the results as the average expression within each cluster of all transcripts up-regulated and down-regulated on average over time.

Cross-Phenotype Comparisons

To assess cross-phenotype differential expression, two approaches were taken. In the first approach, we fit four models including only a line effect, one for each of the time points (0 mins, 30 mins, 60 mins, and 90 mins), where *line* was the only factor were used:

$$y = line$$

This was performed separately in larvae and adults to determine genes that were significantly differentially expressed between lines at each time point. For each genotype within a phenotypic class (HL or HA), and time point, a pairwise comparison was made to a genotype of the other phenotypic designation using linear contrasts. Therefore, we made a total of 9 pairwise comparisons in both larvae and adults per time point, resulting in 9 lists, per stage, of genes that are significantly differentially expressed between the two lines being compared. Next, these lists are concatenated and filtered so that only genes that exist in all 9 lists remain. We then further filter so that only genes that have the same sign of the fold change remain - that is, differentially

expressed in the same direction. This results in 4 lists that include genes that are universally significantly up- or down-regulated between phenotypic classes within larvae and adults.

The second approach is similar to the model utilized in the cross-stage comparison.

$$y = line + rep(line) + time\ point$$

In this model, the two factors are *line* and *time point* and each genotype contributes a third (0.333) to its respective phenotypic class in the pairwise comparison between phenotypes. We made A total of 3 pairwise comparisons within phenotypic classes: 30 mins compared to 0 mins, 60 mins compared to 0 mins, and 90 mins compared to 0 mins. This was followed by 3 more pairwise comparisons between these differences across phenotypes to determine genes that have a significant difference in slope (expression direction) between phenotypes within time point comparisons to 0 mins.

Gene Ontology and Pathway Analysis

Lists containing genes that were found to be significantly differentially expressed between stages or phenotypes were submitted to DAVID (Huang et al. 2009a,b) and Reactome (Fabregat et al. 2018) to determine if significant GO term enrichment and/or biological pathway enrichment exists within them. This was done to illustrate if certain processes or pathways are stage- or phenotype-specific in response to cold stress.

Results

Cross-Stage Differential Expression

This process is aimed at identifying differentially expressed genes averaged across all six lines between stages. The MDS plot illustrates a distinct difference in the expression profiles of

larvae and adults as they separate clearly along the first dimension (Fig. 4.1), however, replicate pools did not visibly cluster by genotype or time point (Figure C.2). A heat map of time series expression profiles for each stage illustrates the largely distinct trajectories across stages (Fig. 4.2A), while clustering revealed that transcripts up- and down-regulated over time in one stage tended to exhibit minimal change over time in the other (Fig. 4.2B). Moreover, the rapidity of gene expression responses appears to differ markedly between larvae and adults. Specifically, two clusters contain transcripts that are either up- or down-regulated 30 minutes into cold stress exposure in larvae (Clusters 1 & 2, Fig. 4.2B), whereas another cluster contains transcripts that are primarily up-regulated at 90 minutes (30 minutes post-stress) in adults (Cluster 3, Fig. 4.2B).

A total of 640, 596, and 543 genes were significantly differentially expressed between larvae and adults for 30 mins compared to 0 mins (30v0), 60 minutes compared to 0 mins (60v0), and 90 mins compared to 0 mins (90v0), respectively (Figure C.3). There is a total of 234 genes that are universally differentially expressed between larvae and adults during or after stress. In other words, these are genes that are significantly differentially expressed between stages across all measured time points during and after cold stress (Figure C.3).

The top ten enriched GO terms and pathways for each pairwise comparison are summarized in Table 4.1 while full lists are available in Tables C.1 and C.2. There are many genes that are highly significantly up-regulated (FDR < 0.0001) in larvae when compared to adults whose expression trajectories roughly follow the average trajectory of cluster 2 (Fig. 4.2B). These genes increase in expression at 30 minutes then drop off in expression over time. Examples of these genes are illustrated in Figure 4.3 and include genes *loco, thor, atg1, paip2, CG8389,* and *CG42502*. Some of these loci, like *Loco* and *Thor*, are involved in regulating and signaling stress responses. Other genes, like *atg1* are involved in autophagy. *Paip2* is involved in

growth while *CG8389* is an integral membrane transporter. In adults, there are also a number of genes significantly differentially expressed between larvae and adults (FDR < 0.0001) that follow the average adult trajectory in cluster 3 (Fig. 4.2B). Examples of these genes are heat-shock proteins (HSPs) that include *HSP70Bb*, *HSP70Bc*, and *HSP68* as well as the loci *Frost* and *CG5550*. Expression trajectories for these loci are illustrated in Figure 4.4.

Enrichments from genes within cluster 1 include GO terms involving autophagic processes, cell death, and immunity (Table C.3). These genes are largely up-regulated in larvae compared to adults (Fig. 4.2). GO terms enriched from cluster 2, which are genes primarily down-regulated in larvae include ribosome biogenesis and lipid metabolism (Fig. 4.2; Table C.3). Finally, enriched GO terms in cluster 3 are related to processes including response to stress, response to temperature, and heat shock proteins. Genes in this cluster are largely up-regulated in adults (Fig. 4.2; Table C.3).

Cross-Phenotype Differential Expression

This procedure aims to identify significantly differentially expressed genes between phenotypic classes (HL or HA) in each life stage. Both cross-phenotype models supported only 2 genes in larvae exhibiting significant differential expression between HL and HA lines in the larval stage: *loco* and the cytochrome P450, *Cyp12a5*. As stated previously *loco* (*locomotion defects*) is involved in many biological processes including stress responses (Fig. 4.5). There are no genes significantly differentially expressed in response to cold stress between phenotypes in the adult stage.

Discussion

Stage-Specific Expression Patterns in Response to Cold Stress

Previously, it has been illustrated that there exists a lack of correlation between thermal hardiness phenotypes across the metamorphic boundary in insects (Tucić 1979; Loeschcke and Krebs 1996; Gilchrist et al. 1997; Dierks et al. 2012; Freda et al. 2017). Additionally, we have shown that the clear majority of SNPs statistically associated with the variation of cold hardiness in larvae and adults are distinct, providing evidence that different genomic regions underlie stage-specific thermal responses (Freda et al. 2017). The current study does not provide much evidence for associations between expression patterns and genetic variation in cold hardiness (see below) but does robustly support distinct physiological responses in each life stage. This is clearly illustrated by the clustering by stage in the MDS plot (Fig. 4.1), the distinct time series expression profiles during and after cold stress (Fig. 4.2), and the large number of transcripts differentially expressed between stages over each time interval (Figure C.3).

Over the development of *D. melanogaster*, much of the transcriptome is differentially regulated as the organism grows and completes its complex life cycle (Arbeitman et al. 2002; Gramates et al. 2017). Additionally, there have been studies that report differential expression of certain genes across holometabolous insect development in response to environmental variation (Bing et al. 2012; Shi et al. 2013) However, to our knowledge, this is the first report of differential expression patterns across the transcriptome in response to thermal stress between larvae and adults of *D. melanogaster*. We achieve this despite using whole body RNA extractions. It may be that our experimental setup misses tissue specific mechanism and signals. However, the purpose of this experiment was to explore all possible stage-specifc mechanisms that may exist between larvae and adults. Our models control for genes that are constitutively

differentially expressed due to developmental stage, leaving only those associated with cold stress response. This result implies that, in addition to genetics underlying cold hardiness, regulatory mechanisms and regions may also be free to evolve independently in each life stage of *D. melanogaster*.

The average expression trajectories of adults and larvae are distinct, with larvae upregulating genes early during stress response and adults activating genes later, after stress and during the recovery phase (Fig. 4.2). The early gene activation of larvae is consistent with elevated levels of cell growth in larvae compared to adults. In particular, autophagy, is inherently linked to cell differentiation and growth. The cell growth and division have large energy requirements, thus processes involving growth and cell differentiation are often slowed or halted during stress (Wang and Levine 2010; Neufeld 2012). This allows cells to sequester nutrients or break down organelles or other structures to create energy reserves via autophagic pathways (Wang and Levine 2010; Neufeld 2012). Indeed, we observe up-regulation of autophagy-related transcripts as a direct response during cold stress in the tested third instar larvae that are still in the feeding and growth phase (not yet wandering), but not in sexually mature adults where cell growth and division should be minimal. This is demonstrated in the enrichment of autophagy-related GO terms in cluster 1 (Fig. 4.2B). Also, in addition to autophagy-related processes, we observe enrichment of growth and development GO terms and pathways early during stress (Tables C.1;C.2). These enrichments are consistent with the shutting down of growth-related processes in larvae. Indeed, it has been observed throughout the literature that stress inhibits the growth of organisms (Denmead and Shaw 1960; Hurkman and Tanaka 1996; Rouault et al. 2006; Cantin et al. 2010). This would also explain the up-regulation of metabolism-related GO terms and pathways like ribosome biogenesis and lipid metabolism. It is of interest why adults do not

respond to stress immediately, however, the 90-min time point and gene cluster 3 (Fig. 4.2) illustrate that adults up-regulate several stress response pathways that are absent in larvae (discussed below).

Cross-Stage GO Terms and Pathway Enrichment

At the 30v0 time point comparison, the top GO terms are involved in ribosome biogenesis, pigmentation, and aging, and determination of lifespan. Enrichment of genes involved in ribosome biogenesis, rRNA processing, aging, and determination of lifespan is not entirely surprising as, in favorable conditions, ribosome biogenesis is promoted to increase cell growth and differentiation (Powers et al. 1999). However, in response to stressful conditions, it has been illustrated that ribosome biogenesis is inhibited in yeast and humans (Powers et al 1999; Marion et al. 2004; Deisenroth and Zhang 2010). In accordance with the GO term enrichment, we observed the up-regulation of genes associated with pigmentation at the 30-min time point in larvae including *black*, *ebony*, and *pale* (Figure C.4). Pigmentation has been linked to temperature as colder developmental temperatures have been illustrated in increase adult pigmentation in *D. melanogaster* (David et al. 1990; Gibert et al. 2000; Gibert et al. 2007). There are plausible explanations for this observation including mate identification, camouflage, and increased absorption of UV light (David et al. 1985; David et al. 1990). The top pathways observed in the 30v0 comparison are involved in macroautophagy, shifts in energy metabolism, and the downregulation of EGFR. Macroautophagic responses are likely implemented as part of a general stress response as it has been implemented as part of the starvation response in *Drosophila* (Reviewed in McPhee and Baehrecke 2009). Furthermore, gene cluster 1 is enriched for a number of autophagic-related processes (Table C.3). There are also pathways implicated including Import of the palmitoyl-CoA into the mitochondrial matrix, AMPK inhibits chREBP

transcriptional activation activity, and fatty acyl-CoA biosynthesis. The enrichment of these pathways likely indicates the shunting of energy from metabolism to stress response as does the enrichment of pathways associated with the downregulation of Epidermal Growth Factor Receptor (EGFR). As the bulk of genes that are differentially expressed are up-regulated in larvae point, large-scale metabolic changes are likely essential to larval cold hardiness.

The 60v0 comparison is enriched for terms and pathways including DNA binding, cell differentiation, growth, and lipid synthesis, including acyl-CoA oxidase. The DNA binding term is likely due to the transcriptional activation of processes that are likely to be involved in stress responses or the downregulation of processes involved in the processes governing cell differentiation and growth. As with the 30v0 comparison, processes that are required for growing larvae are likely to be halted or slowed during stressful conditions (Chippendale et al. 1996). However, the transcriptional shifts in lipid synthesis and acyl-CoA oxidase terms are less clear. Out of the three genes associated in the acyl-CoA oxidase term, *CG4586*, *CG5009*, and *CG9527*, the latter two are downregulated while the first is upregulated in larvae compared to adults (Figure C.5). Acyl-CoA oxidase catalyzes the reaction to produce trans-2,3-dehydroacyl-CoA, an unsaturated fatty acid, from acyl-CoA and oxygen (Kawaguchi et al. 1980). The addition of unsaturated fatty acids to the plasma membrane can stabilize its fluidity during cold stress via the process of homeoviscous adaptation inhibiting cell rupturing (reviewed in Teets and Denlinger 2013). Furthermore, other lipid biosynthetic GO terms are commonly enriched in multiple time points comparisons in addition to 60v0. These terms include cellular lipid catabolic process, lipid catabolic process, lipid oxidation, lipid modification, and lipid biosynthetic process (Table C.1). There are also substantial lipid metabolism-related GO terms enriched in gene cluster 2 (Fig. 4.2; Table C.3). These enrichments may be associated with the termination of lipid biosynthesis and

beta oxidation, however; it is also possible that these pathways are associated with the modification of lipids to combat cold stress via alterations to the plasma membrane. Most of the genes associated with these enriched GO terms are downregulated in larvae compared with adults. However, three genes, *SMSr*, *Pi3K92E*, and *Pi3K59F*, are upregulated in larvae over the course of and after the stress exposure (Figure C.5). *SMSr* is involved in the production of sphingomyelin, an integral component of animal plasma membranes (Huitema et al. 2004) that are commonly found in the myelin sheaths of axons (Ramstedt and Slotte 2002) but also make up 2-15% of all phospholipids, depending on the tissue type (Koval and Pagano 1991). Because of their chemical structure, sphingomyelin can stabilize lipid bilayers via hydrogen bonds (Koynova and Caffrey 1995) and can also interact with cholesterols in the plasma membrane, further fortifying them (Ramstedt and Slotte 2002). The remaining two genes, *Pi3K92E*, and *Pi3K59F* are phosphatidylinositol kinases involved primary in autophagy (Rusten et. al. 2004; Xu et al. 2015) but these kinases have also implicated in lipid homeostasis and lipid modification (Britton et al. 2002). In summary, the possibility of membrane lipid modification in larvae as a pathway to combat cold stress requires further study.

At the 90v0 comparison, GO terms involving responses to stress, hypoxia, and temperature are highly enriched. These GO terms are also found in gene cluster 3 (Fig. 4.2; Table C.3). Most of the genes involved in response to stress, hypoxia, and temperature are heat shock proteins (HSPs) being upregulated in adults compared to larvae (examples in Fig. 4.4). However, also in this list are the genes *Frost* (*Fst*), a gene previously empirically associated with cold acclimation (Qin et al. 2005) and response to cold (Goto 2001; Colinet et al. 2010), and *CG5550*, a gene with unknown function (Fig. 4.4). As their name alludes, HSPs are molecular chaperones that have been widely implicated in heat stress responses in *Drosophila* (Dalgaard et

al. 1998; Lakhotia and Prasanth 2002; Gong and Golic 2006) and other systems (Skidmore et al. 1995; Oehler et al. 2001). However, HSPs have also been implicated in cold stress responses in *Drosophila* as well (Burton et al. 1988; Yiangou et al. 1997; Nielsen et al. 2005; Qin et al. 2005). It is unclear why HSPs are up-regulated in response to cold stress. It may be that they are part of a general stress response but, more likely, since extreme cold can also denature proteins (Privalov 1990), they are likely utilized in the same capacity as in heat stress responses – as molecular chaperones for misfolded proteins (Qin et al. 2005). *Fst*'s function is currently unknown despite its implication in hosts of cold stress studies. However, its cellular location has been inferred to be in the extracellular space (Goto 2001) and most likely is a mucin-type molecule involved in retaining cellular structure during and after cold stress by maintaining ion homeostasis of the cell (Colinet et al. 2010). Interestingly, the HSPs and other genes in these categories are almost universally up-regulated in adults at the 90-minute time point while these genes do not activate during or after stress in larvae. These genes may be interesting targets to assess stage-specific cold hardiness responses in the future.

Finally, GO terms and pathways that enriched in multiple time point comparisons and across all gene clusters are associated with cell/tissue death and apoptosis, macroautophagy, and EGFR signaling. Terms and pathways associated with death and apoptosis are not surprising as cold stress can be fatal or near fatal at the test temperature (-5°C) as observed in our previous study (Freda et al. 2017). Therefore, these signals may be due to tissue loss and mortality. Macroautophagy is likely a commonly enriched term and pathway due to the redistribution of macromolecules and energy during stress responses. Lastly, EGFR signaling is likely downregulated, especially in larvae, as normal processes involving growth and cell differentiation are likely slowed or halted due to the external cold stress response.

Candidate Loci for Further Study

There are multiple genes that are highly significantly differentially expressed between larvae and adults over the whole of the experimental window and, therefore; likely are integral to cold stress response in each life stage. The genes significantly up-regulated in larvae and adults also follow the average stage-specific expression trajectories (Figs. 4.2,4.3,4.4). In larvae, top up-regulated genes include *loco*, *CG8389*, *CG42502*, *thor*, *Atg1*, and *Paip2*. *Loco* and *thor* are both implicated in several pathways with both being experimentally associated with several stress responses including immune stress, heat stress, and starvation (Tettweiler et al. 2005; Wagner et al. 2009; Zid et al. 2009; Lin et al. 2011) (Fig. 4.3). Genes *Atg1* and *Paip2* are associated with the regulation of growth and differentiation with *Atg1* being directly implicated in the processes of autophagy (Xu et al. 2015; Ihry and Bashirullah 2014) and *Paip2* associated with the negative regulation of transcription and in the regulation of cell growth (Roy et al. 2004). Finally, *CG8389* has been inferred as an integral membrane protein, based on phylogenetic similarity (Gramates et al. 2017), which could possibly have a role in maintaining ion homeostasis across the cell membrane in larvae. Further study is required to determine this. There is no ontological information currently available for *CG42502*.

In adults, top genes significantly up-regulated in across the experimental window include *Hsp68*, *Hsp70Bb*, *Hsp70Bc*, *Frost*, and *CG5550*. The heat shock proteins and *Frost* have been implicated in *Drosophila* heat (Dalgaard et al. 1998; Lakhotia and Prasanth 2002; Gong and Golic 2006) and cold (Burton et al. 1988; Yiangou et al. 1997; Goto 2001; Nielsen et al. 2005; Qin et al. 2005; Colinet et al. 2010) hardiness in the literature. However, it is interesting that these genes are not up-regulated in larvae during or after cold stress in our experiment. In Bing et al. 2012, the researchers found that *Frost* was significantly up-regulated 2h after exposure to 0°C

in third instar larvae and 5d old adults. However, we did not detect any significant up-regulation, compared to adults, in third instar larvae during the course of the experiment. It may be possible that *Frost* is upregulated later in larvae or a similar response does not occur within the genotypes tested in this study. Most likely, however, we do not detect a significant upregulation due to the difference in the experimental design. In Bing et al (2012) comparisons are made between controls and treatments within stages while this experimental design explores differences across life stages. There is currently no ontological information available for *CG5550*. From these results, it is apparent that different stress-induced pathways are utilized in adults and larvae. Further study of these loci is required to fully understand the stage-specific responses to cold tolerance across the metamorphic boundary in *Drosophila*.

Phenotypes Achieve Cold Hardiness in Unique Ways

There are only two genes that are significantly differentially regulated in larvae between HL and HA lines: *loco* and *Cyp12a5*. *Loco* was also found to be significantly up-regulated in larvae compared to adults. From the within-stage analysis, larval cold hardiness is also associated with induction of *loco*, with higher expression found in HL lines. *Cyp12a5* is a cytochrome P450, which have been implicated in the metabolism of various toxins (Feyereisen 1997). However, this result provides evidence that cytochrome P450's may be involved in other stress responses. Indeed, in the literature, cytochrome P450s have been implicated in oxidative stress responses (Gonzalez 2005; Li et al. 2008). There were no up-regulated genes that had differential expression among phenotypes in adults. However, three genes have differential expression constitutively between HL and HA lines in adults: *CG13947*, *CR45902*, and *mt:ND3* (Figure C.6). Currently, there is no ontological information for *CG13947* or CR45902. However, *CR45902* codes for a non-protein coding RNA with unknown function. *Mt:ND3* (mitochondrial

NADH-ubiquinone oxidoreductase chain 3) is a subunit of the mitochondrial electron transport chain (Gramates et al. 2017). It is unclear how higher constitutive expression of this gene may combat cold stress, however; one possible explanation is that its expression may be negatively correlated with stress recovery as cells with higher metabolic rates may be slower to shunt energy towards stress responses. These results provide evidence that genotypes achieve cold tolerance in unique ways in larvae and adults. This is likely due to unique polygenic architectures that underlie cold hardiness in each life stage (Freda et al. 2017).

Conclusions

Our results indicate that larvae and adults respond to cold stress in unique ways. Larvae appear to activate pathways involved in ceasing development to react to cold stress. Adult, however; activate stress responses known to be involved in thermal stress after cold exposure, during the recovery phase. Furthermore, the stress associated pathways larvae and adults activate are distinct. Further study into these pathways are required to better understand stage-specific responses to thermal stress. Furthermore, our results indicate that cold hardy phenotypes achieve fitness in unique ways as we implicate a relatively small number of genes universally differentially expressed between phenotypes in both stages. Taken together, these results illustrate the importance of cross-stage and cross-phenotype assessments of fitness in biological systems.

References

Arbeitman MN, Furlong E. EM, Imam F, Johnson E, Null BH, Baker BS, *et al.* (2002). Gene expression during the life cycle of *Drosophila melanogaster*. *Science* **297**: 2270–2275.

Bale JS, Hayward SAL (2010). Insect overwintering in a changing climate. *J Exp Biol* **213**: 980–994.

Bing X, Zhang J, Sinclair BJ (2012). A comparison of *Frost* expression among species and life stages of *Drosophila*. *Insect Mol Biol* **21**: 31–39.

Bowler K, Terblanche JS (2008). Insect thermal tolerance: what is the role of ontogeny, ageing and senescence? *Biol Rev Camb Philos Soc* **83**: 339–355.

Britton JS, Lockwood WK, Li L, Cohen SM, Edgar BA (2002). *Drosophila*'s insulin/PI3-kinase pathway coordinates cellular metabolism with nutritional conditions. *Dev Cell* **2**: 239–249.

Burton V, Mitchell HK, Young P, Petersen NS (1988). Heat shock protection against cold stress of *Drosophila melanogaster*. *Mol Cell Biol* **8**: 3550–3552.

Cantin NE, Cohen AL, Karnauskas KB, Tarrant AM, McCorkle DC (2010). Ocean warming slows coral growth in the central Red Sea. *Science* **329**: 322–325.

Chippindale AK, Chu TJF, Rose MR (1996). Complex trade-offs and the evolution of starvation resistance in *Drosophila Melanogaster*. *Evolution* **50**: 753–766.

Colinet H, Lee SF, Hoffmann A (2010). Functional characterization of the *Frost* Gene in *Drosophila melanogaster*: Importance for recovery from chill coma. *PLoS One* **5**: e10925.

Dahlgaard J, Loeschcke V, Michalak P, Justesen J (1998). Induced thermotolerance and associated expression of the heat-shock protein Hsp70 in adult *Drosophila melanogaster*. *Funct Ecol* **12**: 786–793.

David JR, Capy P, Gauthier J-P (1990). Abdominal pigmentation and growth temperature in *Drosophila melanogaster*: Similarities and differences in the norms of reaction of successive segments. *J Evol Biol* **3**: 429–445.

David JR, Capy P, Payant V, Tsakas S (1985). Thoracic trident pigmentation in Drosophila *melanogaster*: Differentiation of geographical populations. *Genet Sel Evol* **17**: 211–224.

Deisenroth C, Zhang Y (2010). Ribosome biogenesis surveillance: probing the ribosomal protein-Mdm2-p53 pathway. *Oncogene* **29**: 4253–4260.

Denmead OT, Shaw RH (1960). The effects of soil moisture stress at different stages of growth on the development and yield of corn. *Agron J* **52**: 272–274.

Dierks A, Kölzow N, Franke K, Fischer K (2012). Does selection on increased cold tolerance in the adult stage confer resistance throughout development? *J Evol Biol* **25**: 1650–1657.

Dobin A, Davis CA, Schlesinger F, Drenkow J, Zaleski C, Jha S, *et al.* (2013). STAR: ultrafast universal RNA-seq aligner. *Bioinformatics* **29**: 15–21.

Fabregat A, Jupe S, Matthews L, Sidiropoulos K, Gillespie M, Garapati P, *et al.* (2018). The Reactome Pathway Knowledgebase. *Nucleic Acids Res* **46**: D649–D655.

Feyereisen R (1999). Insect P450 enzymes. *Annu Rev Entomol* **44**: 507–533.

Freda PJ, Alex JT, Morgan TJ, Ragland GJ (2017). Genetic decoupling of thermal hardiness across metamorphosis in *Drosophila melanogaster*. *Integr Comp Biol* **57**: 999–1009.

Gibert P, Moreteau B, David JR (2000). Developmental constraints on an adaptive plasticity: reaction norms of pigmentation in adult segments of *Drosophila melanogaster*. *Evol Dev* **2**: 249–260.

Gibert J-M, Peronnet F, Schlötterer C (2007). Phenotypic plasticity in *Drosophila* pigmentation caused by temperature sensitivity of a chromatin regulator network. *PLOS Genetics* **3**: e30.

Gilchrist GW, Huey RB, Partridge L (1997). Thermal sensitivity of *Drosophila melanogaster*: evolutionary responses of adults and eggs to laboratory natural selection at different temperatures. *Physiol Zool* **70**: 403–414.

Gong WJ, Golic KG (2006). Loss of Hsp70 in *Drosophila* is pleiotropic, with effects on thermotolerance, recovery from heat shock and neurodegeneration. *Genetics* **172**: 275–286.

Gonzalez FJ (2005). Role of cytochromes P450 in chemical toxicity and oxidative stress: studies with CYP2E1. *Mutat Res* **569**: 101–110.

Goto SG (2001). A novel gene that is up-regulated during recovery from cold shock in *Drosophila melanogaster*. *Gene* **270**: 259–264.

Gramates LS, Marygold SJ, Santos G dos, Urbano J-M, Antonazzo G, Matthews BB, *et al.* (2017). FlyBase at 25: looking to the future. *Nucleic Acids Res* **45**: D663–D671.

Hoffmann AA, Watson M Geographical variation in the acclimation responses of *Drosophila* to temperature extremes. *Am Nat* **142**: 93–113.

Huang W, Massouras A, Inoue Y, Peiffer J, Ramia M, Tarone AM, *et al.* (2014). Natural variation in genome architecture among 205 *Drosophila melanogaster* Genetic Reference Panel lines. *Genome Res* **24**: 1193–1208.

Huang DW, Sherman BT, Lempicki RA (2009a). Systematic and integrative analysis of large gene lists using DAVID bioinformatics resources. *Nat Protoc* **4**: 44–57.

Huang DW, Sherman BT, Lempicki RA (2009b). Bioinformatics enrichment tools: paths toward the comprehensive functional analysis of large gene lists. *Nucleic Acids Res* **37**: 1–13.

Huitema K, Dikkenberg J van den, Brouwers JF, Holthuis JC (2004). Identification of a family of animal sphingomyelin synthases. *EMBO J* **23**: 33–44.

Hurkman WJ, Tanaka CK (1996). Effect of salt stress on germin gene expression in barley roots. *Plant Physiol* **110**: 971–977.

Ihry RJ, Bashirullah A (2014). Genetic control of specificity to steroid-triggered responses in *Drosophila*. *Genetics* **196**: 767–780.

Kawaguchi A, Tsubotani S, Seyama Y, Yamakawa T, Osumi T, Hashimoto T, *et al.* (1980). Stereochemistry of dehydrogenation catalyzed by Acyl-CoA oxidase. *J Biochem* **88**: 1481–1486.

Kingsolver JG, Arthur Woods H, Buckley LB, Potter KA, MacLean HJ, Higgins JK (2011). Complex life cycles and the responses of insects to climate change. *Integr Comp Biol* **51**: 719–732.

Koval M, Pagano RE (1991). Intracellular transport and metabolism of sphingomyelin. *Biochim Biophys Acta, Lipids Lipid Metab* **1082**: 113–125.

Koynova R, Caffrey M (1995). Phases and phase transitions of the sphingolipids. *Biochim Biophys Acta, Lipids Lipid Metab* **1255**: 213–236.

Krebs RA, Loeschcke V (1995). Resistance to thermal stress in preadult *Drosophila buzzatii*: variation among populations and changes in relative resistance across life stages. *Biol J Linn Soc* **56**: 517–531.

Lakhotia SC, Prasanth KV (2002). Tissue- and development-specific induction and turnover of HSP70 transcripts from loci 87A and 87C after heat shock and during recovery in *Drosophila melanogaster*. *J Exp Biol* **205**: 345–358.

Langfelder P, Horvath S (2008). WGCNA: an R package for weighted correlation network analysis. *BMC Bioinform* **9**.

Li H-M, Buczkowski G, Mittapalli O, Xie J, Wu J, Westerman R, *et al.* (2008). Transcriptomic profiles of *Drosophila melanogaster* third instar larval midgut and responses to oxidative stress. *Insect Mol Biol* **17**: 325–339.

Li B, Dewey CN (2011). RSEM: accurate transcript quantification from RNA-Seq data with or without a reference genome. *BMC Bioinform* **12**: 323.

Lin Y-R, Kim K, Yang Y, Ivessa A, Sadoshima J, Park Y (2011). Regulation of longevity by regulator of G-protein signaling protein, *Loco*. *Aging Cell* **10**: 438–447.

Loeschcke V, Krebs RA (1996). Selection for heat-shock resistance in larval and in adult *Drosophila buzzatii*: comparing direct and indirect responses. *Evolution* **50**: 2354–2359.

Lohman BK, Weber JN, Bolnick DI (2016). Evaluation of TagSeq, a reliable low-cost alternative for RNAseq. *Mol Ecol Resour* **16**: 1315–1321.

Mackay TFC, Richards S, Stone EA, Barbadilla A, Ayroles JF, Zhu D, *et al.* (2012). The *Drosophila melanogaster* Genetic Reference Panel. *Nature* **482**: 173–178.

MacMillan HA, Andersen JL, Davies SA, Overgaard J (2015). The capacity to maintain ion and water homeostasis underlies interspecific variation in *Drosophila* cold tolerance. *Scientific Reports* **5**: 18607.

MacMillan HA, Andersen JL, Loeschcke V, Overgaard J (2015). Sodium distribution predicts the chill tolerance of *Drosophila melanogaster* raised in different thermal conditions. *Am J Physiol Regul Integr Comp Physiol* **308**: R823–R831.

MacMillan HA, Knee JM, Dennis AB, Udaka H, Marshall KE, Merritt TJS, *et al.* (2016). Cold acclimation wholly reorganizes the Drosophila melanogaster transcriptome and metabolome. *Sci Rep* **6**: 28999.

Marion RM, Regev A, Segal E, Barash Y, Koller D, Friedman N, *et al.* (2004). Sfp1 is a stress- and nutrient-sensitive regulator of ribosomal protein gene expression. *Proc Natl Acad Sci USA* **101**: 14315–14322.

McGraw JB, Antonovics J (1983). Experimental ecology of *Dryas octopetala* ecotypes: I. Ecotypic differentiation and life-cycle stages of selection. *J Ecol* **71**: 879.

McPhee CK, Baehrecke EH (2009). Autophagy in *Drosophila melanogaster*. *Biochim Biophys Acta* **1793**: 1452–1460.

Moran N (1994). Adaptation and constraint in the complex life cycles of animals. *Annu Rev Ecol Evol Syst* **2**: 573–600.

Neufeld TP (2012). Autophagy and cell growth – the yin and yang of nutrient responses. *J Cell Sci* **125**: 2359–2368.

Nielsen MM, Overgaard J, Sørensen JG, Holmstrup M, Justesen J, Loeschcke V (2005). Role of HSF activation for resistance to heat, cold and high-temperature knock-down. *J Insect Physiol* **51**: 1320–1329.

Nöthiger R (1970). Sucrose density separation: A method for collecting large numbers of *Drosophila* larvae. *Dros Inf Serv* **45**: 177.

Oehler R, Pusch E, Zellner M, Dungel P, Hergovics N, Homoncik M, *et al.* (2001). Cell type–specific variations in the induction of hsp70 in human leukocytes by feverlike whole body hyperthermia. *Cell Stress Chaperones* **6**: 306–315.

Powers T, Walter P, Kaiser C (1999). Regulation of ribosome biogenesis by the rapamycin-sensitive TOR-signaling pathway in *Saccharomyces cerevisiae*. *Mol Biol Cell* **10**: 987–1000.

Privalov PL (1990). Cold denaturation of proteins. *Crit Rev Biochem Mol Biol* **25**: 281–305.

Qin W, Neal SJ, Robertson RM, Westwood JT, Walker VK (2005). Cold hardening and transcriptional change in *Drosophila melanogaster*. *Insect Mol Biol* **14**: 607–613.

R Core Team (2018). *R: a language and environment for statistical computing.* R Foundation for Statistical Computing: Vienna, Austria.

Ragland GJ, Kingsolver JG (2008). Evolution of thermotolerance in seasonal environments: the effects of annual temperature variation and life-history timing in *Wyeomyia smithii*. *Evolution* **62**: 1345–1357.

Ramstedt B, Slotte JP (2002). Membrane properties of sphingomyelins. *FEBS Lett* **531**: 33–37.

Robinson MD, McCarthy DJ, Smyth GK (2010). edgeR: a Bioconductor package for differential expression analysis of digital gene expression data. *Bioinformatics* **26**: 139–140.

Robinson MD, Oshlack A (2010). A scaling normalization method for differential expression analysis of RNA-seq data. *Genome Biol* **11**: R25.

Rouault G, Candau J-N, Lieutier F, Nageleisen L-M, Martin J-C, Warzée N (2006). Effects of drought and heat on forest insect populations in relation to the 2003 drought in Western Europe. *Ann For Sci* **63**: 613–624.

Roy G, Miron M, Khaleghpour K, Lasko P, Sonenberg N (2004). The *Drosophila* Poly(A) Binding Protein-Interacting Protein, dPaip2, Is a novel rffector of cell growth. *Mol Cell Biol* **24**: 1143–1154.

Rusten TE, Lindmo K, Juhász G, Sass M, Seglen PO, Brech A, *et al.* (2004). Programmed autophagy in the *Drosophila* fat body Is induced by ecdysone through regulation of the PI3K pathway. *Dev Cell* **7**: 179–192.

Schluter D, Price TD, Rowe L (1991). Conflicting selection pressures and life history trade-offs. *Proc Royal Soc Lond [Biol]* **246**: 11–17.

Shi M, Wang Y-N, Zhu N, Chen X-X (2013). Four heat shock protein genes of the endoparasitoid wasp, *Cotesia vestalis*, and their transcriptional profiles in relation to developmental stages and temperature. *PLoS One* **8**: e59721.

Skidmore R, Gutierrez JA, Guerriero V, Kregel KC (1995). HSP70 induction during exercise and heat stress in rats: role of internal temperature. *Am J Physiol Regul Integr Comp Physiol* **268**: R92–R97.

Teets NM, Denlinger DL (2013). Physiological mechanisms of seasonal and rapid cold-hardening in insects: Seasonal and rapid cold-hardening in insects. *Physiol Entomol* **38**: 105–116.

Tettweiler G, Miron M, Jenkins M, Sonenberg N, Lasko PF (2005). Starvation and oxidative stress resistance in *Drosophila* are mediated through the eIF4E-binding protein, d4E-BP. *Genes Dev* **19**: 1840–1843.

Tucić N (1979). Genetic capaticy for adaptation to cold resistance at different developmental stages of *Drosophila melanogaster*. *Evolution* **33**: 350–358.

Wagner C, Isermann K, Roeder T (2009). Infection induces a survival program and local remodeling in the airway epithelium of the fly. *FASEB J* **23**: 2045–2054.

Wang RC, Levine B (2010). Autophagy in cellular growth control. *FEBS Lett* **584**: 1417–1426.

Woods HA (2013). Ontogenetic changes in the body temperature of an insect herbivore (R Wilson, Ed.). *Funct Ecol* **27**: 1322–1331.

Xu T, Nicolson S, Denton D, Kumar S (2015). Distinct requirements of autophagy-related genes in programmed cell death. *Cell Death Differ* **22**: 1792–1802.

Yiangou M, Tsapogas P, Nikolaidis N, Scouras ZG (1997). Heat shock gene expression during recovery after transient cold shock in *Drosophila auraria* (Diptera: Drosophilidae). *Cytobios* **92**: 91–98.

Zid BM, Rogers AN, Katewa SD, Vargas MA, Kolipinski MC, Lu TA, *et al.* (2009). 4E-BP extends lifespan upon dietary restriction by enhancing mitochondrial activity in *Drosophila*. *Cell* **139**: 149–160.

Chapter 4 Figures

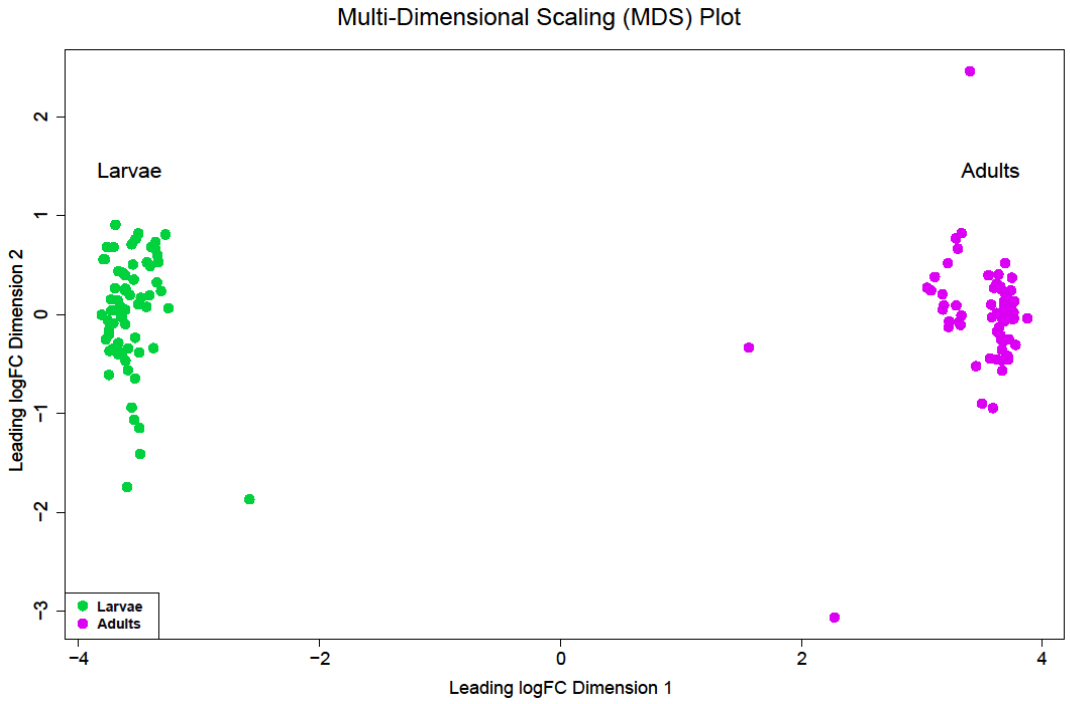

Figure 4.1 Cross-Stage MDS Plot

Multi-Dimensional Scaling (MDS) plot of the experimental samples. Larvae (green) and adults (purple) separate along the first LogFC dimension.

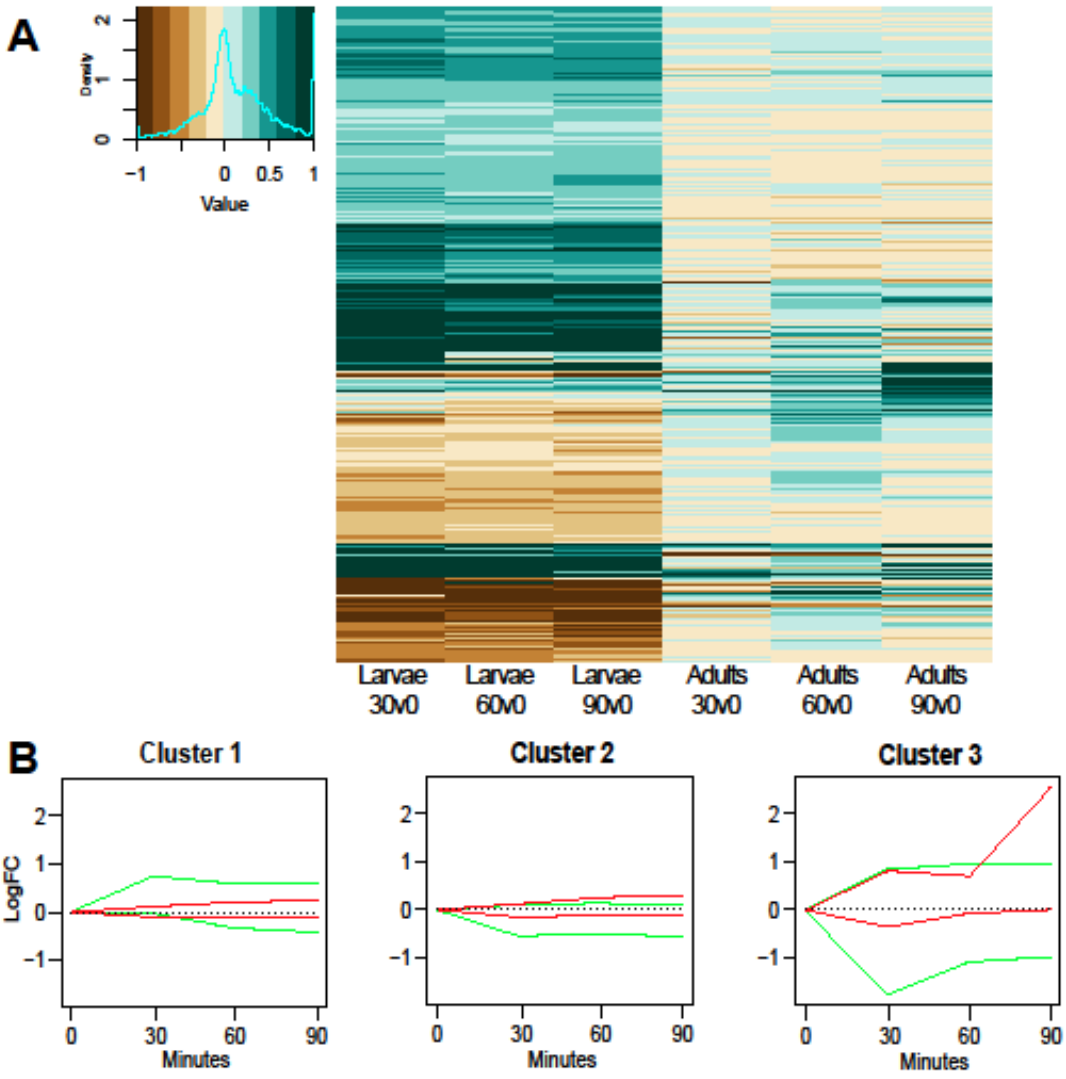

Figure 4.2 Heat Map and Clusters

In A.) Heatmap of 1,561 genes that were found to be significantly differentially expressed between or within stages across time. Genes in brown are downregulated while genes in green are upregulated. In B.) the three clusters are depicted graphically. Red lines depict adult expression trajectories and green depict larval expression trajectories. Lines above the dotted line are up-regulated and lines below this threshold are down-regulated.

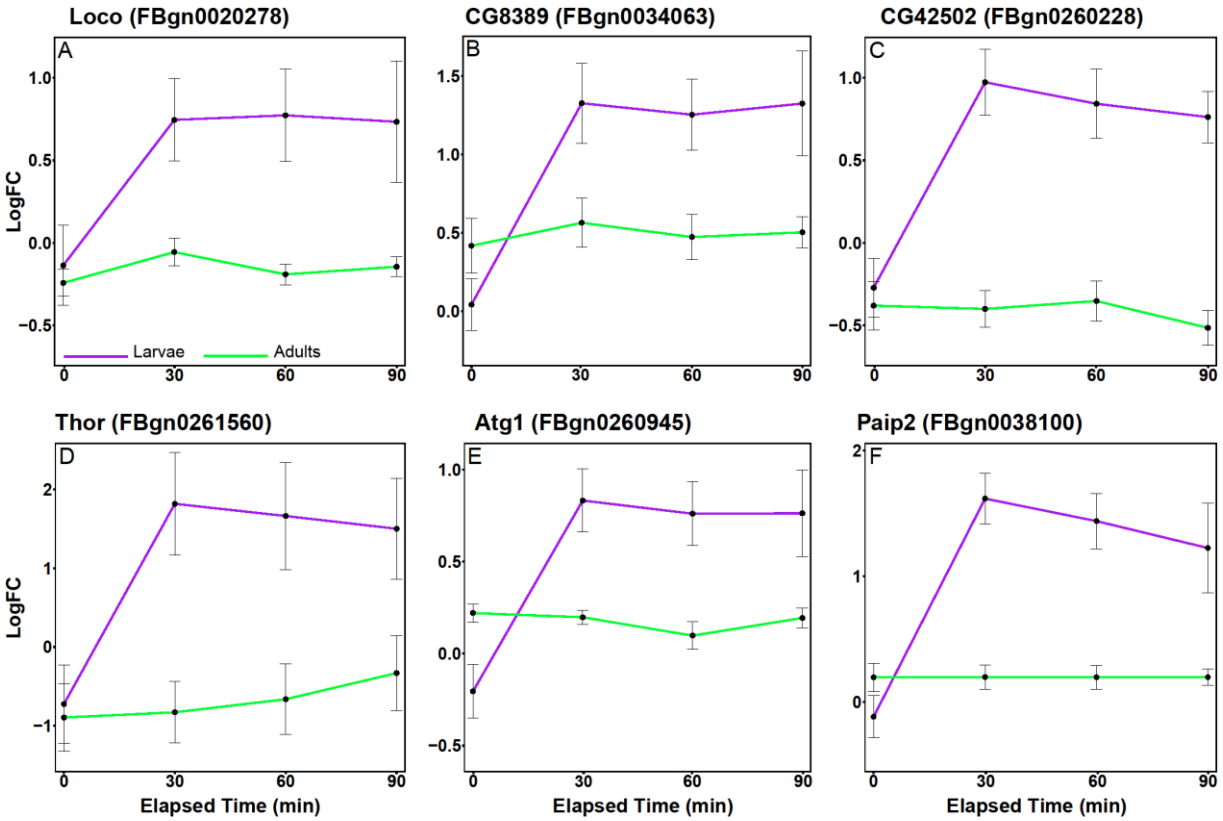

Figure 4.3 Genes Up-Regulated in Larvae

Scatter plots of the most significantly differentially expressed genes with up-regulation in larvae compared to adults. Larval trajectories are in purple while adult trajectories are in green. The x-axes represent each of the four time points and the y-axes are the $\log_2$FC. Gene names and Flybase reference numbers are above each plot.

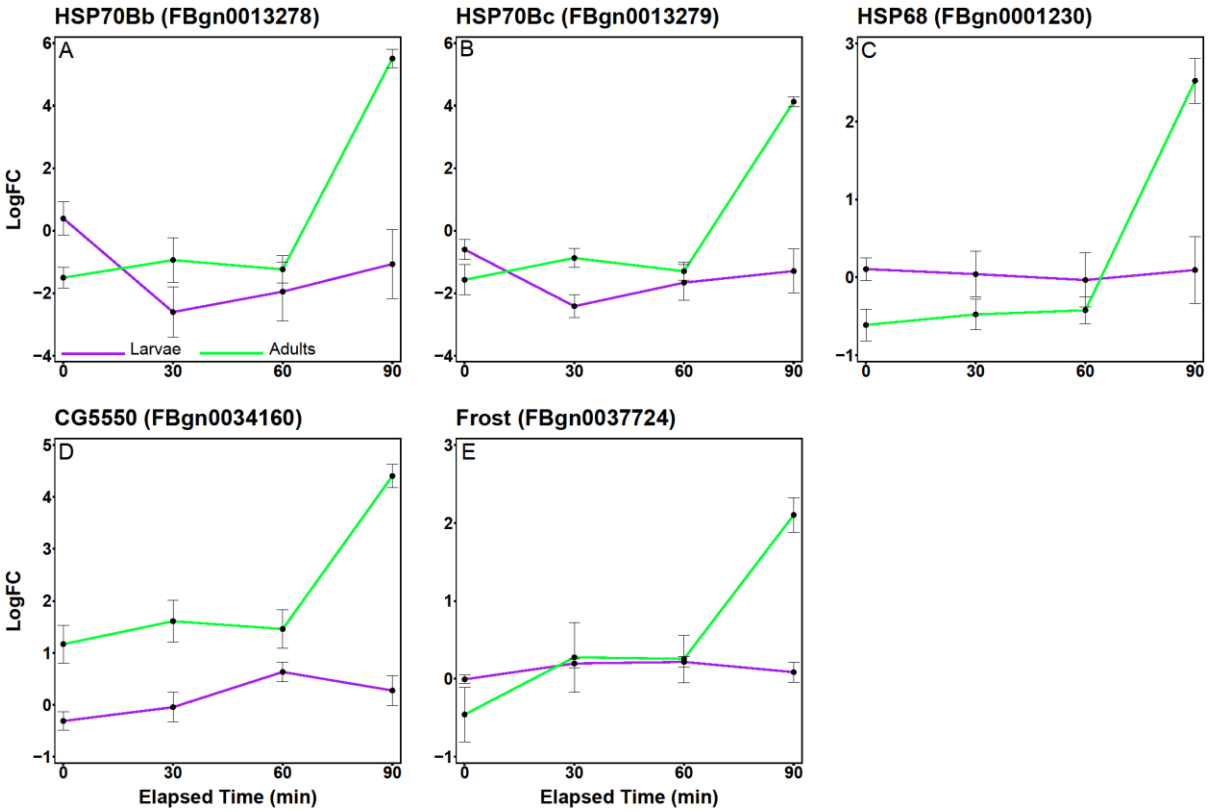

Figure 4.4 Genes Up-Regulated in Adults

Scatter plots of the most significantly differentially expressed genes with up-regulation in adults compared to larvae. Larval trajectories are in purple while adult trajectories are in green. The x-axes represent each of the four time points and the y-axes are the $\log_2$FC. Gene names and Flybase reference numbers are above each plot.

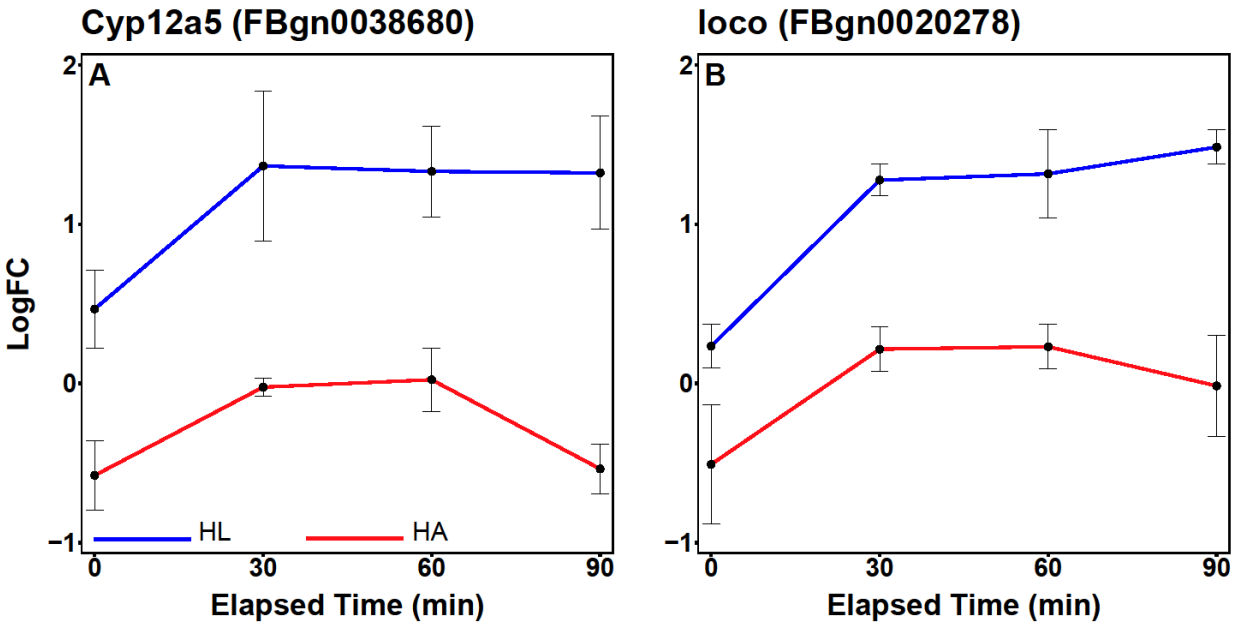

Figure 4.5 Genes with Differential Expression between Larval Phenotypes

Scatter plots of the genes with significant differential expression during stress responses between HL and HA lines in larvae. HL trajectories are in blue while HA trajectories are in red. The x-axes represent each of the four time points and the y-axes are the $\log_2$FC. Gene names and Flybase reference numbers are above each plot.

Chapter 4 Tables

Top 10 Enriched GO Terms and Pathways by Comparison	
GO Terms	***Pathways***
30v0	
ribosome biogenesis	Ion influx/efflux at host-pathogen interface
ribonucleoprotein complex biogenesis	CD28 dependent Vav1 pathway
pigmentation during development	Degradation of GABA
rRNA processing	MAPK6/MAPK4 signaling
pigmentation	HDL remodeling
Ras-related protein Rab	Reproduction
ncRNA processing	Meiosis
multicellular organismal aging	Meiotic recombination
aging	Synthesis of pyrophosphates in the cytosol
determination of adult life span	Urea cycle
60v0	
DNA binding	Synthesis of UDP-N-acetyl-glucosamine
acyl-CoA oxidase	Coenzyme A biosynthesis
cell fate determination	Rhesus glycoproteins mediate ammonium transport.
dorsal/ventral pattern formation	Synthesis of substrates in N-glycan biosythesis
dorsal/ventral axis specification	Mismatch Repair
positive regulation of organ growth	Mismatch repair (MMR) directed by MSH2:MSH6 (MutSalpha)
lyase	HDR through MMEJ (alt-NHEJ)
Glutamine amidotransferase, type II	Vitamin B5 (pantothenate) metabolism
anatomical structure homeostasis	Regulation of TP53 Activity through Association with Co-factors

Lipid synthesis	Biosynthesis of the N-glycan precursor (dolichol lipid-linked oligosaccharide, LLO) and transfer to a nascent protein
90v0	
response to oxygen levels	Common Pathway of Fibrin Clot Formation
response to hypoxia	Formation of Fibrin Clot (Clotting Cascade)
response to temperature stimulus	NOD1/2 Signaling Pathway
apoptosis	Methionine salvage pathway
positive regulation of programmed cell death	ADP signaling through P2Y purinoceptor 1
positive regulation of cell death	Signal amplification
transcription	Apoptotic cleavage of cell adhesion proteins
regulation of retinal cell programmed cell death	p38MAPK events
sugar transmembrane transporter activity	Fibronectin matrix formation
zymogen	via Dependence Receptors in the absence of ligand
Common to Multiple Comparisons	
cell death	Macroautophagy
death	Import of palmitoyl-CoA into the mitochondrial matrix
programmed cell death	Signaling by EGFR
histolysis	AMPK inhibits chREBP transcriptional activation activity
tissue death	EGFR downregulation
intracellular signaling cascade	O2/CO2 exchange in erythrocytes
salivary gland cell autophagic cell death	Erythrocytes take up carbon dioxide and release oxygen
salivary gland histolysis	Erythrocytes take up oxygen and release carbon dioxide
autophagic cell death	Fatty acyl-CoA biosynthesis

endocytosis	Fatty acid metabolism

Table 4.1 Top 10 Enriched GO Terms and Pathways

Table of the top 10 enriched go terms and pathways for each pairwise comparison and for multiple pairwise comparisons.

Chapter 5 - Conclusions & Future Directions

Genetic Decoupling across Metamorphosis – Chapter 2 Conclusions

The results in Chapter 2 provide evidence that thermal hardiness is decoupled across the metamorphic boundary free to evolve independently in *D. melanogaster* larvae and adults. This conclusion is supported from two factors: first, by the non-significant phenotypic and genetic correlation estimates between larvae and adults and, second, by illustration that different genetic architectures underlie the variation in thermal hardiness using Genome-Wide Association (GWA). Our results support and bolster the work of previous researchers, namely Tucić (1979), Loeschcke and Krebs (1996), Gilchrist et al. (1997), and Dierks et al. (2012) using a robust, genomic-level experimental setup. Additionally, these results also provide evidence in support of the adaptive decoupling hypothesis (Moran 1994).

Taken together, these results highlight the importance of whole life history-analysis when predicting the geographic distributions and evolutionary potentials of systems with complex life histories as holometabolous insects are important factors in medicine and agriculture as well as important players in ecosystems worldwide. Furthermore, these results suggest that development, significantly, the metamorphic boundary, can be a barrier to natural selection, facilitating intrinsic biological variation (Bowler and Terblanche 2008) via stage-specific responses to selection.

In the future, it will be of interest to assess genetic correlations for other traits across diverse life histories in other systems. For examples, within Insecta, there exists a continuum of life cycle complexity from ametaboly to hypermetaboly. Assessing correlations across this continuum for a number of different traits would illustrate the potentiality of adaptive decoupling

in many systems and pinpoint which traits are free to evolve independently across of range of life histories to answer if decoupling is correlated with life history complexity.

Stage-Specific GxE and Niche Adaptation – Chapter 3 Conclusions

Chapter 3, in many ways, extends the results of Chapter 2 by illustrating that heat hardiness, in additional to cold hardiness, is also decoupled across the metamorphic boundary across two different rearing conditions. However, there are many other implications that can be made from the results. The results also indicate that larvae and adults respond to changes in the developmental environment uniquely (GxDxE), allowing for stage-specific developmental acclimation and niche adaptation to unique thermal habitats. Furthermore, we illustrate that within each life stage, different genetic variants are associated with both heat and cold hardiness. This had been substantiated in previous work in adults (Morgan and Mackay 2006; Norry et al. 2008). However, when reared at a stressful temperature (18°C), there exists a significant correlation between cold and heat hardiness in larvae. This provides evidence that there may be some universal acclimation response in larvae initiated via stressful rearing, but it also further illustrates potential differences in acclimation response mechanisms across the metamorphic boundary.

Taken together, this chapter further extends the understanding of how decoupled thermal hardiness is between the metamorphic boundary and partially explains the mechanisms for thermal niche adaptation in the species. The lives of *D. melanogaster* larvae and adults are distinct with larvae dedicated to fitness roles such as feeding, and growth and adults dedicated to mating, dispersal, and overwintering (Saunders et al. 1989; Schmidt et al. 2005). The results provide evidence that this fitness partitioning, through selective forces, can lead to the difference in thermal performance we observe in larvae and adults. Furthermore, these results further

bolster the adaptive decoupling hypothesis (Moran 1994) by providing evidence for stage-specific responses to selection on an ecological scale.

In the future, it would be of interest to extend this type of analysis to other, non-model, systems in order to further explore developmental acclamation across life cycle complexity.

Transcriptomic Decoupling across Metamorphosis – Chapter 4 Conclusions

Chapter 4 provides evidence that the transcriptomic responses to acute cold stress is unique in larvae and adults of *D. melanogaster*. One core difference is that classic thermal stress response mechanisms like molecular chaperone activation is significantly upregulated in adults but not larvae. This is an interesting result that requires further study. One possible experiment to evaluate this result would involve knocking down or knocking out these genes and assessing the effect in both life stages to determine if this modification reduces hardiness in adults but not in larvae. In addition to this result, it is apparent that larvae respond to stress early using a variety of genes and pathways during stress exposure while adults activate only a core set of genes immediately after stress. Moreover, larvae, likely due to their active growth and differentiation, regulate genes that are involved with autophagy and metabolic modifications which are likely part of a general stress response regime. It is, at this point, unclear if larvae employ lipid modification as a mechanism to combat cold injury, however, additional testing is required to elucidate this possibility.

The analysis of cross-phenotype transcriptional profiles within stages, provides evidence that genotypes achieve cold hardiness in unique ways. Only two genes were detected to have significant differential expression within or after stress exposure in larvae. In adults, only genes with significantly constitutive differential expression were detected. Taken together, these results

point to polygenic architectures underlying thermal hardiness in larvae and adults with variants exhibiting a wide range of effect sizes.

Concluding Remarks

This body of work, using multiple, robust analyses, provides evidence that complex life cycles evolve decouple life stages in order to adapt to unique habitats and optimally deconstruct fitness across ontogeny. Because of these results and those of others, the adaptive decoupling hypothesis (Moran 1994) has been substantiated with empirical data. Also, this work provides a framework, in the form of thermal hardiness, to test for adaptive decoupling across ontogeny. It would be prudent for future researchers to focus on other, non-model systems and other fitness-related traits to further investigate this phenomenon in order to better prepare for insect-based agricultural and medical threats as well as provide more comprehensive estimates of species distributions in an ever-changing world due to global climate change.

References

Bowler K, Terblanche JS (2008). Insect thermal tolerance: what is the role of ontogeny, ageing and senescence? *Biol Rev Camb Philos Soc* **83**: 339–355.

Dierks A, Kölzow N, Franke K, Fischer K (2012). Does selection on increased cold tolerance in the adult stage confer resistance throughout development? *J Evol Biol* **25**: 1650–1657.

Gilchrist GW, Huey RB, Partridge L (1997). Thermal sensitivity of *Drosophila melanogaster*: evolutionary responses of adults and eggs to laboratory natural selection at different temperatures. *Physiol Zool* **70**: 403–414.

Loeschcke V, Krebs RA (1996). Selection for heat-shock resistance in larval and in adult *Drosophila buzzatii*: comparing direct and indirect responses. *Evolution* **50**: 2354–2359.

Moran N (1994). Adaptation and constraint in the complex life cycles of animals. *Annu Rev Ecol Evol Syst* **2**: 573–600.

Morgan TJ, Mackay TFC (2006). Quantitative trait loci for thermotolerance phenotypes in *Drosophila melanogaster*. *Heredity* **96**: 232.

Norry FM, Scannapieco AC, Sambucetti P, Bertoli CI, Loeschcke V (2008). QTL for the thermotolerance effect of heat hardening, knockdown resistance to heat and chill-coma recovery in an intercontinental set of recombinant inbred lines of *Drosophila melanogaster*. *Mol Ecol* **17**: 4570–4581.

Saunders DS, Henrich VC, Gilbert LI (1989). Induction of diapause in *Drosophila melanogaster*: photoperiodic regulation and the impact of arrhythmic clock mutations on time measurement. *Proc Natl Acad Sci USA* **86**: 3748–3752.

Schmidt PS, Matzkin L, Ippolito M, Eanes WF (2005). Geographic variation in diapause incidence, life-history traits, and climatic adaptation in *Drosophila melanogaster*. *Evolution* **59**: 1721–1732.

Tucić N (1979). Genetic capaticy for adaptation to cold resistance at different developmental stages of *Drosophila melanogaster*. *Evolution* **33**: 350–358.

Appendix A - Chapter 2 Supplementary Data

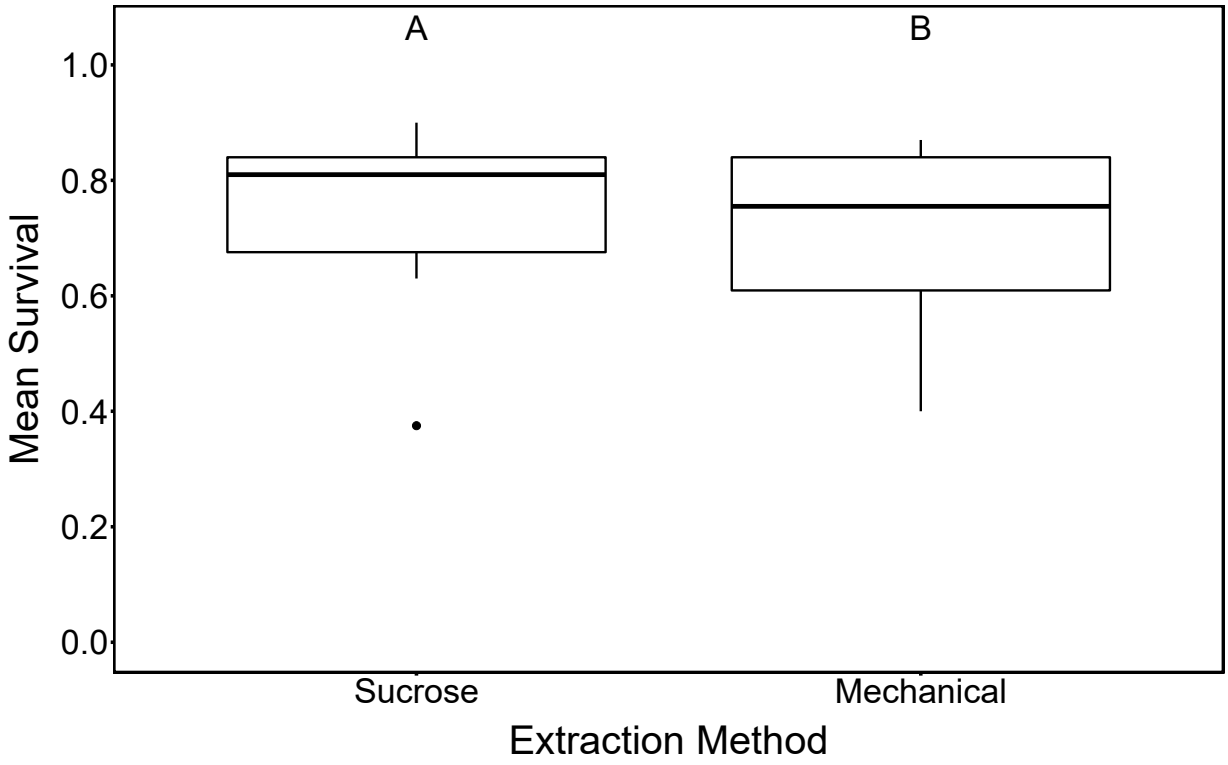

Figure A.1 Extraction Method Comparison

To determine if sucrose extraction influenced larval survival, a subset of 10 DGRP lines were assayed after being extracted either mechanically (physically plucked out of the media with a soft brush) or extracted using a 20% w/v sucrose solution. The solution separates the larvae from the media so the larvae can be removed using a soft brush without disturbing the media and searching for the larvae. Other than the extraction method, the two groups experienced the same conditions (discussed in the "Methods" section of the main manuscript) including all vial transfers and washing in deionized water. A minimum of 4 replicates were performed for each extraction method per line.

The figure shows boxplots depicting the mean survival and quartiles for each extraction method across all lines. We found that survival of flies extracted using the sucrose solution was slightly higher (6.7%). This difference was found to be significant ($p = 0.017$) after analyzing the binomial count data using a generalized linear mixed model in a logit link function implemented in lme4 (glmer function; Bates et al. 2015) in R (R Core Team 2014). To determine if there was any significant interaction between line and extraction method, we reran the data using an interaction term including line and extraction methods. This result was not significant ($p = 0.10$), indicating that the differences among lines are unlikely to be caused by different responses to the sucrose extraction method.

References

Bates D, Mächler M, Bolker B and Walker S (2015) Fitting Linear Mixed-Effects Models Using **lme4**. *Journal of Statistical Software* 67(1). Available at: http://www.jstatsoft.org/v67/i01/ (accessed 17/09/16).

R Core Team (2017) *R: A language and environment for statistical computing.* R Foundation for Statistical Computing, Vienna, Austria. URL: http://www.R-project.org/.

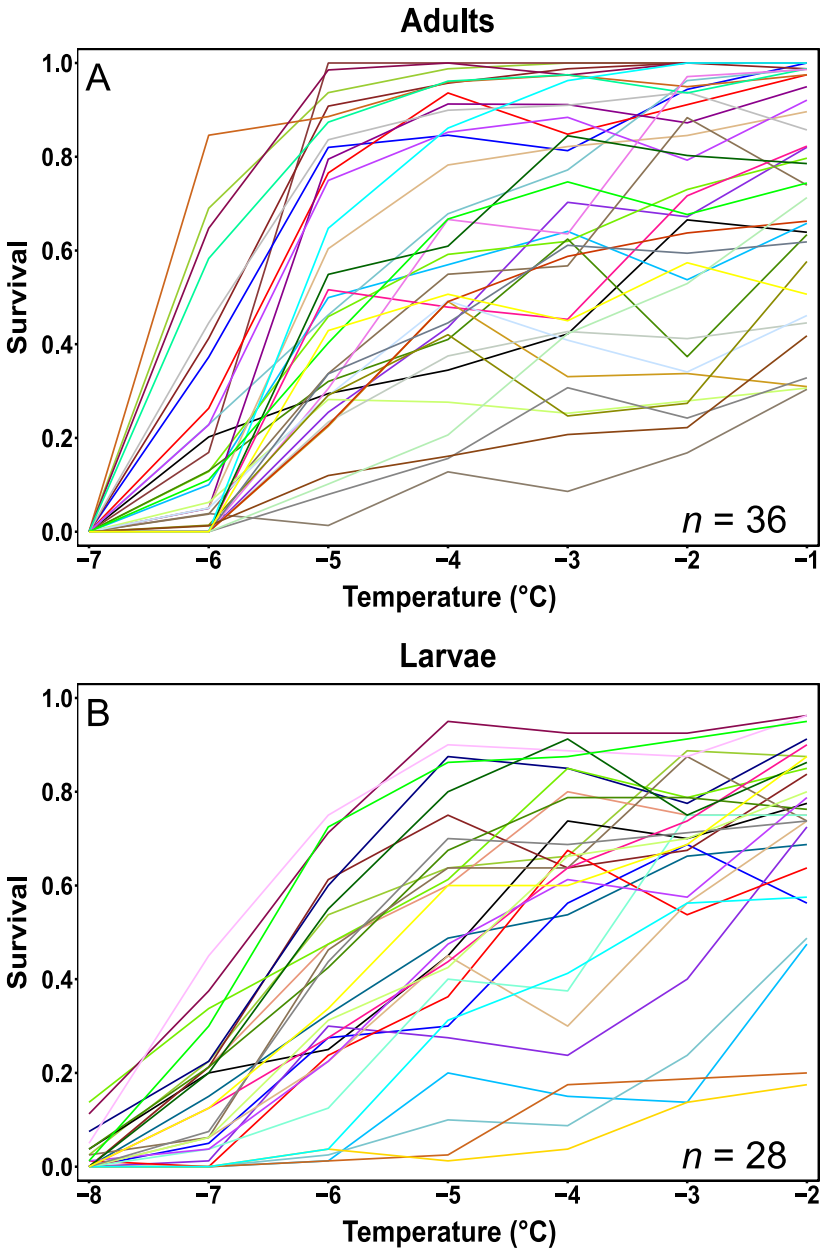

Figure A.2 Survival Curves

Initially, we wished to create survival curves over a set of temperatures for both larvae and adults in a subset of lines to determine whether survival at a single temperature near the LD50 (temperature producing 50% survival) could accurately predict the shape of the full curve. For larvae, a subset of 28 lines were randomly selected and survival was scored after a 1h

exposure to a range of seven temperatures spanning -8° C to -2° C (-8° C, -7° C, -6° C, -5° C, -4° C, -3° C, and -2° C). In adults, 36 lines were randomly selected. Survival was scored after a 1h exposure to a range of seven temperatures spanning -7° C to -1° C (-7° C, -6° C, -5° C, -4° C, -3° C, -2° C, and -1° C). Different ranges were implemented to span as much of the survival range as possible (0% - 100%). Since adults had 100% mortality at -7° C (see figure), a higher range was selected. A minimum of four replicates were performed for each line in each temperature and for both life stages. Larvae and adults were reared, extracted, and assayed as described in the "Methods" section on the main manuscript.

The Figure displays survival curves for each line in A.) adults and B.) larvae. Each colored line represents a DGRP line's survival curve over the range of temperatures in °C. Substantial variation exists in the subset of lines selected for each life stage. The test temperature for future assays was determined from these survival curves (see Figure A.3).

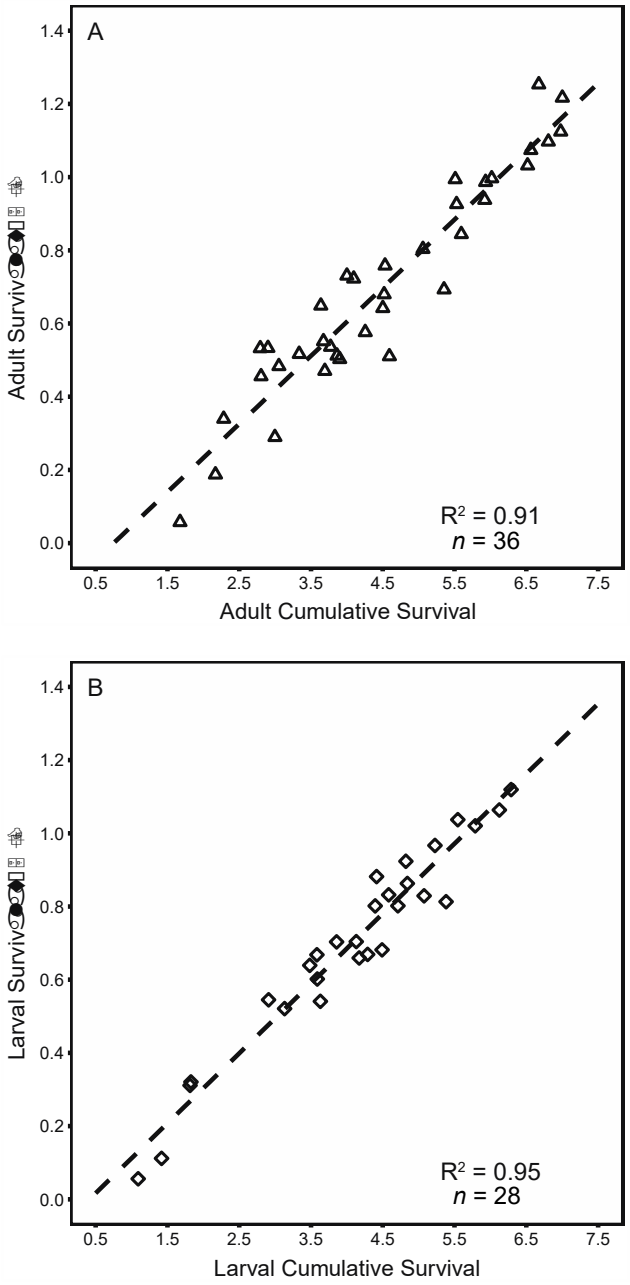

Figure A.3 Selection of Test Temperature

To determine the test temperature to estimate the genetic correlation between larvae and adults and perform genome-wide association, survival at each of the seven temperatures performed on a subset of lines in both larvae and adults (see Figure A.2) were regressed against the cumulative survival (the sum) across all seven test temperatures. Based on these results, we

selected -5° C as the appropriate, single test temperature due to it exhibiting the strongest, highly significant correlation with cumulative survival across all temperatures.

The Figure shows this relationship in both A.) adults and B.) larvae. For both life stages -5° C had the highest coefficient of correlation with cumulative survival (Adults: $R^2 = 0.91$; Larvae, $R^2 = 0.95$). The dashed line in each pane represents the regression line between survival at -5° C and cumulative survival. Proportional survival scores were arcsine transformed to perform correlations.

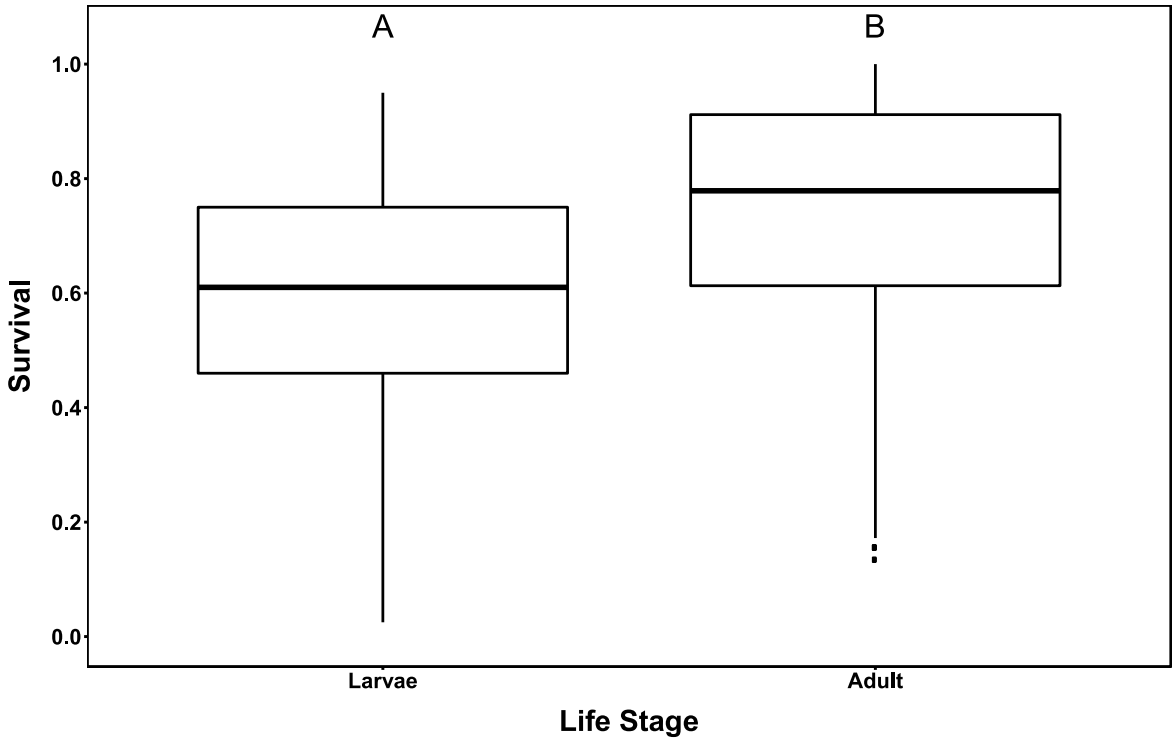

Figure A.4 Life Stage Survival Comparison

Mean survival was found to be significantly higher in adults compared to larvae (mean proportion surviving ± standard error; Adults = 0.73 ± 0.052; Larvae = 0.60 ± 0.064; $p < 0.001$) after analyzing the binomial count data using a generalized linear mixed model in a logit link function implemented in lme4 (glmer function; Bates et al. 2015) in R (R Core Team 2014). Larvae and adults were reared, extracted, and assayed as described in the "Methods" section on the main manuscript.

The figure shows boxplots depicting the mean survival and quartiles for each life stage from all 139 DGRP lines.

References

Bates D, Mächler M, Bolker B and Walker S (2015) Fitting Linear Mixed-Effects Models Using **lme4**. *Journal of Statistical Software* 67(1). Available at: http://www.jstatsoft.org/v67/i01/ (accessed 17/09/16).

R Core Team (2017) *R: A language and environment for statistical computing.* R Foundation for Statistical Computing, Vienna, Austria. URL: http://www.R-project.org/.

Chromosomal position	FlyBase ID	alpha	beta	gamma	Effect Size
2L_9410938_SNP	FBgn0085395	-1.78E-06	-0.1054772	0.27611	-0.0291251
X_10434820_SNP	FBgn0085443	-8.46E-07	-0.2056209	0.07177	-0.0147583
X_12034441_INS	FBgn0267001	-3.00E-07	-0.2124014	0.0559	-0.0118735
2R_17924573_SNP	FBgn0085399	-3.44E-07	-0.1722474	0.06198	-0.0106762
3L_8564344_SNP	FBgn0260442	-7.12E-07	-0.1167976	0.05486	-0.0064082
3L_16878433_SNP	FBgn0261565	-1.23E-06	-0.1334455	0.0477	-0.0063666
3R_10183710_SNP	FBgn0024321	-2.15E-06	-0.0809023	0.06659	-0.0053894
X_2422020_SNP	FBgn0267911	-7.06E-07	-0.1605672	0.0244	-0.0039185
X_2566738_SNP	FBgn0003371	-1.60E-06	-0.1051675	0.03399	-0.0035762
2L_9620991_SNP	FBgn0032135	-8.80E-07	-0.158057	0.01833	-0.0028981
2L_1610547_SNP	FBgn0051935	-2.66E-07	-0.1818248	0.01185	-0.0021549
2L_13129988_SNP	FBgn0032471	-7.79E-07	-0.1041644	0.01932	-0.0020132
X_21191806_SNP	FBgn0029067	-8.59E-07	-0.0712151	0.02293	-0.0016338
X_2421530_SNP	FBgn0267911	-8.37E-07	-0.1519782	0.00999	-0.0015191
X_2421663_SNP	FBgn0267911	-8.37E-07	-0.1538102	0.00843	-0.0012975
2R_15561275_SNP	FBgn0028372	-1.19E-06	-0.0421524	0.03075	-0.0012974
2L_7116390_SNP	FBgn0085407	-8.45E-07	-0.1307974	0.00919	-0.0012029
3R_4602207_SNP	FBgn0261015	-1.40E-06	-0.0559762	0.02092	-0.0011724
3L_1585614_DEL	FBgn0035237	2.37E-07	0.1578575	0.00722	0.00113997
3R_25417092_SNP	FBgn0086361	-2.93E-07	-0.0503111	0.02246	-0.0011303
3R_14413457_SNP	FBgn0038627	-5.19E-07	-0.0516371	0.02097	-0.0010834
3L_945767_SNP	FBgn0264574	-9.79E-07	-0.1682609	0.00636	-0.0010711
3L_13988889_SNP	FBgn0250848	-1.88E-06	-0.072415	0.0132	-0.0009578
3L_479274_SNP	FBgn0001316	-2.22E-07	-0.0540961	0.0166	-0.0008982
2L_16295068_SNP	FBgn0001992	-1.89E-06	-0.0813365	0.01045	-0.0008519
2R_4314695_SNP	FBgn0028836	4.38E-07	0.04113798	0.02032	0.00083636
3R_14816417_SNP	FBgn0026239	-1.62E-07	-0.0411041	0.02016	-0.0008288
3R_9951635_SNP	FBgn0262955	-1.53E-06	-0.0680391	0.01202	-0.0008194
2R_19597874_INS	FBgn0266865	-1.09E-06	-0.0327981	0.02394	-0.0007863
X_16275665_DEL	FBgn0004598	-9.21E-07	-0.0537048	0.0142	-0.0007635
3R_26531988_SNP	FBgn0051010	-7.46E-08	-0.0464884	0.01632	-0.0007588
X_5504700_SNP	FBgn0263511	1.23E-06	0.02742535	0.02657	0.00072992
X_7232011_SNP	FBgn0029941	-9.71E-07	-0.0536339	0.01323	-0.0007105
3R_17253329_SNP	FBgn0008651	-1.29E-06	-0.108384	0.00634	-0.0006884
2R_17961968_SNP	FBgn0034689	-3.10E-07	-0.2268542	0.00298	-0.0006763
X_2421541_SNP	FBgn0267911	-7.63E-07	-0.1692726	0.00396	-0.0006711
X_2421762_SNP	FBgn0267911	-8.38E-07	-0.1559453	0.00429	-0.0006698
3R_6390313_SNP	FBgn0001235	-7.52E-07	-0.0956343	0.00629	-0.0006023

3R_17895271_SNP	FBgn0264491	1.26E-06	0.03392021	0.01655	0.00056264
3R_19966331_SNP	FBgn0039154	6.09E-07	0.02520475	0.02185	0.00055133
2L_22566847_SNP	FBgn0058006	1.06E-06	0.02669317	0.02036	0.00054453
3R_25627692_SNP	FBgn0039697	5.15E-07	0.02166846	0.02442	0.00052966
3R_26836150_SNP	FBgn0004573	5.42E-07	0.07447619	0.00704	0.00052485
X_2241540_SNP	FBgn0003159	6.78E-07	0.08199015	0.00623	0.00051148
3L_20853569_SNP	FBgn0052432	-9.10E-07	-0.034194	0.01491	-0.0005107
2R_7954388_SNP	FBgn0033679	-1.27E-06	-0.0364924	0.01373	-0.0005023
3R_21757901_DEL	FBgn0039396	-1.34E-06	-0.0408069	0.01121	-0.0004588
3L_13988888_SNP	FBgn0250848	-1.99E-06	-0.0717364	0.00619	-0.000446
X_22283756_SNP	FBgn0259677	1.12E-06	0.04771183	0.00924	0.00044198
3L_5592798_SNP	FBgn0035621	1.11E-06	0.03059971	0.01437	0.00044083
3L_11164982_SNP	FBgn0036142	7.47E-07	0.02191463	0.01975	0.00043356
3L_12881724_DEL	FBgn0036321	5.96E-07	0.04800082	0.00893	0.00042924
3R_25326348_SNP	FBgn0039668	1.24E-06	0.05087499	0.00826	0.00042147
3R_26710813_SNP	FBgn0000416	8.83E-07	0.02856034	0.01471	0.00042101
2L_2716753_SNP	FBgn0051690	-5.11E-07	-0.0222969	0.01838	-0.0004103
2L_4337175_SNP	FBgn0020762	-6.98E-07	-0.0268289	0.01479	-0.0003975
2R_7943208_SNP	FBgn0265373	6.96E-07	0.02787128	0.01419	0.00039619
2R_8128751_SNP	FBgn0263020	-7.39E-07	-0.0272942	0.01448	-0.000396
2L_9400715_SNP	FBgn0085395	-1.50E-06	-0.0797052	0.00492	-0.0003937
3L_13709230_SNP	FBgn0264001	-7.12E-07	-0.0259134	0.015	-0.0003894
2L_14406770_SNP	FBgn0004858	-6.58E-07	-0.0529282	0.00731	-0.0003876
3R_7856240_SNP	FBgn0260230	9.70E-07	0.03087292	0.01252	0.0003875
2R_14832611_INS	FBgn0034408	1.17E-07	0.03520331	0.01081	0.00038067
X_10201294_SNP	FBgn0259170	-3.81E-07	-0.0330174	0.01142	-0.0003774
X_7451776_DEL	FBgn0265694	-7.84E-07	-0.0499668	0.00749	-0.000375
X_16708102_SNP	FBgn0030796	-5.58E-07	-0.0414959	0.00885	-0.0003678
2R_14875943_SNP	FBgn0265356	-2.01E-06	-0.0573434	0.00635	-0.0003661
X_8157708_SNP	FBgn0030027	7.94E-07	0.03455899	0.01057	0.00036608
2L_19886715_SNP	FBgn0263873	-2.77E-07	-0.0313863	0.01163	-0.0003653
3L_12630729_SNP	FBgn0052111	4.43E-07	0.0448456	0.00812	0.00036459
3R_10705109_SNP	FBgn0038268	-1.04E-06	-0.0404891	0.00886	-0.0003598
3R_21561447_INS	FBgn0051092	-2.05E-07	-0.0356227	0.00998	-0.0003557
2R_17285081_SNP	FBgn0010415	-4.41E-07	-0.1752671	0.002	-0.000351
2L_4363854_SNP	FBgn0026319	-7.52E-07	-0.0292556	0.01195	-0.0003504
2L_9469513_SNP	FBgn0264269	7.45E-07	0.02021381	0.01719	0.00034822
3R_15045428_SNP	FBgn0267975	-1.82E-06	-0.060344	0.00569	-0.0003452
2L_2061710_SNP	FBgn0053516	-8.66E-07	-0.0779895	0.00436	-0.0003409

3R_25258685_SNP	FBgn0004369	1.71E-07	0.03463589	0.0098	0.0003396
2L_12272831_SNP	FBgn0000114	-7.07E-08	-0.0305152	0.01111	-0.0003391
3R_9951347_SNP	FBgn0010340	-1.55E-06	-0.0805157	0.00414	-0.0003349
3R_12083828_SNP	FBgn0040071	-1.28E-06	-0.04806	0.0067	-0.0003233
2R_15472256_MNP	FBgn0003435	6.39E-07	0.02510734	0.01279	0.00032176
2R_7493372_SNP	FBgn0033636	-1.14E-06	-0.0394364	0.00812	-0.0003214
2R_18070790_SNP	FBgn0034707	-1.79E-06	-0.0556097	0.00574	-0.000321
3L_3615651_SNP	FBgn0035453	7.68E-07	0.0706882	0.00449	0.00031816
2L_9400704_SNP	FBgn0085395	-1.57E-06	-0.0883219	0.00358	-0.0003178
3L_6297968_SNP	FBgn0266589	-9.95E-07	-0.0315992	0.00988	-0.0003132
2L_2356903_SNP	FBgn0031414	4.33E-07	0.01756324	0.01776	0.00031236
3R_13877248_SNP	FBgn0010389	9.74E-07	0.03343783	0.00924	0.00030994
3R_4617292_SNP	FBgn0046874	-1.68E-06	-0.0703341	0.00438	-0.0003097
2L_13253832_SNP	FBgn0051728	-7.68E-07	-0.0514366	0.00599	-0.0003089
3L_8583683_SNP	FBgn0262508	-6.17E-07	-0.0337726	0.00911	-0.0003083
X_14219572_SNP	FBgn0052600	-9.20E-07	-0.0333358	0.00914	-0.0003056
3R_9951276_SNP	FBgn0010340	1.88E-06	0.07712013	0.00387	0.00030033
2L_8062118_SNP	FBgn0011230	9.49E-07	0.06084626	0.00489	0.00029849
2L_10929350_SNP	FBgn0261871	1.18E-06	0.02926422	0.01003	0.0002947
2R_4085639_SNP	FBgn0053087	8.66E-07	0.02932394	0.00996	0.00029293
3R_10170419_SNP	FBgn0024321	-2.66E-07	-0.0483493	0.00605	-0.0002928
X_13603334_SNP	FBgn0265726	4.60E-08	0.01967309	0.01438	0.00028295
3R_9951448_SNP	FBgn0262955	-1.58E-06	-0.0775124	0.0036	-0.0002806

Table A.1 Top 100 Associated Variants, ranked by Effect Size in Larvae

Column 1 is the chromosomal position and bp location of the variant. Column 2 is the FlyBase ID, Columns 3, 4, and 5 are alpha, beta, and gamma, respectively, which are estimated BSLMM parameters. Column 6 is the effect size (beta * gamma).

Chromosomal position	FlyBase ID	alpha	beta	gamma	Effect Size
2R_14120187_INS	FBgn0000658	-1.20E-06	-0.0425806	0.01254	-0.0005352
3L_5909616_SNP	FBgn0035648	1.38E-06	0.1038155	0.00512	0.00053291
2L_847986_SNP	FBgn0020304	1.81E-06	0.08110664	0.00553	0.00045033
2R_11916075_SNP	FBgn0034069	1.81E-06	0.07721365	0.00536	0.00041568
2R_18917000_SNP	FBgn0003900	7.44E-07	0.05147939	0.00749	0.00038633
2R_6741200_SNP	FBgn0050015	-1.13E-06	-0.0394882	0.00945	-0.0003743
X_15752586_INS	FBgn0065035	1.31E-06	0.06394236	0.00567	0.00036386
3L_1406514_SNP	FBgn0267487	-9.14E-07	-0.0509241	0.00683	-0.0003487
2L_11245179_SNP	FBgn0264442	-1.69E-06	-0.0798773	0.00432	-0.0003468
3R_22962431_MNP	FBgn0039492	6.31E-07	0.0361658	0.00865	0.00031347
3R_5822630_SNP	FBgn0045473	8.01E-07	0.03845667	0.00768	0.00029615
3L_5495928_SNP	FBgn0085371	-1.89E-06	-0.0493909	0.00584	-0.0002903
2R_13767669_SNP	FBgn0011589	8.32E-07	0.05120382	0.00562	0.0002886
2R_17143259_SNP	FBgn0085426	-2.01E-06	-0.062776	0.00449	-0.0002839
2L_17745404_SNP	FBgn0015609	1.25E-06	0.01704199	0.0162	0.00027733
3L_4486149_SNP	FBgn0035553	-8.02E-07	-0.192142	0.00143	-0.0002756
3R_2502765_SNP	FBgn0002522	-6.71E-07	-0.0218484	0.01214	-0.0002659
2L_15953384_SNP	FBgn0028645	-3.15E-07	-0.0835653	0.00296	-0.0002477
X_12091204_INS	FBgn0267001	-8.65E-07	-0.0191947	0.01266	-0.0002439
X_19367250_SNP	FBgn0052533	2.16E-06	0.05112829	0.00442	0.00022815
2R_11916074_SNP	FBgn0034069	1.77E-06	0.08582983	0.00261	0.00022579
2L_3302839_SNP	FBgn0031516	-9.49E-07	-0.0381618	0.00585	-0.0002242
X_18515658_SNP	FBgn0262981	7.35E-07	0.0333572	0.00613	0.00020522
3R_6156976_DEL	FBgn0266717	-7.77E-07	-0.0411152	0.00486	-0.0002006
3L_11751538_SNP	FBgn0036202	8.28E-07	0.05944772	0.00335	0.00019998
X_19509948_SNP	FBgn0031040	-1.26E-06	-0.0147213	0.01307	-0.0001937
2R_12035599_SNP	FBgn0029175	1.74E-06	0.05363669	0.00352	0.00019054
X_8919116_SNP	FBgn0264384	-9.55E-07	-0.0168767	0.01115	-0.0001891
2L_12240398_SNP	FBgn0000114	-3.35E-07	-0.0440052	0.00429	-0.0001891
3L_11917339_SNP	FBgn0036222	1.08E-06	0.04203076	0.00446	0.00018854
2R_18838687_DEL	FBgn0052835	1.15E-06	0.0304661	0.00613	0.00018791
3R_2521220_SNP	FBgn0004781	-7.29E-07	-0.028647	0.00628	-0.0001806
2R_18916932_SNP	FBgn0261705	-1.11E-06	-0.1291992	0.00137	-0.0001781
X_5279545_SNP	FBgn0029761	4.45E-07	0.0318604	0.0055	0.00017568
2L_13883152_SNP	FBgn0028509	-1.26E-06	-0.0599332	0.00289	-0.0001745
2R_17143254_SNP	FBgn0085426	-2.00E-06	-0.0594552	0.00289	-0.0001738
3R_20348560_SNP	FBgn0039202	1.31E-06	0.08186794	0.00204	0.00016832
X_22009400_SNP	FBgn0052499	9.78E-07	0.00917051	0.01805	0.00016651

3L_3806532_SNP	FBgn0052264	-1.21E-06	-0.0158306	0.01041	-0.000166
2R_10729921_DEL	FBgn0016684	-1.73E-06	-0.0560846	0.00283	-0.0001605
3L_5495045_SNP	FBgn0265712	-9.88E-07	-0.036326	0.00432	-0.0001579
3R_23671227_SNP	FBgn0085382	6.47E-07	0.0532309	0.00295	0.00015768
3R_11025670_SNP	FBgn0260659	6.63E-07	0.02729811	0.00572	0.00015681
X_16298438_DEL	FBgn0030746	-9.00E-07	-0.0159778	0.00968	-0.0001556
2R_12043524_DEL	FBgn0034083	1.10E-06	0.02261865	0.00677	0.00015423
2R_9422119_SNP	FBgn0260964	9.29E-07	0.03961636	0.00373	0.0001487
2R_13150821_SNP	FBgn0265487	-8.68E-07	-0.0254104	0.00579	-0.000148
2L_5069089_SNP	FBgn0028572	7.69E-07	0.06396431	0.00228	0.00014661
3R_17961195_SNP	FBgn0051163	-2.09E-06	-0.0622815	0.00227	-0.0001435
X_15620785_SNP	FBgn0030674	-5.51E-07	-0.2588975	0.00055	-0.0001429
2R_12390998_DEL	FBgn0011260	-8.66E-07	-0.0114453	0.01226	-0.0001412
X_8796011_DEL	FBgn0030067	7.46E-07	0.01417304	0.0099	0.00014106
3R_16442945_SNP	FBgn0038814	8.77E-07	0.00634981	0.02165	0.00013835
X_6211136_SNP	FBgn0029864	1.15E-06	0.01992707	0.00683	0.00013725
3L_4446340_SNP	FBgn0267303	-5.81E-07	-0.0187261	0.00725	-0.0001363
X_436860_SNP	FBgn0000108	1.17E-06	0.01672384	0.00804	0.00013563
3R_13015006_SNP	FBgn0038492	1.15E-06	0.02195126	0.00599	0.00013264
2R_5690850_SNP	FBgn0027589	8.99E-07	0.0314531	0.00406	0.0001286
X_1876798_SNP	FBgn0264562	-3.98E-07	-0.0260528	0.00491	-0.0001283
2L_9951706_SNP	FBgn0032168	6.98E-07	0.02653922	0.0048	0.00012809
X_22128961_SNP	FBgn0266348	-1.10E-06	-0.1075353	0.00118	-0.000128
X_22122676_SNP	FBgn0266348	-4.64E-07	-0.0663135	0.00188	-0.0001251
2R_5896723_SNP	FBgn0022382	-1.25E-06	-0.0325782	0.0038	-0.000125
2R_13592862_DEL	FBgn0028494	5.17E-07	0.03284789	0.00369	0.00012173
3R_12514367_SNP	FBgn0003944	-3.64E-07	-0.0470595	0.00257	-0.0001213
X_4879125_SNP	FBgn0266096	8.56E-07	0.04090952	0.00294	0.00012113
X_1641330_SNP	FBgn0025391	-8.08E-07	-0.0268987	0.00446	-0.0001208
3L_1462304_SNP	FBgn0266116	-1.01E-06	-0.0365261	0.00317	-0.0001168
2R_4585667_SNP	FBgn0033321	-1.09E-06	-0.0137854	0.00837	-0.0001165
2L_12212541_SNP	FBgn0000114	1.03E-06	0.01615778	0.00712	0.00011607
2L_4412767_SNP	FBgn0031602	-5.63E-07	-0.0048084	0.0235	-0.0001136
2L_4454897_SNP	FBgn0040705	1.20E-06	0.01814421	0.00617	0.00011315
3L_15642716_SNP	FBgn0004588	-3.64E-07	-0.0087879	0.01282	-0.000113
3R_27164884_SNP	FBgn0085376	1.85E-06	0.05613204	0.00198	0.00011299
3R_12366145_SNP	FBgn0259244	7.30E-07	0.00934717	0.01198	0.00011271
2L_11354610_SNP	FBgn0265797	1.82E-06	0.04702264	0.00234	0.00011186
X_10745712_SNP	FBgn0030240	8.64E-07	0.01388524	0.00792	0.00011084

2L_12137390_SNP	FBgn0032416	-8.77E-07	-0.0387293	0.00278	-0.0001085
X_22068387_SNP	FBgn0266348	1.05E-06	0.02887356	0.0037	0.00010788
X_16467314_SNP	FBgn0267912	-8.75E-07	-0.0132152	0.00802	-0.0001069
3R_12099909_SNP	FBgn0250823	-5.32E-07	-0.020478	0.00517	-0.0001064
2L_22623171_SNP	FBgn0058006	-3.53E-07	-0.1100967	0.00095	-0.0001049
2L_3398119_SNP	FBgn0085204	-1.60E-06	-0.0666376	0.00155	-0.0001049
3L_18652232_SNP	FBgn0036801	-3.65E-07	-0.0114859	0.0091	-0.0001049
2L_8771844_SNP	FBgn0032067	-1.30E-06	-0.0263711	0.00392	-0.0001047
3R_1056405_SNP	FBgn0040208	-1.10E-06	-0.0274994	0.00372	-0.0001034
3L_14556532_SNP	FBgn0054039	-2.21E-07	-0.044431	0.0023	-0.0001024
2L_18061327_SNP	FBgn0243486	-9.85E-07	-0.0240251	0.00422	-0.0001024
X_4231109_SNP	FBgn0262738	-8.12E-07	-0.0080029	0.01268	-0.0001023
X_10317984_SNP	FBgn0052683	-1.26E-06	-0.0443812	0.00224	-0.0001007
X_3048718_SNP	FBgn0004647	-5.62E-07	-0.0115881	0.00856	-9.98E-05
X_14766806_SNP	FBgn0264078	1.05E-06	0.04974688	0.00198	9.95E-05
3R_23381793_SNP	FBgn0004387	4.40E-07	0.01449748	0.00677	9.86E-05
3R_7937498_SNP	FBgn0051361	-2.14E-06	-0.0561296	0.00171	-9.81E-05
3L_5909619_SNP	FBgn0035648	1.23E-06	0.0837185	0.00115	9.75E-05
X_15973337_DEL	FBgn0028397	-1.06E-06	-0.0158372	0.00609	-9.75E-05
X_4410555_SNP	FBgn0052773	5.77E-07	0.01467445	0.0066	9.74E-05
2R_11710157_SNP	FBgn0034046	-2.70E-07	-0.0232992	0.00416	-9.72E-05
3L_5494285_SNP	FBgn0265712	9.14E-07	0.01738697	0.00553	9.71E-05
3L_18818427_SNP	FBgn0000261	-1.12E-06	-0.0096314	0.00996	-9.70E-05

Table A.2 Top 100 Associated Variants, Ranked by Effect Size in Adults

Column 1 is the chromosomal position and bp location of the variant. Column 2 is the FlyBase ID, Columns 3, 4, and 5 are alpha, beta~, and gamma, respectively, which are estimated BSLMM parameters. Column 6 is the effect size (beta * gamma).

Annotation Cluster 1	Enrichment Score: 3.4101029380737353											
Category	Term	Count	%	PValue	Genes	List Total	Pop Hits	Pop Total	Fold Enrichment	Bonferroni	Benjamini	FDR
UP_KEYWORDS	Alternative splicing	15	16.66666667	2.25E-05	FBGN0263873,	85	631	13921	3.893259998	0.002266448	0.002266448	0.024978884
UP_SEQ_FEATURE	splice variant	15	16.66666667	9.91E-05	FBGN0263873,	27	610	3113	2.835154827	0.012118934	0.012118934	0.114237561
UP_KEYWORDS	Developmental protein	9	10	0.026423862	FBGN0001235,	85	593	13921	2.485646265	0.933109874	0.187836941	25.75420102
Annotation Cluster 2	Enrichment Score: 2.6762560504932833											
Category	Term	Count	%	PValue	Genes	List Total	Pop Hits	Pop Total	Fold Enrichment	Bonferroni	Benjamini	FDR
INTERPRO	IPR023415:Low-density lipoprotein (LDL) receptor class A, conserved site	5	5.555555556	3.44E-05	FBGN0030027,	75	28	10984	26.15238095	0.007194734	0.007194734	0.043432098
INTERPRO	IPR002172:Low-density lipoprotein (LDL) receptor class A repeat	5	5.555555556	1.06E-04	FBGN0030027,	75	37	10984	19.79099099	0.022003149	0.011062767	0.133764206
INTERPRO	IPR000742:Epidermal growth factor-like domain	6	6.666666667	1.36E-04	FBGN0053087,	75	74	10984	11.87459459	0.028120817	0.009462869	0.17145805
UP_KEYWORDS	Disulfide bond	14	15.55555556	1.76E-04	FBGN0004573,	85	670	13921	3.422194908	0.017646707	0.008862626	0.195833681
SMART	SM00192:LDLa	5	5.555555556	3.66E-04	FBGN0030027,	53	35	5218	14.06469003	0.020982034	0.020982034	0.363095598
SMART	SM00181:EGF	6	6.666666667	4.56E-04	FBGN0053087,	53	66	5218	8.95025729	0.026112721	0.013142726	0.452862545
INTERPRO	IPR013032:EGF-like, conserved site	5	5.555555556	7.41E-04	FBGN0053087,	75	61	10984	12.00437158	0.144158005	0.038169824	0.932169425
INTERPRO	IPR011042:Six-bladed beta-propeller, TolB-like	4	4.444444444	0.002090714	FBGN0053087,	75	38	10984	15.41614035	0.355647623	0.070633018	2.60953169
UP_KEYWORDS	EGF-like domain	4	4.444444444	0.002505175	FBGN0053087,	85	45	13921	14.5579085	0.223796197	0.041344369	2.750743968
INTERPRO	IPR018097:EGF-like calcium-binding, conserved site	3	3.333333333	0.017244331	FBGN0053087,	75	30	10984	14.64533333	0.974084052	0.30600441	19.72935076
INTERPRO	IPR000152:EGF-type aspartate/asparagine hydroxylation site	3	3.333333333	0.017244331	FBGN0053087,	75	30	10984	14.64533333	0.974084052	0.30600441	19.72935076
INTERPRO	IPR009030:Insulin-like growth factor binding protein, N-terminal	3	3.333333333	0.023083536	FBGN0053087,	75	35	10984	12.55314286	0.992585872	0.359721233	25.55111087
INTERPRO	IPR001881:EGF-like calcium-binding	3	3.333333333	0.024336293	FBGN0053087,	75	36	10984	12.20444444	0.994337196	0.350240512	26.74832957
SMART	SM00179:EGF_CA	3	3.333333333	0.049474729	FBGN0053087,	53	36	5218	8.204402516	0.947290036	0.387674819	39.63948822
GOTERM_MF_DIRECT	GO:0005509~calcium ion binding	4	4.444444444	0.153968902	FBGN0053087,	61	210	9284	2.898985168	0.999999954	0.965864694	84.4214963
Annotation Cluster 3	Enrichment Score: 2.181330147022585											
Category	Term	Count	%	PValue	Genes	List Total	Pop Hits	Pop Total	Fold Enrichment	Bonferroni	Benjamini	FDR
UP_SEQ_FEATURE	transmembrane region	14	15.55555556	2.12E-04	FBGN0004573,	27	566	3113	2.851851852	0.025722527	0.012945051	0.243992986
GOTERM_CC_DIRECT	GO:0016021~integral component of membrane	29	32.22222222	0.010670701	FBGN0262508,	68	2814	10026	1.519471968	0.566900264	0.566900264	10.72771719
UP_KEYWORDS	Transmembrane helix	28	31.11111111	0.014594876	FBGN0262508,	85	2985	13921	1.536261701	0.773485269	0.152101142	15.08276202
UP_KEYWORDS	Transmembrane	28	31.11111111	0.014911112	FBGN0262508,	85	2990	13921	1.533692701	0.780710713	0.140785215	15.38531299
UP_KEYWORDS	Membrane	29	32.22222222	0.025202113	FBGN0262508,	85	3266	13921	1.454230755	0.924077152	0.193326653	24.71151451
Annotation Cluster 4	Enrichment Score: 1.881867397414338											
Category	Term	Count	%	PValue	Genes	List Total	Pop Hits	Pop Total	Fold Enrichment	Bonferroni	Benjamini	FDR
INTERPRO	IPR013783:Immunoglobulin-like fold	7	7.777777778	0.001203507	FBGN0010389,	75	177	10984	5.791939736	0.2234456	0.049319958	1.509916939
INTERPRO	IPR007110:Immunoglobulin-like domain	6	6.666666667	0.002127609	FBGN0010389,	75	135	10984	6.509037037	0.360631185	0.061897686	2.655013705
GOTERM_BP_DIRECT	GO:0050808~synapse organization	4	4.444444444	0.004825363	FBGN0261871,	66	58	10996	11.49007315	0.816914481	0.572115063	6.404068729
INTERPRO	IPR003598:Immunoglobulin subtype 2	5	5.555555556	0.006198796	FBGN0010389,	75	109	10984	6.718042813	0.729043912	0.15059979	7.555308911
INTERPRO	IPR003599:Immunoglobulin subtype	5	5.555555556	0.006606396	FBGN0010389,	75	111	10984	6.596996997	0.751408931	0.143294165	8.033193679
SMART	SM00406:IGv	3	3.333333333	0.012039782	FBGN0261871,	53	17	5218	17.3702886	0.504676974	0.208781975	11.35361256
SMART	SM00408:IGc2	5	5.555555556	0.022622369	FBGN0010389,	53	109	5218	4.516184871	0.73477227	0.282363149	20.36071785
SMART	SM00409:IG	5	5.555555556	0.024003323	FBGN0010389,	53	111	5218	4.434812171	0.75565489	0.245601649	21.47320426
INTERPRO	IPR013106:Immunoglobulin V-set	3	3.333333333	0.025616369	FBGN0261871,	75	37	10984	11.87459459	0.99570171	0.342424202	27.95332161
GOTERM_BP_DIRECT	GO:0007606~sensory perception of chemical stimulus	3	3.333333333	0.102730093	FBGN0261871,	66	92	10996	5.432806324	1	0.968535633	77.30834981
GOTERM_CC_DIRECT	GO:0005887~integral component of plasma membrane	6	6.666666667	0.228914436	FBGN0004573,	68	490	10026	1.805402161	0.999999998	0.982669938	93.60569936
Annotation Cluster 5	Enrichment Score: 1.7744566810961027											
Category	Term	Count	%	PValue	Genes	List Total	Pop Hits	Pop Total	Fold Enrichment	Bonferroni	Benjamini	FDR
UP_SEQ_FEATURE	transmembrane region	14	15.55555556	2.12E-04	FBGN0004573,	27	566	3113	2.851851852	0.025722527	0.012945051	0.243992986
UP_KEYWORDS	Glycoprotein	11	12.22222222	8.70E-04	FBGN0010389,	85	503	13921	3.581592796	0.084167375	0.028881927	0.963350719
UP_SEQ_FEATURE	glycosylation site:N-linked (GlcNAc...)	10	11.11111111	0.005333323	FBGN0010389,	27	423	3113	2.725680764	0.481986671	0.19688024	5.979854941
UP_SEQ_FEATURE	topological domain:Cytoplasmic	9	10	0.012619363	FBGN0004573,	27	397	3113	2.613769941	0.790296074	0.323291486	13.62181608
UP_SEQ_FEATURE	topological domain:Extracellular	6	6.666666667	0.111773931	FBGN0004573,	27	312	3113	2.217236467	0.999999534	0.911949453	74.50564562
UP_SEQ_FEATURE	disulfide bond	4	4.444444444	0.383436677	FBGN0004573,	27	265	3113	1.740321454	1	0.997389489	99.62128569
UP_SEQ_FEATURE	signal peptide	4	4.444444444	0.713081817	FBGN0010389,	27	427	3113	1.080058982	1	0.999999136	99.99994407
Annotation Cluster 6	Enrichment Score: 1.321307523280036											
Category	Term	Count	%	PValue	Genes	List Total	Pop Hits	Pop Total	Fold Enrichment	Bonferroni	Benjamini	FDR
UP_KEYWORDS	Metal-binding	16	17.77777778	9.31E-04	FBGN0038627,	85	1008	13921	2.599626517	0.08974072	0.023232325	1.029887766
UP_KEYWORDS	Zinc-finger	8	8.888888889	0.008441971	FBGN0038627,	85	384	13921	3.412009804	0.575251647	0.115137159	8.996697939
UP_KEYWORDS	Zinc	10	11.11111111	0.009817808	FBGN0038627,	85	598	13921	2.738736966	0.630830115	0.117116738	10.39103983
GOTERM_MF_DIRECT	GO:0004842~ubiquitin-protein transferase activity	4	4.444444444	0.108956386	FBGN0038627,	61	179	9284	3.401044052	0.999991294	0.979428543	72.27513671
GOTERM_MF_DIRECT	GO:0008270~zinc ion binding	8	8.888888889	0.119998632	FBGN0038627,	61	644	9284	1.890642501	0.999997529	0.960353531	75.86501604
INTERPRO	IPR013083:Zinc finger, RING/FYVE/PHD-type	4	4.444444444	0.164910721	FBGN0038627,	75	208	10984	2.816410256	1	0.892062783	89.73947886
SMART	SM00184:RING	3	3.333333333	0.182033341	FBGN0038627,	53	78	5218	3.786647315	0.999991317	0.767012236	86.45508303
INTERPRO	IPR001841:Zinc finger, RING-type	3	3.333333333	0.198510004	FBGN0038627,	75	122	10984	3.601311475	1	0.924349599	93.8927797
GOTERM_BP_DIRECT	GO:0016567~protein ubiquitination	3	3.333333333	0.213520315	FBGN0026319,	66	146	10996	3.423412204	1	0.996376838	96.26117722
Annotation Cluster 7	Enrichment Score: 0.7915793750582981											
Category	Term	Count	%	PValue	Genes	List Total	Pop Hits	Pop Total	Fold Enrichment	Bonferroni	Benjamini	FDR
UP_KEYWORDS	Homeobox	4	4.444444444	0.024949925	FBGN0001235,	85	104	13921	6.299095023	0.922067443	0.207047495	24.49463555
INTERPRO	IPR001356:Homeodomain	4	4.444444444	0.031349729	FBGN0001235,	75	102	10984	5.743267974	0.998755282	0.379838126	33.12971108
INTERPRO	IPR009057:Homeodomain-like	4	4.444444444	0.079115332	FBGN0001235,	75	149	10984	3.93163311	0.99999997	0.684591502	64.70061527
SMART	SM00389:HOX	4	4.444444444	0.080593951	FBGN0001235,	53	102	5218	3.860895302	0.992354134	0.501537624	56.65668945
INTERPRO	IPR017970:Homeobox, conserved site	3	3.333333333	0.127488417	FBGN0024321,	75	92	10984	4.775652174	1	0.833036318	82.1474516
UP_KEYWORDS	Nucleus	9	10	0.376628586	FBGN0034707,	85	1134	13921	1.299813259	1	0.885790666	99.47813704
GOTERM_MF_DIRECT	GO:0043565~sequence-specific DNA binding	3	3.333333333	0.510470931	FBGN0024321,	61	263	9284	1.736084274	1	0.999878814	99.9644947
UP_KEYWORDS	DNA-binding	4	4.444444444	0.631683647	FBGN0001235,	85	535	13921	1.224496976	1	0.98231794	99.99849922
GOTERM_CC_DIRECT	GO:0005634~nucleus	8	8.888888889	0.972892427	FBGN0001235,	68	1832	10026	0.643847932	1	0.999999993	100
Annotation Cluster 8	Enrichment Score: 0.5499607156258718											
Category	Term	Count	%	PValue	Genes	List Total	Pop Hits	Pop Total	Fold Enrichment	Bonferroni	Benjamini	FDR
GOTERM_MF_DIRECT	GO:0003729~mRNA binding	4	4.444444444	0.098324141	FBGN0264001,	61	171	9284	3.560157224	0.999971153	0.994629097	68.36596445
INTERPRO	IPR000504:RNA recognition motif domain	3	3.333333333	0.230656907	FBGN0264001,	75	135	10984	3.254518519	1	0.944877746	96.35888162
INTERPRO	IPR012677:Nucleotide-binding, alpha-beta plait	3	3.333333333	0.295663477	FBGN0264001,	75	161	10984	2.728944099	1	0.974783071	98.80643215
SMART	SM00360:RRM	3	3.333333333	0.355280762	FBGN0264001,	53	125	5218	2.362867925	1	0.940911956	98.73128956
GOTERM_MF_DIRECT	GO:0000166~nucleotide binding	3	3.333333333	0.399681669	FBGN0264001,	61	212	9284	2.153727188	1	0.999814038	99.65678024
GOTERM_MF_DIRECT	GO:0003723~RNA binding	3	3.333333333	0.526654114	FBGN0264001,	61	271	9284	1.684834553	1	0.999773649	99.97556905
Annotation Cluster 9	Enrichment Score: 0.2070797891567501											
Category	Term	Count	%	PValue	Genes	List Total	Pop Hits	Pop Total	Fold Enrichment	Bonferroni	Benjamini	FDR
GOTERM_BP_DIRECT	GO:0006468~protein phosphorylation	3	3.333333333	0.468928242	FBGN0010389,	66	266	10996	1.879015721	1	0.999974524	99.98264663
UP_KEYWORDS	Kinase	3	3.333333333	0.492852937	FBGN0010389,	85	273	13921	1.799741435	1	0.942574442	99.9473925
UP_KEYWORDS	Transferase	7	7.777777778	0.643862726	FBGN0262955,	85	1081	13921	1.060532187	1	0.981877998	99.99896742
UP_KEYWORDS	ATP-binding	4	4.444444444	0.660117921	FBGN0010389,	85	558	13921	1.174024879	1	0.979609208	99.99938581
GOTERM_MF_DIRECT	GO:0005524~ATP binding	5	5.555555556	0.726288065	FBGN0263873,	61	751	9284	1.01329375	1	0.999993187	99.99994471
UP_KEYWORDS	Nucleotide-binding	4	4.444444444	0.801998971	FBGN0010389,	85	701	13921	0.934530503	1	0.995713392	99.99999849

Table A.3 Gene Enrichment

Table containing functional annotation information from DAVID (https://david.ncifcrf.gov/home.jsp) for the top 100 adult genes most strongly associated with cold hardiness.

Script A.1 Enrichment Tests for Strength of Association of Top Genes Identified in One Life Stage vs. the Other

We applied an enrichment approach to test the hypothesis that inclusion probabilities for a 'test' list of genes is higher than expected for a random 'background' list of the same size (containing the same number of genes). Prior to applying these tests, we calculated the maximum inclusion probability for variants in each gene model (Flybase Id). Here, the test lists were the 100 genes from the larval and adult analyses that yielded the highest inclusion probabilities. The larval test list was tested against the background of all adult inclusion probabilities. Likewise, the adult test list was tested against the background of all larval inclusion probabilities. The point estimates were simply the median of 100 inclusion probabilities in the background list for the genes designated in the test list. We then generated a random destruction of median values by sampling a random subset of 100 genes from the background list and estimating the median 10,000 times. We then estimated the percentile of the point estimate in this random distribution.

R script

```
#R
#GJR 3/10/17
# perform enrichment tests, asking whether the median gamma in larvae for the top 100 associated genes in adults is higher (or lower) than expected by chance
# then perform the reciprocal, top 100 larval associated genes in adults

#load workspace with data frames containing larval and adult output of BSLMM
#data/workspace available upon request: gregory.ragland@ucdenver.edu
setwd('/media/raglandlab/ExtraDrive1/dmel/dgrpGenotypes/output')
load('temp.R')

#calculate maximum gamma value for variants within a given gene
maxProb<-function(x,data) {
  id<-x
  maxVal<-max ( data$gamma[grep(id,data$flyid)] )
  out<-c(id,maxVal)
```

```
  return(out)
}

#parellelize for speed, and apply across larval and adult data frames
library(parallel)
#create a virtual cluster, reserving computational space for a parallel loop
cl <- makeCluster( (8) )
#need to export variable/functions so that they are visible in the virtual machine
clusterExport(cl=cl, varlist=c("adatAnno","maxProb"),envir = .GlobalEnv)
maxGammaAdult<-t( parSapply(cl, unique(adatAnno$flyid), function (x) maxProb(x,data=adatAnno)) )
#save.image('temp.R')
stopCluster(cl)

library(parallel)
#create a virtual cluster, reserving computational space for a parallel loop
cl <- makeCluster( (8) )
#need to export variable/functions so that they are visible in the virtual machine
clusterExport(cl=cl, varlist=c("ldatAnno","maxProb"),envir = .GlobalEnv)
maxGammaLarv<-t( parSapply(cl, unique(ldatAnno$flyid), function (x) maxProb(x,data=ldatAnno)) )
#save.image('temp.R')
stopCluster(cl)

#condition output
maxGammaAdult<-data.frame(maxGammaAdult,stringsAsFactors=F)
maxGammaAdult[,2]<-as.numeric(maxGammaAdult[,2])
names(maxGammaAdult)<-c("flyid","gamma")
maxGammaAdult<-maxGammaAdult[order(maxGammaAdult$gamma,decreasing=T),]

maxGammaLarv<-data.frame(maxGammaLarv,stringsAsFactors=F)
maxGammaLarv[,2]<-as.numeric(maxGammaLarv[,2])
names(maxGammaLarv)<-c("flyid","gamma")

#calculate empirical quantiles
ind<-maxGammaLarv$flyid %in% maxGammaAdult$flyid[1:100]
quantile(maxGammaLarv$gamma,c(0.025,0.5,0.975))
quantile(maxGammaLarv$gamma[ind],c(0.025,0.5,0.975))
```

```
#median of a random subset of 100 from data$gamma
randMedian<-function(x,data) {
   out<-median(sample(data$gamma,100))
}

#estimate distribution of median of random samples, 10k iterations
library(parallel)
cl <- makeCluster( (8) )
clusterExport(cl=cl, varlist=c("maxGammaLarv","randMedian"),envir = .GlobalEnv)
randDistLarvGammaMedian<-parSapply(cl, 1:10000, function (x) randMedian(x,data=maxGammaLarv))
stopCluster(cl)

#find percentile of point estimate in random distribution
pointEst<-median(maxGammaLarv$gamma[ind])
ecdf(randDistLarvGammaMedian)(pointEst)
#[1]
#So, none of the 10k random samples produced a value as extreme (top 100 adult in larval dist)

#do same for top 100 larval in adult

maxGammaLarv<-maxGammaLarv[order(maxGammaLarv$gamma,decreasing=T),]
ind<-maxGammaAdult$flyid %in% maxGammaLarv$flyid[1:100]
quantile(maxGammaAdult$gamma,c(0.025,0.5,0.975))
quantile(maxGammaAdult$gamma[ind],c(0.025,0.5,0.975))

library(parallel)
cl <- makeCluster( (8) )
clusterExport(cl=cl, varlist=c("maxGammaAdult","randMedian"),envir = .GlobalEnv)
randDistAdultGammaMedian<-parSapply(cl, 1:10000, function (x) randMedian(x,data=maxGammaAdult))
stopCluster(cl)

pointEst<-median(maxGammaAdult$gamma[ind])
ecdf(randDistAdultGammaMedian)(pointEst)
#[1]
#So, none of the 10k random samples produced a value as extreme (top 100 larval in adult dist)
```

Script A.2 Phylogenetically Independent contrast of LT90 Data from Mitchell *et al.* 2013

```
#R
#GJR 10/6/2016
#conduct phylogentically independent contrast on LLT90 data from:

#"Mitchell, Katherine A., Brent J. Sinclair, and John S. Terblanche. "Ontogenetic variation in cold tolerance
 plasticity in Drosophila: is the Bogert effect bogus?." Naturwissenschaften 100.3 (2013): 281-284."

#obtained the phylogenetic tree from John Terblanche, jst@sun.ac.za

library(ape)
#read in tree in newick format; contents of tree file listed at end of script
tree<-read.tree('/Users/gregoryragland/Downloads/prunedtree.nwk')

#LLT90 data from table 1, in degrees C
larval<-c(-3.8,-5.4,-9.5,-3.4,-6.1,-5.2,-4.7,-6.8,-9.6,-10.7,-1.6,-3.7,-4.1,-10.7,-3.8,-4.3)

adult<-c(-3,-8,-13,-5,-7,-4,-5,-6,-12,-12,-4,-5,-4,-11,-4,-4)

names(larval)<-names(adult)<-c("Drosophila_ananassae",
 "Drosophila_auraria","Drosophila_borealis","Drosophila_erecta",
 "Drosophila_hydei","Drosophila_immigrans","Drosophila_melanogaster","Drosophila_mojavensis",
 "Drosophila_persimilis","Drosophila_pseudoobscura","Drosophila_sechellia", "Drosophila_simulans",
  "Drosophila_takahashii","Drosophila_virilis","Drosophila_willistoni","Drosophila_yakuba")

#perform phylogenetic corrections
pic.l <- pic(larval, tree)
pic.a <- pic(adult, tree)

#correlation
cor.test(pic.l, pic.a)

#           Pearson's product-moment correlation

#data:  pic.l and pic.a
#t = 3.4791, df = 13, p-value = 0.004074
#alternative hypothesis: true correlation is not equal to 0
#95 percent confidence interval:
# 0.2826501 0.8900457
#sample estimates:
#      cor
#0.6943737

#tree file in newick format (pruned triauraria from the tree, no tolerance data):
#(((((((((Drosophila_sechellia:0.01493538,Drosophila_simulans:0.00980485):0.0087678,Drosophila_melanogaster:
 0.01900845):0.00998612,(Drosophila_erecta:0.0299889,Drosophila_yakuba:0.02500882):0.00239455):0.00555352
 ,Drosophila_takahashii:0.02520013):0.01086504,Drosophila_ananassae:0.04778839):0.00224421,Drosophila_aurar
 ia:0.04218731):0.00320987,(Drosophila_persimilis:0.0023642,Drosophila_pseudoobscura:-
 0.00024683):0.04885695):0.00517698,(Drosophila_immigrans:0.06135893,((Drosophila_hydei:0.05750723,Droso
 phila_mojavensis:0.04327141):0.00431859,(Drosophila_borealis:0.03260168,Drosophila_virilis:0.02222114):0.02
 719413):0.00159046):0.00633753):0.0149843,Drosophila_willistoni:0.04040619);
```

~

Script A.3 Enrichment Tests for Common Allelic Effects in Adults and Larvae

We applied an enrichment approach to test the hypothesis that the correlation in effect sizes between larva and adults for a 'test' list of genes is higher than expected for a random 'background' list of the same size (containing the same number of genes). Here, the effect size ε is:

$$\varepsilon = (\beta \times \gamma) + \alpha$$

where β is the 'major' effect size, γ, is the inclusion probability, and α is the infinitesimal effect, as defined in the BSLMM model in the main document .The correlation is the Pearson correlation coefficient. Prior to applying these tests, we calculated the maximum effect size ε for variants in each gene model (Flybase Id). Here, the test lists were all Gene Ontology (GO) and Kyoto Encyclopedia of Genes and Genomes (KEGG) functional categories with at least 10 representative genes in the data set as identified using the 'org.Dm.eg.db' R package, part of the 'Annotate' suite in Bioconductor (https://www.bioconductor.org/packages/release/bioc/html/annotate.html).

We generated null distributions by estimating the correlation for 10,000 random samples of *n* genes, where *n* represents the size of a given gene list. We then estimated the percentile of the point estimate in these random distributions to generate p-values (two-tailed), then applied a multiple comparison False Discovery Rate (FDR) correction using the Benjamini-Hochberg method.

R script

```
#first, need to estimate max effect size for each gene

maxEffect<-function(x,data) {
  id<-x
  vec<-data$effectSize[grep(id,data$flyid)]
  maxInd<-which.max(abs(vec))
```

```
  maxVal<-vec[maxInd]
  out<-c(id,maxVal)
  return(out)
}

library(parallel)
#create a virtual cluster, reserving computational space for a parallel loop
cl <- makeCluster( (10) )
#need to export variable/functions so that they are visible in the virtual machine
clusterExport(cl=cl, varlist=c("adatAnno","maxEffect"),envir = .GlobalEnv)
maxEffectAdult<-t( parSapply(cl, unique(adatAnno$flyid), function (x) maxEffect(x,data=adatAnno)) )
save.image('temp.R')
stopCluster(cl)

library(parallel)
#create a virtual cluster, reserving computational space for a parallel loop
cl <- makeCluster( (10) )
#need to export variable/functions so that they are visible in the virtual machine
clusterExport(cl=cl, varlist=c("ldatAnno","maxEffect"),envir = .GlobalEnv)
maxEffectLarv<-t( parSapply(cl, unique(ldatAnno$flyid), function (x) maxEffect(x,data=ldatAnno)) )
save.image('temp.R')
stopCluster(cl)

maxEffectAdult<-data.frame(maxEffectAdult,stringsAsFactors=F)
maxEffectAdult[,2]<-as.numeric(maxEffectAdult[,2])
names(maxEffectAdult)<-c("flyid","effectSizeAd")
#maxEffectAdult<-maxEffectAdult[order(maxEffectAdult$effectSize,decreasing=T),]

maxEffectLarv<-data.frame(maxEffectLarv,stringsAsFactors=F)
maxEffectLarv[,2]<-as.numeric(maxEffectLarv[,2])
names(maxEffectLarv)<-c("flyid","effectSizeLarv")

maxEffectBoth<-merge(maxEffectAdult,maxEffectLarv)

#next, re-do enrichment using the pearson correlation as the metric

# Go and Kegg lists generated using:
```

```
# https://github.com/gjragland/r-misc/blob/master/extractDrosGeneSets.r
load('DrosGoAndKeggGeneLists.rdat')

#generate enrichment scores for each list
# currently, the enrichment score is just the median value

#minimum number of genes present in a list to proceed
minLen=10

GoScores<-data.frame(catId='na',n=0,score=0,stringsAsFactors=F)
for (i in names(DrosGoLists)) {
   ind<-maxEffectBoth$flyid %in% DrosGoLists[[i]]
   if (sum(ind) > minLen) {
      GoScores<-rbind(GoScores,c(i,sum(ind),
cor(maxEffectBoth$effectSizeAd[ind],maxEffectBoth$effectSizeLarv[ind]) ))
   }
}
GoScores<-GoScores[-1,]
GoScores$score<-as.numeric(GoScores$score)
GoScores$n<-as.numeric(GoScores$n)

KeggScores<-data.frame(catId='na',n=0,score=0,stringsAsFactors=F)
for (i in names(DrosKeggLists)) {
   ind<-maxEffectBoth$flyid %in% DrosKeggLists[[i]]
   if (sum(ind) > minLen) {
      KeggScores<-rbind(KeggScores,c(i,sum(ind),
cor(maxEffectBoth$effectSizeAd[ind],maxEffectBoth$effectSizeLarv[ind]) ))
   }
}
KeggScores<-KeggScores[-1,]
KeggScores$score<-as.numeric(KeggScores$score)
KeggScores$n<-as.numeric(KeggScores$n)

#generate null distributions
#length(unique(c(KeggScores$n,GoScores$n))) # 165 different sized lists, each needs null distribution

perm<-function(n,it,data) {
```

```
   out<-vector(length=it)
   for (i in 1:it) {
      ind<-sample(1:nrow(data),n)
      out[i]<-cor(data$effectSizeAd[ind],data$effectSizeLarv[ind])
   }
   return(out)
}

it=10000

listSizes<-unique(c(KeggScores$n,GoScores$n))
nullDists<-matrix(nrow=length(listSizes),ncol=it)
for (i in 1:length(listSizes)) {
   nullDists[i,]<-perm(listSizes[i],it,maxEffectBoth)
}
save.image('temp.R')

#estimate p val from point estimate and null (random) distribution
permPval<-function(vec,est) {
  prob<-ecdf(vec)(est)
  if (prob <= 0.5) {p=prob} else {p=1-prob}
  p=p*2 #accounts for 2-tailed search
  return(p)
}

est<-cor(maxEffectBoth$effectSizeAd,maxEffectBoth$effectSizeLarv)

GoScores<-
data.frame(GoScores,representation=rep('na',nrow(GoScores)),pval=rep(0,nrow(GoScores)),stringsAsFactors=F)
for (i in 1:nrow(GoScores)) {
   rep='over'
   n=GoScores$n[i]
   score=GoScores$score[i]
   pval<-permPval(nullDists[listSizes==n,],score)
   if (score < est) {rep='under'}
   GoScores[i,4]<-rep
   GoScores[i,5]<-pval
```

```
}
GoScores<-GoScores[order(GoScores$pval),]

KeggScores<-
data.frame(KeggScores,representation=rep('na',nrow(KeggScores)),pval=rep(0,nrow(KeggScores)),stringsAsFactors
=F)
for (i in 1:nrow(KeggScores)) {
   rep='over'
   n=KeggScores$n[i]
   score=KeggScores$score[i]
   pval<-permPval(nullDists[listSizes==n,],score)
   if (score < est) {rep='under'}
   KeggScores[i,4]<-rep
   KeggScores[i,5]<-pval
}
KeggScores<-KeggScores[order(KeggScores$pval),]

# after p.adjust(x,method='BH'), no GO or Kegg categories are significantly enriched
```

Appendix B - Chapter 3 Supplementary Data

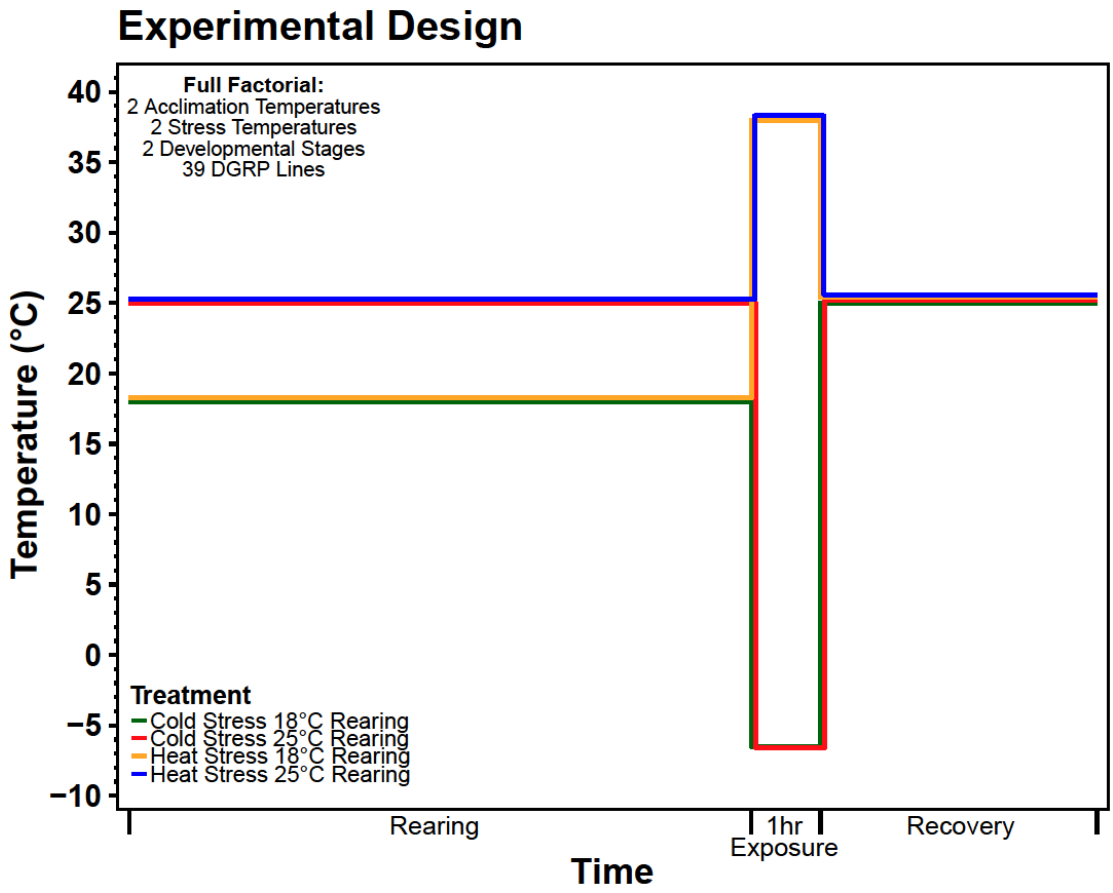

Figure B.1 Conceptual Figure of Factorial Design

Conceptual figure illustrating the full factorial experimental design. Larvae and adults from 39 DGRP lines were reared in two possible conditions and then exposed to both acute cold stress (-6.5°C for 1h) and heat stress (38°C 1h). Colored lines represent the four treatments used in this study as seen in the legend: Yellow and green lines represent adults and larvae reared at 18°C and either cold stressed at -6.5°C (green line) or heat stressed at 38°C (yellow line). Red and blue lines represent adults and larvae reared at 25°C and either cold stressed at -6.5°C (red line) or heat stressed at 38°C (blue line). Regardless of rearing temperature or stress temperature, all treatment combinations recovered at 25°C before survival scoring.

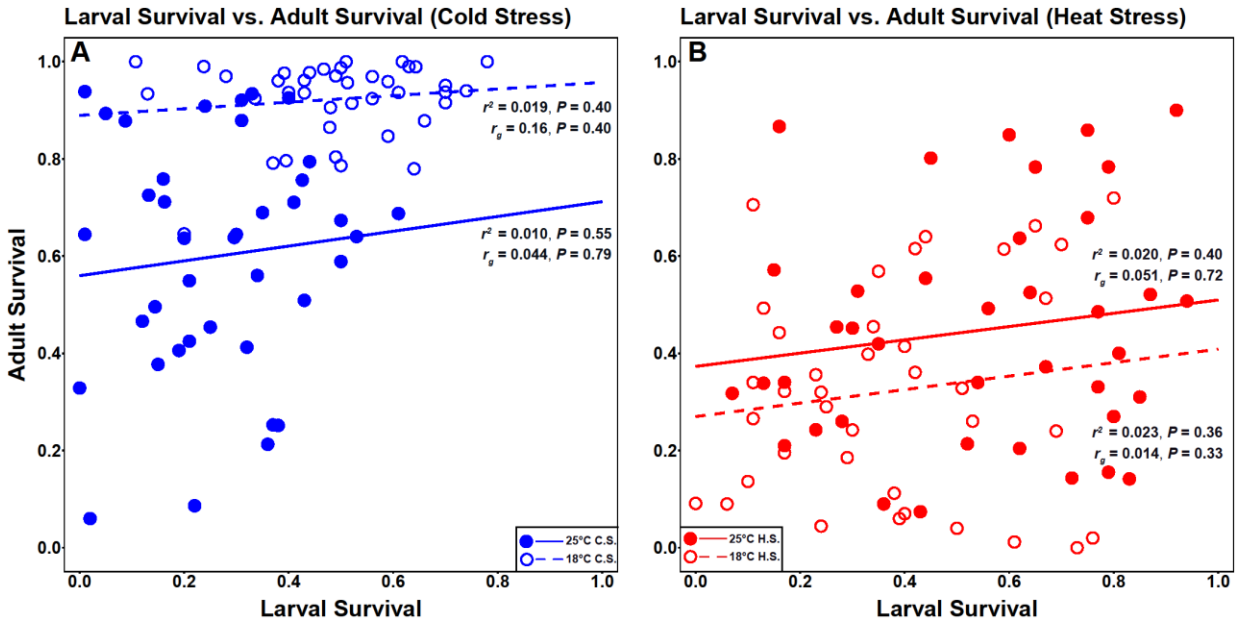

Figure B.2 Thermal Hardiness across Life Stages

Linear relationships of thermal hardiness (proportion surviving after 1h thermal stress) at different acclimation temperatures across life stages. Scatter plots depict the relationship between cold (A) and heat (B) hardiness for each genotype (DGRP line) measured in larval and adult stages acclimated at 18°C (dashed line) and 25°C (solid line).

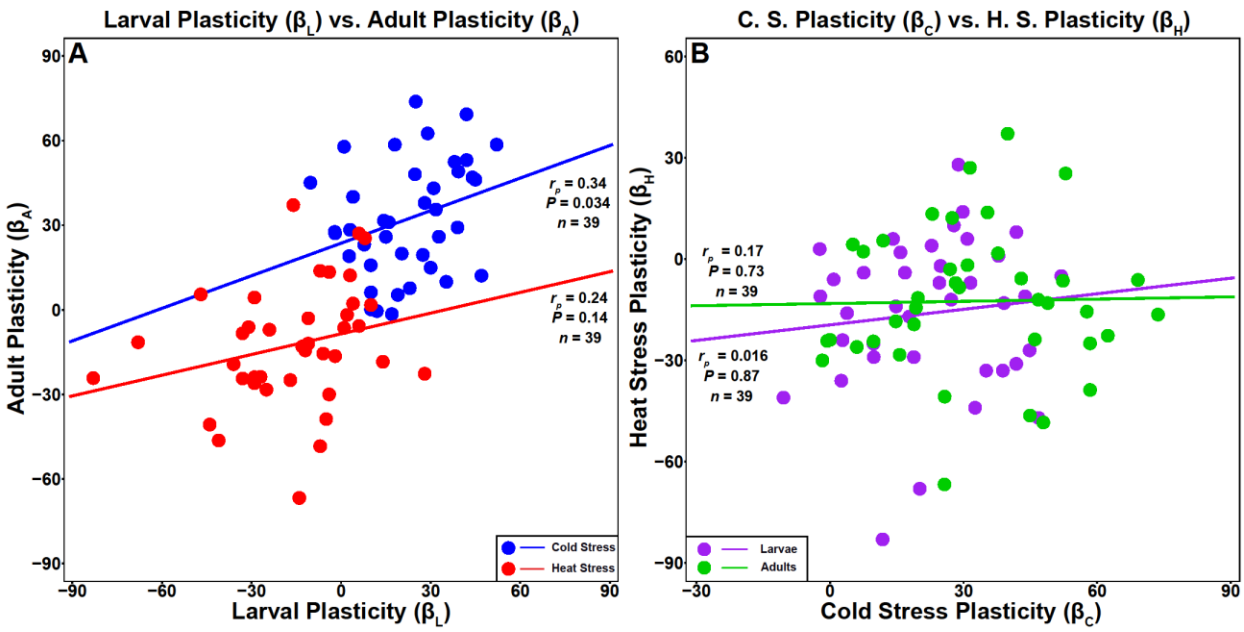

Figure B.3 Thermal Plasticity across Life Stages

Scatter plots depicting larval vs. adult cold stress and heat stress plasticity (A) and cold stress plasticity vs. heat stress plasticity in larvae and adults (B). Plasticity score is calculated as survival when reared at 18°C minus survival when reared at 25°C for both cold stress and heat stress. Blue circles and blue regression lines and red circles and red regression lines represent cold stress plasticity data and heat stress plasticity data, respectively, for between-stage comparisons. Purple circles and purple regression lines and green circles and green regression lines represent larval plasticity data and adult plasticity data, respectively, for between-stress type comparisons.

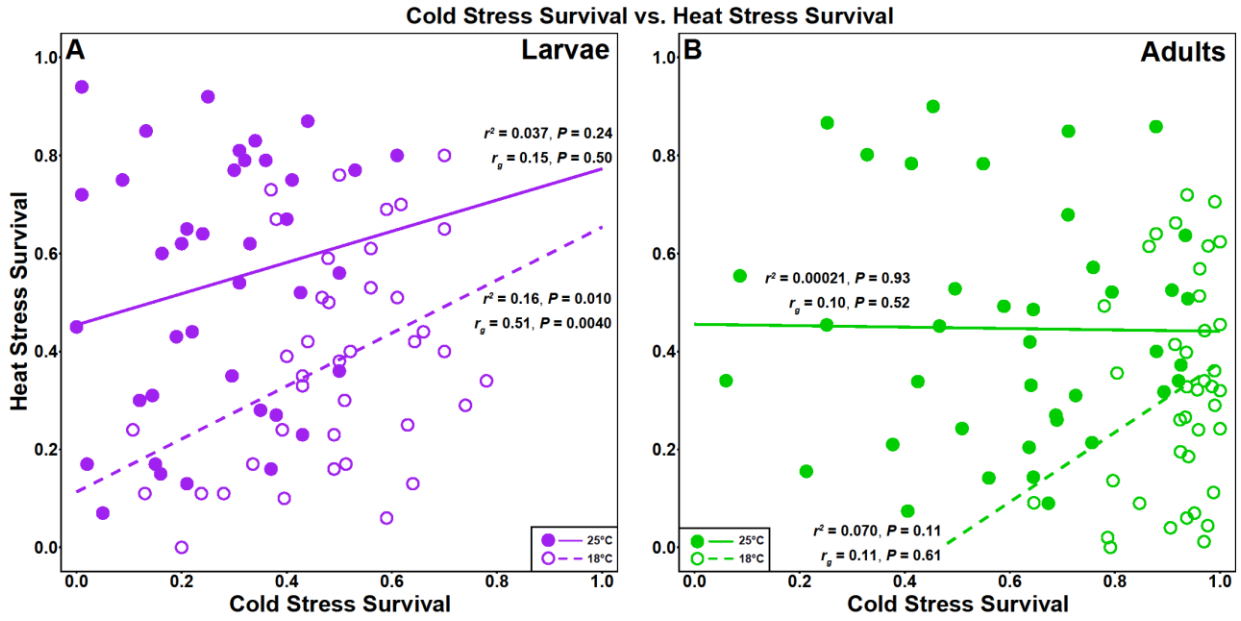

Figure B.4 Thermal Hardiness within Life Stages

Scatter plots of cold hardiness vs. heat hardiness, as the proportion surviving 1h thermal stress, in larvae (A) and adults (B). Dashed lines and open circles represent survival data and linear regression from rearing at 18°C. Solid lines and solid circles represent survival data and linear regression from rearing at 25°C. Purple circles and regression lines represent larval data. Green circles and green regression lines represent adult data.

a. Cold Hardiness

(logit survival) = stage + temp + stage*temp + line + line*stage + line*stage*temp

model	Fixed terms	Random terms	Drop	AIC
full	stage,temp, stage*temp	line,line*temp,line*stage, line*stage*temp		14143
reduced			line*stage*temp	14203
reduced			line*stage	14159
reduced			**line*temp**	**14142**
reduced			line*stage,line*temp	14158
reduced			line*temp,stage*temp	14163

b. Heat Hardiness

(logit survival) = stage + temp + line + line*stage + line*stage*temp

model	Fixed terms	Random terms	Drop	AIC
full	stage,temp, stage*temp	line,line*temp,line*stage, line*stage*temp		17179
reduced			line*stage*temp	17420
reduced			line*stage	17193
reduced			line*temp	17178
reduced			line*stage, line*temp	17191
reduced			**line*temp, stage*temp**	**17176**

Table B.1 Generalized Linear Models

Generalized linear models for cold hardiness (a) and heat hardiness (b). The full model is indicated in the top row, followed by reduced models dropping one or more terms. The best model for each trait appears in bold above each table, and the dropped terms and the AIC for the best model are also bolded.

Appendix C - Chapter 4 Supplementary Data

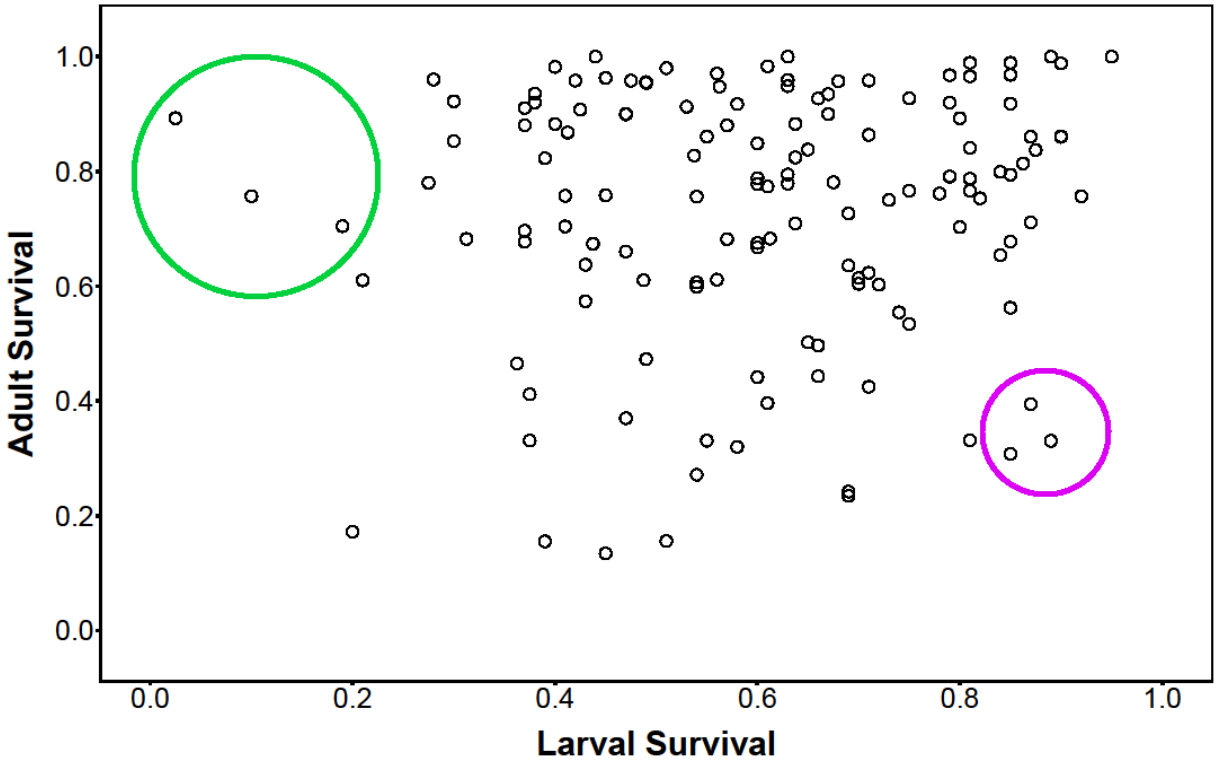

Figure C.1 HL and HA Lines

A total of six DGRP lines were used in this study. These lines were selected because they exhibited the greatest difference in survival between larvae and adults in a previous study (Freda *et al.* 2017). Three of the lines (441, 832, 913) are deemed high larval (HL) lines because they exhibited high cold hardiness as larvae but low cold hardiness as adults after a 1h exposure to -5°C. Conversely, the remaining three lines (358, 380, 486), deemed high adult (HA) lines, exhibited high cold hardiness as adults but low cold hardiness as larvae after a 1h exposure to -5°C. Below are a scatter plot depicted the lines chosen for the study with HL lines circled in purple and HA lines circled in green and a table containing the average survival for each line as both larvae and adults and the absolute difference between the average survival between stages.

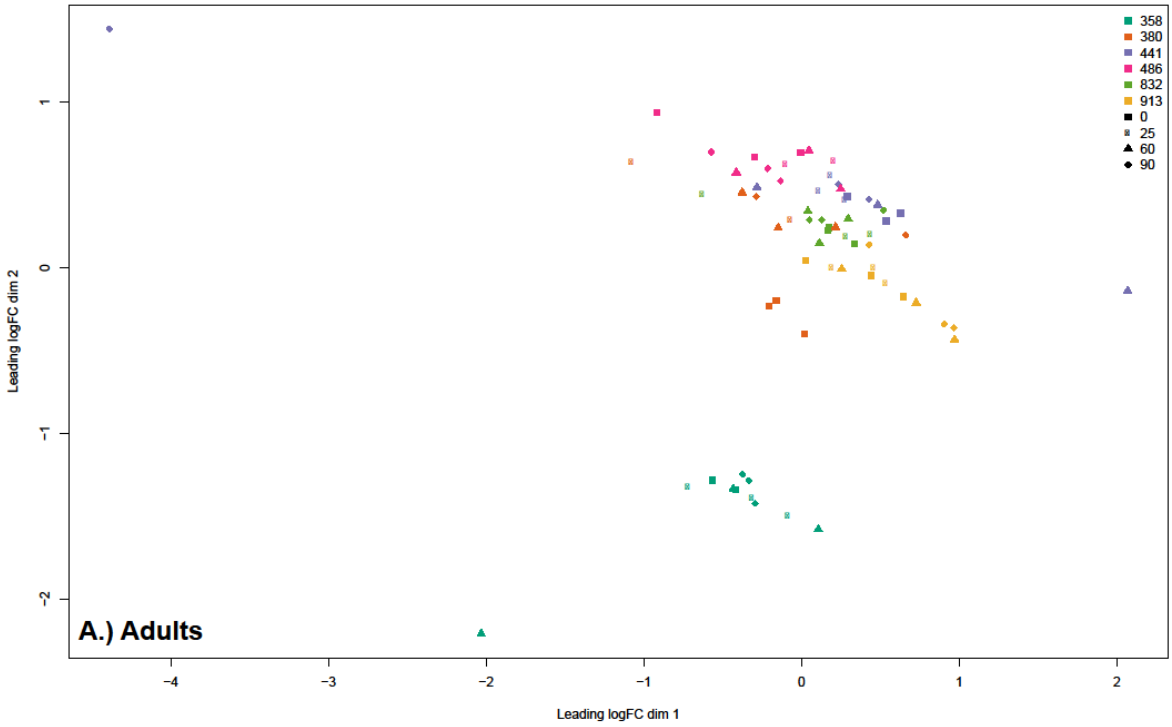
358
380
441
486
832
913
0
25
60
90
Leading logFC dim 2
Leading logFC dim 1
A.) Adults

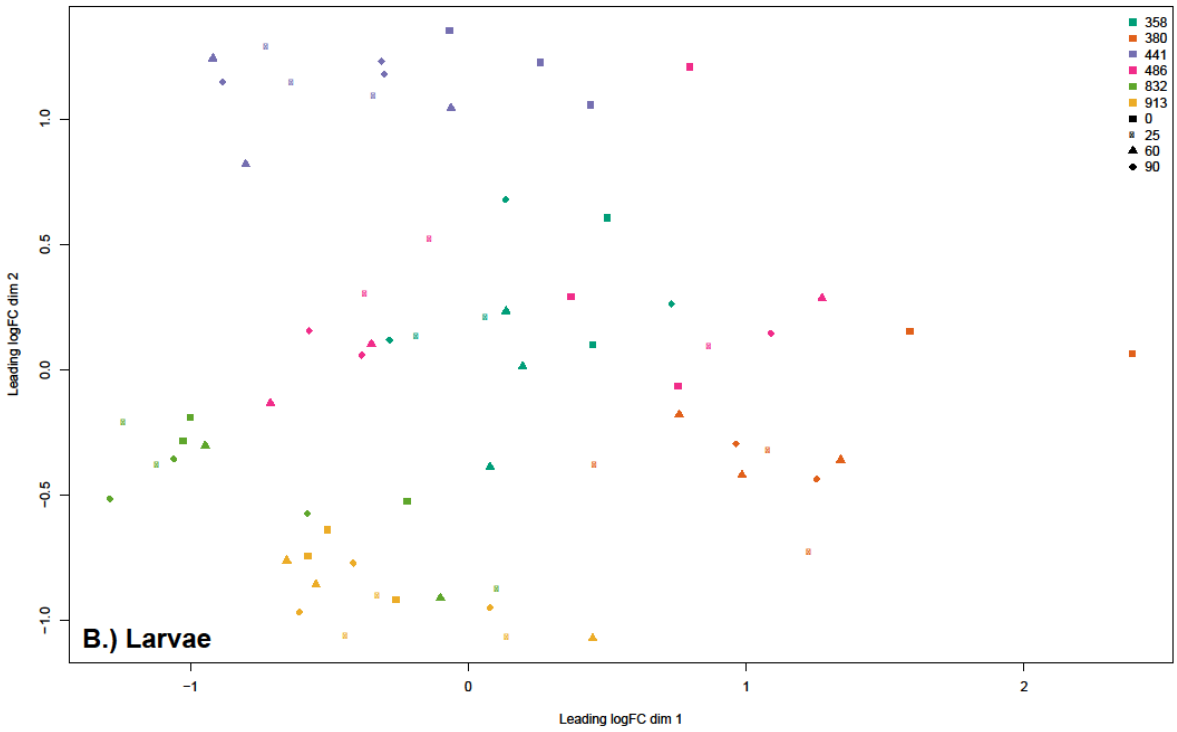
358
380
441
486
832
913
0
25
60
90
Leading logFC dim 2
Leading logFC dim 1
B.) Larvae

Figure C.2 Stage-Specific MDS Plots by Time Point and Genotype

The following two Multi- Dimensional Scaling (MDS) plots depict the 2D expression associated in (A) adults and (B) larvae. Different colors in each plot represent the different genotypes while shapes represent time points. In both life stages, there is no clear clustering by genotype or time point except line 832, which clusters in adults by genotype but not by time point.

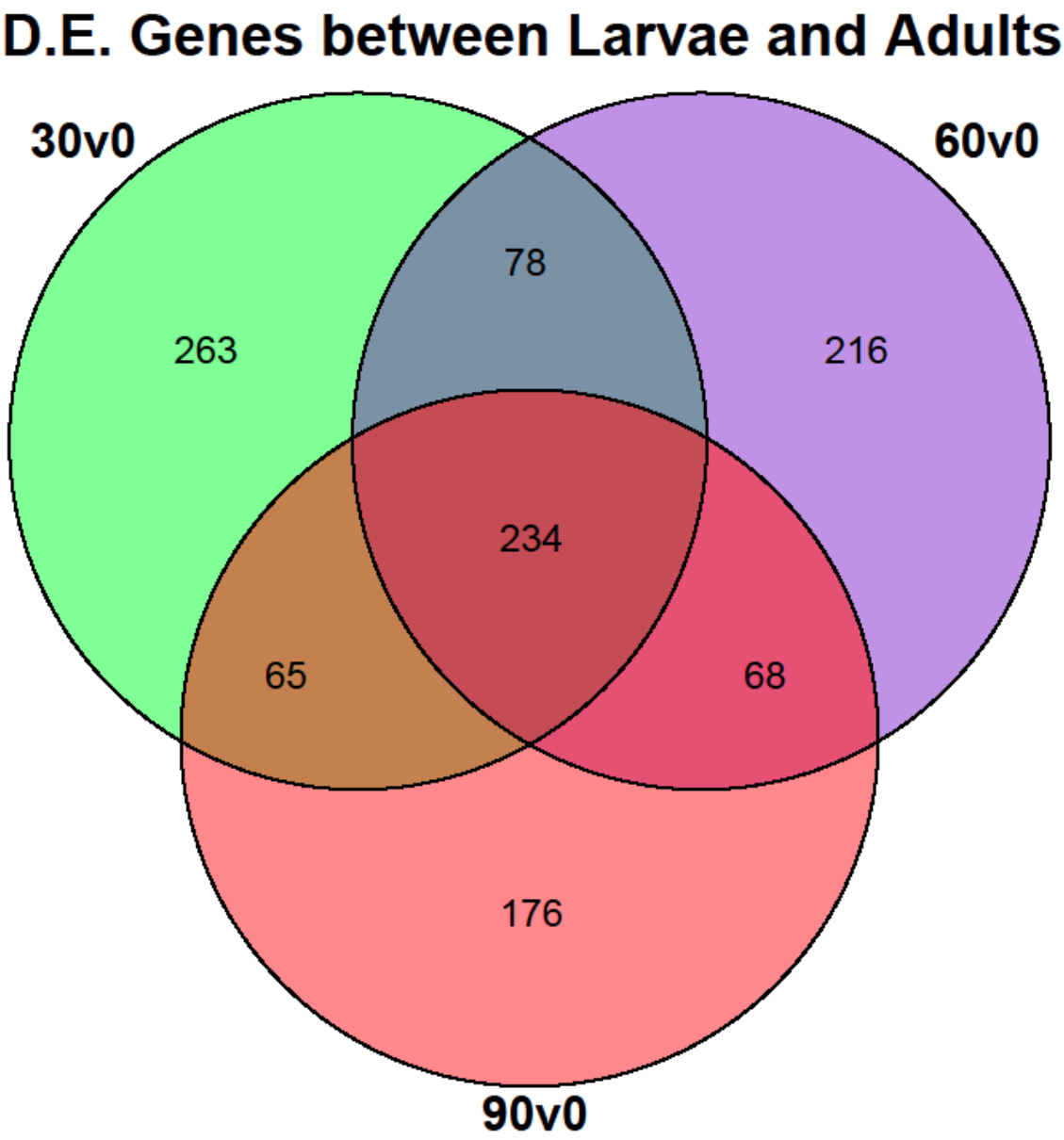

Figure C.3 Venn Diagram of Differentially Expressed Genes

Venn Diagram of significantly differentially expressed genes between larvae and adults in each of the three time point comparisons. Overlapping circles provide a count of which genes are differentially expressed in multiple comparisons.

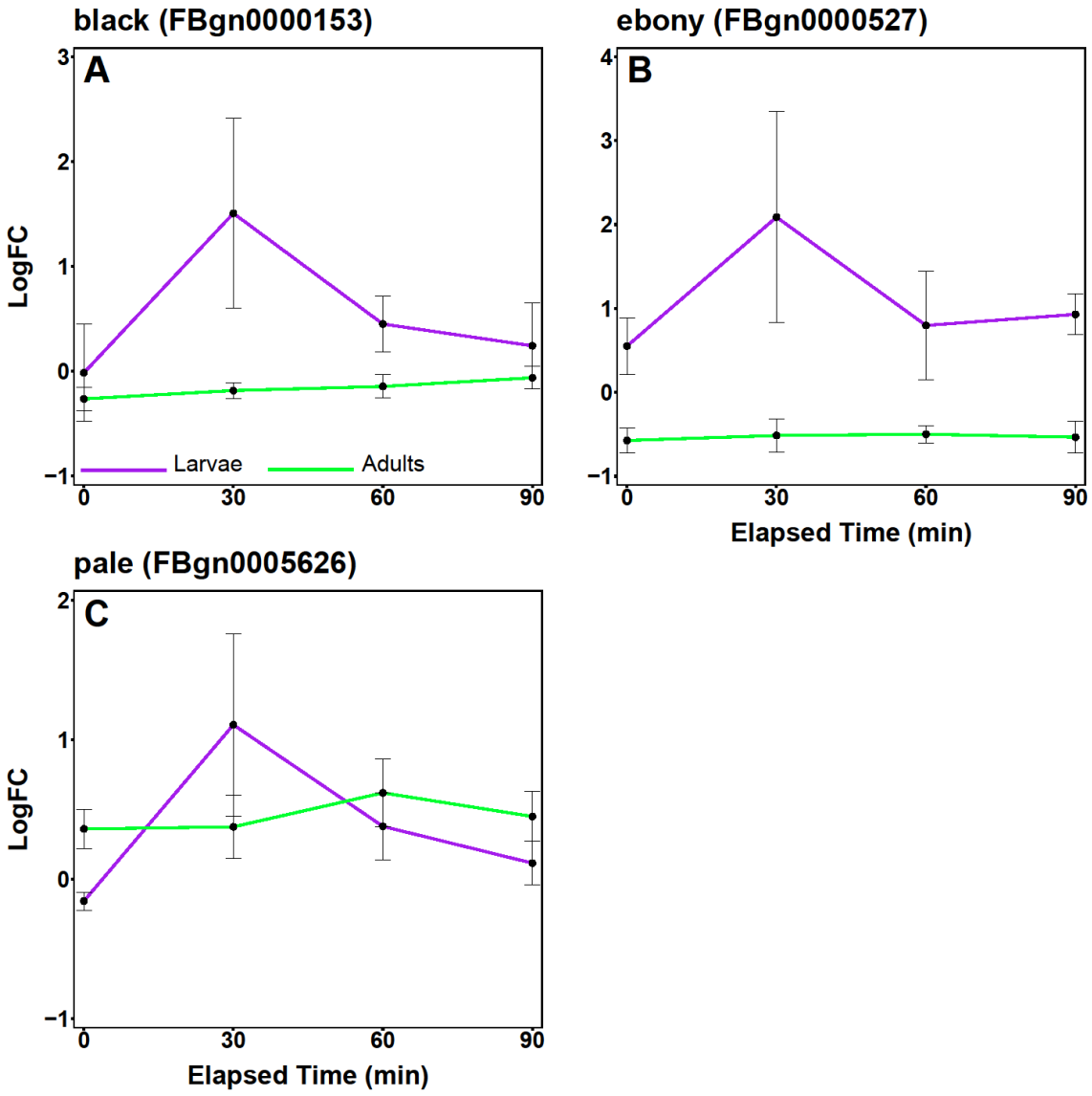

Figure C.4 Pigmentation Cross-Stage Expression Trajectories

Pigmentation related GO terms were enriched in the analysis at the 30v0 time point comparison (Table C.1). Below are the expression trajectories of several genes involved in the pigmentation pathway: *black* (A), *ebony* (B), and *pale* (C). Larvae up-regulated the expression of these genes at the 30-minute time point. Larval trajectories are in purple. Adult trajectories are in green.

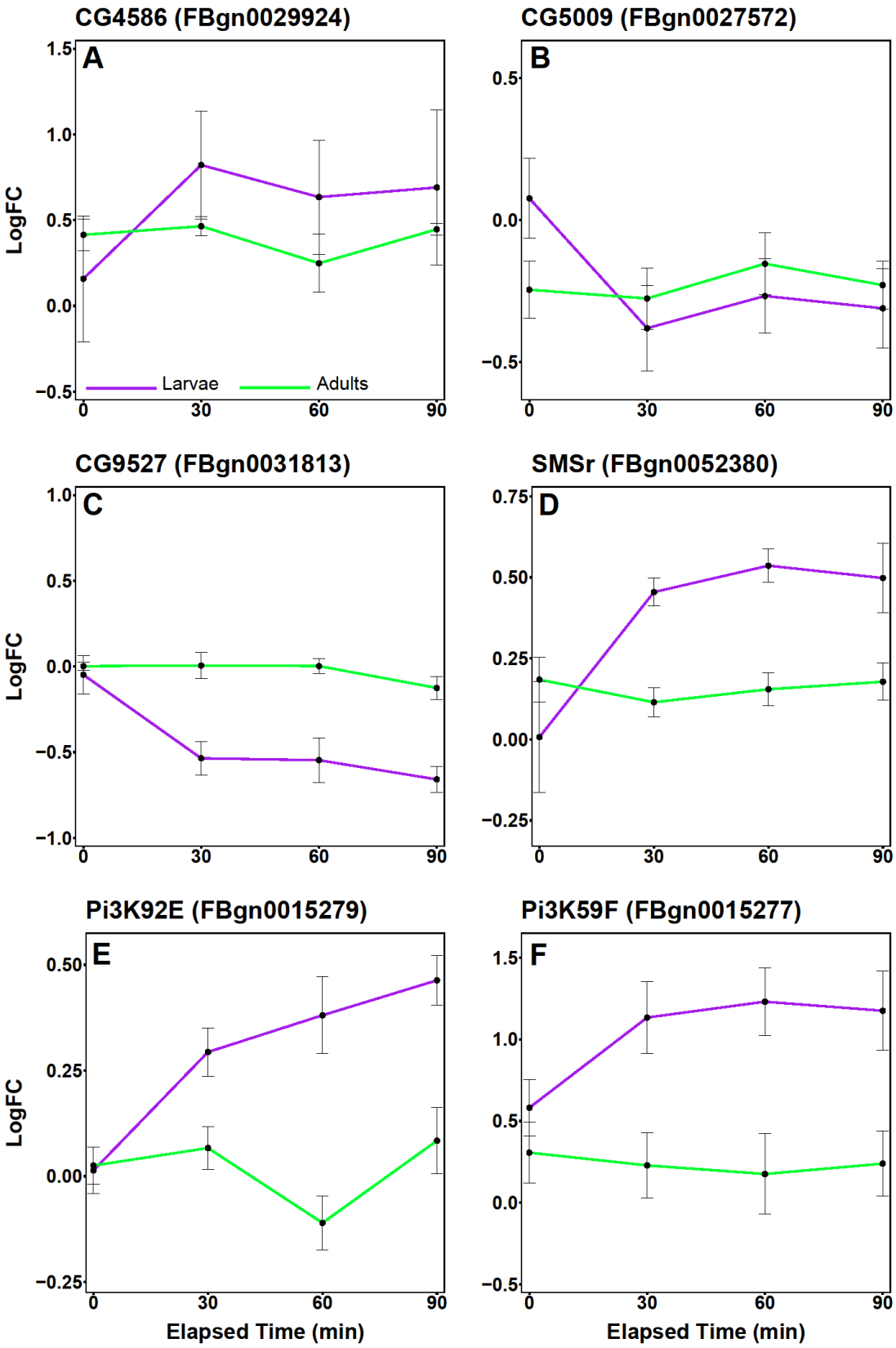
CG4586 (FBgn0029924)
A
CG5009 (FBgn0027572)
B
CG9527 (FBgn0031813)
C
SMSr (FBgn0052380)
D
Pi3K92E (FBgn0015279)
E
Pi3K59F (FBgn0015277)
F
LogFC
Larvae
Adults
Elapsed Time (min)

Figure C.5 Lipid Cross-Stage Expression Trajectories

Lipid synthesis related GO terms were enriched in the analysis at the 60v0 time point comparison (Table C.1). Below are the expression trajectories of several genes involved in numerous lipid pathways: *CG4586* (A), *CG5009* (B), *CG9527* (C), *SMSr* (D), *Pi3k92E* (E), and *Pi3K59F* (F). Larvae have differential expression in these genes at the 60-minute time point. Larval trajectories are in purple. Adult trajectories are in green.

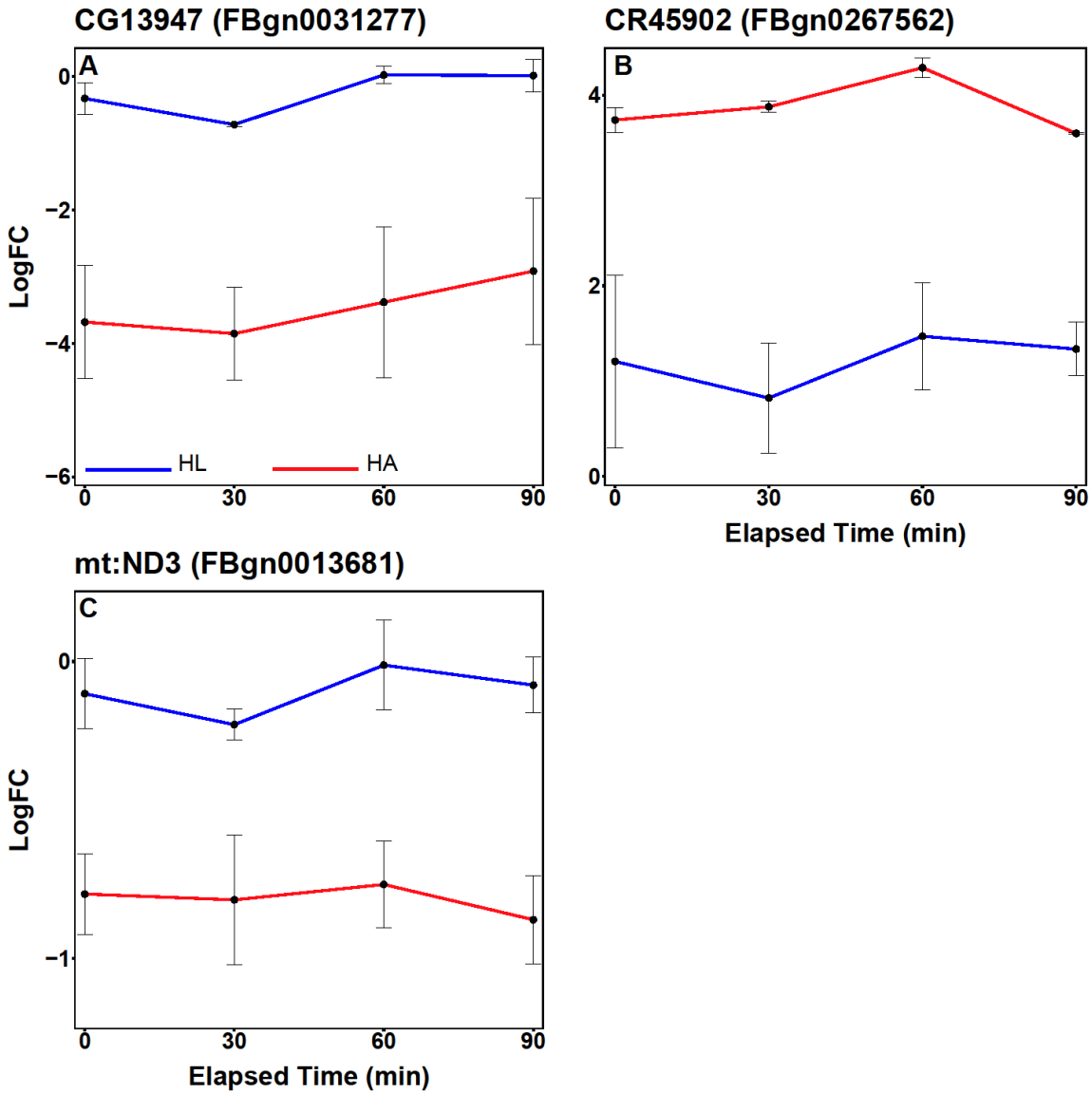

Figure C.6 Adult Cross-Phenotype Expression Trajectories

There is a total of three genes that are constitutively differentially expressed between phenotypes in adults. Below are the expression trajectories of these genes: *CG13947* (A), *CR45902* (B), and *mt:ND3* (C). HL trajectories are in blue. HA trajectories are in red.

30v0 GO Terms

GO:0042254~ribosome biogenesis
GO:0022613~ribonucleoprotein complex biogenesis
GO:0048066~pigmentation during development
GO:0006364~rRNA processing
GO:0043473~pigmentation
GO:0016072~rRNA metabolic process
ribosome biogenesis
PIRSF001710:Ras-related protein Rab
GO:0034470~ncRNA processing
GO:0010259~multicellular organismal aging
GO:0007568~aging
GO:0008340~determination of adult life span
gtp-binding
GO:0031396~regulation of protein ubiquitination
GO:0042594~response to starvation
GO:0060326~cell chemotaxis
GO:0005525~GTP binding
GO:0016477~cell migration
GO:0009309~amine biosynthetic process
wd repeat
GO:0032561~guanyl ribonucleotide binding
GO:0043408~regulation of MAPKKK cascade
GO:0016645~oxidoreductase activity, acting on the CH-NH group of donors
GO:0019001~guanyl nucleotide binding
GO:0006836~neurotransmitter transport
domain:Leucine-zipper
GO:0007298~border follicle cell migration
GO:0048870~cell motility
lipid metabolism
GO:0016646~oxidoreductase activity, acting on the CH-NH group of donors, NAD or NADP as acceptor
GO:0046528~imaginal disc fusion
GO:0017076~purine nucleotide binding
GO:0003924~GTPase activity
IPR013753:Ras
IPR001806:Ras GTPase
fatty acid metabolism
binding site:FAD
GO:0051674~localization of cell
GO:0042127~regulation of cell proliferation
GO:0060429~epithelium development
GO:0008652~cellular amino acid biosynthetic process

GO:0005730~nucleolus
GO:0048584~positive regulation of response to stimulus
IPR016118:Phosphatidic acid phosphatase/chloroperoxidase, N-terminal
IPR006011:Syntaxin, N-terminal
GO:0006904~vesicle docking during exocytosis
GO:0048278~vesicle docking
GO:0022406~membrane docking
GO:0001505~regulation of neurotransmitter levels
GO:0010741~negative regulation of protein kinase cascade
SM00503:SynN
GO:0001736~establishment of planar polarity
GO:0030707~ovarian follicle cell development
DNA binding
GO:0002009~morphogenesis of an epithelium
GO:0007164~establishment of tissue polarity
dme04130:SNARE interactions in vesicular transport
GO:0048729~tissue morphogenesis
GO:0016192~vesicle-mediated transport
GO:0007444~imaginal disc development
GO:0008544~epidermis development
IPR019775:WD40 repeat, conserved site
nucleotide-binding
GO:0042440~pigment metabolic process
GO:0006887~exocytosis
GO:0007269~neurotransmitter secretion
GO:0016814~hydrolase activity, acting on carbon-nitrogen (but not peptide) bonds, in cyclic amidines
GO:0008195~phosphatidate phosphatase activity
GO:0003001~generation of a signal involved in cell-cell signaling
IPR001680:WD40 repeat
dme00565:Ether lipid metabolism
GO:0048056~R3/R4 cell differentiation
GO:0007464~R3/R4 cell fate commitment
IPR019781:WD40 repeat, subgroup
GO:0001738~morphogenesis of a polarized epithelium
GO:0030036~actin cytoskeleton organization
GO:0032555~purine ribonucleotide binding
GO:0032553~ribonucleotide binding
GO:0007423~sensory organ development
GO:0030029~actin filament-based process
dme00564:Glycerophospholipid metabolism
GO:0042624~ATPase activity, uncoupled
GO:0048598~embryonic morphogenesis
GO:0016311~dephosphorylation

GO:0046148~pigment biosynthetic process
dme00250:Alanine, aspartate and glutamate metabolism
IPR015943:WD40/YVTN repeat-like
IPR019782:WD40 repeat 2
IPR011701:Major facilitator superfamily MFS-1
IPR000326:Phosphatidic acid phosphatase type 2/haloperoxidase
propeptide:Activation peptide
GO:0000902~cell morphogenesis
GO:0043628~ncRNA 3'-end processing
GO:0035233~germ cell repulsion
GO:0006935~chemotaxis
GO:0004487~methylenetetrahydrofolate dehydrogenase (NAD+) activity
GO:0070279~vitamin B6 binding
GO:0030170~pyridoxal phosphate binding
IPR015897:CHK kinase-like
IPR004119:Protein of unknown function DUF227
GO:0034660~ncRNA metabolic process
rrna processing
GO:0004091~carboxylesterase activity
SM00014:acidPPc
GO:0016831~carboxy-lyase activity
SM00320:WD40
IPR002167:Graves disease carrier protein
GO:0002064~epithelial cell development
GO:0001885~endothelial cell development
GO:0045446~endothelial cell differentiation
GO:0043409~negative regulation of MAPKKK cascade
IPR017986:WD40 repeat, region
GO:0006979~response to oxidative stress
GO:0018130~heterocycle biosynthetic process

60v0 GO Terms

GO:0003677~DNA binding
PIRSF000168:acyl-CoA oxidase
GO:0001709~cell fate determination
dna-binding
GO:0009953~dorsal/ventral pattern formation
GO:0009950~dorsal/ventral axis specification
GO:0046622~positive regulation of organ growth
lyase
IPR017932:Glutamine amidotransferase, type II
IPR000583:Glutamine amidotransferase, class-II
GO:0060249~anatomical structure homeostasis

lipid synthesis
GO:0016476~regulation of embryonic cell shape
GO:0001742~oenocyte differentiation
GO:0042592~homeostatic process
GO:0033293~monocarboxylic acid binding
GO:0003684~damaged DNA binding
GO:0032869~cellular response to insulin stimulus
GO:0008286~insulin receptor signaling pathway
GO:0032868~response to insulin stimulus
GO:0043434~response to peptide hormone stimulus
GO:0010557~positive regulation of macromolecule biosynthetic process
GO:0016620~oxidoreductase activity, acting on the aldehyde or oxo group of donors, NAD or NADP as acceptor
IPR015876:Fatty acid desaturase, type 1, core
GO:0043492~ATPase activity, coupled to movement of substances
GO:0042626~ATPase activity, coupled to transmembrane movement of substances
GO:0008654~phospholipid biosynthetic process
GO:0016820~hydrolase activity, acting on acid anhydrides, catalyzing transmembrane movement of substances
GO:0015405~P-P-bond-hydrolysis-driven transmembrane transporter activity
GO:0015399~primary active transmembrane transporter activity
GO:0004768~stearoyl-CoA 9-desaturase activity
GO:0046845~branched duct epithelial cell fate determination, open tracheal system
IPR013172:DIM, Drosophila melanogaster
GO:0006355~regulation of transcription, DNA-dependent
GO:0016331~morphogenesis of embryonic epithelium
golgi apparatus
GO:0035225~determination of genital disc primordium
GO:0007445~determination of imaginal disc primordium
GO:0019730~antimicrobial humoral response
GO:0007294~germarium-derived oocyte fate determination
GO:0035152~regulation of tube architecture, open tracheal system
GO:0031406~carboxylic acid binding
GO:0006417~regulation of translation
Fatty acid biosynthesis
cytoplasm
GO:0030716~oocyte fate determination
GO:0030706~germarium-derived oocyte differentiation
GO:0035160~maintenance of epithelial integrity, open tracheal system
GO:0016717~oxidoreductase activity, acting on paired donors, with oxidation of a pair of donors resulting in the reduction of molecular oxygen to two molecules of water
GO:0008374~O-acyltransferase activity
IPR005804:Fatty acid desaturase, type 1

IPR002198:Short-chain dehydrogenase/reductase SDR
GO:0045767~regulation of anti-apoptosis
GO:0035202~sac formation, open tracheal system
GO:0010669~epithelial structure maintenance
GO:0006308~DNA catabolic process
domain:BESS
GO:0032870~cellular response to hormone stimulus
dme00340:Histidine metabolism
GO:0009891~positive regulation of biosynthetic process
GO:0031328~positive regulation of cellular biosynthetic process
SM00563:PlsC
GO:0019731~antibacterial humoral response
GO:0007310~oocyte dorsal/ventral axis specification
GO:0005700~polytene chromosome
IPR014352:FERM/acyl-CoA-binding protein, 3-helical bundle
PIRSF028804:protein yippee-like
PIRSF002411:endozepine
PIRSF017270:ESCRT-3 complex, Chmp1/Chmp2/Chmp3 subunits
GO:0017124~SH3 domain binding
GO:0006909~phagocytosis
GO:0051252~regulation of RNA metabolic process

90v0 GO Terms

GO:0070482~response to oxygen levels
GO:0001666~response to hypoxia
GO:0009266~response to temperature stimulus
GO:0006915~apoptosis
GO:0043068~positive regulation of programmed cell death
GO:0010942~positive regulation of cell death
GO:0006350~transcription
GO:0046668~regulation of retinal cell programmed cell death
GO:0051119~sugar transmembrane transporter activity
zymogen
GO:0005355~glucose transmembrane transporter activity
GO:0042214~terpene metabolic process
GO:0009408~response to heat
GO:0012502~induction of programmed cell death
GO:0030723~ovarian fusome organization
GO:0043065~positive regulation of apoptosis
IPR011600:Peptidase C14, caspase catalytic
IPR001309:Peptidase C14, ICE, catalytic subunit p20
IPR015917:Peptidase C14, caspase precursor p45, core
IPR002138:Peptidase C14, caspase non-catalytic subunit p10

IPR002398:Peptidase C14, caspase precursor p45
SM00115:CASc
GO:0015149~hexose transmembrane transporter activity
GO:0008080~N-acetyltransferase activity
IPR005829:Sugar transporter, conserved site
zinc-finger
GO:0004197~cysteine-type endopeptidase activity
GO:0016410~N-acyltransferase activity
GO:0006721~terpenoid metabolic process
GO:0009636~response to toxin
GO:0015145~monosaccharide transmembrane transporter activity
GO:0009628~response to abiotic stimulus
stress response
dme00903:Limonene and pinene degradation
GO:0006917~induction of apoptosis
GO:0007282~cystoblast division
GO:0043066~negative regulation of apoptosis
PIRSF002581:chaperone HSP70
GO:0016407~acetyltransferase activity
microsome
GO:0008284~positive regulation of cell proliferation
GO:0045478~fusome organization
PIRSF000050:cytochrome P450 CYP4B1
GO:0006401~RNA catabolic process
metal-binding
GO:0006090~pyruvate metabolic process
GO:0032012~regulation of ARF protein signal transduction
IPR001529:DNA-directed RNA polymerase, M/15 kDa subunit
IPR005479:Carbamoyl phosphate synthetase, large subunit, ATP-binding
IPR018181:Heat shock protein 70, conserved site
IPR002401:Cytochrome P450, E-class, group I
GO:0043069~negative regulation of programmed cell death
SM00661:RPOL9
Transcription
GO:0007474~imaginal disc-derived wing vein specification
dme00360:Phenylalanine metabolism
IPR001023:Heat shock protein Hsp70
IPR013126:Heat shock protein 70
IPR013816:ATP-grasp fold, subdomain 2
GO:0007276~gamete generation
GO:0016405~CoA-ligase activity
GO:0045182~translation regulator activity
GO:0014070~response to organic cyclic substance

GO:0043279~response to alkaloid
GO:0045449~regulation of transcription
ligase
GO:0060548~negative regulation of cell death

Common GO Terms

GO:0008219~cell death
GO:0016265~death
GO:0012501~programmed cell death
GO:0007559~histolysis
GO:0016271~tissue death
GO:0007242~intracellular signaling cascade
GO:0035071~salivary gland cell autophagic cell death
GO:0035070~salivary gland histolysis
GO:0048102~autophagic cell death
dme04144:Endocytosis
GO:0015031~protein transport
GO:0007435~salivary gland morphogenesis
GO:0022612~gland morphogenesis
GO:0045184~establishment of protein localization
GO:0040008~regulation of growth
IPR005024:Snf7
GO:0007431~salivary gland development
GO:0035272~exocrine system development
GO:0008104~protein localization
IPR004827:Basic-leucine zipper (bZIP) transcription factor
GO:0009791~post-embryonic development
GO:0007243~protein kinase cascade
GO:0007552~metamorphosis
GO:0002165~instar larval or pupal development
GO:0048707~instar larval or pupal morphogenesis
dme04140:Regulation of autophagy
SM00338:BRLZ
GO:0007254~JNK cascade
GO:0009886~post-embryonic morphogenesis
GO:0008028~monocarboxylic acid transmembrane transporter activity
GO:0006631~fatty acid metabolic process
GO:0031098~stress-activated protein kinase signaling pathway
GO:0007264~small GTPase mediated signal transduction
GO:0010627~regulation of protein kinase cascade
GO:0000165~MAPKKK cascade
GO:0010623~developmental programmed cell death
GO:0048732~gland development

GO:0016877~ligase activity, forming carbon-sulfur bonds
IPR003579:Ras small GTPase, Rab type
GO:0044242~cellular lipid catabolic process
IPR000727:Target SNARE coiled-coil region
IPR011993:Pleckstrin homology-type
GO:0015645~fatty-acid ligase activity
GO:0004467~long-chain-fatty-acid-CoA ligase activity
GO:0007297~ovarian follicle cell migration
GO:0030307~positive regulation of cell growth
SM00175:RAB
GO:0046578~regulation of Ras protein signal transduction
GO:0051056~regulation of small GTPase mediated signal transduction
SM00397:t_SNARE
GO:0015803~branched-chain aliphatic amino acid transport
GO:0015820~leucine transport
GO:0060356~leucine import
GO:0005484~SNAP receptor activity
GO:0046983~protein dimerization activity
GO:0009055~electron carrier activity
GO:0043190~ATP-binding cassette (ABC) transporter complex
IPR003903:Ubiquitin interacting motif
GO:0045793~positive regulation of cell size
alternative splicing
GO:0030695~GTPase regulator activity
IPR001849:Pleckstrin homology
GO:0001558~regulation of cell growth
GO:0006635~fatty acid beta-oxidation
SM00726:UIM
GO:0016042~lipid catabolic process
GO:0035234~germ cell programmed cell death
GO:0042802~identical protein binding
GO:0060589~nucleoside-triphosphatase regulator activity
splice variant
GO:0034440~lipid oxidation
GO:0009062~fatty acid catabolic process
GO:0019395~fatty acid oxidation
GO:0033554~cellular response to stress
GO:0045165~cell fate commitment
GO:0007163~establishment or maintenance of cell polarity
GO:0016081~synaptic vesicle docking during exocytosis
SM00233:PH
GO:0016053~organic acid biosynthetic process
GO:0046394~carboxylic acid biosynthetic process

IPR003439:ABC transporter-like
GO:0019637~organophosphate metabolic process
GO:0042981~regulation of apoptosis
IPR002110:Ankyrin
GO:0031667~response to nutrient levels
GO:0009991~response to extracellular stimulus
GO:0042169~SH2 domain binding
GO:0005083~small GTPase regulator activity
IPR001251:Cellular retinaldehyde-binding/triple function, C-terminal
IPR017871:ABC transporter, conserved site
GO:0015849~organic acid transport
GO:0046942~carboxylic acid transport
GO:0030258~lipid modification
GO:0006644~phospholipid metabolic process
GO:0016079~synaptic vesicle exocytosis
GO:0009968~negative regulation of signal transduction
GO:0006865~amino acid transport
GO:0015804~neutral amino acid transport
GO:0010648~negative regulation of cell communication
GO:0005777~peroxisome
GO:0042579~microbody
SM00248:ANK
SM00516:SEC14
GO:0003995~acyl-CoA dehydrogenase activity
GO:0003997~acyl-CoA oxidase activity
GO:0015355~secondary active monocarboxylate transmembrane transporter activity
GO:0015837~amine transport
IPR006091:Acyl-CoA oxidase/dehydrogenase, central region
IPR013786:Acyl-CoA dehydrogenase/oxidase, N-terminal
IPR013764:Acyl-CoA oxidase/dehydrogenase, type1/2, C-terminal
GO:0019842~vitamin binding
IPR006578:MADF domain
GO:0048489~synaptic vesicle transport
GO:0008356~asymmetric cell division
GO:0005938~cell cortex
IPR002655:Acyl-CoA oxidase, C-terminal
IPR012258:Acyl-CoA oxidase
GO:0019904~protein domain specific binding
GO:0007169~transmembrane receptor protein tyrosine kinase signaling pathway
GO:0007167~enzyme linked receptor protein signaling pathway
GO:0016044~membrane organization
Apoptosis
DNA-binding region:ETS

GO:0043067~regulation of programmed cell death
GO:0001751~compound eye photoreceptor cell differentiation
GO:0045927~positive regulation of growth
SM00595:MADF
GO:0005096~GTPase activator activity
PIRSF000168:Acyl-CoA_oxidase
GO:0046620~regulation of organ growth
GO:0043565~sequence-specific DNA binding
GO:0032312~regulation of ARF GTPase activity
GO:0001752~compound eye photoreceptor fate commitment
GO:0042706~eye photoreceptor cell fate commitment
IPR000873:AMP-dependent synthetase and ligase
GO:0016298~lipase activity
GO:0010941~regulation of cell death
growth regulation
GO:0001754~eye photoreceptor cell differentiation
IPR013525:ABC-2 type transporter
GO:0007424~open tracheal system development
GO:0060541~respiratory system development
GO:0048610~reproductive cellular process
dme00640:Propanoate metabolism
ank repeat
GO:0042803~protein homodimerization activity
GO:0032318~regulation of Ras GTPase activity
dme00592:alpha-Linolenic acid metabolism
IPR001164:Arf GTPase activating protein
IPR000418:Ets
IPR000108:Neutrophil cytosol factor 2
oxidoreductase
Acyltransferase
GO:0046552~photoreceptor cell fate commitment
GO:0048037~cofactor binding
GO:0008060~ARF GTPase activator activity
GO:0010324~membrane invagination
GO:0006897~endocytosis
Monooxygenase
GO:0055114~oxidation reduction
SM00105:ArfGap
SM00413:ETS
dme01040:Biosynthesis of unsaturated fatty acids
GO:0005624~membrane fraction
GO:0007422~peripheral nervous system development
GO:0042058~regulation of epidermal growth factor receptor signaling pathway

GO:0042598~vesicular fraction
GO:0005792~microsome
IPR008942:ENTH/VHS
GO:0048663~neuron fate commitment
IPR002076:GNS1/SUR4 membrane protein
GO:0005070~SH3/SH2 adaptor activity
GO:0046530~photoreceptor cell differentiation
GO:0005626~insoluble fraction
compositionally biased region:Gln-rich
GO:0043087~regulation of GTPase activity
GO:0032268~regulation of cellular protein metabolic process
GO:0003006~reproductive developmental process
IPR011700:Basic leucine zipper
phosphoprotein
GO:0016634~oxidoreductase activity, acting on the CH-CH group of donors, oxygen as acceptor
GO:0005770~late endosome
GO:0000267~cell fraction
oogenesis
domain:FH1
GO:0043548~phosphoinositide 3-kinase binding
endoplasmic reticulum
GO:0007391~dorsal closure
GO:0030674~protein binding, bridging
IPR002123:Phospholipid/glycerol acyltransferase
IPR019018:Rab11-binding domain , FIP domain, C-terminal
IPR019458:Telomerase activating protein Est1
IPR004910:Yippee-like protein
GO:0008047~enzyme activator activity
PIRSF031070:PIRSF031070
GO:0031399~regulation of protein modification process
GO:0006633~fatty acid biosynthetic process
GO:0008610~lipid biosynthetic process
IPR016040:NAD(P)-binding domain
GO:0007390~germ-band shortening
developmental protein
IPR006596:Nucleotide binding protein, PINc
SM00670:PINc
GO:0010033~response to organic substance
GO:0019748~secondary metabolic process
dme00620:Pyruvate metabolism
dme00071:Fatty acid metabolism
GO:0010604~positive regulation of macromolecule metabolic process
GO:0005811~lipid particle

GO:0045471~response to ethanol
GO:0051336~regulation of hydrolase activity
Lipid metabolism / Secondary metabolites biosynthesis, transport, and catabolism
GO:0040007~growth
GO:0031224~intrinsic to membrane
GO:0016021~integral to membrane
GO:0008361~regulation of cell size
dme04150:mTOR signaling pathway
IPR002293:Amino acid/polyamine transporter I
GO:0045941~positive regulation of transcription
GO:0010628~positive regulation of gene expression
PIRSF001552:4-coumarate-CoA ligase
PIRSF006060:AA_transporter

Table C.1 Enriched GO Terms from Pairwise Comparisons

GO Terms were retrieved from genes groups uploaded to DAVID (Gibert et al. 2000) from each of the three pairwise comparisons. The "Common Go Terms" section refers to GO Terms from genes in more than one pairwise comparison.

References

Gibert P, Moreteau B, David JR (2000). Developmental constraints on an adaptive plasticity: reaction norms of pigmentation in adult segments of *Drosophila melanogaster*. *Evol Dev* **2**: 249–260.

30v0 Pathways

R-DME-6803544 Ion influx/efflux at host-pathogen interface
R-DME-389359 CD28 dependent Vav1 pathway
R-DME-916853 Degradation of GABA
R-DME-5687128 MAPK6/MAPK4 signaling
R-DME-8964058 HDL remodeling
R-DME-1474165 Reproduction
R-DME-1500620 Meiosis
R-DME-912446 Meiotic recombination
R-DME-1855167 Synthesis of pyrophosphates in the cytosol
R-DME-70635 Urea cycle
R-DME-83936 Transport of nucleosides and free purine and pyrimidine bases across the plasma membrane
R-DME-888590 GABA synthesis, release, reuptake and degradation
R-DME-6803157 Antimicrobial peptides
R-DME-8939247 RUNX1 regulates transcription of genes involved in interleukin signaling
R-DME-209478 Dephosphorylation of BSK
R-DME-202040 G-protein activation
R-DME-8963899 Plasma lipoprotein remodeling
R-DME-70688 Proline catabolism
R-DME-3928664 Ephrin signaling
R-DME-212676 Dopamine Neurotransmitter Release Cycle
R-DME-204626 Hypusine synthesis from eIF5A-lysine
R-DME-209471 Formation and transport of the N-HH ligand
R-DME-5632681 Ligand-receptor interactions
R-DME-77288 mitochondrial fatty acid beta-oxidation of unsaturated fatty acids
R-DME-77348 Beta oxidation of octanoyl-CoA to hexanoyl-CoA
R-DME-73614 Pyrimidine salvage
R-DME-77346 Beta oxidation of decanoyl-CoA to octanoyl-CoA-CoA
R-DME-8939245 RUNX1 regulates transcription of genes involved in BCR signaling
R-DME-189451 Heme biosynthesis
R-DME-5362798 Release of Hh-Np from the secreting cell
R-DME-209338 Assembly of the 'signalling complexes'
R-DME-189445 Metabolism of porphyrins
R-DME-77286 mitochondrial fatty acid beta-oxidation of saturated fatty acids
R-DME-1614558 Degradation of cysteine and homocysteine
R-DME-112310 Neurotransmitter release cycle
R-DME-8866427 VLDLR internalisation and degradation
R-DME-5627123 RHO GTPases activate PAKs
R-DME-68962 Activation of the pre-replicative complex
R-DME-69002 DNA Replication Pre-Initiation
R-DME-68874 M/G1 Transition
R-DME-176187 Activation of ATR in response to replication stress

R-DME-8956321 Nucleotide salvage
R-DME-69481 G2/M Checkpoints
R-DME-4090294 SUMOylation of intracellular receptors
R-DME-3928662 EPHB-mediated forward signaling
R-DME-163841 Gamma carboxylation, hypusine formation and arylsulfatase activation
R-DME-977606 Regulation of Complement cascade
R-DME-166658 Complement cascade
R-DME-1236978 Cross-presentation of soluble exogenous antigens (endosomes)

60v0 Pathways

R-DME-446210 Synthesis of UDP-N-acetyl-glucosamine
R-DME-196783 Coenzyme A biosynthesis
R-DME-444411 Rhesus glycoproteins mediate ammonium transport.
R-DME-446219 Synthesis of substrates in N-glycan biosythesis
R-DME-5358508 Mismatch Repair
R-DME-5358565 Mismatch repair (MMR) directed by MSH2:MSH6 (MutSalpha)
R-DME-5685939 HDR through MMEJ (alt-NHEJ)
R-DME-199220 Vitamin B5 (pantothenate) metabolism
R-DME-6804759 Regulation of TP53 Activity through Association with Co-factors
R-DME-446193 Biosynthesis of the N-glycan precursor (dolichol lipid-linked oligosaccharide, LLO) and transfer to a nascent protein
R-DME-1483148 Synthesis of PG
R-DME-2559586 DNA Damage/Telomere Stress Induced Senescence
R-DME-5693548 Sensing of DNA Double Strand Breaks
R-DME-3214841 PKMTs methylate histone lysines
R-DME-5693607 Processing of DNA double-strand break ends
R-DME-6798163 Choline catabolism
R-DME-5693616 Presynaptic phase of homologous DNA pairing and strand exchange
R-DME-5693538 Homology Directed Repair
R-DME-71262 Carnitine synthesis
R-DME-418457 cGMP effects
R-DME-1483115 Hydrolysis of LPC
R-DME-392154 Nitric oxide stimulates guanylate cyclase
R-DME-1482922 Acyl chain remodelling of PI
R-DME-2022857 Keratan sulfate degradation
R-DME-72695 Formation of the ternary complex, and subsequently, the 43S complex
R-DME-201451 Signaling by BMP
R-DME-1638074 Keratan sulfate/keratin metabolism
R-DME-156581 Methylation
R-DME-214874 PLL kinase binds to TUB in the TL receptor 'signalling complex'
R-DME-214862 Activated PLL kinase is autophosphorylated in the TL receptor 'signalling complex'
R-DME-111957 Cam-PDE 1 activation
R-DME-5693567 HDR through Homologous Recombination (HRR) or Single Strand Annealing (SSA)

R-DME-1251985 Nuclear signaling by ERBB4
R-DME-1483226 Synthesis of PI
R-DME-727802 Transport of nucleotide sugars
R-DME-174362 Transport and synthesis of PAPS
R-DME-196836 Vitamin C (ascorbate) metabolism
R-DME-209442 Formation of the trans-membrane 'signalling complex'
R-DME-5693571 Nonhomologous End-Joining (NHEJ)
R-DME-189085 Digestion of dietary carbohydrate
R-DME-5633007 Regulation of TP53 Activity
R-DME-72649 Translation initiation complex formation
R-DME-72702 Ribosomal scanning and start codon recognition
R-DME-3928663 EPHA-mediated growth cone collapse
R-DME-3928665 EPH-ephrin mediated repulsion of cells
R-DME-5173214 O-glycosylation of TSR domain-containing proteins
R-DME-2024096 HS-GAG degradation
R-DME-5693579 Homologous DNA Pairing and Strand Exchange
R-DME-71064 Lysine catabolism
R-DME-913709 O-linked glycosylation of mucins
R-DME-5685942 HDR through Homologous Recombination (HRR)
R-DME-2672351 Stimuli-sensing channels
R-DME-156584 Cytosolic sulfonation of small molecules
R-DME-975956 Nonsense Mediated Decay (NMD) independent of the Exon Junction Complex (EJC)
R-DME-72689 Formation of a pool of free 40S subunits
R-DME-427601 Multifunctional anion exchangers
R-DME-429593 Inositol transporters
R-DME-3214815 HDACs deacetylate histones
R-DME-5173105 O-linked glycosylation
R-DME-74259 Purine catabolism
R-DME-1638091 Heparan sulfate/heparin (HS-GAG) metabolism
R-DME-8963676 Intestinal absorption
R-DME-8981373 Intestinal hexose absorption
R-DME-156827 L13a-mediated translational silencing of Ceruloplasmin expression
R-DME-428643 Organic anion transporters
R-DME-209968 Thyroxine biosynthesis
R-DME-72706 GTP hydrolysis and joining of the 60S ribosomal subunit
R-DME-1630316 Glycosaminoglycan metabolism
R-DME-432722 Golgi Associated Vesicle Biogenesis

90v0 Pathways

R-DME-140875 Common Pathway of Fibrin Clot Formation
R-DME-140877 Formation of Fibrin Clot (Clotting Cascade)
R-DME-168638 NOD1/2 Signaling Pathway
R-DME-1237112 Methionine salvage pathway

R-DME-418592 ADP signalling through P2Y purinoceptor 1
R-DME-392518 Signal amplification
R-DME-351906 Apoptotic cleavage of cell adhesion proteins
R-DME-171007 p38MAPK events
R-DME-1566977 Fibronectin matrix formation
R-DME-418889 via Dependence Receptors in the absence of ligand
R-DME-5357769 Caspase activation via extrinsic apoptotic signalling pathway
R-DME-2142700 Synthesis of Lipoxins (LX)
R-DME-140342 Apoptosis induced DNA fragmentation
R-DME-211227 Activation of DNA fragmentation factor
R-DME-2028269 Signaling by Hippo
R-DME-1855183 Synthesis of IP2, IP, and Ins in the cytosol
R-DME-442380 Zinc influx into cells by the SLC39 gene family
R-DME-3000170 Syndecan interactions
R-DME-9018896 Biosynthesis of E-series 18(S)-resolvins
R-DME-9018676 Biosynthesis of D-series resolvins
R-DME-9018679 Biosynthesis of EPA-derived SPMs
R-DME-1855204 Synthesis of IP3 and IP4 in the cytosol
R-DME-435354 Zinc transporters
R-DME-372708 p130Cas linkage to MAPK signaling for integrins
R-DME-432142 Platelet sensitization by LDL
R-DME-113418 Formation of the Early Elongation Complex
R-DME-264870 Caspase-mediated cleavage of cytoskeletal proteins
R-DME-3000171 Non-integrin membrane-ECM interactions
R-DME-3000178 ECM proteoglycans
R-DME-425410 Metal ion SLC transporters
R-DME-77075 RNA Pol II CTD phosphorylation and interaction with CE
R-DME-77387 Insulin receptor recycling
R-DME-917977 Transferrin endocytosis and recycling
R-DME-1222556 ROS, RNS production in phagocytes
R-DME-72086 mRNA Capping
R-DME-8936459 RUNX1 regulates genes involved in megakaryocyte differentiation and platelet function
R-DME-216083 Integrin cell surface interactions
R-DME-5389840 Mitochondrial translation elongation
R-DME-5578749 Transcriptional regulation by small RNAs
R-DME-5419276 Mitochondrial translation termination
R-DME-5368287 Mitochondrial translation
R-DME-211000 Gene Silencing by RNA

Common Pathways

R-DME-1632852 Macroautophagy
R-DME-200425 Import of palmitoyl-CoA into the mitochondrial matrix
R-DME-177929 Signaling by EGFR

R-DME-163680 AMPK inhibits chREBP transcriptional activation activity
R-DME-182971 EGFR downregulation
R-DME-1480926 O2/CO2 exchange in erythrocytes
R-DME-1237044 Erythrocytes take up carbon dioxide and release oxygen
R-DME-1247673 Erythrocytes take up oxygen and release carbon dioxide
R-DME-75105 Fatty acyl-CoA biosynthesis
R-DME-8978868 Fatty acid metabolism
R-DME-5668599 RHO GTPases Activate NADPH Oxidases
R-DME-6807004 Negative regulation of MET activity
R-DME-917729 Endosomal Sorting Complex Required For Transport (ESCRT)
R-DME-426048 Arachidonate production from DAG
R-DME-1855191 Synthesis of IPs in the nucleus
R-DME-163765 ChREBP activates metabolic gene expression
R-DME-425381 Bicarbonate transporters
R-DME-6806834 Signaling by MET
R-DME-75876 Synthesis of very long-chain fatty acyl-CoAs
R-DME-1227986 Signaling by ERBB2
R-DME-1660516 Synthesis of PIPs at the early endosome membrane
R-DME-5620916 VxPx cargo-targeting to cilium
R-DME-5205647 Mitophagy
R-DME-163685 Integration of energy metabolism
R-DME-427975 Proton/oligopeptide cotransporters
R-DME-74749 Signal attenuation
R-DME-400685 Sema4D in semaphorin signaling
R-DME-416572 Sema4D induced cell migration and growth-cone collapse
R-DME-2871796 FCERI mediated MAPK activation
R-DME-5620920 Cargo trafficking to the periciliary membrane
R-DME-1483213 Synthesis of PE
R-DME-5654741 Signaling by FGFR3
R-DME-5654743 Signaling by FGFR4
R-DME-1482839 Acyl chain remodelling of PE
R-DME-2404192 Signaling by Type 1 Insulin-like Growth Factor 1 Receptor (IGF1R)
R-DME-2428924 IGF1R signaling cascade
R-DME-1295596 Spry regulation of FGF signaling
R-DME-71240 Tryptophan catabolism
R-DME-425986 Sodium/Proton exchangers
R-DME-2428933 SHC-related events triggered by IGF1R
R-DME-74751 Insulin receptor signalling cascade
R-DME-8856825 Cargo recognition for clathrin-mediated endocytosis
R-DME-5205685 Pink/Parkin Mediated Mitophagy
R-DME-2424491 DAP12 signaling
R-DME-2172127 DAP12 interactions
R-DME-1250347 SHC1 events in ERBB4 signaling

R-DME-5628897 TP53 Regulates Metabolic Genes
R-DME-373755 Semaphorin interactions
R-DME-1660517 Synthesis of PIPs at the late endosome membrane
R-DME-209560 NF-kB is activated and signals survival
R-DME-193639 p75NTR signals via NF-kB
R-DME-380972 Energy dependent regulation of mTOR by LKB1-AMPK
R-DME-8866376 Reelin signalling pathway
R-DME-8863795 Downregulation of ERBB2 signaling
R-DME-196780 Biotin transport and metabolism
R-DME-5654736 Signaling by FGFR1
R-DME-1369062 ABC transporters in lipid homeostasis
R-DME-180336 SHC1 events in EGFR signaling
R-DME-112409 RAF-independent MAPK1/3 activation
R-DME-168138 Toll Like Receptor 9 (TLR9) Cascade
R-DME-556833 Metabolism of lipids
R-DME-428559 Proton-coupled neutral amino acid transporters
R-DME-8866652 Synthesis of active ubiquitin: roles of E1 and E2 enzymes
R-DME-2730905 Role of LAT2/NTAL/LAB on calcium mobilization
R-DME-1236394 Signaling by ERBB4
R-DME-5654732 Negative regulation of FGFR3 signaling
R-DME-5654727 Negative regulation of FGFR2 signaling
R-DME-5654733 Negative regulation of FGFR4 signaling
R-DME-2046106 alpha-linolenic acid (ALA) metabolism
R-DME-2046104 alpha-linolenic (omega3) and linoleic (omega6) acid metabolism
R-DME-2173788 Downregulation of TGF-beta receptor signaling
R-DME-3322077 Glycogen synthesis
R-DME-450341 Activation of the AP-1 family of transcription factors
R-DME-109704 PI3K Cascade
R-DME-5654726 Negative regulation of FGFR1 signaling
R-DME-2428928 IRS-related events triggered by IGF1R
R-DME-112399 IRS-mediated signalling
R-DME-8934903 Receptor Mediated Mitophagy
R-DME-425393 Transport of inorganic cations/anions and amino acids/oligopeptides
R-DME-1660514 Synthesis of PIPs at the Golgi membrane
R-DME-450724 JNK signalling
R-DME-389356 CD28 co-stimulation
R-DME-5654688 SHC-mediated cascade:FGFR1
R-DME-5654719 SHC-mediated cascade:FGFR4
R-DME-5654704 SHC-mediated cascade:FGFR3
R-DME-5654699 SHC-mediated cascade:FGFR2
R-DME-5621575 CD209 (DC-SIGN) signaling
R-DME-114508 Effects of PIP2 hydrolysis
R-DME-983231 Factors involved in megakaryocyte development and platelet production

R-DME-1482788 Acyl chain remodelling of PC
R-DME-209394 Transcriptional activtion and repression of REL-68 target genes
R-DME-1250196 SHC1 events in ERBB2 signaling
R-DME-162658 Golgi Cisternae Pericentriolar Stack Reorganization
R-DME-5617833 Cilium Assembly
R-DME-180292 GAB1 signalosome
R-DME-112412 SOS-mediated signalling
R-DME-209905 Catecholamine biosynthesis
R-DME-8949664 Processing of SMDT1
R-DME-390918 Peroxisomal lipid metabolism
R-DME-165159 mTOR signalling
R-DME-389887 Beta-oxidation of pristanoyl-CoA
R-DME-174403 Glutathione synthesis and recycling
R-DME-5213460 RIPK1-mediated regulated necrosis
R-DME-5675482 Regulation of necroptotic cell death
R-DME-5218859 Regulated Necrosis
R-DME-879518 Transport of organic anions
R-DME-1483257 Phospholipid metabolism
R-DME-2046105 Linoleic acid (LA) metabolism
R-DME-167044 Signalling to RAS
R-DME-187687 Signalling to ERKs
R-DME-8852135 Protein ubiquitination
R-DME-5654687 Downstream signaling of activated FGFR1
R-DME-5654716 Downstream signaling of activated FGFR4
R-DME-5654696 Downstream signaling of activated FGFR2
R-DME-5654708 Downstream signaling of activated FGFR3
R-DME-209425 Transcriptional activtion by AP-1 transcription factor
R-DME-209409 Formation of the nuclear AP-1 transcription factor 'scaffolding complex'
R-DME-5223345 Miscellaneous transport and binding events
R-DME-8873719 RAB geranylgeranylation
R-DME-1253288 Downregulation of ERBB4 signaling
R-DME-6788656 Histidine, lysine, phenylalanine, tyrosine, proline and tryptophan catabolism
R-DME-2173789 TGF-beta receptor signaling activates SMADs
R-DME-70268 Pyruvate metabolism
R-DME-8849469 PTK6 Regulates RTKs and Their Effectors AKT1 and DOK1
R-DME-937042 IRAK2 mediated activation of TAK1 complex
R-DME-110523 TOR signaling pathway
R-DME-1482925 Acyl chain remodelling of PG
R-DME-1482883 Acyl chain remodeling of DAG and TAG
R-DME-975163 IRAK2 mediated activation of TAK1 complex upon TLR7/8 or 9 stimulation
R-DME-2122948 Activated NOTCH1 Transmits Signal to the Nucleus
R-DME-1980143 Signaling by NOTCH1
R-DME-5654738 Signaling by FGFR2

R-DME-5682910 LGI-ADAM interactions
R-DME-937039 IRAK1 recruits IKK complex
R-DME-975144 IRAK1 recruits IKK complex upon TLR7/8 or 9 stimulation
R-DME-168898 Toll-Like Receptors Cascades
R-DME-445989 TAK1 activates NFkB by phosphorylation and activation of IKKs complex
R-DME-1810476 RIP-mediated NFkB activation via ZBP1
R-DME-1606322 ZBP1(DAI) mediated induction of type I IFNs
R-DME-168928 DDX58/IFIH1-mediated induction of interferon-alpha/beta
R-DME-933542 TRAF6 mediated NF-kB activation
R-DME-5218920 VEGFR2 mediated vascular permeability
R-DME-210993 Tie2 Signaling
R-DME-352230 Amino acid transport across the plasma membrane
R-DME-8856828 Clathrin-mediated endocytosis
R-DME-1483255 PI Metabolism
R-DME-5689877 Josephin domain DUBs
R-DME-390247 Beta-oxidation of very long chain fatty acids
R-DME-3134963 DEx/H-box helicases activate type I IFN and inflammatory cytokines production
R-DME-8851805 MET activates RAS signaling
R-DME-74752 Signaling by Insulin receptor
R-DME-190236 Signaling by FGFR
R-DME-209459 Imd pathway
R-DME-376172 DSCAM interactions
R-DME-1852241 Organelle biogenesis and maintenance
R-DME-168188 Toll Like Receptor TLR6:TLR2 Cascade
R-DME-168176 Toll Like Receptor 5 (TLR5) Cascade
R-DME-166058 MyD88:Mal cascade initiated on plasma membrane
R-DME-975871 MyD88 cascade initiated on plasma membrane
R-DME-166016 Toll Like Receptor 4 (TLR4) Cascade
R-DME-168179 Toll Like Receptor TLR1:TLR2 Cascade
R-DME-181438 Toll Like Receptor 2 (TLR2) Cascade
R-DME-8949215 Mitochondrial calcium ion transport
R-DME-416476 G alpha (q) signalling events
R-DME-8982491 Glycogen metabolism
R-DME-964827 Progressive trimming of alpha-1,2-linked mannose residues from Man9/8/7GlcNAc2 to produce Man5GlcNAc2
R-DME-209400 Transcriptional activtion by phosphorylated DL/DIF dimer
R-DME-165158 Activation of AKT2
R-DME-877312 Regulation of IFNG signaling
R-DME-210693 STAT92E dimer dephosphorylated in the nucleus and transported to the cytosol
R-DME-877300 Interferon gamma signaling
R-DME-1483206 Glycerophospholipid biosynthesis
R-DME-168164 Toll Like Receptor 3 (TLR3) Cascade
R-DME-166166 MyD88-independent TLR4 cascade

R-DME-937061 TRIF(TICAM1)-mediated TLR4 signaling
R-DME-912631 Regulation of signaling by CBL
R-DME-1482801 Acyl chain remodelling of PS
R-DME-445144 Signal transduction by L1
R-DME-210688 Dephosphorylation by PTP61F phosphatases
R-DME-198693 AKT phosphorylates targets in the nucleus
R-DME-1358803 Downregulation of ERBB2:ERBB3 signaling
R-DME-9006934 Signaling by Receptor Tyrosine Kinases
R-DME-5689901 Metalloprotease DUBs
R-DME-8866654 E3 ubiquitin ligases ubiquitinate target proteins
R-DME-110524 DINR-mediated activation
R-DME-110526 Insulin receptor mediated signaling
R-DME-168142 Toll Like Receptor 10 (TLR10) Cascade
R-DME-975138 TRAF6 mediated induction of NFkB and MAP kinases upon TLR7/8 or 9 activation
R-DME-975155 MyD88 dependent cascade initiated on endosome
R-DME-168181 Toll Like Receptor 7/8 (TLR7/8) Cascade
R-DME-1483191 Synthesis of PC
R-DME-389599 Alpha-oxidation of phytanate
R-DME-163560 Triglyceride catabolism
R-DME-512988 Interleukin-3, Interleukin-5 and GM-CSF signaling
R-DME-8948747 Regulation of PTEN localization
R-DME-6785631 ERBB2 Regulates Cell Motility
R-DME-1963640 GRB2 events in ERBB2 signaling
R-DME-432408 Transcription regulation of cwo gene
R-DME-2395516 Electron transport from NADPH to Ferredoxin
R-DME-193048 Androgen biosynthesis
R-DME-209931 Serotonin and melatonin biosynthesis
R-DME-8953897 Cellular responses to external stimuli
R-DME-209405 JAK/STAT pathway
R-DME-425397 Transport of vitamins, nucleosides, and related molecules
R-DME-383280 Nuclear Receptor transcription pathway
R-DME-388841 Costimulation by the CD28 family
R-DME-193648 NRAGE signals death through JNK
R-DME-204998 Cell death signalling via NRAGE, NRIF and NADE
R-DME-450321 JNK (c-Jun kinases) phosphorylation and activation mediated by activated human TAK1
R-DME-70614 Amino acid synthesis and interconversion (transamination)
R-DME-450736 Activation of Downstream Effectors
R-DME-561048 Organic anion transport
R-DME-179812 GRB2 events in EGFR signaling
R-DME-350407 RHO1 GTPase cycle
R-DME-432560 Transcription activation by CLK:CYC and repression by VRI
R-DME-5676934 Protein repair
R-DME-174048 APC/C:Cdc20 mediated degradation of Cyclin B

R-DME-450302 activated TAK1 mediates p38 MAPK activation
R-DME-5654710 PI-3K cascade:FGFR3
R-DME-5654695 PI-3K cascade:FGFR2
R-DME-5654720 PI-3K cascade:FGFR4
R-DME-5654689 PI-3K cascade:FGFR1
R-DME-881907 Gastrin-CREB signalling pathway via PKC and MAPK
R-DME-450294 MAP kinase activation
R-DME-448424 Interleukin-17 signaling
R-DME-71403 Citric acid cycle (TCA cycle)
R-DME-975110 TRAF6 mediated IRF7 activation in TLR7/8 or 9 signaling
R-DME-211979 Eicosanoids
R-DME-8979227 Triglyceride metabolism
R-DME-9033241 Peroxisomal protein import
R-DME-354192 Integrin alphaIIb beta3 signaling
R-DME-9006921 Integrin signaling
R-DME-425407 SLC-mediated transmembrane transport
R-DME-964739 N-glycan trimming and elongation in the cis-Golgi
R-DME-2559585 Oncogene Induced Senescence
R-DME-211958 Miscellaneous substrates
R-DME-350431 Planar Cell Polarity pathway
R-DME-2173796 SMAD2/SMAD3:SMAD4 heterotrimer regulates transcription
R-DME-416482 G alpha (12/13) signalling events
R-DME-8851907 MET activates PI3K/AKT signaling
R-DME-381038 XBP1(S) activates chaperone genes
R-DME-9027307 Biosynthesis of maresin-like SPMs
R-DME-9018682 Biosynthesis of maresins
R-DME-983189 Kinesins
R-DME-76009 Platelet Aggregation (Plug Formation)
R-DME-193704 p75 NTR receptor-mediated signalling
R-DME-936837 Ion transport by P-type ATPases
R-DME-433137 Sodium-coupled sulphate, di- and tri-carboxylate transporters
R-DME-199920 CREB phosphorylation
R-DME-352238 Breakdown of the nuclear lamina
R-DME-442720 CREB phosphorylation through the activation of Adenylate Cyclase
R-DME-5675221 Negative regulation of MAPK pathway
R-DME-110478 Insulin signaling pathway
R-DME-73817 Purine ribonucleoside monophosphate biosynthesis
R-DME-5683826 Surfactant metabolism
R-DME-2173791 TGF-beta receptor signaling in EMT (epithelial to mesenchymal transition)
R-DME-901032 ER Quality Control Compartment (ERQC)
R-DME-450282 MAPK targets/ Nuclear events mediated by MAP kinases
R-DME-381070 IRE1alpha activates chaperones
R-DME-179409 APC-Cdc20 mediated degradation of Nek2A

R-DME-9012852 Signaling by NOTCH3
R-DME-9013507 NOTCH3 Activation and Transmission of Signal to the Nucleus
R-DME-214416 Phosphorylated REL is cleaved by and dissociates from DREDD
R-DME-214411 REL binds to DREDD in the PGN:PGRP-LC/LE receptor 'signalling complex'
R-DME-2179392 EGFR Transactivation by Gastrin
R-DME-209438 Formation of the PGN:PGRP-LC/LE receptor 'signalling complex'
R-DME-432501 Transcription repression by PER and activation by PDP1
R-DME-375170 CDO in myogenesis
R-DME-525793 Myogenesis
R-DME-211981 Xenobiotics
R-DME-73887 Death Receptor Signalling
R-DME-8875656 MET receptor recycling
R-DME-8956320 Nucleobase biosynthesis
R-DME-432720 Lysosome Vesicle Biogenesis
R-DME-198203 PI3K/AKT activation
R-DME-390696 Adrenoceptors
R-DME-196819 Vitamin B1 (thiamin) metabolism
R-DME-442742 CREB phosphorylation through the activation of Ras
R-DME-192456 Digestion of dietary lipid
R-DME-351202 Metabolism of polyamines
R-DME-1660661 Sphingolipid de novo biosynthesis
R-DME-2559582 Senescence-Associated Secretory Phenotype (SASP)
R-DME-5655862 Translesion synthesis by POLK
R-DME-110312 Translesion synthesis by REV1
R-DME-9010553 Regulation of expression of SLITs and ROBOs
R-DME-622312 Inflammasomes
R-DME-844456 The NLRP3 inflammasome
R-DME-209465 Catalytic processing of the nuclear factor, REL
R-DME-214842 DL and DIF homodimers bind to TUB and phosphorylated PLL in the TL receptor 'signalling complex'
R-DME-214869 Phosphorylated CACT, DL and DIF homodimers dissociate from the TL receptor 'signalling complex'
R-DME-214844 DL and DIF homodimers complexed with CACT are all phosphorylated in the TL receptor 'signalling complex'
R-DME-214399 Activated IkappaB kinase (IKK) complex, Phospho IRD5:KEY dimer, phosphorylates REL in the PGN:PGRP-LC/LE receptor 'signalling complex'
R-DME-389357 CD28 dependent PI3K/Akt signaling
R-DME-8875555 MET activates RAP1 and RAC1
R-DME-1474151 Tetrahydrobiopterin (BH4) synthesis, recycling, salvage and regulation
R-DME-1834949 Cytosolic sensors of pathogen-associated DNA
R-DME-211897 Cytochrome P450 - arranged by substrate type
R-DME-5656121 Translesion synthesis by POLI
R-DME-5689896 Ovarian tumor domain proteases
R-DME-166520 Signaling by NTRKs

R-DME-187037 Signaling by NTRK1 (TRKA)
R-DME-1362409 Mitochondrial iron-sulfur cluster biogenesis
R-DME-5654693 FRS-mediated FGFR1 signaling
R-DME-5654712 FRS-mediated FGFR4 signaling
R-DME-5654700 FRS-mediated FGFR2 signaling
R-DME-5654706 FRS-mediated FGFR3 signaling
R-DME-210991 Basigin interactions
R-DME-73864 RNA Polymerase I Transcription
R-DME-73854 RNA Polymerase I Promoter Clearance
R-DME-73762 RNA Polymerase I Transcription Initiation
R-DME-209447 Activation of the IkappaB kinase complex, KEY:IRD5 dimer:KEY
R-DME-977347 Serine biosynthesis
R-DME-202733 Cell surface interactions at the vascular wall
R-DME-157118 Signaling by NOTCH
R-DME-376176 Signaling by ROBO receptors
R-DME-75109 Triglyceride biosynthesis
R-DME-381119 Unfolded Protein Response (UPR)
R-DME-428157 Sphingolipid metabolism
R-DME-5620924 Intraflagellar transport
R-DME-110320 Translesion Synthesis by POLH
R-DME-168643 Nucleotide-binding domain, leucine rich repeat containing receptor (NLR) signaling pathways
R-DME-8951664 Neddylation
R-DME-201722 Formation of the beta-catenin:TCF transactivating complex
R-DME-1660662 Glycosphingolipid metabolism
R-DME-2454202 Fc epsilon receptor (FCERI) signaling
R-DME-196071 Metabolism of steroid hormones
R-DME-2029482 Regulation of actin dynamics for phagocytic cup formation
R-DME-71384 Ethanol oxidation
R-DME-3769402 Deactivation of the beta-catenin transactivating complex
R-DME-196757 Metabolism of folate and pterines
R-DME-450408 AUF1 (hnRNP D0) binds and destabilizes mRNA
R-DME-5696394 DNA Damage Recognition in GG-NER
R-DME-538864 Degradation of CRY
R-DME-382556 ABC-family proteins mediated transport
R-DME-1483249 Inositol phosphate metabolism
R-DME-216167 Nuclear CI is degraded
R-DME-901042 Calnexin/calreticulin cycle
R-DME-449836 Other interleukin signaling
R-DME-1679131 Trafficking and processing of endosomal TLR
R-DME-9018677 Biosynthesis of DHA-derived SPMs
R-DME-9018678 Biosynthesis of specialized proresolving mediators (SPMs)
R-DME-375165 NCAM signaling for neurite out-growth
R-DME-156590 Glutathione conjugation

R-DME-174824 Plasma lipoprotein assembly, remodeling, and clearance
R-DME-432524 Degradation of PER
R-DME-110314 Recognition of DNA damage by PCNA-containing replication complex
R-DME-176412 Phosphorylation of the APC/C
R-DME-8875878 MET promotes cell motility
R-DME-170834 Signaling by TGF-beta Receptor Complex
R-DME-6811436 COPI-independent Golgi-to-ER retrograde traffic
R-DME-2162123 Synthesis of Prostaglandins (PG) and Thromboxanes (TX)
R-DME-209406 Degradation of NF-kappa-B inhibitor, CACT
R-DME-8948751 Regulation of PTEN stability and activity
R-DME-2559583 Cellular Senescence
R-DME-5252538 Drosophila signaling pathways
R-DME-194840 Rho GTPase cycle
R-DME-8876198 RAB GEFs exchange GTP for GDP on RABs
R-DME-432395 Degradation of TIM
R-DME-442729 CREB phosphorylation through the activation of CaMKII
R-DME-196108 Pregnenolone biosynthesis
R-DME-1614635 Sulfur amino acid metabolism
R-DME-2559580 Oxidative Stress Induced Senescence
R-DME-6809371 Formation of the cornified envelope
R-DME-6805567 Keratinization
R-DME-983168 Antigen processing: Ubiquitination & Proteasome degradation
R-DME-5656169 Termination of translesion DNA synthesis
R-DME-8978934 Metabolism of cofactors
R-DME-432626 Circadian Clock pathway
R-DME-71406 Pyruvate metabolism and Citric Acid (TCA) cycle
R-DME-201681 TCF dependent signaling in response to WNT
R-DME-4755510 SUMOylation of immune response proteins
R-DME-549132 Organic cation/anion/zwitterion transport
R-DME-983695 Antigen activates B Cell Receptor (BCR) leading to generation of second messengers
R-DME-4419969 Depolymerisation of the Nuclear Lamina
R-DME-450799 RHO1 signalling
R-DME-5683057 MAPK family signaling cascades
R-DME-209449 Toll pathway
R-DME-176407 Conversion from APC/C:Cdc20 to APC/C:Cdh1 in late anaphase
R-DME-73621 Pyrimidine catabolism
R-DME-203615 eNOS activation
R-DME-6791226 Major pathway of rRNA processing in the nucleolus and cytosol
R-DME-72312 rRNA processing
R-DME-8868773 rRNA processing in the nucleus and cytosol
R-DME-538848 Degradation of CLK
R-DME-77289 Mitochondrial Fatty Acid Beta-Oxidation
R-DME-2132295 MHC class II antigen presentation

R-DME-193368 Synthesis of bile acids and bile salts via 7alpha-hydroxycholesterol
R-DME-203765 eNOS activation and regulation
R-DME-202131 Metabolism of nitric oxide
R-DME-2029480 Fcgamma receptor (FCGR) dependent phagocytosis
R-DME-69202 Cyclin E associated events during G1/S transition
R-DME-141430 Inactivation of APC/C via direct inhibition of the APC/C complex
R-DME-141405 Inhibition of the proteolytic activity of APC/C required for the onset of anaphase by mitotic spindle checkpoint components
R-DME-69618 Mitotic Spindle Checkpoint
R-DME-209461 Ubiquitination and degradation of phosphorylated ARM
R-DME-69231 Cyclin D associated events in G1
R-DME-69236 G1 Phase
R-DME-8854214 TBC/RABGAPs
R-DME-8935690 Digestion
R-DME-5689880 Ub-specific processing proteases
R-DME-199418 Negative regulation of the PI3K/AKT network
R-DME-69656 Cyclin A:Cdk2-associated events at S phase entry
R-DME-209452 N-HH ligand bound to PTC receptor complex
R-DME-209441 WG ligand not bound to FZ receptors
R-DME-198725 Nuclear Events (kinase and transcription factor activation)
R-DME-6811434 COPI-dependent Golgi-to-ER retrograde traffic
R-DME-195258 RHO GTPase Effectors
R-DME-1660499 Synthesis of PIPs at the plasma membrane
R-DME-8856688 Golgi-to-ER retrograde transport
R-DME-5663220 RHO GTPases Activate Formins
R-DME-9018519 Estrogen-dependent gene expression
R-DME-9006936 Signaling by TGF-beta family members
R-DME-209360 Ubiquitination and proteolysis of phosphorylated CI
R-DME-5607761 Dectin-1 mediated noncanonical NF-kB signaling
R-DME-5668541 TNFR2 non-canonical NF-kB pathway
R-DME-5676590 NIK-->noncanonical NF-kB signaling
R-DME-8877627 Vitamin E
R-DME-499943 Interconversion of nucleotide di- and triphosphates
R-DME-5423646 Aflatoxin activation and detoxification
R-DME-1266738 Developmental Biology
R-DME-6811558 PI5P, PP2A and IER3 Regulate PI3K/AKT Signaling
R-DME-5693565 Recruitment and ATM-mediated phosphorylation of repair and signaling proteins at DNA double strand breaks
R-DME-5693606 DNA Double Strand Break Response
R-DME-1169091 Activation of NF-kappaB in B cells
R-DME-1433559 Regulation of KIT signaling
R-DME-194315 Signaling by Rho GTPases
R-DME-5621481 C-type lectin receptors (CLRs)

R-DME-9020702 Interleukin-1 signaling
R-DME-2173793 Transcriptional activity of SMAD2/SMAD3:SMAD4 heterotrimer
R-DME-3899300 SUMOylation of transcription cofactors
R-DME-166208 mTORC1-mediated signalling
R-DME-3700989 Transcriptional Regulation by TP53
R-DME-429947 Deadenylation of mRNA
R-DME-430039 mRNA decay by 5' to 3' exoribonuclease
R-DME-8964043 Plasma lipoprotein clearance
R-DME-9007101 Rab regulation of trafficking
R-DME-422475 Axon guidance
R-DME-9006927 Signaling by Non-Receptor Tyrosine Kinases
R-DME-8848021 Signaling by PTK6
R-DME-373752 Netrin-1 signaling
R-DME-8939211 ESR-mediated signaling
R-DME-532668 N-glycan trimming in the ER and Calnexin/Calreticulin cycle
R-DME-373760 L1CAM interactions
R-DME-5358346 Hedgehog ligand biogenesis
R-DME-174084 Autodegradation of Cdh1 by Cdh1:APC/C
R-DME-390666 Serotonin receptors
R-DME-71291 Metabolism of amino acids and derivatives
R-DME-446652 Interleukin-1 family signaling
R-DME-110313 Translesion synthesis by Y family DNA polymerases bypasses lesions on DNA template
R-DME-209412 Wingless pathway
R-DME-209392 Hedgehog pathway
R-DME-69613 p53-Independent G1/S DNA damage checkpoint
R-DME-69601 Ubiquitin Mediated Degradation of Phosphorylated Cdc25A
R-DME-69610 p53-Independent DNA Damage Response
R-DME-69615 G1/S DNA Damage Checkpoints
R-DME-983169 Class I MHC mediated antigen processing & presentation
R-DME-202670 ERKs are inactivated
R-DME-192105 Synthesis of bile acids and bile salts
R-DME-6807070 PTEN Regulation
R-DME-4608870 Asymmetric localization of PCP proteins
R-DME-4570464 SUMOylation of RNA binding proteins
R-DME-194068 Bile acid and bile salt metabolism
R-DME-5673001 RAF/MAP kinase cascade
R-DME-2173795 Downregulation of SMAD2/3:SMAD4 transcriptional activity
R-DME-209446 N-HH ligand not bound to PTC receptor complex
R-DME-5684996 MAPK1/MAPK3 signaling
R-DME-4641257 Degradation of AXIN
R-DME-69229 Ubiquitin-dependent degradation of Cyclin D1
R-DME-75815 Ubiquitin-dependent degradation of Cyclin D
R-DME-438064 Post NMDA receptor activation events

R-DME-8953750 Transcriptional Regulation by E2F6
R-DME-5362517 Signaling by Retinoic Acid
R-DME-449147 Signaling by Interleukins
R-DME-5632684 Hedgehog 'on' state
R-DME-5696400 Dual Incision in GG-NER
R-DME-1433557 Signaling by SCF-KIT
R-DME-174178 APC/C:Cdh1 mediated degradation of Cdc20 and other APC/C:Cdh1 targeted proteins in late mitosis/early G1
R-DME-8848584 Wax biosynthesis
R-DME-69206 G1/S Transition
R-DME-1257604 PIP3 activates AKT signaling
R-DME-1234176 Oxygen-dependent proline hydroxylation of Hypoxia-inducible Factor Alpha
R-DME-70263 Gluconeogenesis
R-DME-1442490 Collagen degradation
R-DME-73893 DNA Damage Bypass
R-DME-4641258 Degradation of DVL
R-DME-174184 Cdc20:Phospho-APC/C mediated degradation of Cyclin A
R-DME-179419 APC:Cdc20 mediated degradation of cell cycle proteins prior to satisfation of the cell cycle checkpoint
R-DME-69017 CDK-mediated phosphorylation and removal of Cdc6
R-DME-388396 GPCR downstream signalling
R-DME-3371497 HSP90 chaperone cycle for steroid hormone receptors (SHR)
R-DME-2871837 FCERI mediated NF-kB activation
R-DME-176409 APC/C:Cdc20 mediated degradation of mitotic proteins
R-DME-156580 Phase II - Conjugation of compounds
R-DME-198753 ERK/MAPK targets
R-DME-176814 Activation of APC/C and APC/C:Cdc20 mediated degradation of mitotic proteins
R-DME-209776 Amine-derived hormones
R-DME-442755 Activation of NMDA receptor and postsynaptic events
R-DME-70895 Branched-chain amino acid catabolism
R-DME-8854050 FBXL7 down-regulates AURKA during mitotic entry and in early mitosis
R-DME-8943724 Regulation of PTEN gene transcription
R-DME-197264 Nicotinamide salvaging
R-DME-8941858 Regulation of RUNX3 expression and activity
R-DME-450531 Regulation of mRNA stability by proteins that bind AU-rich elements
R-DME-375280 Amine ligand-binding receptors
R-DME-202424 Downstream TCR signaling
R-DME-174113 SCF-beta-TrCP mediated degradation of Emi1
R-DME-1234174 Regulation of Hypoxia-inducible Factor (HIF) by oxygen
R-DME-2262749 Cellular response to hypoxia
R-DME-1168372 Downstream signaling events of B Cell Receptor (BCR)
R-DME-3108214 SUMOylation of DNA damage response and repair proteins
R-DME-5610780 Degradation of GLI1 by the proteasome

R-DME-187577 SCF(Skp2)-mediated degradation of p27/p21
R-DME-9006931 Signaling by Nuclear Receptors
R-DME-8956319 Nucleobase catabolism
R-DME-6781823 Formation of TC-NER Pre-Incision Complex
R-DME-202403 TCR signaling
R-DME-5607764 CLEC7A (Dectin-1) signaling
R-DME-8964038 LDL clearance
R-DME-5610785 GLI3 is processed to GLI3R by the proteasome
R-DME-2022090 Assembly of collagen fibrils and other multimeric structures
R-DME-6806667 Metabolism of fat-soluble vitamins
R-DME-1280218 Adaptive Immune System
R-DME-5357801 Programmed Cell Death
R-DME-983705 Signaling by the B Cell Receptor (BCR)
R-DME-382551 Transport of small molecules
R-DME-913531 Interferon Signaling
R-DME-75953 RNA Polymerase II Transcription Initiation
R-DME-73779 RNA Polymerase II Transcription Pre-Initiation And Promoter Opening
R-DME-76042 RNA Polymerase II Transcription Initiation And Promoter Clearance
R-DME-73776 RNA Polymerase II Promoter Escape
R-DME-8939243 RUNX1 interacts with co-factors whose precise effect on RUNX1 targets is not known
R-DME-1280215 Cytokine Signaling in Immune system
R-DME-8963743 Digestion and absorption
R-DME-199991 Membrane Trafficking
R-DME-5653656 Vesicle-mediated transport
R-DME-5696395 Formation of Incision Complex in GG-NER
R-DME-176408 Regulation of APC/C activators between G1/S and early anaphase
R-DME-2142753 Arachidonic acid metabolism
R-DME-69620 Cell Cycle Checkpoints
R-DME-109582 Hemostasis
R-DME-3371453 Regulation of HSF1-mediated heat shock response
R-DME-3371556 Cellular response to heat stress
R-DME-4086400 PCP/CE pathway
R-DME-5663213 RHO GTPases Activate WASPs and WAVEs
R-DME-112043 PLC beta mediated events
R-DME-1592389 Activation of Matrix Metalloproteinases
R-DME-372790 Signaling by GPCR
R-DME-68875 Mitotic Prophase
R-DME-6782210 Gap-filling DNA repair synthesis and ligation in TC-NER
R-DME-3214847 HATs acetylate histones
R-DME-112040 G-protein mediated events
R-DME-1474290 Collagen formation
R-DME-211945 Phase I - Functionalization of compounds
R-DME-453279 Mitotic G1-G1/S phases

R-DME-354194 GRB2:SOS provides linkage to MAPK signaling for Integrins
R-DME-111885 Opioid Signalling
R-DME-196849 Metabolism of water-soluble vitamins and cofactors
R-DME-453276 Regulation of mitotic cell cycle
R-DME-174143 APC/C-mediated degradation of cell cycle proteins
R-DME-983712 Ion channel transport
R-DME-5688426 Deubiquitination
R-DME-9006925 Intracellular signaling by second messengers
R-DME-389661 Glyoxylate metabolism and glycine degradation
R-DME-373076 Class A/1 (Rhodopsin-like receptors)
R-DME-381426 Regulation of Insulin-like Growth Factor (IGF) transport and uptake by Insulin-like Growth Factor Binding Proteins (IGFBPs)
R-DME-8957275 Post-translational protein phosphorylation
R-DME-429914 Deadenylation-dependent mRNA decay
R-DME-69275 G2/M Transition
R-DME-189200 Cellular hexose transport
R-DME-453274 Mitotic G2-G2/M phases
R-DME-6811440 Retrograde transport at the Trans-Golgi-Network
R-DME-6811438 Intra-Golgi traffic
R-DME-2682334 EPH-Ephrin signaling
R-DME-917937 Iron uptake and transport
R-DME-5693532 DNA Double-Strand Break Repair
R-DME-69052 Switching of origins to a post-replicative state
R-DME-6811442 Intra-Golgi and retrograde Golgi-to-ER traffic
R-DME-6807505 RNA polymerase II transcribes snRNA genes
R-DME-68949 Orc1 removal from chromatin
R-DME-445355 Smooth Muscle Contraction
R-DME-975957 Nonsense Mediated Decay (NMD) enhanced by the Exon Junction Complex (EJC)
R-DME-927802 Nonsense-Mediated Decay (NMD)
R-DME-15869 Metabolism of nucleotides
R-DME-1483166 Synthesis of PA
R-DME-204005 COPII-mediated vesicle transport
R-DME-8957322 Metabolism of steroids
R-DME-70326 Glucose metabolism
R-DME-195253 Degradation of beta-catenin by the destruction complex
R-DME-418555 G alpha (s) signalling events
R-DME-8878159 Transcriptional regulation by RUNX3
R-DME-6782135 Dual incision in TC-NER
R-DME-199992 trans-Golgi Network Vesicle Budding
R-DME-421837 Clathrin derived vesicle budding
R-DME-69306 DNA Replication
R-DME-194138 Signaling by VEGF
R-DME-4420097 VEGFA-VEGFR2 Pathway

R-DME-195721 Signaling by WNT
R-DME-111465 Apoptotic cleavage of cellular proteins
R-DME-5689603 UCH proteinases
R-DME-500792 GPCR ligand binding
R-DME-5696399 Global Genome Nucleotide Excision Repair (GG-NER)
R-DME-196807 Nicotinate metabolism
R-DME-8878171 Transcriptional regulation by RUNX1
R-DME-1428517 The citric acid (TCA) cycle and respiratory electron transport
R-DME-425366 Transport of bile salts and organic acids, metal ions and amine compounds
R-DME-6781827 Transcription-Coupled Nucleotide Excision Repair (TC-NER)
R-DME-196854 Metabolism of vitamins and cofactors
R-DME-3858494 Beta-catenin independent WNT signaling
R-DME-211859 Biological oxidations
R-DME-75153 Apoptotic execution phase
R-DME-5658442 Regulation of RAS by GAPs
R-DME-674695 RNA Polymerase II Pre-transcription Events
R-DME-69242 S Phase
R-DME-2980766 Nuclear Envelope Breakdown
R-DME-109581 Apoptosis
R-DME-1236975 Antigen processing-Cross presentation
R-DME-5610787 Hedgehog 'off' state
R-DME-69239 Synthesis of DNA
R-DME-1430728 Metabolism
R-DME-611105 Respiratory electron transport
R-DME-72662 Activation of the mRNA upon binding of the cap-binding complex and eIFs, and subsequent binding to 43S
R-DME-3108232 SUMO E3 ligases SUMOylate target proteins
R-DME-76002 Platelet activation, signaling and aggregation
R-DME-4839726 Chromatin organization
R-DME-3247509 Chromatin modifying enzymes
R-DME-5358351 Signaling by Hedgehog
R-DME-2990846 SUMOylation
R-DME-5696398 Nucleotide Excision Repair
R-DME-397014 Muscle contraction
R-DME-68886 M Phase
R-DME-163200 Respiratory electron transport, ATP synthesis by chemiosmotic coupling, and heat production by uncoupling proteins.
R-DME-2262752 Cellular responses to stress
R-DME-212436 Generic Transcription Pathway
R-DME-159236 Transport of Mature mRNA derived from an Intron-Containing Transcript
R-DME-72202 Transport of Mature Transcript to Cytoplasm
R-DME-6807878 COPI-mediated anterograde transport
R-DME-71387 Metabolism of carbohydrates

R-DME-112315 Transmission across Chemical Synapses
R-DME-199977 ER to Golgi Anterograde Transport
R-DME-1640170 Cell Cycle
R-DME-1474228 Degradation of the extracellular matrix
R-DME-162582 Signal Transduction
R-DME-418594 G alpha (i) signalling events
R-DME-69278 Cell Cycle, Mitotic
R-DME-948021 Transport to the Golgi and subsequent modification
R-DME-72737 Cap-dependent Translation Initiation
R-DME-72613 Eukaryotic Translation Initiation
R-DME-72163 mRNA Splicing - Major Pathway
R-DME-112314 Neurotransmitter receptors and postsynaptic signal transmission
R-DME-72172 mRNA Splicing
R-DME-168249 Innate Immune System
R-DME-114608 Platelet degranulation
R-DME-446203 Asparagine N-linked glycosylation
R-DME-76005 Response to elevated platelet cytosolic Ca2+
R-DME-73894 DNA Repair
R-DME-73857 RNA Polymerase II Transcription
R-DME-1474244 Extracellular matrix organization
R-DME-168256 Immune System
R-DME-8953854 Metabolism of RNA
R-DME-72203 Processing of Capped Intron-Containing Pre-mRNA
R-DME-112316 Neuronal System
R-DME-6798695 Neutrophil degranulation
R-DME-74160 Gene expression (Transcription)
R-DME-597592 Post-translational protein modification
R-DME-72766 Translation
R-DME-392499 Metabolism of proteins
R-DME-380612 Metabolism of serotonin
R-DME-380615 Serotonin clearance from the synaptic cleft
R-DME-112311 Neurotransmitter clearance
R-DME-163754 Insulin effects increased synthesis of Xylulose-5-Phosphate
R-DME-170660 Adenylate cyclase activating pathway
R-DME-997269 Inhibition of adenylate cyclase pathway
R-DME-170670 Adenylate cyclase inhibitory pathway
R-DME-5365859 RA biosynthesis pathway
R-DME-163359 Glucagon signaling in metabolic regulation
R-DME-432040 Vasopressin regulates renal water homeostasis via Aquaporins
R-DME-164378 PKA activation in glucagon signalling
R-DME-111996 Ca-dependent events
R-DME-111997 CaM pathway
R-DME-111933 Calmodulin induced events

R-DME-1489509 DAG and IP3 signaling
R-DME-6783984 Glycine degradation
R-DME-418597 G alpha (z) signalling events
R-DME-163615 PKA activation
R-DME-111931 PKA-mediated phosphorylation of CREB
R-DME-2453902 The canonical retinoid cycle in rods (twilight vision)
R-DME-114604 GPVI-mediated activation cascade
R-DME-211976 Endogenous sterols
R-DME-975634 Retinoid metabolism and transport
R-DME-445717 Aquaporin-mediated transport
R-DME-2187335 The retinoid cycle in cones (daylight vision)
R-DME-71182 Phenylalanine and tyrosine catabolism
R-DME-216119 Activation of CI
R-DME-71336 Pentose phosphate pathway
R-DME-991365 Activation of GABAB receptors
R-DME-977444 GABA B receptor activation
R-DME-2187338 Visual phototransduction
R-DME-977443 GABA receptor activation
R-DME-1234158 Regulation of gene expression by Hypoxia-inducible Factor
R-DME-8937144 Aryl hydrocarbon receptor signalling
R-DME-1236973 Cross-presentation of particulate exogenous antigens (phagosomes)
R-DME-2173782 Binding and Uptake of Ligands by Scavenger Receptors
R-DME-3000471 Scavenging by Class B Receptors
R-DME-5674135 MAP2K and MAPK activation
R-DME-5686938 Regulation of TLR by endogenous ligand
R-DME-209159 Assembly of the CI containing complexes
R-DME-72165 mRNA Splicing - Minor Pathway
R-DME-1799339 SRP-dependent cotranslational protein targeting to membrane
R-DME-5673000 RAF activation
R-DME-6803529 FGFR2 alternative splicing
R-DME-418346 Platelet homeostasis
R-DME-6796648 TP53 Regulates Transcription of DNA Repair Genes
R-DME-112382 Formation of RNA Pol II elongation complex
R-DME-75955 RNA Polymerase II Transcription Elongation

Table C.2 Enriched Pathways from Pairwise Comparisons

Pathways were retrieved from genes groups uploaded to Reactome (Fabregat et al. 2018) from each of the three pairwise comparisons. The “Common Pathways” section refers to pathways from genes in more than one pairwise comparison.

References

Fabregat A, Jupe S, Matthews L, Sidiropoulos K, Gillespie M, Garapati P, *et al.* (2018). The Reactome Pathway Knowledgebase. *Nucleic Acids Res* **46**: D649–D655.

Cluster 1 GO Terms

GO:0012501~programmed cell death
GO:0008219~cell death
GO:0016265~death
GO:0007435~salivary gland morphogenesis
GO:0022612~gland morphogenesis
GO:0007242~intracellular signaling cascade
GO:0007559~histolysis
GO:0016271~tissue death
GO:0048732~gland development
GO:0007431~salivary gland development
GO:0035272~exocrine system development
GO:0035071~salivary gland cell autophagic cell death
GO:0035070~salivary gland histolysis
GO:0048102~autophagic cell death
GO:0007552~metamorphosis
GO:0009886~post-embryonic morphogenesis
GO:0006955~immune response
GO:0048707~instar larval or pupal morphogenesis
GO:0009791~post-embryonic development
GO:0002165~instar larval or pupal development
GO:0019730~antimicrobial humoral response
GO:0007264~small GTPase mediated signal transduction
GO:0006959~humoral immune response
GO:0006952~defense response
GO:0060541~respiratory system development
GO:0007424~open tracheal system development
GO:0007243~protein kinase cascade
GO:0016477~cell migration
GO:0033554~cellular response to stress
GO:0046578~regulation of Ras protein signal transduction
dme04144:Endocytosis
dme04140:Regulation of autophagy
dme04630:Jak-STAT signaling pathway
GO:0009968~negative regulation of signal transduction
GO:0010648~negative regulation of cell communication
GO:0048870~cell motility
GO:0051056~regulation of small GTPase mediated signal transduction
GO:0051674~localization of cell
Apoptosis
GO:0045087~innate immune response
GO:0040008~regulation of growth

IPR005024:Snf7
IPR013172:DIM, Drosophila melanogaster
innate immunity
IPR001849:Pleckstrin homology
immune response
IPR003579:Ras small GTPase, Rab type
GO:0048066~pigmentation during development
IPR011993:Pleckstrin homology-type
GO:0048610~reproductive cellular process
GO:0042058~regulation of epidermal growth factor receptor signaling pathway
GO:0043473~pigmentation
IPR000980:SH2 motif
GO:0045165~cell fate commitment
GO:0008270~zinc ion binding
GO:0008104~protein localization
GO:0007297~ovarian follicle cell migration
GO:0015031~protein transport
GO:0043067~regulation of programmed cell death
GO:0007167~enzyme linked receptor protein signaling pathway
GO:0003677~DNA binding
IPR013753:Ras
IPR001806:Ras GTPase
SM00175:RAB
GO:0005083~small GTPase regulator activity
PIRSF001710:Ras-related protein Rab
GO:0000165~MAPKKK cascade
GO:0045184~establishment of protein localization
GO:0010941~regulation of cell death
GO:0030695~GTPase regulator activity
GO:0003006~reproductive developmental process
GO:0010623~developmental programmed cell death
SM00233:PH
GO:0007254~JNK cascade
GO:0060589~nucleoside-triphosphatase regulator activity
GO:0042802~identical protein binding
SM00252:SH2
GO:0006928~cell motion
GO:0007298~border follicle cell migration
GO:0016311~dephosphorylation
GO:0007169~transmembrane receptor protein tyrosine kinase signaling pathway
GO:0008360~regulation of cell shape
GO:0004725~protein tyrosine phosphatase activity
GO:0005096~GTPase activator activity

GO:0008063~Toll signaling pathway
GO:0006915~apoptosis
GO:0031098~stress-activated protein kinase signaling pathway
DNA binding
GO:0042742~defense response to bacterium
GO:0007276~gamete generation
GO:0000902~cell morphogenesis
IPR003903:Ubiquitin interacting motif
GO:0030307~positive regulation of cell growth
GO:0046914~transition metal ion binding
GO:0030097~hemopoiesis
GO:0032268~regulation of cellular protein metabolic process
GO:0007389~pattern specification process
GO:0048477~oogenesis
GO:0010627~regulation of protein kinase cascade
GO:0031399~regulation of protein modification process
IPR001496:SOCS protein, C-terminal
GO:0019953~sexual reproduction
GO:0032318~regulation of Ras GTPase activity
GO:0042981~regulation of apoptosis
GO:0007444~imaginal disc development
IPR013087:Zinc finger, C2H2-type/integrase, DNA-binding
compositionally biased region:Ser-rich
GO:0007163~establishment or maintenance of cell polarity
IPR004827:Basic-leucine zipper (bZIP) transcription factor
GO:0043066~negative regulation of apoptosis
GO:0019731~antibacterial humoral response
GO:0007280~pole cell migration
GO:0007292~female gamete generation
GO:0007259~JAK-STAT cascade
GO:0032989~cellular component morphogenesis
GO:0046983~protein dimerization activity
GO:0042440~pigment metabolic process
GO:0042067~establishment of ommatidial polarity
SM00726:UIM
developmental protein
GO:0006796~phosphate metabolic process
GO:0006793~phosphorus metabolic process
GO:0032504~multicellular organism reproduction
GO:0048609~reproductive process in a multicellular organism
IPR006578:MADF domain
GO:0002520~immune system development
GO:0042127~regulation of cell proliferation

GO:0048534~hemopoietic or lymphoid organ development
GO:0045793~positive regulation of cell size
IPR005225:Small GTP-binding protein
GO:0005525~GTP binding
GO:0048569~post-embryonic organ development
GO:0009617~response to bacterium
GO:0000922~spindle pole
GO:0030707~ovarian follicle cell development
GO:0032561~guanyl ribonucleotide binding
GO:0019904~protein domain specific binding
PIRSF036514:alpha-crystallin-related small heat shock protein
GO:0016814~hydrolase activity, acting on carbon-nitrogen (but not peptide) bonds, in cyclic amidines
GO:0019001~guanyl nucleotide binding
GO:0006468~protein amino acid phosphorylation
gtp-binding
GO:0006470~protein amino acid dephosphorylation
GO:0046982~protein heterodimerization activity
GO:0048729~tissue morphogenesis
GO:0051336~regulation of hydrolase activity
SM00253:SOCS
GO:0043069~negative regulation of programmed cell death
GO:0043087~regulation of GTPase activity
GO:0035099~hemocyte migration
GO:0022604~regulation of cell morphogenesis
GO:0045927~positive regulation of growth
GO:0006355~regulation of transcription, DNA-dependent
splice variant
dme04150:mTOR signaling pathway
GO:0008047~enzyme activator activity
GO:0005615~extracellular space
IPR002110:Ankyrin
GO:0005576~extracellular region
IPR015880:Zinc finger, C2H2-like
GO:0001558~regulation of cell growth
GO:0007143~female meiosis
IPR012934:Zinc finger, AD-type
SM00338:BRLZ
GO:0060356~leucine import
GO:0015803~branched-chain aliphatic amino acid transport
GO:0035096~larval midgut cell programmed cell death
GO:0015820~leucine transport
GO:0001751~compound eye photoreceptor cell differentiation
GO:0007560~imaginal disc morphogenesis

GO:0048563~post-embryonic organ morphogenesis
GO:0009719~response to endogenous stimulus
GO:0009725~response to hormone stimulus
dna-binding
GO:0003924~GTPase activity
GO:0060548~negative regulation of cell death
IPR016130:Protein-tyrosine phosphatase, active site
GO:0043408~regulation of MAPKKK cascade
domain:RHD
IPR000306:Zinc finger, FYVE-type
zinc-finger
GO:0004857~enzyme inhibitor activity
IPR007087:Zinc finger, C2H2-type
GO:0016791~phosphatase activity
GO:0046580~negative regulation of Ras protein signal transduction
GO:0051058~negative regulation of small GTPase mediated signal transduction
GO:0005938~cell cortex
zinc finger
IPR000387:Dual-specific/protein-tyrosine phosphatase, conserved region
GO:0006974~response to DNA damage stimulus
GO:0046148~pigment biosynthetic process
IPR000108:Neutrophil cytosol factor 2
IPR000451:NF-kappa-B/Rel/dorsal
GO:0046530~photoreceptor cell differentiation
GO:0060429~epithelium development
GO:0001754~eye photoreceptor cell differentiation
GO:0009168~purine ribonucleoside monophosphate biosynthetic process
GO:0009126~purine nucleoside monophosphate metabolic process
GO:0046668~regulation of retinal cell programmed cell death
GO:0016476~regulation of embryonic cell shape
GO:0009127~purine nucleoside monophosphate biosynthetic process
GO:0009167~purine ribonucleoside monophosphate metabolic process
GO:0001709~cell fate determination
GO:0046872~metal ion binding
GO:0007423~sensory organ development
GO:0048749~compound eye development
IPR004841:Amino acid permease-associated region
GO:0007098~centrosome cycle
GO:0002009~morphogenesis of an epithelium
GO:0060284~regulation of cell development
GO:0031023~microtubule organizing center organization
GO:0042706~eye photoreceptor cell fate commitment
GO:0001752~compound eye photoreceptor fate commitment

GO:0008356~asymmetric cell division
SM00595:MADF
GO:0048598~embryonic morphogenesis
GO:0031396~regulation of protein ubiquitination
GO:0048056~R3/R4 cell differentiation
GO:0007464~R3/R4 cell fate commitment
GO:0005886~plasma membrane
GO:0001738~morphogenesis of a polarized epithelium
GO:0008286~insulin receptor signaling pathway
GO:0032869~cellular response to insulin stimulus
GO:0043434~response to peptide hormone stimulus
GO:0032868~response to insulin stimulus
GO:0043169~cation binding
GO:0035069~larval midgut histolysis
GO:0035234~germ cell programmed cell death
GO:0006303~double-strand break repair via nonhomologous end joining
GO:0060326~cell chemotaxis
GO:0048010~vascular endothelial growth factor receptor signaling pathway
IPR001436:Alpha crystallin/Heat shock protein
alternative splicing
PIRSF015810:Caenorhabditis elegans hypothetical protein R06B9.1
GO:0005099~Ras GTPase activator activity
IPR017455:Zinc finger, FYVE-related
GO:0008354~germ cell migration
GO:0005070~SH3/SH2 adaptor activity
GO:0007494~midgut development
GO:0051174~regulation of phosphorus metabolic process
GO:0019220~regulation of phosphate metabolic process
GO:0035162~embryonic hemopoiesis
signal peptide
GO:0043167~ion binding
GO:0006979~response to oxidative stress
GO:0001736~establishment of planar polarity
GO:0048565~gut development
GO:0035081~induction of programmed cell death by hormones
GO:0042594~response to starvation
PIRSF006060:AA_transporter
GO:0007164~establishment of tissue polarity
SM00064:FYVE
GO:0035295~tube development
ank repeat
GO:0009967~positive regulation of signal transduction
GO:0046552~photoreceptor cell fate commitment

GO:0006865~amino acid transport
GO:0006310~DNA recombination
GO:0045449~regulation of transcription
IPR011539:Rel homology
IPR011700:Basic leucine zipper
GO:0050829~defense response to Gram-negative bacterium
GO:0005788~endoplasmic reticulum lumen
GO:0035220~wing disc development
GO:0005097~Rab GTPase activator activity
GO:0004721~phosphoprotein phosphatase activity
GO:0051252~regulation of RNA metabolic process
IPR011021:Arrestin-like, N-terminal
IPR011022:Arrestin-like, C-terminal
GO:0051298~centrosome duplication
GO:0048568~embryonic organ development
GO:0009161~ribonucleoside monophosphate metabolic process
GO:0009156~ribonucleoside monophosphate biosynthetic process
GO:0007426~tracheal outgrowth, open tracheal system
GO:0006281~DNA repair
GO:0010647~positive regulation of cell communication
GO:0034976~response to endoplasmic reticulum stress
GO:0045742~positive regulation of epidermal growth factor receptor signaling pathway
GO:0000726~non-recombinational repair
GO:0042325~regulation of phosphorylation
GO:0030031~cell projection assembly
GO:0015837~amine transport
IPR017956:AT hook, DNA-binding, conserved site
GO:0005815~microtubule organizing center
GO:0004672~protein kinase activity
GO:0008083~growth factor activity
GO:0048663~neuron fate commitment
GO:0030674~protein binding, bridging
GO:0042169~SH2 domain binding
IPR002293:Amino acid/polyamine transporter I
GO:0046620~regulation of organ growth
signal
GO:0051297~centrosome organization
GO:0001700~embryonic development via the syncytial blastoderm
GO:0043565~sequence-specific DNA binding
GO:0004674~protein serine/threonine kinase activity
GO:0001654~eye development
domain:Leucine-zipper
GO:0003002~regionalization

SM00248:ANK
GO:0007155~cell adhesion
GO:0008340~determination of adult life span
GO:0010259~multicellular organismal aging
GO:0007568~aging
GO:0009880~embryonic pattern specification
GO:0008293~torso signaling pathway
GO:0051225~spindle assembly
GO:0002164~larval development
domain:PH
IPR004182:GRAM
IPR006596:Nucleotide binding protein, PINc
GO:0044421~extracellular region part
GO:0043068~positive regulation of programmed cell death
GO:0010942~positive regulation of cell death
IPR002068:Heat shock protein Hsp20
IPR013128:Peptidase C1A, papain
GO:0007391~dorsal closure
GO:0032012~regulation of ARF protein signal transduction
GO:0008088~axon cargo transport
GO:0046622~positive regulation of organ growth
GO:0042417~dopamine metabolic process
GO:0015804~neutral amino acid transport
GO:0001745~compound eye morphogenesis
antibiotic
zinc
GO:0051094~positive regulation of developmental process
GO:0005813~centrosome
GO:0040007~growth
GO:0035239~tube morphogenesis
IPR000719:Protein kinase, core
GO:0051726~regulation of cell cycle
GO:0009792~embryonic development ending in birth or egg hatching
GO:0042059~negative regulation of epidermal growth factor receptor signaling pathway
GO:0046528~imaginal disc fusion
GO:0016318~ommatidial rotation
IPR000340:Dual specificity phosphatase, catalytic domain
IPR017442:Serine/threonine protein kinase-related
GO:0006836~neurotransmitter transport
IPR008271:Serine/threonine protein kinase, active site
GO:0005819~spindle
GO:0008283~cell proliferation
GO:0004197~cysteine-type endopeptidase activity

IPR006331:Adenosine deaminase-related growth factor
IPR016118:Phosphatidic acid phosphatase/chloroperoxidase, N-terminal
IPR013659:Adenosine/AMP deaminase N-terminal
GO:0005275~amine transmembrane transporter activity
GO:0009952~anterior/posterior pattern formation
GO:0048067~cuticle pigmentation
GO:0034331~cell junction maintenance
GO:0032870~cellular response to hormone stimulus
GO:0032313~regulation of Rab GTPase activity
GO:0050832~defense response to fungus
GO:0032483~regulation of Rab protein signal transduction
SM00568:GRAM
SM00670:PINc
GO:0003700~transcription factor activity
GO:0005769~early endosome
GO:0042803~protein homodimerization activity
compositionally biased region:Gln-rich
GO:0008361~regulation of cell size
GO:0008092~cytoskeletal protein binding
IPR000727:Target SNARE coiled-coil region
GO:0004869~cysteine-type endopeptidase inhibitor activity
GO:0051240~positive regulation of multicellular organismal process
GO:0022404~molting cycle process
GO:0042461~photoreceptor cell development
SM00384:AT_hook
GO:0015171~amino acid transmembrane transporter activity
GO:0022610~biological adhesion
GO:0016765~transferase activity, transferring alkyl or aryl (other than methyl) groups
kinase
Secreted
compositionally biased region:Poly-Gln
DNA-binding region:ETS
GO:0048489~synaptic vesicle transport
GO:0003684~damaged DNA binding
GO:0040003~chitin-based cuticle development
GO:0004364~glutathione transferase activity
GO:0048584~positive regulation of response to stimulus
GO:0005768~endosome
GO:0051301~cell division
IPR000626:Ubiquitin
IPR015940:Ubiquitin-associated/translation elongation factor EF1B, N-terminal, eukaryote
IPR000195:RabGAP/TBC
IPR018957:Zinc finger, C3HC4 RING-type

GO:0009620~response to fungus
GO:0002920~regulation of humoral immune response
GO:0002831~regulation of response to biotic stimulus
GO:0043900~regulation of multi-organism process
GO:0002759~regulation of antimicrobial humoral response
GO:0006967~positive regulation of antifungal peptide biosynthetic process
GO:0032312~regulation of ARF GTPase activity
GO:0006984~ER-nuclear signaling pathway
GO:0006570~tyrosine metabolic process
GO:0002788~regulation of antifungal peptide production
GO:0030723~ovarian fusome organization
GO:0002810~regulation of antifungal peptide biosynthetic process
GO:0007561~imaginal disc eversion
zinc finger region:RING-type
GO:0000278~mitotic cell cycle
IPR003118:Sterile alpha motif/pointed
GO:0016331~morphogenesis of embryonic epithelium
GO:0015849~organic acid transport
GO:0046942~carboxylic acid transport
GO:0005484~SNAP receptor activity
GO:0004428~inositol or phosphatidylinositol kinase activity
GO:0009953~dorsal/ventral pattern formation
GO:0006914~autophagy
GO:0010741~negative regulation of protein kinase cascade
GO:0007099~centriole replication
GO:0042386~hemocyte differentiation
GO:0007427~epithelial cell migration, open tracheal system
GO:0010631~epithelial cell migration
GO:0004000~adenosine deaminase activity
GO:0048069~eye pigmentation
GO:0048592~eye morphogenesis
dme00600:Sphingolipid metabolism
GO:0048589~developmental growth
GO:0045995~regulation of embryonic development
GO:0010033~response to organic substance
growth regulation
IPR002656:Acyltransferase 3
GO:0003702~RNA polymerase II transcription factor activity
GO:0035072~ecdysone-mediated induction of salivary gland cell autophagic cell death
GO:0016044~membrane organization
GO:0009072~aromatic amino acid family metabolic process
dme00565:Ether lipid metabolism
GO:0010324~membrane invagination

GO:0006897~endocytosis
GO:0005700~polytene chromosome
GO:0030528~transcription regulator activity
GO:0048737~imaginal disc-derived appendage development
IPR017441:Protein kinase, ATP binding site
GO:0045177~apical part of cell
GO:0060249~anatomical structure homeostasis
IPR001365:Adenosine/AMP deaminase
IPR001164:Arf GTPase activating protein
IPR000418:Ets
GO:0007015~actin filament organization
GO:0045179~apical cortex
GO:0008195~phosphatidate phosphatase activity
GO:0008060~ARF GTPase activator activity
IPR013525:ABC-2 type transporter
IPR000242:Protein-tyrosine phosphatase, receptor/non-receptor type
IPR019955:Ubiquitin supergroup
SM00355:ZnF_C2H2
SM00397:t_SNARE
GO:0007346~regulation of mitotic cell cycle
GO:0060560~developmental growth involved in morphogenesis
GO:0007390~germ-band shortening
GO:0030178~negative regulation of Wnt receptor signaling pathway
GO:0048736~appendage development

Cluster 2 GO Terms

GO:0042254~ribosome biogenesis
GO:0022613~ribonucleoprotein complex biogenesis
GO:0055114~oxidation reduction
oxidoreductase
GO:0006364~rRNA processing
GO:0016072~rRNA metabolic process
GO:0006631~fatty acid metabolic process
ribosome biogenesis
Acyltransferase
IPR016040:NAD(P)-binding domain
GO:0034470~ncRNA processing
GO:0005730~nucleolus
GO:0015405~P-P-bond-hydrolysis-driven transmembrane transporter activity
GO:0015399~primary active transmembrane transporter activity
GO:0048037~cofactor binding
GO:0008610~lipid biosynthetic process
GO:0019748~secondary metabolic process

GO:0044242~cellular lipid catabolic process
lyase
GO:0050662~coenzyme binding
SM00563:PlsC
rrna processing
GO:0042579~microbody
GO:0005777~peroxisome
GO:0022884~macromolecule transmembrane transporter activity
GO:0015450~P-P-bond-hydrolysis-driven protein transmembrane transporter activity
GO:0006612~protein targeting to membrane
GO:0006633~fatty acid biosynthetic process
GO:0016042~lipid catabolic process
GO:0016634~oxidoreductase activity, acting on the CH-CH group of donors, oxygen as acceptor
IPR002123:Phospholipid/glycerol acyltransferase
dme01040:Biosynthesis of unsaturated fatty acids
GO:0031974~membrane-enclosed lumen
GO:0046394~carboxylic acid biosynthetic process
GO:0016053~organic acid biosynthetic process
GO:0008374~O-acyltransferase activity
dme00561:Glycerolipid metabolism
GO:0034660~ncRNA metabolic process
GO:0043190~ATP-binding cassette (ABC) transporter complex
GO:0006839~mitochondrial transport
GO:0043603~cellular amide metabolic process
GO:0016877~ligase activity, forming carbon-sulfur bonds
IPR003439:ABC transporter-like
dme00071:Fatty acid metabolism
GO:0008320~protein transmembrane transporter activity
dme00620:Pyruvate metabolism
GO:0051186~cofactor metabolic process
GO:0033293~monocarboxylic acid binding
GO:0005784~translocon complex
GO:0006721~terpenoid metabolic process
GO:0042626~ATPase activity, coupled to transmembrane movement of substances
GO:0043492~ATPase activity, coupled to movement of substances
GO:0016620~oxidoreductase activity, acting on the aldehyde or oxo group of donors, NAD or NADP as acceptor
SM00382:AAA
GO:0009055~electron carrier activity
GO:0055085~transmembrane transport
GO:0016820~hydrolase activity, acting on acid anhydrides, catalyzing transmembrane movement of substances
GO:0006396~RNA processing

GO:0005811~lipid particle
nucleotidyltransferase
IPR000873:AMP-dependent synthetase and ligase
binding site:NAD
GO:0042624~ATPase activity, uncoupled
GO:0001676~long-chain fatty acid metabolic process
GO:0046496~nicotinamide nucleotide metabolic process
GO:0009820~alkaloid metabolic process
GO:0006769~nicotinamide metabolic process
IPR011701:Major facilitator superfamily MFS-1
dme00640:Propanoate metabolism
GO:0005786~signal recognition particle, endoplasmic reticulum targeting
GO:0048500~signal recognition particle
GO:0005739~mitochondrion
GO:0019842~vitamin binding
GO:0019362~pyridine nucleotide metabolic process
IPR002076:GNS1/SUR4 membrane protein
GO:0043233~organelle lumen
GO:0070013~intracellular organelle lumen
IPR015590:Aldehyde dehydrogenase
PIRSF031070:PIRSF031070
short sequence motif:Twin CX3C motif
GO:0006732~coenzyme metabolic process
IPR017871:ABC transporter, conserved site
GO:0044429~mitochondrial part
nucleotide phosphate-binding region:NAD
GO:0006605~protein targeting
IPR016162:Aldehyde dehydrogenase, N-terminal
PIRSF000147:NAD-dependent aldehyde dehydrogenase
GO:0030529~ribonucleoprotein complex
GO:0050660~FAD binding
GO:0030867~rough endoplasmic reticulum membrane
GO:0044271~nitrogen compound biosynthetic process
transmembrane
GO:0016021~integral to membrane
GO:0051761~sesquiterpene metabolic process
GO:0006716~juvenile hormone metabolic process
GO:0006714~sesquiterpenoid metabolic process
GO:0051188~cofactor biosynthetic process
GO:0005758~mitochondrial intermembrane space
SM00587:CHK
GO:0031406~carboxylic acid binding
GO:0005759~mitochondrial matrix

GO:0031980~mitochondrial lumen
IPR013764:Acyl-CoA oxidase/dehydrogenase, type1/2, C-terminal
IPR006091:Acyl-CoA oxidase/dehydrogenase, central region
IPR013786:Acyl-CoA dehydrogenase/oxidase, N-terminal
IPR002198:Short-chain dehydrogenase/reductase SDR
binding site:Substrate
transferase
GO:0005791~rough endoplasmic reticulum
GO:0031224~intrinsic to membrane
GO:0042214~terpene metabolic process
GO:0006613~cotranslational protein targeting to membrane
GO:0006626~protein targeting to mitochondrion
GO:0070585~protein localization in mitochondrion
GO:0003995~acyl-CoA dehydrogenase activity
GO:0003997~acyl-CoA oxidase activity
IPR012258:Acyl-CoA oxidase
IPR004217:Zinc finger, Tim10/DDP-type
IPR002655:Acyl-CoA oxidase, C-terminal
lipid synthesis
translocation
GO:0031970~organelle envelope lumen
GO:0006098~pentose-phosphate shunt
GO:0006739~NADP metabolic process
GO:0006720~isoprenoid metabolic process
dme00280:Valine, leucine and isoleucine degradation
PIRSF000168:Acyl-CoA_oxidase
Monooxygenase
GO:0016411~acylglycerol O-acyltransferase activity
IPR004217:Mitochondrial inner membrane translocase complex, Tim8/9/10/13-zinc finger-like
IPR015876:Fatty acid desaturase, type 1, core
GO:0042623~ATPase activity, coupled
GO:0006733~oxidoreduction coenzyme metabolic process
GO:0016407~acetyltransferase activity
GO:0030684~preribosome
GO:0016779~nucleotidyltransferase activity
IPR000618:Insect cuticle protein
GO:0005744~mitochondrial inner membrane presequence translocase complex
GO:0007007~inner mitochondrial membrane organization
GO:0045039~protein import into mitochondrial inner membrane
GO:0033365~protein localization in organelle
GO:0001882~nucleoside binding
dme02010:ABC transporters
GO:0007005~mitochondrion organization

GO:0008509~anion transmembrane transporter activity
IPR003593:ATPase, AAA+ type, core
GO:0005792~microsome
GO:0042598~vesicular fraction
IPR001993:Mitochondrial substrate carrier
GO:0005214~structural constituent of chitin-based cuticle
GO:0004467~long-chain-fatty-acid-CoA ligase activity
GO:0015645~fatty-acid ligase activity
GO:0004768~stearoyl-CoA 9-desaturase activity
GO:0045471~response to ethanol
GO:0008028~monocarboxylic acid transmembrane transporter activity
GO:0001522~pseudouridine synthesis
GO:0031301~integral to organelle membrane
GO:0015370~solute:sodium symporter activity
GO:0042719~mitochondrial intermembrane space protein transporter complex
Lipid metabolism
GO:0000166~nucleotide binding
GO:0009636~response to toxin
GO:0019637~organophosphate metabolic process
GO:0008080~N-acetyltransferase activity
GO:0015294~solute:cation symporter activity
IPR016160:Aldehyde dehydrogenase, conserved site
dme00480:Glutathione metabolism
IPR002347:Glucose/ribitol dehydrogenase
IPR005829:Sugar transporter, conserved site
GO:0016229~steroid dehydrogenase activity
GO:0006635~fatty acid beta-oxidation
IPR003689:Zinc/iron permease
GO:0030001~metal ion transport
GO:0030258~lipid modification
GO:0009108~coenzyme biosynthetic process
IPR015897:CHK kinase-like
IPR004119:Protein of unknown function DUF227
GO:0016410~N-acyltransferase activity
GO:0019395~fatty acid oxidation
GO:0034440~lipid oxidation
GO:0009062~fatty acid catabolic process
GO:0015293~symporter activity
GO:0030554~adenyl nucleotide binding
Fatty acid biosynthesis
GO:0005048~signal sequence binding
GO:0000062~acyl-CoA binding

GO:0016717~oxidoreductase activity, acting on paired donors, with oxidation of a pair of donors resulting in the reduction of molecular oxygen to two molecules of water
GO:0031090~organelle membrane
GO:0007443~Malpighian tubule morphogenesis
IPR005804:Fatty acid desaturase, type 1
GO:0042302~structural constituent of cuticle
GO:0008565~protein transporter activity
GO:0016887~ATPase activity
GO:0001883~purine nucleoside binding
GO:0046395~carboxylic acid catabolic process
GO:0016054~organic acid catabolic process
GO:0035202~sac formation, open tracheal system
GO:0006644~phospholipid metabolic process
GO:0044452~nucleolar part
GO:0005783~endoplasmic reticulum
GO:0007006~mitochondrial membrane organization
GO:0015103~inorganic anion transmembrane transporter activity
microsome
GO:0009165~nucleotide biosynthetic process
transport
GO:0006820~anion transport
Flavoprotein
IPR017940:ABC transporter integral membrane type 1
GO:0070279~vitamin B6 binding
GO:0030170~pyridoxal phosphate binding
dme00410:beta-Alanine metabolism
SM00487:DEXDc
Lipid metabolism / Secondary metabolites biosynthesis, transport, and catabolism
GO:0008654~phospholipid biosynthetic process
GO:0006090~pyruvate metabolic process
dme00981:Insect hormone biosynthesis
IPR010509:ABC transporter, N-terminal
IPR006183:6-phosphogluconate dehydrogenase
SM00490:HELICc
transit peptide:Mitochondrion
GO:0016831~carboxy-lyase activity
dme00903:Limonene and pinene degradation
GO:0005624~membrane fraction
GO:0009124~nucleoside monophosphate biosynthetic process
mitochondrion
GO:0006812~cation transport
GO:0034404~nucleobase, nucleoside and nucleotide biosynthetic process
GO:0034654~nucleobase, nucleoside, nucleotide and nucleic acid biosynthetic process

PIRSF038447:mitochondrial import inner membrane translocase Tim9-Tim10, subunit Tim9
PIRSF002411:endozepine
PIRSF001552:4-coumarate-CoA ligase
GO:0030176~integral to endoplasmic reticulum membrane
endoplasmic reticulum
GO:0031300~intrinsic to organelle membrane
IPR000629:RNA helicase, ATP-dependent, DEAD-box, conserved site
GO:0048619~embryonic hindgut morphogenesis
lipid metabolism
metal ion-binding site:Iron (heme axial ligand)
GO:0006621~protein retention in ER lumen
GO:0006573~valine metabolic process

Cluster 3 GO Terms

stress response
GO:0009266~response to temperature stimulus
GO:0009408~response to heat
IPR018181:Heat shock protein 70, conserved site
IPR013126:Heat shock protein 70
IPR001023:Heat shock protein Hsp70
GO:0009628~response to abiotic stimulus
PIRSF002581:chaperone HSP70
GO:0001666~response to hypoxia
GO:0070482~response to oxygen levels
IPR005521:Attacin, C-terminal region
GO:0035080~heat shock-mediated polytene chromosome puffing
GO:0035079~polytene chromosome puffing
GO:0005576~extracellular region
GO:0034605~cellular response to heat
dme04144:Endocytosis
stress-induced protein
heat shock
dme03040:Spliceosome
GO:0006952~defense response
GO:0009617~response to bacterium
GO:0019731~antibacterial humoral response
polymorphism
GO:0006955~immune response
innate immunity
immune response
GO:0042742~defense response to bacterium
GO:0019730~antimicrobial humoral response
GO:0006959~humoral immune response

GO:0045087~innate immune response
IPR001436:Alpha crystallin/Heat shock protein
molecular chaperone
GO:0006986~response to unfolded protein
GO:0051789~response to protein stimulus
sequence variant
IPR002068:Heat shock protein Hsp20
PIRSF036514:alpha-crystallin-related small heat shock protein
GO:0044421~extracellular region part
antibiotic
GO:0004252~serine-type endopeptidase activity
GO:0033554~cellular response to stress
GO:0008236~serine-type peptidase activity
GO:0005524~ATP binding
GO:0017171~serine hydrolase activity
GO:0032559~adenyl ribonucleotide binding
Antimicrobial
GO:0030554~adenyl nucleotide binding
GO:0001883~purine nucleoside binding
GO:0001882~nucleoside binding
Secreted
GO:0032553~ribonucleotide binding
GO:0032555~purine ribonucleotide binding
GO:0004175~endopeptidase activity
GO:0017076~purine nucleotide binding
GO:0051276~chromosome organization

All Go Terms

GO:0012501~programmed cell death
GO:0008219~cell death
GO:0016265~death
GO:0048732~gland development
GO:0016271~tissue death
GO:0007559~histolysis
GO:0007431~salivary gland development
GO:0035272~exocrine system development
GO:0022612~gland morphogenesis
GO:0007435~salivary gland morphogenesis
GO:0035071~salivary gland cell autophagic cell death
GO:0048102~autophagic cell death
GO:0035070~salivary gland histolysis
GO:0042254~ribosome biogenesis
GO:0019730~antimicrobial humoral response

GO:0007242~intracellular signaling cascade
GO:0006955~immune response
GO:0006959~humoral immune response
GO:0044242~cellular lipid catabolic process
GO:0033554~cellular response to stress
GO:0006952~defense response
GO:0009886~post-embryonic morphogenesis
GO:0007552~metamorphosis
dme04144:Endocytosis
GO:0048707~instar larval or pupal morphogenesis
dme04630:Jak-STAT signaling pathway
GO:0009791~post-embryonic development
innate immunity
GO:0045087~innate immune response
GO:0016072~rRNA metabolic process
GO:0006631~fatty acid metabolic process
GO:0007243~protein kinase cascade
immune response
GO:0022613~ribonucleoprotein complex biogenesis
GO:0060541~respiratory system development
GO:0007424~open tracheal system development
GO:0002165~instar larval or pupal development
Apoptosis
Acyltransferase
GO:0055114~oxidation reduction
GO:0019731~antibacterial humoral response
GO:0016042~lipid catabolic process
dme04140:Regulation of autophagy
oxidoreductase
IPR005024:Snf7
IPR013172:DIM, Drosophila melanogaster
GO:0019748~secondary metabolic process
GO:0042058~regulation of epidermal growth factor receptor signaling pathway
GO:0046578~regulation of Ras protein signal transduction
GO:0006364~rRNA processing
GO:0042440~pigment metabolic process
GO:0015031~protein transport
GO:0010623~developmental programmed cell death
GO:0040008~regulation of growth
GO:0048066~pigmentation during development
GO:0043067~regulation of programmed cell death
GO:0016477~cell migration
ribosome biogenesis

stress response
GO:0030097~hemopoiesis
GO:0045184~establishment of protein localization
GO:0043190~ATP-binding cassette (ABC) transporter complex
GO:0008104~protein localization
GO:0010941~regulation of cell death
GO:0043473~pigmentation
IPR005521:Attacin, C-terminal region
IPR000980:SH2 motif
GO:0007264~small GTPase mediated signal transduction
GO:0051056~regulation of small GTPase mediated signal transduction
IPR004827:Basic-leucine zipper (bZIP) transcription factor
GO:0009968~negative regulation of signal transduction
GO:0010648~negative regulation of cell communication
SM00252:SH2
SM00338:BRLZ
GO:0035234~germ cell programmed cell death
GO:0042981~regulation of apoptosis
GO:0016634~oxidoreductase activity, acting on the CH-CH group of donors, oxygen as acceptor
GO:0007167~enzyme linked receptor protein signaling pathway
PIRSF036514:alpha-crystallin-related small heat shock protein
GO:0048870~cell motility
GO:0042742~defense response to bacterium
GO:0010033~response to organic substance
GO:0006986~response to unfolded protein
GO:0051789~response to protein stimulus
GO:0007254~JNK cascade
GO:0006915~apoptosis
GO:0005777~peroxisome
GO:0042579~microbody
IPR003579:Ras small GTPase, Rab type
GO:0007169~transmembrane receptor protein tyrosine kinase signaling pathway
dme00561:Glycerolipid metabolism
GO:0042127~regulation of cell proliferation
GO:0048534~hemopoietic or lymphoid organ development
GO:0002520~immune system development
GO:0007280~pole cell migration
SM00175:RAB
GO:0000165~MAPKKK cascade
GO:0031098~stress-activated protein kinase signaling pathway
GO:0009617~response to bacterium
GO:0048565~gut development
IPR001849:Pleckstrin homology

IPR003439:ABC transporter-like
GO:0034976~response to endoplasmic reticulum stress
GO:0045742~positive regulation of epidermal growth factor receptor signaling pathway
antibiotic
GO:0051674~localization of cell
IPR013525:ABC-2 type transporter
GO:0048037~cofactor binding
dme00600:Sphingolipid metabolism
GO:0007390~germ-band shortening
GO:0045793~positive regulation of cell size
GO:0030258~lipid modification
GO:0045165~cell fate commitment
GO:0009055~electron carrier activity
SM00233:PH
dme01040:Biosynthesis of unsaturated fatty acids
IPR016040:NAD(P)-binding domain
IPR011993:Pleckstrin homology-type
GO:0006865~amino acid transport
GO:0042598~vesicular fraction
GO:0005792~microsome
GO:0006721~terpenoid metabolic process
GO:0009161~ribonucleoside monophosphate metabolic process
GO:0009156~ribonucleoside monophosphate biosynthetic process
splice variant
GO:0007297~ovarian follicle cell migration
IPR003903:Ubiquitin interacting motif
IPR001436:Alpha crystallin/Heat shock protein
GO:0007494~midgut development
DNA binding
GO:0046148~pigment biosynthetic process
GO:0016814~hydrolase activity, acting on carbon-nitrogen (but not peptide) bonds, in cyclic amidines
SM00726:UIM
GO:0015837~amine transport
IPR006091:Acyl-CoA oxidase/dehydrogenase, central region
IPR013764:Acyl-CoA oxidase/dehydrogenase, type1/2, C-terminal
IPR013786:Acyl-CoA dehydrogenase/oxidase, N-terminal
GO:0003995~acyl-CoA dehydrogenase activity
GO:0006635~fatty acid beta-oxidation
GO:0006612~protein targeting to membrane
GO:0009124~nucleoside monophosphate biosynthetic process
GO:0009266~response to temperature stimulus
GO:0003677~DNA binding
PIRSF001710:Ras-related protein Rab

GO:0009127~purine nucleoside monophosphate biosynthetic process
GO:0009126~purine nucleoside monophosphate metabolic process
GO:0009167~purine ribonucleoside monophosphate metabolic process
GO:0009168~purine ribonucleoside monophosphate biosynthetic process
GO:0030307~positive regulation of cell growth
GO:0046668~regulation of retinal cell programmed cell death
GO:0007298~border follicle cell migration
GO:0003997~acyl-CoA oxidase activity
GO:0008063~Toll signaling pathway
IPR001496:SOCS protein, C-terminal
IPR011700:Basic leucine zipper
IPR015897:CHK kinase-like
IPR004119:Protein of unknown function DUF227
dna-binding
GO:0043565~sequence-specific DNA binding
GO:0033293~monocarboxylic acid binding
GO:0035295~tube development
Monooxygenase
PIRSF000168:Acyl-CoA_oxidase
SM00253:SOCS
GO:0034440~lipid oxidation
GO:0009062~fatty acid catabolic process
GO:0019395~fatty acid oxidation
GO:0007259~JAK-STAT cascade
GO:0043068~positive regulation of programmed cell death
GO:0010942~positive regulation of cell death
GO:0043066~negative regulation of apoptosis
GO:0019904~protein domain specific binding
IPR002655:Acyl-CoA oxidase, C-terminal
IPR012258:Acyl-CoA oxidase
IPR013659:Adenosine/AMP deaminase N-terminal
IPR016118:Phosphatidic acid phosphatase/chloroperoxidase, N-terminal
IPR006331:Adenosine deaminase-related growth factor
GO:0045927~positive regulation of growth
GO:0032868~response to insulin stimulus
GO:0008286~insulin receptor signaling pathway
GO:0043434~response to peptide hormone stimulus
GO:0032869~cellular response to insulin stimulus
GO:0008354~germ cell migration
GO:0042214~terpene metabolic process
GO:0048067~cuticle pigmentation
GO:0001742~oenocyte differentiation
GO:0009408~response to heat

GO:0034470~ncRNA processing
dme00640:Propanoate metabolism
GO:0035239~tube morphogenesis
SM00587:CHK
GO:0015849~organic acid transport
GO:0046942~carboxylic acid transport
dme00410:beta-Alanine metabolism
GO:0001736~establishment of planar polarity
GO:0005615~extracellular space
GO:0005624~membrane fraction
GO:0042067~establishment of ommatidial polarity
GO:0035096~larval midgut cell programmed cell death
GO:0015820~leucine transport
GO:0060356~leucine import
GO:0015803~branched-chain aliphatic amino acid transport
DNA-binding region:ETS
IPR002656:Acyltransferase 3
GO:0005525~GTP binding
GO:0009123~nucleoside monophosphate metabolic process
GO:0008610~lipid biosynthetic process
PIRSF014263:Drosophila hypothetical protein EG_34F3.5
IPR002123:Phospholipid/glycerol acyltransferase
GO:0016877~ligase activity, forming carbon-sulfur bonds
GO:0007164~establishment of tissue polarity
GO:0001738~morphogenesis of a polarized epithelium
GO:0001666~response to hypoxia
GO:0070482~response to oxygen levels
domain:RHD
GO:0001709~cell fate determination
compositionally biased region:Ser-rich
SM00563:PlsC
IPR000873:AMP-dependent synthetase and ligase
dme00903:Limonene and pinene degradation
GO:0017076~purine nucleotide binding
GO:0032561~guanyl ribonucleotide binding
GO:0032268~regulation of cellular protein metabolic process
GO:0015405~P-P-bond-hydrolysis-driven transmembrane transporter activity
GO:0015399~primary active transmembrane transporter activity
zinc finger
dme00071:Fatty acid metabolism
GO:0022884~macromolecule transmembrane transporter activity
GO:0015450~P-P-bond-hydrolysis-driven protein transmembrane transporter activity
GO:0005783~endoplasmic reticulum

IPR001806:Ras GTPase
IPR013753:Ras
GO:0006984~ER-nuclear signaling pathway
GO:0002788~regulation of antifungal peptide production
GO:0002810~regulation of antifungal peptide biosynthetic process
GO:0006967~positive regulation of antifungal peptide biosynthetic process
GO:0048729~tissue morphogenesis
GO:0016053~organic acid biosynthetic process
GO:0046394~carboxylic acid biosynthetic process
GO:0019001~guanyl nucleotide binding
GO:0005626~insoluble fraction
GO:0006720~isoprenoid metabolic process
PIRSF001894:attacin
dme00565:Ether lipid metabolism
GO:0012502~induction of programmed cell death
gtp-binding
IPR000451:NF-kappa-B/Rel/dorsal
IPR019761:DNA-directed RNA polymerase M, 15 kDa subunit, conserved site
endoplasmic reticulum
GO:0051186~cofactor metabolic process
GO:0005784~translocon complex
GO:0035099~hemocyte migration
transferase
IPR002068:Heat shock protein Hsp20
GO:0030031~cell projection assembly
GO:0008360~regulation of cell shape
rrna processing
GO:0004725~protein tyrosine phosphatase activity
GO:0043069~negative regulation of programmed cell death
GO:0046983~protein dimerization activity
GO:0032318~regulation of Ras GTPase activity
lyase
GO:0008028~monocarboxylic acid transmembrane transporter activity
dme04150:mTOR signaling pathway
GO:0042802~identical protein binding
PIRSF000051:cytochrome P450 CYP3A5
heat shock
stress-induced protein
GO:0000267~cell fraction
GO:0004467~long-chain-fatty-acid-CoA ligase activity
GO:0015645~fatty-acid ligase activity
GO:0004000~adenosine deaminase activity
alternative splicing

GO:0009719~response to endogenous stimulus
GO:0060249~anatomical structure homeostasis
GO:0009725~response to hormone stimulus
GO:0070279~vitamin B6 binding
GO:0030170~pyridoxal phosphate binding
GO:0016311~dephosphorylation
GO:0007163~establishment or maintenance of cell polarity
GO:0048598~embryonic morphogenesis
GO:0051058~negative regulation of small GTPase mediated signal transduction
GO:0046580~negative regulation of Ras protein signal transduction
IPR013087:Zinc finger, C2H2-type/integrase, DNA-binding
GO:0006644~phospholipid metabolic process
GO:0050660~FAD binding
GO:0050662~coenzyme binding
GO:0007176~regulation of epidermal growth factor receptor activity
GO:0001676~long-chain fatty acid metabolic process
GO:0010469~regulation of receptor activity
GO:0060326~cell chemotaxis
GO:0048010~vascular endothelial growth factor receptor signaling pathway
GO:0035069~larval midgut histolysis
GO:0007593~chitin-based cuticle tanning
GO:0006303~double-strand break repair via nonhomologous end joining
GO:0031399~regulation of protein modification process
GO:0010627~regulation of protein kinase cascade
lipid metabolism
GO:0051188~cofactor biosynthetic process
dme00250:Alanine, aspartate and glutamate metabolism
IPR017871:ABC transporter, conserved site
IPR000108:Neutrophil cytosol factor 2
IPR001365:Adenosine/AMP deaminase
IPR000418:Ets
GO:0005083~small GTPase regulator activity
GO:0005942~phosphoinositide 3-kinase complex
microsome
propeptide:Removed by a dipeptidylpeptidase
GO:0006928~cell motion
GO:0016054~organic acid catabolic process
GO:0046395~carboxylic acid catabolic process
SM00413:ETS
GO:0015171~amino acid transmembrane transporter activity
GO:0007391~dorsal closure
GO:0050829~defense response to Gram-negative bacterium
GO:0009112~nucleobase metabolic process

GO:0006468~protein amino acid phosphorylation
GO:0005730~nucleolus
nucleotide-binding
GO:0030695~GTPase regulator activity
GO:0045471~response to ethanol
GO:0042624~ATPase activity, uncoupled
GO:0008195~phosphatidate phosphatase activity
GO:0035152~regulation of tube architecture, open tracheal system
GO:0016645~oxidoreductase activity, acting on the CH-NH group of donors
GO:0048663~neuron fate commitment
GO:0060548~negative regulation of cell death
GO:0048056~R3/R4 cell differentiation
GO:0007445~determination of imaginal disc primordium
GO:0031396~regulation of protein ubiquitination
GO:0035225~determination of genital disc primordium
GO:0007464~R3/R4 cell fate commitment
nucleotidyltransferase
IPR000727:Target SNARE coiled-coil region
IPR000306:Zinc finger, FYVE-type
IPR013027:FAD-dependent pyridine nucleotide-disulphide oxidoreductase
GO:0044271~nitrogen compound biosynthetic process
PIRSF015810:Caenorhabditis elegans hypothetical protein R06B9.1
PIRSF000147:NAD-dependent aldehyde dehydrogenase
PIRSF000168:acyl-CoA oxidase
GO:0006633~fatty acid biosynthetic process
GO:0019637~organophosphate metabolic process
IPR005520:Attacin, N-terminal region
IPR011539:Rel homology
IPR005520:Attacin, N-terminal
IPR000759:Adrenodoxin reductase
IPR001251:Cellular retinaldehyde-binding/triple function, C-terminal
IPR015421:Pyridoxal phosphate-dependent transferase, major region, subdomain 1
GO:0000922~spindle pole
GO:0005786~signal recognition particle, endoplasmic reticulum targeting
GO:0048500~signal recognition particle
GO:0002009~morphogenesis of an epithelium
GO:0040003~chitin-based cuticle development
GO:0001752~compound eye photoreceptor fate commitment
GO:0042706~eye photoreceptor cell fate commitment
SM00064:FYVE
SM00397:t_SNARE
GO:0030855~epithelial cell differentiation
GO:0060429~epithelium development

GO:0048871~multicellular organismal homeostasis
GO:0016476~regulation of embryonic cell shape
GO:0001894~tissue homeostasis
GO:0043603~cellular amide metabolic process
Antimicrobial
GO:0060589~nucleoside-triphosphatase regulator activity
IPR003689:Zinc/iron permease
GO:0005096~GTPase activator activity
GO:0042335~cuticle development
GO:0008374~O-acyltransferase activity
GO:0005275~amine transmembrane transporter activity
GO:0001558~regulation of cell growth
GO:0046620~regulation of organ growth
GO:0000726~non-recombinational repair
GO:0035079~polytene chromosome puffing
GO:0035080~heat shock-mediated polytene chromosome puffing
GO:0043043~peptide biosynthetic process
GO:0008365~adult chitin-based cuticle development
GO:0043087~regulation of GTPase activity
SM00516:SEC14
GO:0016410~N-acyltransferase activity
IPR004841:Amino acid permease-associated region
GO:0007444~imaginal disc development
GO:0003684~damaged DNA binding
GO:0035081~induction of programmed cell death by hormones
GO:0006582~melanin metabolic process
GO:0042594~response to starvation
GO:0035160~maintenance of epithelial integrity, open tracheal system
GO:0005048~signal sequence binding
GO:0000062~acyl-CoA binding
GO:0005070~SH3/SH2 adaptor activity
GO:0000902~cell morphogenesis
GO:0016318~ommatidial rotation
GO:0001882~nucleoside binding
compositionally biased region:Poly-Gln
dme00480:Glutathione metabolism
dme00564:Glycerophospholipid metabolism
IPR017973:Cytochrome P450, C-terminal region
GO:0042386~hemocyte differentiation
GO:0006613~cotranslational protein targeting to membrane
short sequence motif:Twin CX3C motif
GO:0048569~post-embryonic organ development
GO:0008293~torso signaling pathway

GO:0019842~vitamin binding
GO:0008083~growth factor activity
metal ion-binding site:Iron (heme axial ligand)
IPR006578:MADF domain
GO:0008356~asymmetric cell division
IPR001128:Cytochrome P450
PIRSF002581:chaperone HSP70
PIRSF031070:PIRSF031070
GO:0004857~enzyme inhibitor activity
GO:0042169~SH2 domain binding
GO:0008340~determination of adult life span
GO:0010259~multicellular organismal aging
GO:0007568~aging
GO:0016331~morphogenesis of embryonic epithelium
Lipid metabolism / Secondary metabolites biosynthesis, transport, and catabolism
GO:0032870~cellular response to hormone stimulus
GO:0006917~induction of apoptosis
compositionally biased region:Gln-rich
IPR000326:Phosphatidic acid phosphatase type 2/haloperoxidase
GO:0007442~hindgut morphogenesis
GO:0043408~regulation of MAPKKK cascade
GO:0032555~purine ribonucleotide binding
GO:0032553~ribonucleotide binding
GO:0005484~SNAP receptor activity
GO:0016620~oxidoreductase activity, acting on the aldehyde or oxo group of donors, NAD or NADP as acceptor
IPR017455:Zinc finger, FYVE-related
IPR016130:Protein-tyrosine phosphatase, active site
GO:0009072~aromatic amino acid family metabolic process
GO:0035162~embryonic hemopoiesis
GO:0010669~epithelial structure maintenance
GO:0046496~nicotinamide nucleotide metabolic process
GO:0006769~nicotinamide metabolic process
GO:0006308~DNA catabolic process
GO:0009820~alkaloid metabolic process
polymorphism
GO:0002164~larval development
GO:0046552~photoreceptor cell fate commitment
GO:0009967~positive regulation of signal transduction
SM00014:acidPPc
GO:0031974~membrane-enclosed lumen
GO:0001883~purine nucleoside binding
SM00595:MADF
GO:0005214~structural constituent of chitin-based cuticle

IPR001222:Zinc finger, TFIIS-type
IPR006596:Nucleotide binding protein, PINc
IPR004182:GRAM
GO:0000166~nucleotide binding
GO:0022404~molting cycle process
GO:0015370~solute:sodium symporter activity
GO:0043065~positive regulation of apoptosis
GO:0048563~post-embryonic organ morphogenesis
GO:0007560~imaginal disc morphogenesis
GO:0006714~sesquiterpenoid metabolic process
GO:0015804~neutral amino acid transport
GO:0042417~dopamine metabolic process
GO:0034605~cellular response to heat
GO:0007438~oenocyte development
GO:0002683~negative regulation of immune system process
GO:0006716~juvenile hormone metabolic process
GO:0006616~SRP-dependent cotranslational protein targeting to membrane, translocation
GO:0046622~positive regulation of organ growth
GO:0006684~sphingomyelin metabolic process
GO:0051761~sesquiterpene metabolic process
GO:0050777~negative regulation of immune response
GO:0042438~melanin biosynthetic process

Table C.3 Enriched GO Terms from Clusters

GO Terms were retrieved from genes groups uploaded to DAVID (Gibert et al. 2000) from each of the three clusters from Figure 4.2. The "All GO Terms" section is the GO Terms enriched when all clusters are combined.

References

Gibert P, Moreteau B, David JR (2000). Developmental constraints on an adaptive plasticity: reaction norms of pigmentation in adult segments of *Drosophila melanogaster*. *Evol Dev* **2**: 249–260.